

WISCONSIN GEOLOGICAL SURVEY

Bulletin No. 78

Scientific Series
No. 15

GEOPHYSICAL METHODS
APPLIED TO GEOLOGIC PROBLEMS IN WISCONSIN

By

GEORGE P. WOOLLARD
Professor of Geophysics
University of Wisconsin

and

GEORGE F. HANSON
State Geologist

University of Wisconsin
1954

Preface

This report covers a series of geophysical studies made in connection with subsurface investigations in various parts of the State of Wisconsin which were carried out cooperatively by the Wisconsin Geological Survey and the University of Wisconsin Department of Geology, Geophysics Section. Many of the investigations undertaken owe their conception to Mr. E.F. Bean, State Geologist retired, whose enthusiastic encouragement and support played a vital role.

The studies reported are part of the University of Wisconsin's program of specialized research for the development of the natural resources of the state. Although the work was supported in part by research grants from the Wisconsin Alumni Research Foundation, the cost of much of the work was borne on an actual cost basis by the municipalities and organizations directly concerned.

The purpose of this report is to show the degree to which geophysical studies can be of assistance in resolving some of the problems of subsurface water supply, mineral exploration, engineering, and subsurface geology encountered in Wisconsin.

Table of Contents

Part I Introduction

I-1	General Statement	1
1-2	Types of Geophysical Measurements	1
1-3	General Description of Geophysical Measurements	3
	1-3a Gravity Measurements	3
	1-3b Magnetic Measurements	4
	1-3c Electrical Measurements	10
	1-3d Seismic Measurements	12
	1-3e Electro-magnetic Measurements	13
1-4	Work Covered in Present Report	15
1-5	Equipment Used	15
1-6	Acknowledgements	17

Part II

Ground Water Investigations

II-1	Lake Mills, Wisconsin. University of Wisconsin Emmons Blaine Farm	19
	II-1a General Statement	19
	II-1b Seismic Investigations	19
	II-1c Evaluation of Seismic Results from Drilling	20
	II-1d Magnetic and Gravity Study of Lake Mills Area	24
	II-1e Concluding Statement on Investigation	34
II-2	Antigo, Wisconsin	34
	II-2a General Statement	34
	II-2b Seismic Studies	35
	II-2c Electrical Resistivity Studies	37
	II-2d Magnetic Survey	49
	II-2e Gravity Investigation	49
	II-2f Magnetic and Gravity Results	53
	II-2g Interpretation of Gravity and Magnetic Results	53
	II-2h Conclusion on Study at Antigo	63
II-3	Seismic Investigations at Gresham, Wisconsin	64
	II-3a General Statement	64
	II-3b Seismic Investigation	64
II-4	Campbellsport, Wisconsin	68
	II-4a General Statement	68
	II-4b Seismic Investigation	68
II-5	Hudson, Wisconsin	78
	II-5a General Statement	78
	II-5b Seismic Investigation	78
	II-5c Evaluation of Results	79
II-6	Clark County Hospital, Wisconsin	82
	II-6a General Statement	82
	II-6b Seismic Investigation	83
	II-6c Evaluation of Results	83
II-7	Vesper, Wisconsin	87
	II-7a General Statement	87

II-7b	Seismic Investigation	88
II-7c	Discussion of Results	88
II-8	Greenwood, Clark County, Wisconsin	93
II-8a	General Statement	93
II-8b	Seismic Investigation	93
II-8c	Discussion of Results	93
II-8d	Evaluation of Results	99
II-9	University of Wisconsin, Willows Athletic Field Madison, Wisconsin	100
II-9a	General Statement	100
II-9b	Seismic Investigation	101
II-9c	Discussion of Results	101
II-10	Elkhorn, Wisconsin	105
II-10a	General Statement	105
II-10b	Seismic Investigation	106
II-10c	Discussion of Seismic Results	106
II-10d	Electrical Resistivity Investigation	106
II-10e	Electrical Resistivity Results	107
II-11	Neillsville, Wisconsin	118
II-11a	General Statement	118
II-11b	Seismic Investigation	118
II-11c	Remarks on Test	119
II-12	Marshfield, Wisconsin	119
II-12a	General Statement	119
II-12b	Gravity and Magnetic Study	119

Part III Subsurface Engineering Studies

III-1	General Statement	126
III-2	Lower Paint River Dam Diversion Canal	126
III-2a	General Statement	126
III-2b	Seismic Investigation	127
III-2c	Evaluation of Results	127
III-3	Wisconsin Dells, Wisconsin. Subsurface Materials Investigations	133
III-3a	General Statement	133
III-3b	Seismic Investigation	133
III-3c	Resistivity Studies	134
III-4	Argyle, Wisconsin, Yellowstone River Dam Site	140
III-4a	General Statement	140
III-4b	Seismic Investigation	140
III-4c	Evaluation of Results	141
III-5	Madison, Wisconsin. Second Point Nuclear Accelerator Site	141
III-5a	General Statement	141
III-5b	Seismic Investigation	143
III-6	Madison, Wisconsin. Hydraulics Building University of Wisconsin	148
III-6a	General Statement	148
III-6b	Results of Seismic Measurement	148
III-7	Cave of the Mounds Gravity Study	149
III-7a	General Statement	149

III-7b Gravity Survey	149
III-8 Oshkosh, Wisconsin. Gravel Pit Extension	153
III-8a General Statement	153
III-8b Seismic Results	153
III-9 Milwaukee Harbor. Thickness of the Lake Bottom Sediment	157
III-9a General Statement	157
III-9b Seismic Results	157

Part IV

Mineral Deposit Studies

IV-1 General Statement	162
IV-2 Geophysical Studies over Iron Formation	163
IV-2a General Statement	163
IV-3 Vermillion Range, Minnesota	163
IV-3a General Description	163
IV-3b Gravity Studies	164
IV-3b ₁ Area A	164
IV-3b ₂ Area B	165
IV-3b ₃ Area C	165
IV-3c Conclusion on Vermillion Range Studies	170
IV-4 Gogebic Range, Wisconsin	170
IV-4a General Statement	170
IV-4b Lake Namakagon-Mellen Area	172
IV-4c Upsan Area, Wisconsin. Electro-Magnetic Study	172
IV-4c ₁ General Statement	172
IV-4c ₂ Electro-magnetic Study	172
IV-5 Baraboo Syncline	175
IV-5a General Statement	175
IV-5b Gravity and Magnetic Study	179
IV-5c Magnetic Investigation at the Illinois Mine	179
IV-6 Mesabi Range, Minnesota	180
IV-6a General Statement	180
IV-6b Seismic Studies	180
IV-6b ₁ Area 1	181
IV-6b ₂ Area 2	182
IV-6b ₃ Area 3	185
IV-6b ₄ Area 4	185
IV-6b ₅ Area 5	188
IV-6c Summary on Seismic Investigations	190
IV-6d Electrical Resistivity Studies	190
IV-6d ₁ Area 1	193
IV-6d ₂ Area 3	195
IV-6d ₃ Area 4	197
IV-6d ₄ Area 5	197
IV-6d ₅ Summary of Electrical Measurements	198

IV-7	Electro-magnetic Investigations Along the Boundary of the Keweenaw Volcanic Flows. Northern Wisconsin	203
IV-7a	General Statement	203
IV-7b	Electro-magnetic Study	203
IV-7c	Barabee Test, Ashland County	203
IV-7d	Davis Hill Area, Bayfield County	204
IV-8	Magnetic Survey of Peridotite Body	204
IV-8a	General Statement	204
IV-8b	Magnetic Survey	204
IV-9	Lead-Zinc Deposit Gravity Study. Shullsburg, Wisconsin	207
IV-9a	General Statement	207
IV-9b	Gravity Survey	207
IV-9c	Conclusion	210

Part V

General Geologic Studies

V-1	General Statement	211
V-2	Subsurface Topographic Studies	211
V-2a	Lake Mills, Waterloo, Fond du Lac Areas	211
V-2b	Madison Area	211
V-3	Crypto-Volcanic Structure Investigations	213
V-4	Petrologic Investigations	213
V-5	Structural Studies	214

Part VI

Appendix

on

Geophysical Theory and Method of Reductions

VI-1	Gravity Methods	218
VI-1a	Gravity Theory	218
VI-1b	Observed Gravity	220
VI-1c	Example of Gravity Reductions	220
VI-1d	Residual Anomaly Values	222
VI-1e	Gravity Interpretation	222
VI-2	Magnetics	222
VI-2a	General Statement	222
VI-2b	Magnetic Quantities Measured	224
VI-2c	Example of Magnetic Reduction	225
VI-2d	Analysis of Anomaly Values	226
VI-3	Electrical Resistivity Measurements	227
VI-3a	General Statement	227
VI-3b	Reduction of Resistivity Data	229
VI-3c	Traverse (Constant Depth) Resistivity Measurements	231
VI-3d	Remarks on the Interpretation of Traverse Measurements	235
VI-4	Seismic Methods	236
VI-4a	General Statement	236

VI-4b	Fundamentals of Refraction Method	237
VI-5	Electro-magnetic Method	252
VI-5a	General Statement	252
VI-5b	General Theory	252
VI-5c	Field Procedure	253
VI-6	Conclusion	254

List of Figures

Figure	Page
1 Regional Network of Gravity Stations in Wisconsin and Vicinity	5
2 Bouguer Anomaly Gravity Map. Southeast Wisconsin	6
3 Anomaly Pattern for Different Magnetic Components	8
4 Effect of Observation Level on Anomaly Profile	9
5 Wenner Electrode Configuration for Resistivity Measurements	11
6 Relation of Seismic Paths to Travel-Time Graph	14
7 Location of Geophysical Studies in Wisconsin	16
8 Location of Emmons Blaine Farm	21
9 Seismic Station Layout and Section at Blaine Farm. Lake Mills Area	23
10 Location of Gravity & Magnetic Stations. Lake Mills Area	27
11 Bouguer Isoanomaly Gravity Map. Lake Mills Area	28
12 Isoanomaly Magnetic Map. Lake Mills Area	29
13 Determination of Residual Anomalies, Section A-A. Lake Mills Area	30
14 Comparative Gravity, Magnetic & Geologic Profiles. Lake Mills, Wisconsin	31
15 Bouguer Gravity Anomaly Profiles. Lake Mills Area	32
16 Vertical Magnetic Anomaly Profiles. Lake Mills Area	33
17 Location of Gravity & Magnetic Stations. Antigo, Wisconsin	36
18 Seismic and Electrical Resistivity Profile A-A. Antigo, Wisconsin	41
19 Seismic and Electrical Resistivity Profile B-B. Antigo, Wisconsin	42
20 Comparison of Resistivity Profiles Along Traverse A-A. Antigo, Wisconsin	43
21 Comparative Interpretation Plots, Resistivity Data. Antigo, Wisconsin	44

22	Comparisons of Differences. Resistivity & Seismic Depths	45
23	Comparative Depths. Antigo Area	47
24	Basement Rock Configuration Based on Resistivity Measurements After USGS	48
25	Magnetic Anomaly Map. Antigo, Wisconsin	57
26	Bouguer Gravity Anomaly Map. Antigo, Wisconsin	58
27	Anomaly Sections. Antigo, Wisconsin	59
28	Analysis of Anomalies. Antigo Area	61
29	Seismic Station Map Granite Surface Configuration	66
30	Seismic Profiles. Gresham, Wisconsin	67
31	Seismic Station Map and Configuration of Niagara Dolomite Surface Area I. Campbellsport, Wisconsin	73
32	Seismic Station Map & Configuration of Niagara Dolomite Surface Area II. Campbellsport, Wisconsin	74
33	Seismic Station Map & Configuration of Niagara Dolomite Surface Area III. Campbellsport, Wisconsin	75
34	Seismic Sections. Campbellsport, Wisconsin	76
35	Seismic Sections Area II. Campbellsport, Wisconsin	77
36	Seismic Station Map and Configuration of Sandstone Surface Hudson, Wisconsin	80
37	Seismic Section. Hudson, Wisconsin	81
38	Seismic Station Map and Granite Configuration. Clark County Hospital	85
39	Seismic Sections. Clark County Hospital	86
40	Seismic Station Map. Vesper, Wisconsin	89
41	Seismic Sections. Vesper, Wisconsin	92
42	Seismic Station Map & Location of Sandstone. Greenwood, Wisconsin	97
43	Seismic Profiles. Greenwood, Wisconsin	98

44	Madison Area Willows Project	102
45	Depth to Bed Rock. Madison Area Willows Project	103
46	Seismic Sections. Willows Athletic Field, University of Wisconsin	104
47	Seismic Stations Map & Configuration of Bedrock. Elkhorn, Wisconsin	108
48	Seismic Sections. Elkhorn, Wisconsin	109
49	Seismic Section. Elkhorn, Wisconsin	110
50	Electrical Resistivity Stations & Area of High Resistivity. Elkhorn, Wisconsin	114
51	Resistivity Traverses. Elkhorn, Wisconsin	115
52	Resistivity Traverses. Elkhorn, Wisconsin	116
53	Resistivity Traverses. Elkhorn, Wisconsin	117
54	Neillsville Area	120
55	Location of Gravity & Magnetic Measurements in Relation to Buried Channel Found by USGS Resistivity Study. Marshfield Wisconsin	123
56	a. Marshfield, Wisconsin. Observed Bouguer Anomaly	124
	b. Residual Bouguer Anomaly	
57	Magnetic Anomaly Map Sec. 28 & 33. Marshfield, Wisconsin	125
58	Seismic Station Map & Configuration of Granite Surface. Crystal Falls, Michigan	129
59	Seismic Sections Diversion Canal. Crystal Falls, Michigan	130
60	Seismic Section Diversion Canal. Crystal Falls, Michigan	131
61	Comparison of Seismic & Actual Depths to Bedrock along Center Line of Canal. Crystal Falls, Michigan	132
62	Wisconsin Dells Area Resistivity & Seismic Stations	136
63	Electrode Spacing. Wisconsin Dells	139
64	Seismic Station Location & Profiles. Yellowstone River Dam	142

65	Surface Topography & Depth of Bedrock. Second Point, Lake Mendota	144
66	Travel-Time Graph. Second Point, Lake Mendota	146
67	Seismic Profiles. Second Point, Lake Mendota	147
68	Bouguer Gravity Anomaly Map. Blue Mounds Area, Wisconsin	150
69	Residual Gravity Anomaly Map. Blue Mounds	151
70	Comparison of Observed & Computed Gravity Profiles. Cave of the Mounds	152
71	Seismic Station Map and Depth of Till. Oshkosh, Wisconsin	154
72	Seismic Depth Profiles. Oshkosh, Wisconsin	156
73	Location of Seismic Stations Off Milwaukee Harbor	158
74	Seismic Section of Milwaukee Harbor	160
75	Comparative Magnetic Gravity Profiles. Vermillion District, Minnesota	166
76	Comparative Magnetic & Gravity Profile. Vermillion District, Minnesota	167
77	Comparative Magnetic & Gravity Profile in Vermillion District, Minnesota	168
78	Gravity Profile over Iron Formation in Vermillion District Minnesota	169
79	Comparative Magnetic & Gravity Profiles. Gogebic District Wisconsin	173
80	Comparative Magnetic Dip Needle Profiles Across Gogebic Range	174
81	Comparative Magnetic & Electro-Magnetic Measurements Iron Formation. Upson, Wisconsin	176
82	Comparative Magnetic & Electro-Magnetic Measurements Iron Formation. Upson, Wisconsin	177
83	Gravity & Magnetic Traverses across Baraboo Syncline	178
84	Seismic Station Map and Profile Area 1 Mesabi Range	183
85	Seismic Station Map and Profile Area 2 Mesabi Range	184

86	Seismic Station Map and Profile Area 3 Mesabi Range	186
87	Seismic Station Map & Profile Area 4 Mesabi Range	187
88	Seismic Station Map Profile Area 5 Mesabi Range	189
89	Observed Resistivity Site Ao Area I	191
90	Cumulative Resistivity Plot Site Ao Area I	192
91	Comparative Resistivity Profiles in N-S and E-W Directions Site A-1 Area I	194
92	Correlation Electrical, Seismic, & Drill Data Mesabi Range	196
93	Correlation Electrical, Seismic & Drill Area Mesabi Range	199
94	Depth Coefficients for Converting Electrical Depths to Geologic Depths Mesabi Range, Minnesota	202
95	Comparative Reversed Electro-Magnetic Profiles. Trout Brook Area	205
96	Magnetic Map of Peridotite Plug. Marinette County	206
97	Magnetic Profile Across Periodotite Plug. Marinette County	208
98	Location of Gravity Traverses over Lead-Zinc Ore Body Shullsburg, Wisconsin	209
99	Gravity Anomaly Traverses, Shullsburg, Wisconsin	211
100	Gravity Station Map. Madison & Vicinity	212
101	Gravity Profile. East Side Lake Superior Syncline	215
102	Vertical Component Magnetic Anomaly Map. Baraboo Syncline	216
103	Distribution of Magnetic Stations over Baraboo Syncline	217
104	Current Flow Lines in Homogeneous and Non-homogeneous Media	230
105	2 Empirical Methods of Interpreting Resistivity Data as Compared to Well Log at Site	232
106	Constant Depth Resistivity Traverse across Dolomite Ridge Covered by Glacial Till	233
107	Effect of Local Anomalous Resistivity Area When Running Constant Depth Resistivity Traverse	234

108	Refracted Path of Sound Wave	238
109	Relation of Time Intercept and Critical Distance on Travel-Time Graph	240
110	Illustration of Snell's Law in Three Layer Situation	242
111	Effect of Dip on V_2 Velocity Line of Travel-Time Graph	245
112	Reverse Travel Time Graph Location 3. Blaine Farm, Lake Mills, Wisconsin	246
113	Seismic Travel Paths in Multiple Dipping Layers	247
114	Refraction Travel-Time Graphs over Faults	251
115	Electro-Magnetic Indications of a Buried Sheet Conductor	255

List of Tables

Table	Page
1 Seismic Velocities and Depths. Blaine Farm, Lake Mills, Wisconsin	22
2 Comparison of Drill Data and Seismic Data. Blaine Farm, Lake Mills, Wisconsin	24
3 Table of Gravity and Magnetic Anomaly Values. Lake Mills, Wisconsin	26
4 Seismic Data. Antigo, Wisconsin. Traverse A-A	38
5 Seismic Data. Antigo, Wisconsin. Traverse B-B	39
6 Seismic Data. Antigo Area, Wisconsin	40
7 Comparative Interpretations of Resistivity Data and Seismic Data. Antigo Area	43
8 Electrode Spacings at Which Layers are Indicated on Accumulative Basis of Interpretation. Antigo Area	50
9 Table of Magnetic and Gravity Anomaly Values. Antigo, Wisconsin	54
10 Seismic Data. Gresham, Wisconsin	65
11 Seismic Data at Campbellsport, Wisconsin. Area I	70
12 Seismic Data at Campbellsport, Wisconsin. Area II	71
13 Seismic Data at Campbellsport, Wisconsin. Area III	72
14 Seismic Data at Campbellsport, Wisconsin. Area IV	72
15 Seismic Values. Hudson, Wisconsin	79
16 Seismic Data for Clark County Hospital, Wisconsin	84
17 Seismic Data. Vesper, Wisconsin	90
18 Seismic Data. Greenwood, Clark County, Wisconsin	95
19 Seismic Stations with Alternate Values	96
20 Comparison of Well and Seismic Depths. Greenwood, Clark County, Wisconsin	100

21	Seismic Data. Willows Athletic Field, University of Wisconsin	105
22	Seismic Data. Elkhorn, Wisconsin	107
23	Resistivity Values, Elkhorn, Wisconsin	111
24	Seismic Data. Neillsville, Wisconsin	118
25	Gravity and Magnetic Anomaly Values. Marshfield, Wisconsin	122
26	Seismic Data. Lower Paint River Dam Diversion Canal Crystal Falls, Michigan	128
27	a. Seismic Results in Test Areas. Wisconsin Dells, Wisconsin b. Observations near Burke, Wisconsin	135
28	Seismic Values. Wisconsin Dells Area	137
29	Resistivity Values. Wisconsin Dells, Wisconsin	138
30	Seismic Data at Yellowstone River Dam Site	140
31	Seismic Data at Second Point	143
32	Alternate Interpretation of the Seismic Data. Second Point	145
33	Seismic Results. Hydraulics Laboratory	148
34	Seismic Results. Oshkosh, Wisconsin	155
35	Seismic Results. Milwaukee Harbor	159
36	Density Values. Vermillion Range	164
37	Divisions of Ironwood Formation	171
38	Characteristic Velocity Values. Mesabi Range, Minnesota	180
39	Seismic Results. Area 1	181
40	Seismic Results. Area 2	182
41	Seismic Results. Area 3	185
42	Seismic Results. Area 4	188
43	Seismic Results. Area 5	188

44	Electrical Resistivity Values, Area 1	193
45	Electrical Resistivity Results, Area 3	195
46	Electrical Resistivity Results, Area 4	197
47	Electrical Resistivity Results, Area 5	197
48	Table of Electrical Resistivity Coefficients. Mesabi Range, Minnesota	200

Part I

Introduction

I-1 - General Statement

At the outset it should be stated that geophysics should not be confused with the art of "water witching", "dowsing" or "divining". A water diviner depends entirely upon his personal and presumably uncontrollable reaction to the presence of water; geophysical measurements are only influenced by water through its effect upon earth materials. In contrast to a water diviner, who apparently reacts only to water in highly permeable media, a geophysicist cannot differentiate by his measurements between water that is locked up in an impermeable clay from the same amount of water free to flow in a permeable sand. As geophysical equipment may cost several thousand dollars in contrast to the nominal cost of a forked willow twig, and as the labor and man hours of a single geophysical measurement will exceed that required by a water diviner by a factor of over a hundred to one, it is quite obvious that the laws of economics definitely do not favor the use of geophysics on a competitive basis with divining. The only factor in favor of the use of geophysics on subsurface problems is that experience has shown that of the two methods geophysics has proved the more reliable. Certainly, as regards consistency in results, a better case can be made for geophysics than for divining. An example in point is the test conducted in Milwaukee in which a water diviner of some reputation failed in a blindfold test to recognize the fact that he was over abundant water when standing on a bridge over the Milwaukee River.

However, it is not our purpose to compare the relative merits of geophysics and divining so much as to point out that the two are not even distantly related. One depends for its success upon measurable changes in physical quantities, and the other upon psychic phenomena and involuntary muscular reactions which if real are not understood.

I-2 - Types of Geophysical Measurements

Geophysical measurements employed in studying subsurface conditions can be divided into seven basic types. These are:

- Gravity measurements
- Magnetic measurements
- Electrical measurements
- Electro-magnetic measurements
- Seismic measurements
- Thermal measurements
- Radioactive measurements

All depend for their successful utilization upon there being a contrast in physical properties either associated directly with the materials being studied, or indirectly related to them through some associated geologic factor such as the accumulation of oil and gas in traps formed by the deformation of rock strata. To utilize gravity measurements there must be a density contrast. In the case of magnetics there must be a marked change in the percentage of the naturally magnetic mineral, magnetite. Successful use of electrical and electro-magnetic measurements depends upon a change in electrical conductivity and resistance. Seismic measurements can only be used where there are changes in the velocity of propagation of sound.

It is obvious that a certain amount of general geologic knowledge concerning the area, as well as specific knowledge as to the nature of the local problem, is necessary before an intelligent choice of geophysical methods can be made. For example, local problems in groundwater investigations might be ; (a) locating an underground buried ridge which acts as a subsurface dam; (b) defining the boundary of salt water encroachment in an aquifer; (c) locating a buried former stream valley having alluvial sands which might serve as aquifers; (d) locating a buried sand and gravel lens in dense impermeable clay; (e) defining the buried boundary of a large sand area; (f) finding the depth at which a permeable sand occurs; (g) tracing the flow of possibly polluted water from sink holes to a producing well. Even in a completed well there may be a problem of determining the depths at which water is entering and where water that is polluted or contaminated with mineral matter needs to be sealed off.

The problems associated with the use and development of groundwater supplies are therefore numerous and not merely confined to locating water as such, and the choice of a suitable geophysical method of study will vary accordingly. Very little is to be gained by trying geophysical methods at random. There is enough of a gambling element in such investigations without increasing the odds against success. If the right method can be picked the first time, it is much better from all standpoints. If the first methods chosen do not yield positive results, there is little to be gained by trying methods which have been evaluated as having small chance of success. Failure on some problems is inevitable. It may be caused by some combination of geologic factors that prevent positive geophysical results or, in the case of water, because of inadequate quantities or contamination by mineral matter which render it unusable. Since there is no way of anticipating such results, all subsurface studies will always incorporate a large degree of uncertainty, but in most areas the odds are that geophysical measurements will be helpful. Even if the results of a geophysical survey

cannot be correctly interpreted without auxiliary bore hole data, the savings over the cost required for a strictly drilling program are usually appreciable. The ideal method of making an investigation is, (a) to carry out a geophysical study and place the best possible geological interpretation on it; (b) to conduct exploratory drilling to test the interpretation; (c) to reevaluate the significance of the geophysical results in the light of the test drilling data.

I-3 - General Description of Geophysical Measurements

I-3a Gravity Measurements:

Gravity measurements are usually carried out with a gravimeter. This instrument consists of a very delicate, calibrated spring balance to which is attached a small weight. The length of the spring varies with elevation, latitude, and rock type as the instrument is moved from one place to another, and this change in length of the spring can be translated into terms of change in gravitational attraction. Changes as small as one ten millionth of the normal pull of gravity can be accurately determined. The instrument is most useful for outlining horizontal changes in rock type involving changes in density. In order to separate that part of the observed changes in gravity attributable to change in latitude and elevation from those due to geologic causes, the observed gravity values must be corrected for the theoretical changes in gravity as calculated from the observed changes in elevation and latitude. In areas where there is considerable relief (hills and valleys) the gravitational effect of these topographic irregularities must also be allowed for. The residual left after making the theoretical corrections for change in latitude, elevation, the mass of rocks beneath the observation point above sea level, and the topography is called the gravity anomaly. The anomaly represents the gravitational effect of the subsurface geology. An illustrative example in the determination of a gravity anomaly is given in the Appendix.

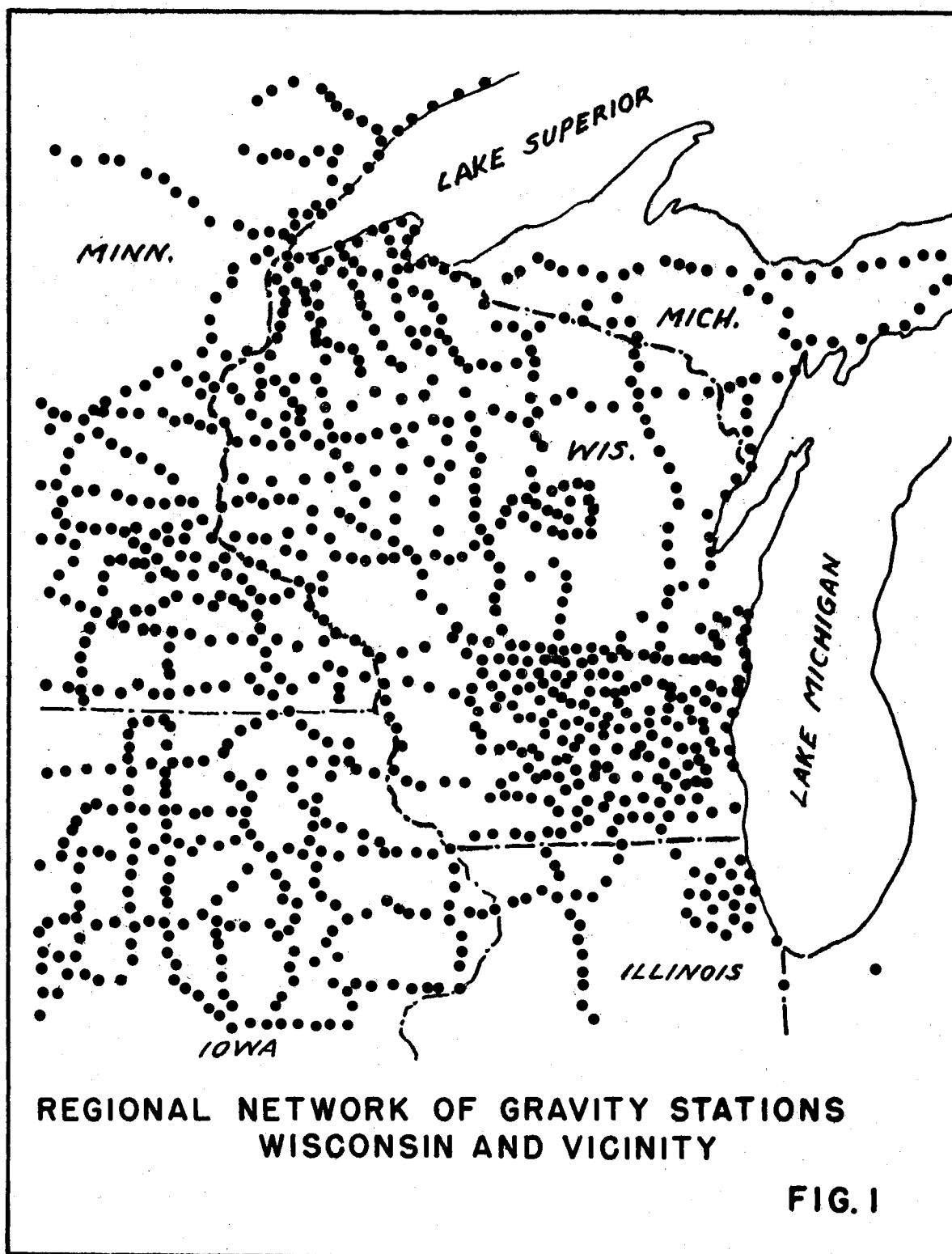
The successful use of gravity in geologic studies depends first on there being an anomaly, and second upon the correct geologic interpretation of its significance. The last usually involves quantitative calculations based upon different, though probable, geological assumptions to see which has a gravitational effect approximating that of the anomaly. Even when an exact fit between the computed effect of a geologic model and the anomaly is obtained, there is no guarantee that the model assumed is the correct one. Another mass distribution with a different density contrast originating from a different depth might satisfy the anomaly equally well. So even though gravity measurements indicate very accurately places where there are irregularities in the horizontal mass distribution, they do not permit an accurate evaluation of the depth at which these mass irregularities take place.

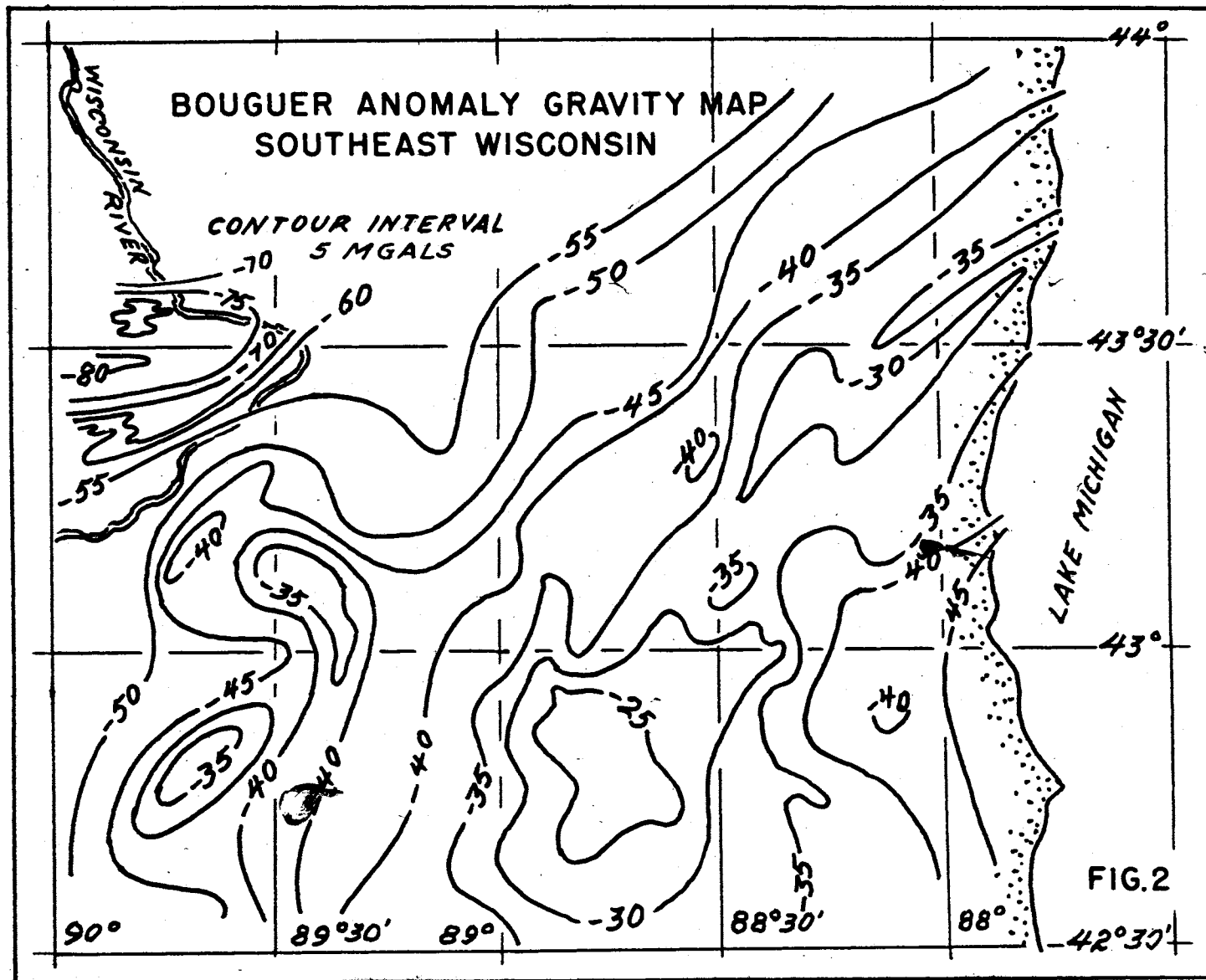
As the method is very rapid (only five minutes are required for an observation), and therefore inexpensive from an operational standpoint, gravity measurements are frequently used as a reconnaissance method in outlining areas where other more expensive and precise methods are to be used. In Wisconsin, the University is building up a regional reconnaissance gravity anomaly map of the entire state so that this information on a broad basis will be available for all types of studies, whether related to general geology, ground-water or mineral deposits. This map is based upon a network of gravity observations at about ten mile intervals following the principle roads covering the state. The locations at which observations have been made to date in developing this regional gravity map of the state and adjoining territory are shown in Fig. 1. How gravity anomalies reveal the structural grain of an area is shown by the Bouguer Anomaly map of Southeastern Wisconsin, Fig. 2.

I-3b Magnetic Methods of Measurement:

In contrast to gravity studies which usually involve only the change in the intensity of the vertical component of the earth's gravitational field, magnetic studies may involve measurements of the total intensity of the earth's magnetic field, its vertical and horizontal components, the direction of the earth's field relative to true North, or its inclination relative to the earth's surface.

The measurements themselves therefore may be carried out with instruments as simple as a compass or a dip needle or as complex as the total intensity continuous recording magnetometer which is towed through the air from an aeroplane. The choice of instruments and the associated field of measurement studied will depend upon (a) the sensitivity required to map the variations in magnetic field intensity associated with the problem being studied, (b) the accessibility of the area, and (c) the magnetic latitude of the area. In a densely wooded or swamp area, the air-borne magnetometer has obvious advantages over instruments that must be read at ground level. At very high latitudes near to the magnetic poles significant measurements may only be possible through the use of a sun compass and the measurement recorded would be the difference between the direction of magnetic North and true North. As all of the magnetic components are intimately related to each other, any factor producing a distortion in one will produce a distortion in all. The distortion may be related to the local geology, a mineral deposit, a steel structure, pipe line, well casing, electrical ground current or an ionospheric disturbance. Such distortions are referred to as magnetic anomalies. As with gravity, it is the anomaly values that must be determined and mapped. These anomalies are then analyzed as to their cause on the basis of probable geologic models and their computed magnetic effects.



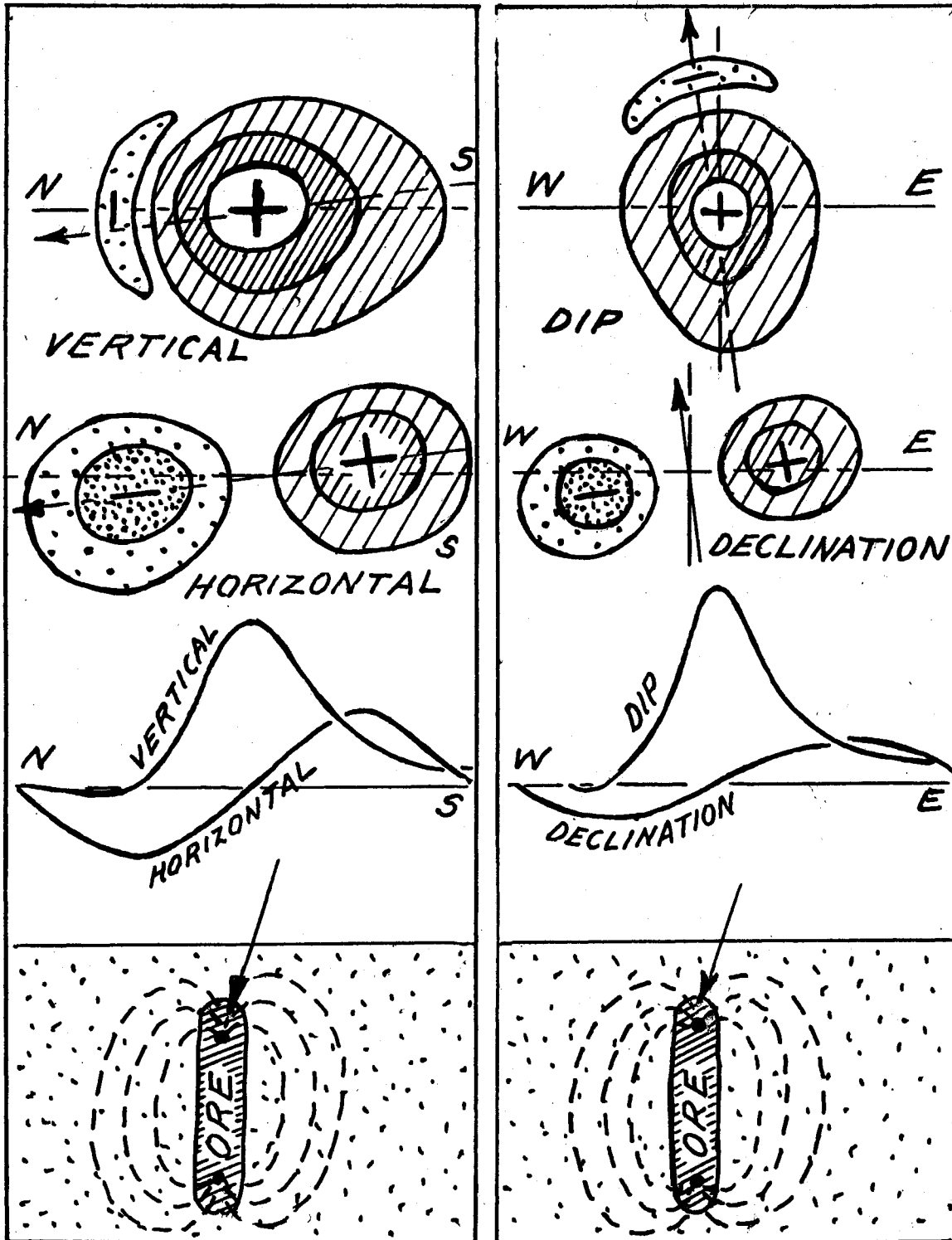


In Fig. 3 is shown a schematic representation of the anomaly patterns that would be produced by the same disturbing body in each of the component elements of magnetic measurement in mid-latitudes in the Northern Hemisphere. The same disturbing body near the Equator would produce markedly different patterns in the component measurements because of the change in intensity and direction of inclination of the earth's field. The vertical component would have very small values, and the horizontal component very large values, while the angle of inclination would be essentially zero. These effects related to change in latitude will not be considered further here since we are more concerned with measurements in Wisconsin where the vertical component is dominant. Another change in pattern that should be mentioned is obtained in airborne magnetic work with change in altitude. As measurements are made at progressively higher levels of flight, the power to resolve individual anomalies that are observable at low flight levels or on the ground becomes progressively less, because the effects of adjacent anomaly areas will overlap and merge. This is illustrated schematically in Fig. 4. In order to keep this effect to a minimum, most airborne magnetic surveys conducted for exploration purposes are carried out at an elevation of about 1000 feet.

The instruments used for magnetic exploration measurements are as follows:

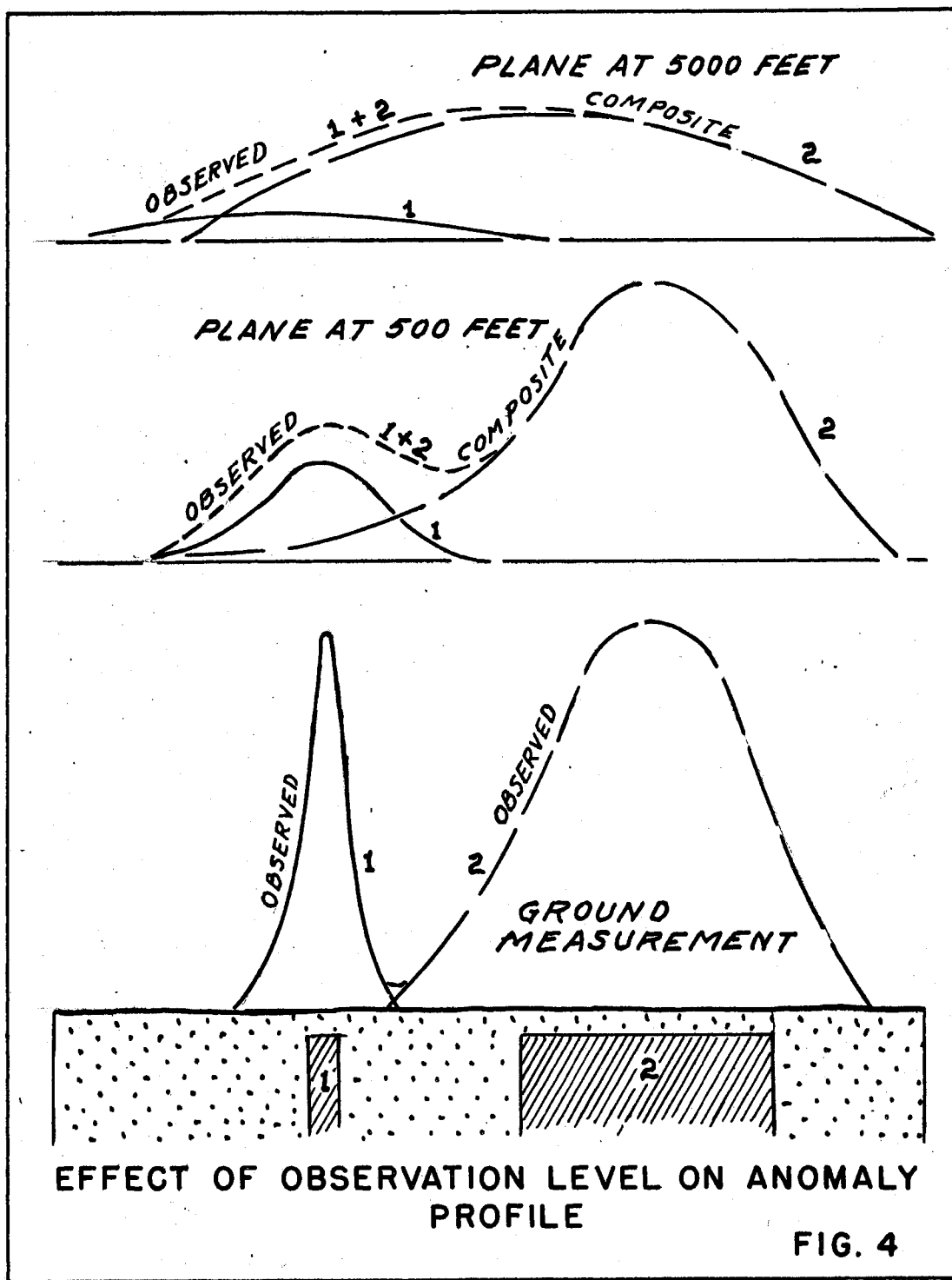
Total magnetic intensityHotchkiss superdip magnetometer
	Airborne magnetometer
Vertical componentVertical component variometer
Horizontal componentHorizontal component variometer
Inclination of fieldDip needle
Direction of fieldCompass and sun compass

A considerable amount of dip needle work was done by the Wisconsin Geological Survey during the early days of iron exploration in the northern part of the state. Little other magnetic work was done until the University started a regional reconnaissance network of magnetic bases as a companion study to the gravity study mentioned in the previous section. This study, involving observations at approximately ten mile intervals on all the main roads in the state, has been made using a vertical component magnetometer. This instrument, which measures only the vertical component of the earth's magnetic field, has sufficient sensitivity to map variations of one part in ten thousand in the strength of the earth's magnetic field. It is the standard instrument used in carrying out most ground surveys as it is readily portable and can be read in less than five minutes.



ANOMALY PATTERN FOR DIFFERENT MAGNETIC COMPONENTS

FIG. 3



Mechanically, the instrument is essentially a delicate balance composed of two magnetized steel blades mounted on a central aluminum block. This unit is balanced horizontally on a central quartz or sapphire knife edge which rests on a flat surface of the same material. Tilting of the balance in response to changes in magnetic field strength is observed through a telescope, and the observed angle of tilt is converted to give the equivalent change in magnetic field.

Once the changes in magnetic field are determined, they must be reduced further to yield anomalies. This is done by subtracting from the observed values the corrections for temperature, changes in the earth's field during the time of the survey and changes in magnetic latitude. An example of a magnetic anomaly reduction is given in the Appendix.

Because of the very large magnetic effects produced by relatively small percentages of the mineral magnetite, which is a common accessory mineral in most rocks, magnetic measurements can frequently be used to map horizontal variations in rock types beneath the surface and for locating subsurface ridges composed of crystalline rock as well as economic mineral deposits. As with gravity data, it is difficult to evaluate the depth at which a magnetic disturbance originates.

In a study of the buried ridges in the Waterloo and Fond du Lac regions of Wisconsin, magnetic studies are being carried out together with gravity measurements as a method for outlining the location of the ridges.

I-3c Electrical Measurements:

Although there are a variety of methods for making electrical measurements, the method most commonly used is based upon determining the apparent resistivity of the rocks. This is done by measuring the change in electrical potential between one pair of electrodes when a current is introduced into the ground through another pair of electrodes. With this type of measurement, the electrodes are usually laid out in a line with the two current electrodes at the end positions. The intervening distance is divided into equal thirds and the potential electrodes located at the central division points. With this arrangement the depth of effective current penetration is assumed to be approximately equal to the distance between the individual electrodes; that is, one third the distance between the two end current electrodes. See the schematic diagram in Fig. 5.

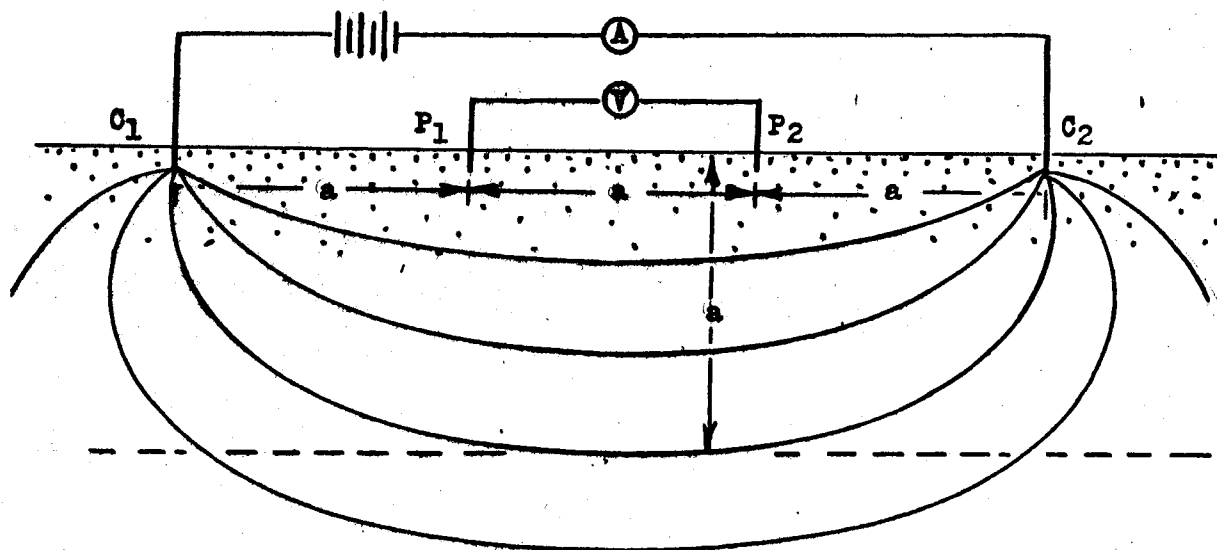


Fig. 5

C_1 and C_2 = Current electrodes
 P_1 and P_2 = Potential electrodes
 \textcircled{A} = ammeter \textcircled{V} = Potentiometer
 a = electrode spacing, and assumed effective depth of current penetration

This system of measurement, whereby the resistivity is determined mathematically from the measured current and potential difference at the central pair of electrodes, P_1 and P_2 , is used in two ways. (1) To determine changes in resistivity with depth by progressively increasing the electrode spacing. (2) To determine horizontal changes in resistivity to a given depth by maintaining the electrode spacing at a constant value and moving the entire spread of equipment across country in increments equal to the spacing between two adjacent electrodes. Results are not always reproducible because of variations in soil moisture and also because at times there are strong natural ground currents. However, despite the limitations, the method has proved applicable for the study of many problems.

While the determination of resistivity values is a relatively simple operation, the results are frequently difficult to interpret. Theoretical relationships are difficult to apply except for very simple geologic situations, and empirical methods of interpretation must be varied constantly with changes in area. Opinion varies strongly among those using such measurements as to the best method of interpretation. From an operating standpoint, the most generally reliable method appears to be an empirical one whereby test measurements conducted alongside a well with a known log are used to establish an interpretation standard for that particular local area.

The successful application of electrical resistivity measurements for determining the depth to geologic horizons constituting electrical discontinuities has varied greatly in Wisconsin and, as a result, the method has only been used to a limited extent. However on problems involving the determination of horizontal changes in resistivity such as locating a sand lens in glacial till or the boundary between outwash sands and glacial till, the electrical method has proved to be more effective than any of the other geophysical methods. Such measurements have been conducted in several areas in the state as at Elkhorn where the principal aquifer supplying the town with water is a lens of sand and gravel in otherwise relatively impervious glacial till. A more complete discussion of the resistivity method and the theory involved is given in the Appendix.

I-3d Seismic Measurements:

Seismic measurements which consist of firing a small charge of explosive, and recording the time it takes for the shock wave to reach a series of detectors, constitute the most reliable of the geophysical measurements for determining depth. Although these measurements can be subdivided into reflection and refraction measurements, only the latter will be considered here since there has been no known reflection work in Wisconsin to date.

At the outset, it should be pointed out that the refraction method will only give reliable results so long as the velocity of seismic (shock) wave propagation increases with depth. If there are reversals in velocity gradient, as sometimes happens, then the depths determined may be considerably in error. Fortunately areas where this occurs are not the rule.

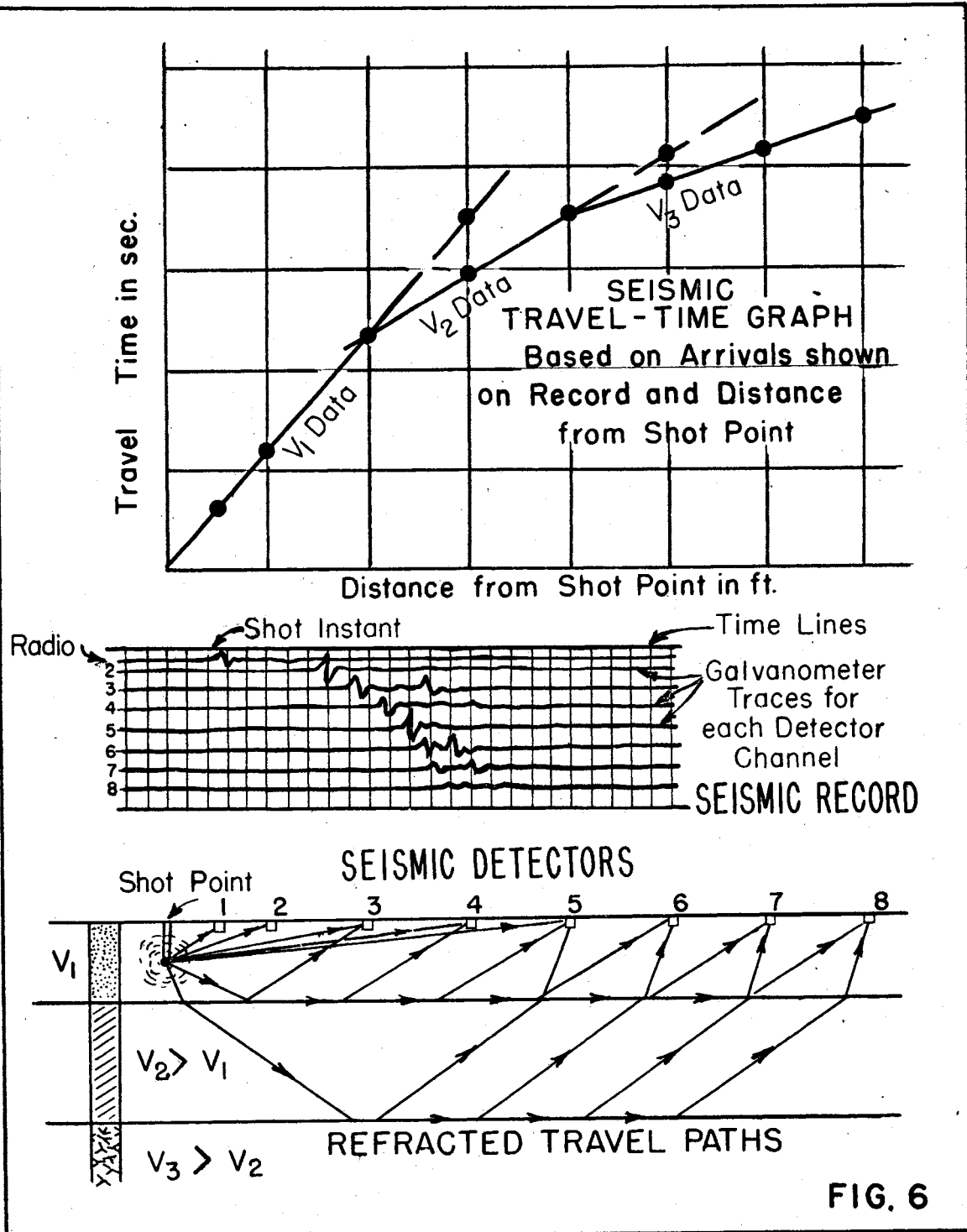
The basis of the refraction method is to generate a sound impulse, usually with a small charge of explosive, in a hole varying from a few feet to twenty feet or more beneath the surface, and to record the arrival of the seismic wave generated at varying distances. The arrival of the wave is picked up by a detector which is essentially a miniature vertical component seismograph as is used in studying earthquakes. The signal is then passed through an electronic amplifier and fed to a galvanometer which is deflected by the arriving signal. This deflection of the galvanometer is recorded photographically by the reflection of a light beam from a mirror on the galvanometer to a moving strip of photographic paper. On this same film strip are also recorded time lines at .01 second intervals and a galvanometer trace connected to a radio for indicating the instant the explosive was fired. From this photographic record the travel time of the explosive signal through the ground to each of the seismic detectors can be accurately determined. A graph is then constructed in which travel time is plotted as a function of distance to each detector. From the travel time data plot lines are defined whose number defines the number of seismic discontinuities (layers of rock) present, and whose slopes are the reciprocal of the velocity of seismic propagation in each layer. These velocity values serve to identify the kinds of rock present. The data are then used, along with optical theory for refracted wave paths through different media, to determine the depths to each of the seismic discontinuities. A schematic representation of the above is shown in Fig. 6.

A more complete description of seismic theory and an example of a seismic depth computation are given in the Appendix. In general an accuracy on depths between 5 and 10 % is possible, and the more nearly the geology approaches the physical model visualized, the more accurate the results are. However, where the actual conditions do not approximate the physical situation visualized in the theory, the results may be considerably in error. Some knowledge of the subsurface geology therefore must be had in determining whether the seismic method can be successfully applied. In areas where there is little or no advance geologic information, it is generally worth-while to gamble on the method being applicable since conditions generally favor its application.

In Wisconsin the seismic method has been the geophysical method most successfully used in connection with water supply and engineering problems. Twenty such studies have been made at different locations throughout the state.

I-3e Electro-magnetic Methods

Electro-magnetic methods involve the following: (1) The creation of a primary artificial electro-magnetic field at the surface of the ground.



(2) The excitation of a secondary electro-magnetic field resulting from a flow of electric current induced in a subsurface conductor as a result of the primary exciting field. (3) The detection of a distortional change in direction, intensity, or quality of the primary field produced by the secondary induced field. This method is applicable primarily to the search of the metallic sulfide ores, and to the more mundane search for lost buried pipe lines. The primary exciting field is produced by means of an alternating current in a coil of wire. The distortion produced by a subsurface conductor is detected by means of a second (search) coil with suitable indicating instruments. The method is complicated by the fact that the search coil receives radiations from all conductors in the area as well as from the primary exciting coil. The resultant recorded is always a vector quality and by plotting these vectors an indication of the location of a buried conductor can be determined.

Although several investigations of this type have been carried out in Wisconsin only one such study has been made during the period concerned by this report. An example of a reduction of field observations is given in the Appendix.

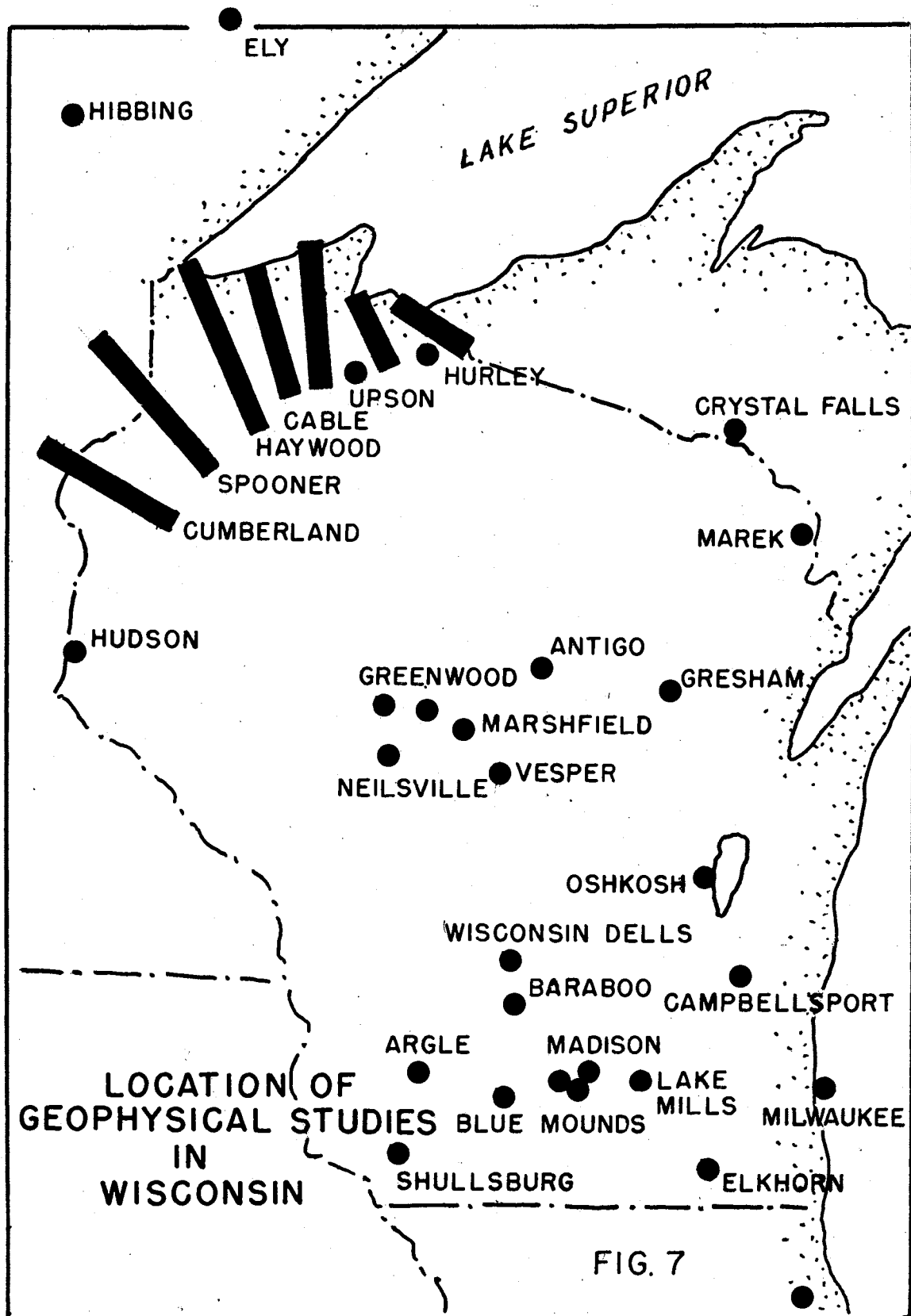
I-4 - Work Covered in Present Report

Although Wisconsin pioneered in the use of geophysical measurements both as applied to mineral exploration problems and to engineering problems, the interest shown in the early investigations was not maintained for various reasons. Chief of these was probably the moving away of the principal investigators. Following the end of World War II, however, interest was revived by the work of Professor Louis Slichter at the University and several investigations were made under his direction. As results are not available for most of Professor Slichter's studies, the present report is limited to the work carried out under the writer, who succeeded Professor Slichter as Professor of Geophysics in 1948.

In presenting the results, the studies have been divided on the basis of ground water supply investigations, mineral exploration studies, engineering subsurface studies, and scientific geological investigations. The general locations in which geophysical studies have been made are shown in Fig. 7.

I-5 - Equipment Used

All of the seismic measurements reported except those made in Lake Michigan were carried out with Century, 12 channel portable refraction equipment using geophones peaked at a frequency of 12 cycles per second. Although this equipment was designed for shallow studies applicable to engineering investigations, it has been used successfully in working to depths of 2000 feet in the course of the investigations carried out by the University.



In making the seismic studies in Lake Michigan, the equipment was a modified refraction-reflection instrument built by the Humble Oil and Refining Co. which was loaned along with underwater, gimbal mounted geophones for this investigation.

The magnetic investigations were made with a temperature compensated, Askania, Schmidt type, vertical component variometer having a sensitivity of about 33 gammas per scale division.

The gravity measurements were made chiefly with Worden temperature compensated gravimeters having sensitivity values ranging from .01 to 0.1 mgals per scale unit. Other instruments used on the gravity studies were a North American constant temperature gravimeter, a Humble Oil Co. compound "X" type gravimeter, and a Humble Oil Co. "Z" type gravimeter. All of the measurements made in connection with the studies of mineral deposits where extreme portability was required were made with the Worden meters which weigh only 5 pounds and hence are readily adaptable to work in rough country.

In establishing the absolute gravity value at the University of Wisconsin, which was used as a base for all the gravity studies, relative gravity measurements were made to the absolute gravity base at the Bureau of Standards and the national gravity base of the U.S. Coast and Geodetic Survey in Washington. In making these measurements, the quartz pendulums of the Gulf Research and Development Co. were used as well as Geodetic type Worden gravimeters.

The electrical measurements were carried out using standard four electrode resistivity equipment built by the Geophysical Instrument Co.

The electro-magnetic measurements were made with equipment designed and built by the Palmerton Laboratory of the New Jersey Zinc Co.

Unless otherwise specified, the above equipment was that used in each of the series of measurements reported.

I-6 - Acknowledgements

The investigations reported are primarily the work of the group of students in geophysics at the University of Wisconsin. These men carried out the field observations, made the necessary computations for reducing the results, analyzed the results as to their geological significance, and prepared the reports covering the investigations. Some of the work was done on a remunerative basis, and some was done with no other reward than the satisfaction of having contributed to the solution of a scientific problem. Some of the work was done under pleasant working conditions; some was done during the black fly season in swamps, and some was done with temperatures as low as 40° below zero.

As nearly all of the projects required the coordinated efforts of several men, it is not feasible to make individual acknowledgements of the part each man played on each project. On one project a man might serve as chief of a party, whereas on another project the same man might serve as a "roustabout". No one could wish to be associated with a finer group of men than the following:

Graduate Students

Virgil Mann
Norman Harding
William Bonini
John Rose
Robert Meyer
Rodger Chapman
Roger Pemberton
Ned Ostenso
Wendel Weart
Budd Adams

William Black
Edward Thiel
William Hinze
John Sumner
Jack Richgels
Anthony Amante
Gaither Randall
Richard Haubrick
John Belshe

Under-graduates

William Laing
Richard Randolph
Lawrence Machesky
Jogi Tomei
Jack Mack
Donald Plouff

Tom Larsen
Robert Bruce
Ronald Ulrich
Wayne Zwick
Richard Hecht
John Chyle

Part II

Ground Water Investigations

II-1 - Lake Mills, Wisconsin
University of Wisconsin Emmons Blaine Farm

II-1a General Statement

The Emmons Blaine Farm is a dairy research farm of the University of Wisconsin located near Lake Mills and lies over the crest of a subsurface crystalline rock ridge covered by Paleozoic sediments and glacial till. The ridge itself is about 70 feet beneath the surface at the farm and outcrops about 3 miles to the north where it is seen to be composed of quartzite. See Fig. 8. Available well log data indicate that it rises at least 1,000 feet above the surrounding crystalline rock floor and must have constituted an island in early Paleozoic time when the sediments, now constituting the aquifers of the region, were being deposited. The existing farm well was 80 feet deep and terminated in what the driller had termed "granite". The material between the surface and the "granite" was not classified.

The problem here was to see if there was any local geologic situation that could be exploited to get more water; in particular to see if there was any buried valley cutting the crystalline rock surface or if Paleozoic sandstones were present beneath the till in the farm area. It was felt that a buried valley might have sand or gravel associated with it which would constitute a local aquifer or, lacking such material, the valley would at least give a local thickening of the overlying material and define the area having maximum reservoir capacity. If sandstones were present they might constitute a sheet aquifer that could be developed to obtain a higher yield of water.

As depth and recognition of rock types were the primary quantities to be determined, the seismic refraction method was chosen as the principal method of study.

II-1b Seismic Investigations

The reverse refraction shooting technique was employed as described in the Appendix in carrying out the seismic investigation. This method permits the true velocity values to be determined which are necessary for the identification of the rock types present, and the establishment of the slope of the subsurface geologic horizons and their depths.

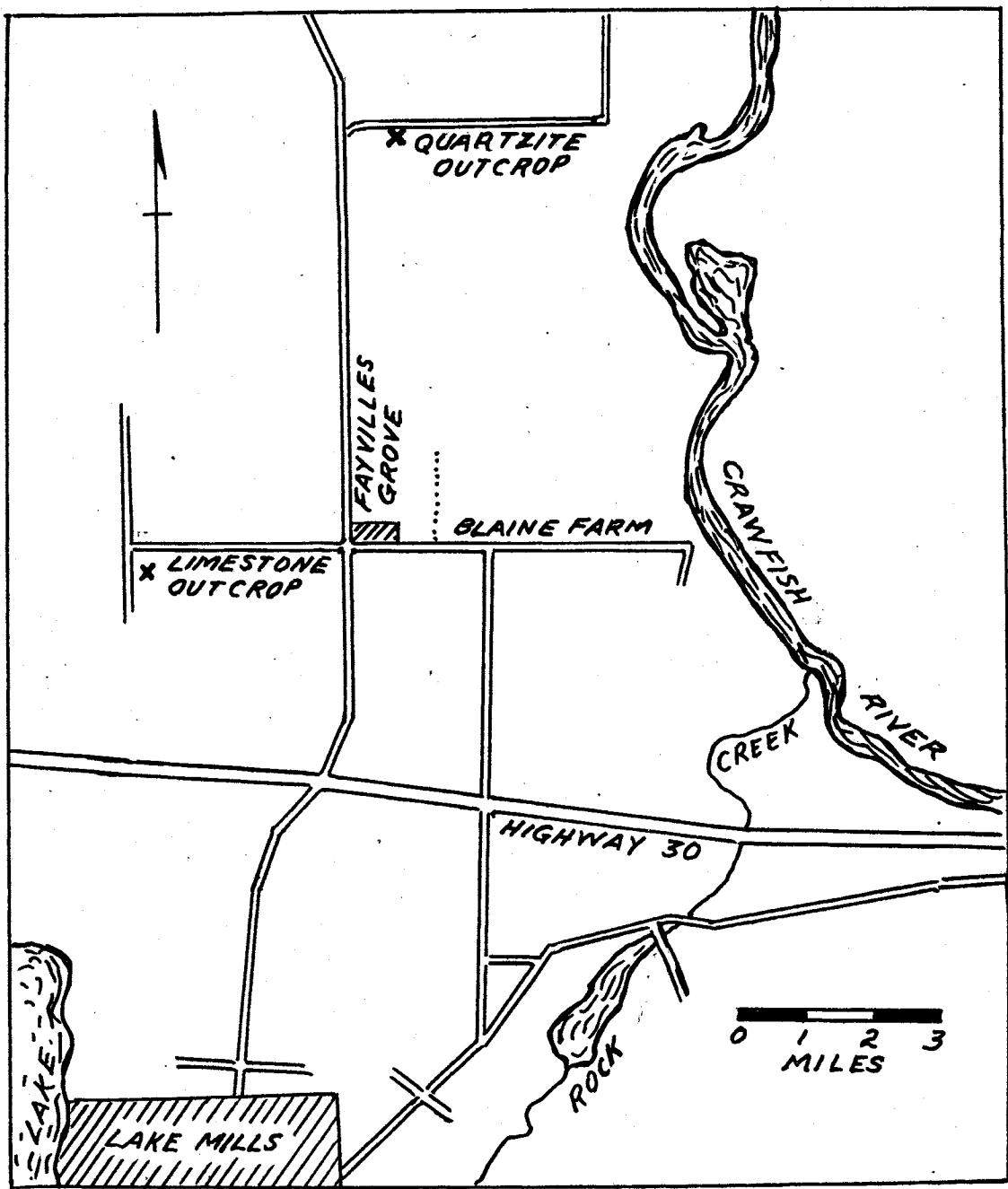
In Fig. 9, a map of the farm area is shown with the positions of the shot points at which depth measurements were made. Three layers were found to be present. The top layer (V_1) had a velocity of about 3500 ft./sec. and was identified as unsaturated glacial till. The second layer (V_2) had a velocity varying from 7100 ft./sec. to 12,340 ft./sec. and was identified as probably sandstone or a sandy limestone. The third layer (V_3) had a velocity varying from 14,240 ft./sec. to 15,000 ft./sec. and was identified as crystalline basement rock.

In Table 1 the velocity values and depths determined for each layer at each shot point are given. Fig. 9, a vertical cross-section based on the seismic data and subsequent well and test hole data, shows the subsurface geology.

From an inspection of the sectional profile in Fig. 9, it is seen that there is no pronounced subsurface bedrock valley within the limits of the farm and that the location of the present well is at about the optimum location as regards thickness of material overlying the impervious basement of crystalline rocks. As the velocities in the rock beneath the till, identified as probably sandstone or limestone, are appreciably higher west of the entrance road to the farm than to the east of this location, it was postulated that there is a change in lithology at this point with limestone to the West and sandstone to the East. It was also noted that at locations 2N and 7E that there was very pronounced time delay when shooting towards these locations which was not apparent on the records when shooting in the opposite directions at these sites. This was interpreted as indicating a greater thickness of surface till material in this area, and on the basis of these data a pocket or channel in the pre-glacial surface was inferred.

II-1c Evaluation of Seismic Results from Drilling

Upon completion of the geophysical work, two shallow holes were drilled at sites 3W and 3E to ascertain the nature of the material having a velocity of 7095 ft./sec. which appeared to be within 18 feet of the surface at these sites. In each case, sandstone was encountered at depths agreeing within 2 feet of that indicated by the seismic measurements. Two years after the completion of the survey, a new well was drilled very close to the site of the original farm well which lay between seismic locations 2N and 5E. The log of this new well checks very closely with the seismic measurements as is indicated by the comparisons given in Table 2.



LOCATION OF EMMONS BLAINE FARM

FIG.8

Table 1

Seismic Velocities and Depths
Blaine Farm, Lake Mills, Wisconsin

Station	Apparent Velocities(ft./sec.)			Depth from Surface	
	V ₁	V ₂	V ₃	V ₂	V ₃
1N	3500	11530	16020	17	52
1S	3500	10180	14270	6	83
2N	3500	11560	-----	11	—
2S	3500	11850	-----	15	—
3E	3500	7150	13900	14	30
3W	3500	7040	15580	18	51
4E	3500	7970	14500	18	62
4W	3500	7450	12390	14	72
5E	4490	11770	-----	12	—
5W	4490	12990	-----	27	—
6W	1920	11000	13470	15	76
7E	2640	9530	-----	11	—
7W	2640	9530	14290	12	105
8	gneiss outcrop		22000		
9	limestone outcrop		10500		

V₁ = Velocity of surface material (glacial till).

V₂ = Velocity of second layer material (sandstone = 7500 ft./sec.),
(limestone = 11,000 ft./sec.)

V₃ = Velocity of third layer crystalline complex, average true
velocity = 13,600 ft./sec.

SEISMIC STATION LAYOUT AND SECTION AT BLAINE FARM LAKE MILLS AREA

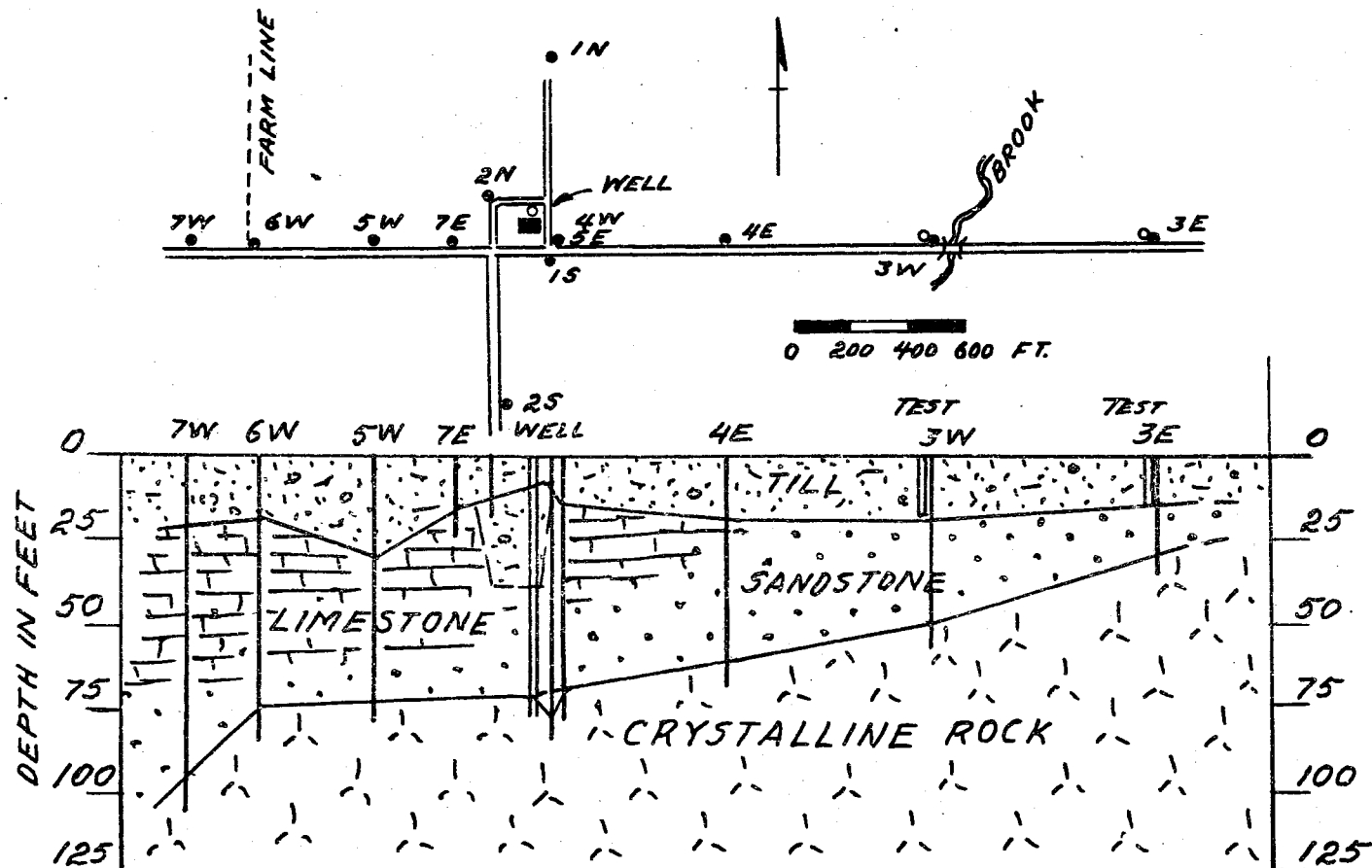


FIG. 9

Table 2

Comparison of Drill Data and Seismic Data
Blaine Farm, Lake Mills, Wisconsin

Driller's Log

0 -	15 feet	-----	glacial till
15 -	30 feet	-----	coarse gravel and silt
30 -	55 feet	-----	sandy dolomitic limestone
55 -	70 feet	-----	sandstone and silt stone
70 -	116 feet	-----	crystalline quartzite

Seismic Section

Based on Sites 2N, 5E, and 4W

0 -	13 feet	-----	till (V ₁)
13 -	< 30 feet	-----	channel fill (V ₁)
< 30 -	72 feet	-----	sandstone and limestone (V ₂)
> 72 feet		-----	crystalline rock (V ₃)

This log, therefore verified the following: (1) the existence of the channel incised in the pre-glacial surface that was indicated at locations 2N and 7E by the seismic data and showed it to be 15 feet deep and filled with gravel. (2) the presence of both sandstone and limestone beneath the till and above the basement rock as postulated on the basis of seismic velocities, and (3) the depth of till and the depth to the basement crystalline rock surface. For both depths the accuracy was of the order of 2 feet.

In drawing the geologic section shown in Fig. 9, the data for this new well have been added to show the degree of agreement between this later geologic information and the earlier seismic data.

II-1d Magnetic and Gravity Study of Lake Mills Area

Following the seismic survey at the Emmons Blaine Farm, a gravity and magnetic reconnaissance survey was carried out over the Lake Mills area to see to what extent the buried ridge, indicated by well data to the north of the farm, was reflected in these geophysical measurements.

In all, 71 sets of gravity and magnetic measurements were made in an area of approximately 150 square miles. The locations of these observation points are shown in Fig. 10, and the anomaly values at each site are listed in Table 3. These values are contoured and shown as a Bouguer iso-anomaly map in Fig. 11, and as a magnetic vertical component iso-anomaly map in Fig. 12.

As these anomaly maps reflect in large measure intra-basement variations in petrology rather than the near surface geology, a sectional profile was constructed so that the anomalies could be compared directly with the subsurface geology as indicated by the outcrop pattern and well data. In Figure 13, the observed gravity and magnetic anomaly profiles along traverse A-A of Figs. 11 and 12 are shown, along with the geologic section based on well and outcrop data. In each case a smooth "regional" anomaly curve has been plotted in order to separate that portion of the anomaly value related to the near surface geology from that related to intra-basement petrology and crustal structure which account for the bulk of the anomaly.

On the gravity profile a single residual anomaly of 5 mgals is found which is about 3 miles wide, and on the magnetic profile it is seen that there is a magnetic counterpart whose value is about 80 gammas. Both of these residual anomalies occur over that area which is underlaid by the crystalline rock ridge as revealed by the well data, and the correlation between the position of the geophysical anomalies and that of the buried ridge, as shown in Fig. 14, is quite striking. It therefore appears that this ridge may be traced beneath the surface by the application of either gravity or magnetic data.

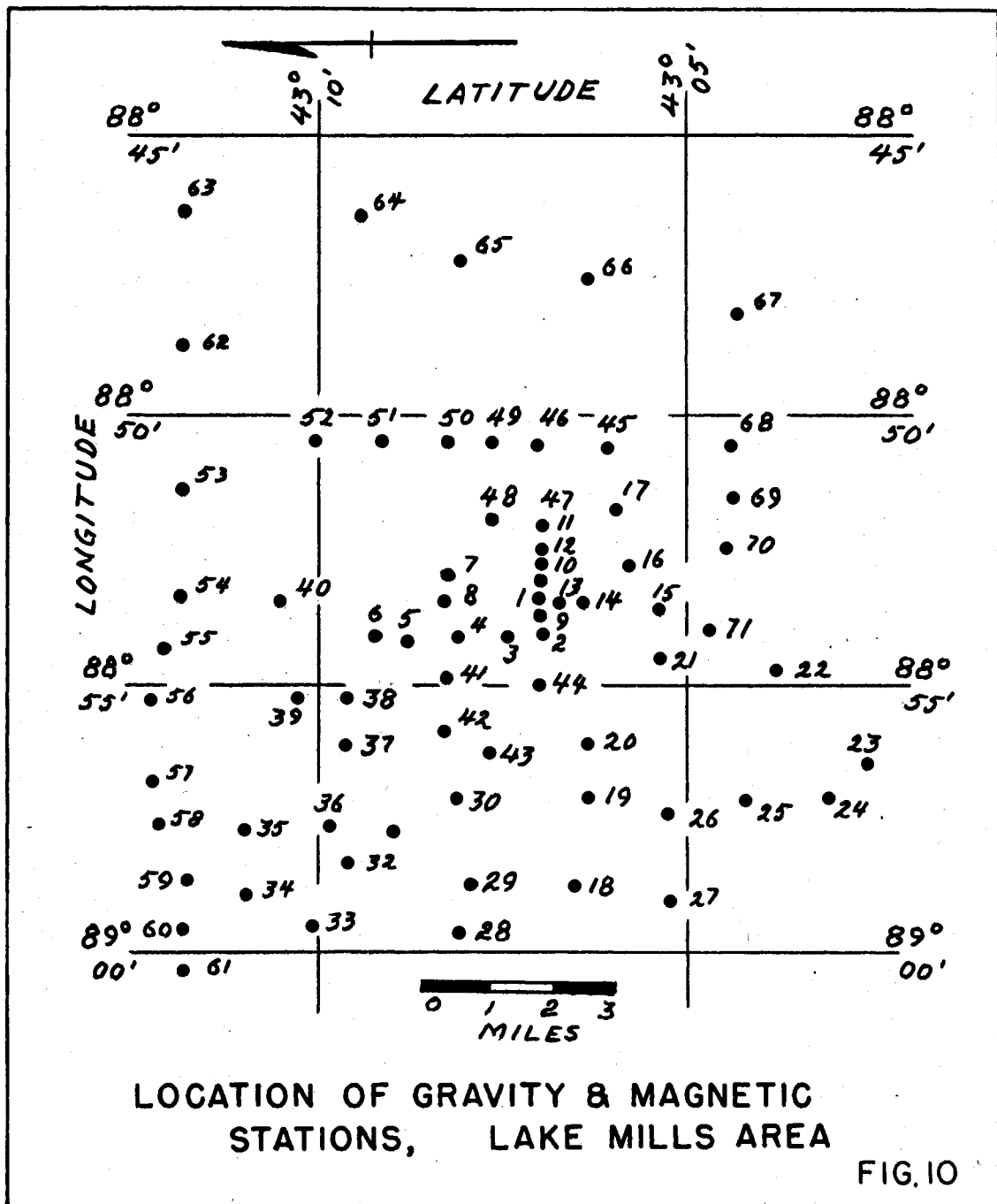
To facilitate tracing the ridge south of section A-A, anomaly profiles were constructed along traverses B-B, C-C, D-D, E-E and F-F. (See Figs. 11 and 12) The strike of these traverses is approximately perpendicular to that of the ridge which seems to be striking roughly North-South and plunging to the South. For comparative purposes, a North-South profile, G-G, is also included. This last traverse starts off the east side of the ridge and crosses it near the Blaine Farm on traverse D-D. These profiles are shown in Fig. 15 and Fig. 16. In order to bring out that part of the anomaly related to the buried ridge, the regional trend on each is shown.

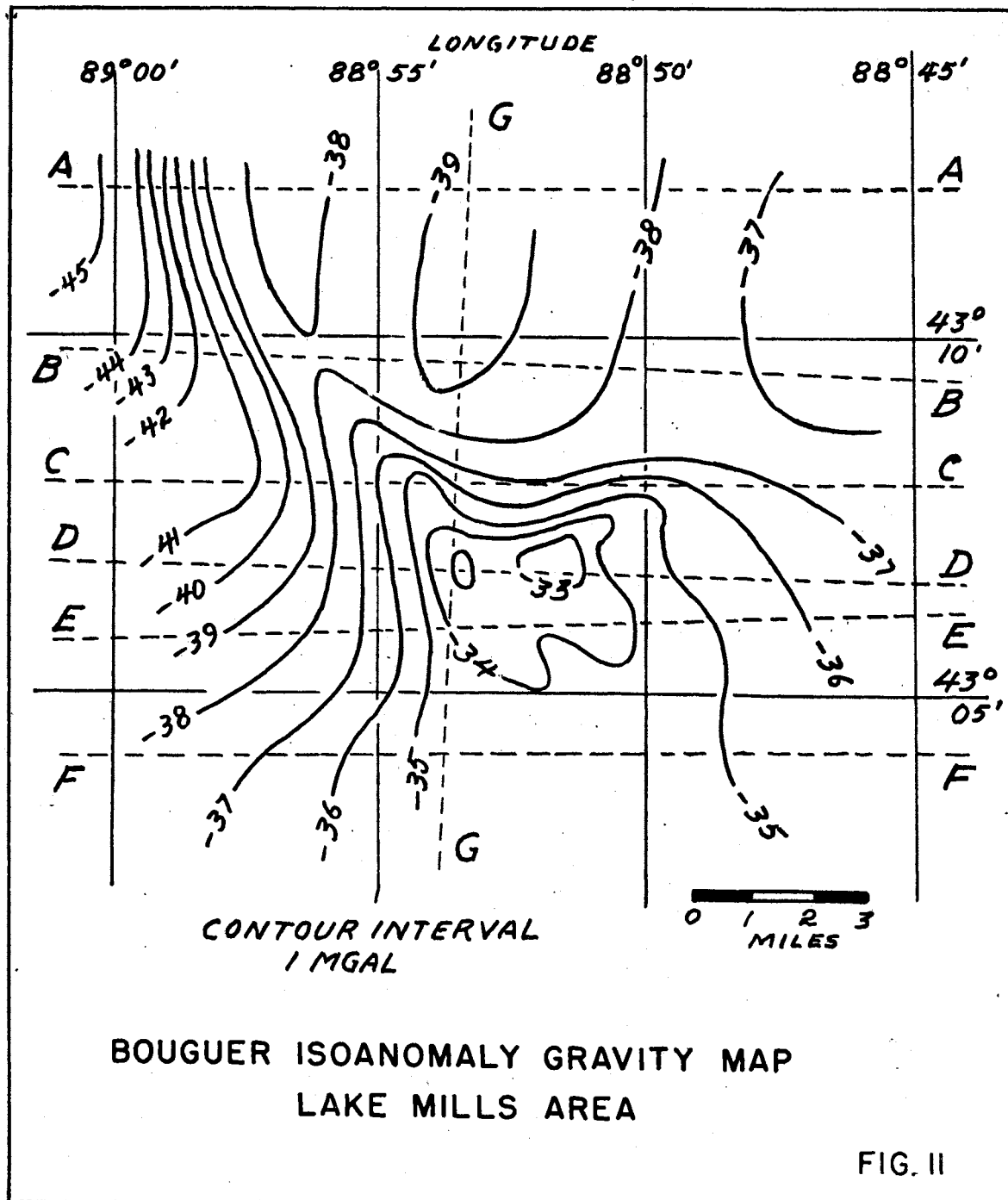
Examination of these profiles shows that, whereas the gravity profiles indicate a relatively simple pattern with a single residual "high" superimposed upon the regional anomaly defining the position of the ridge, the magnetic profiles show considerable variability particularly on the three southern traverses. This change in character of the magnetic values is believed to be related to either a fault or a pronounced change in the petrology of the crystalline rock complex.

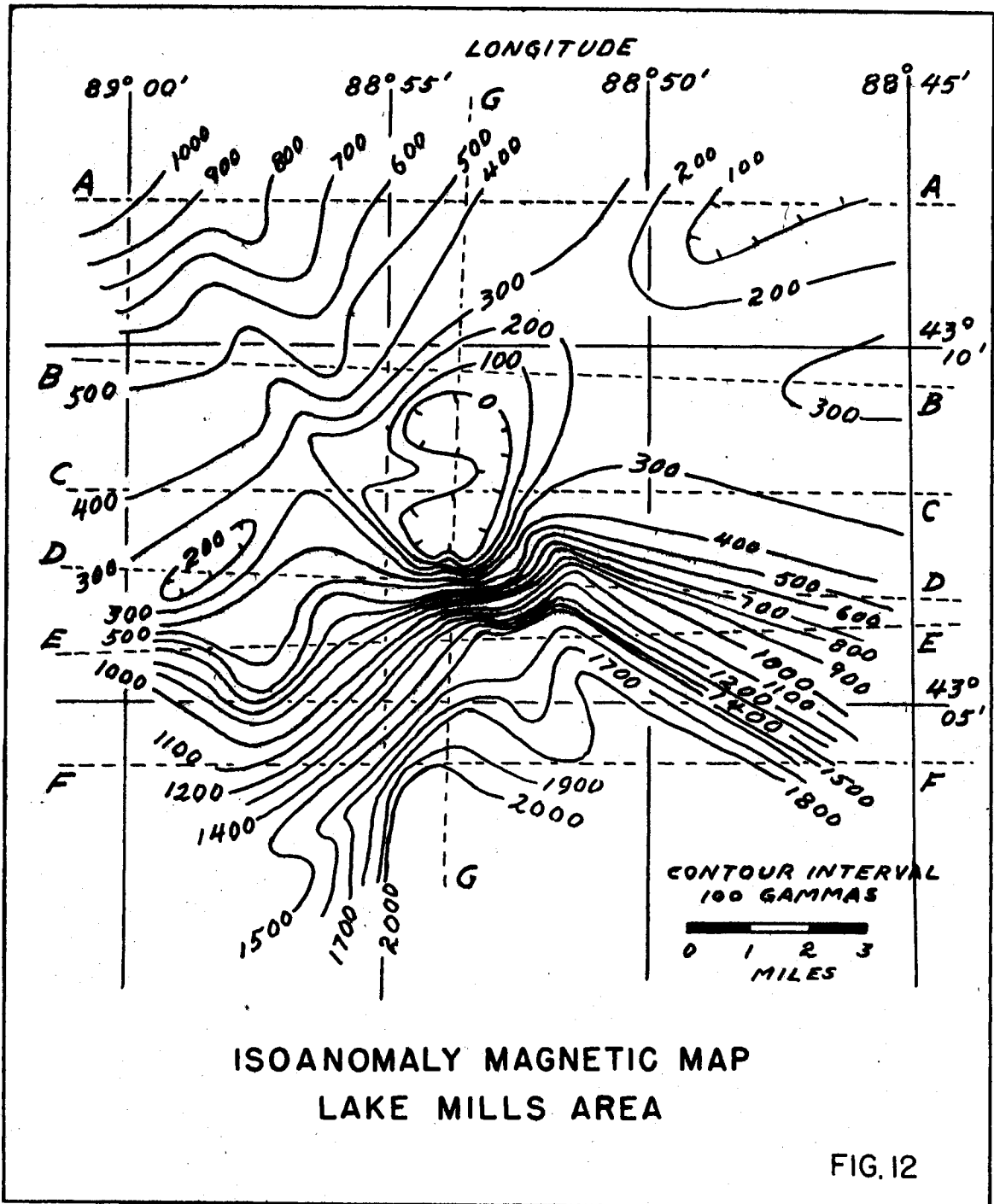
Table 3

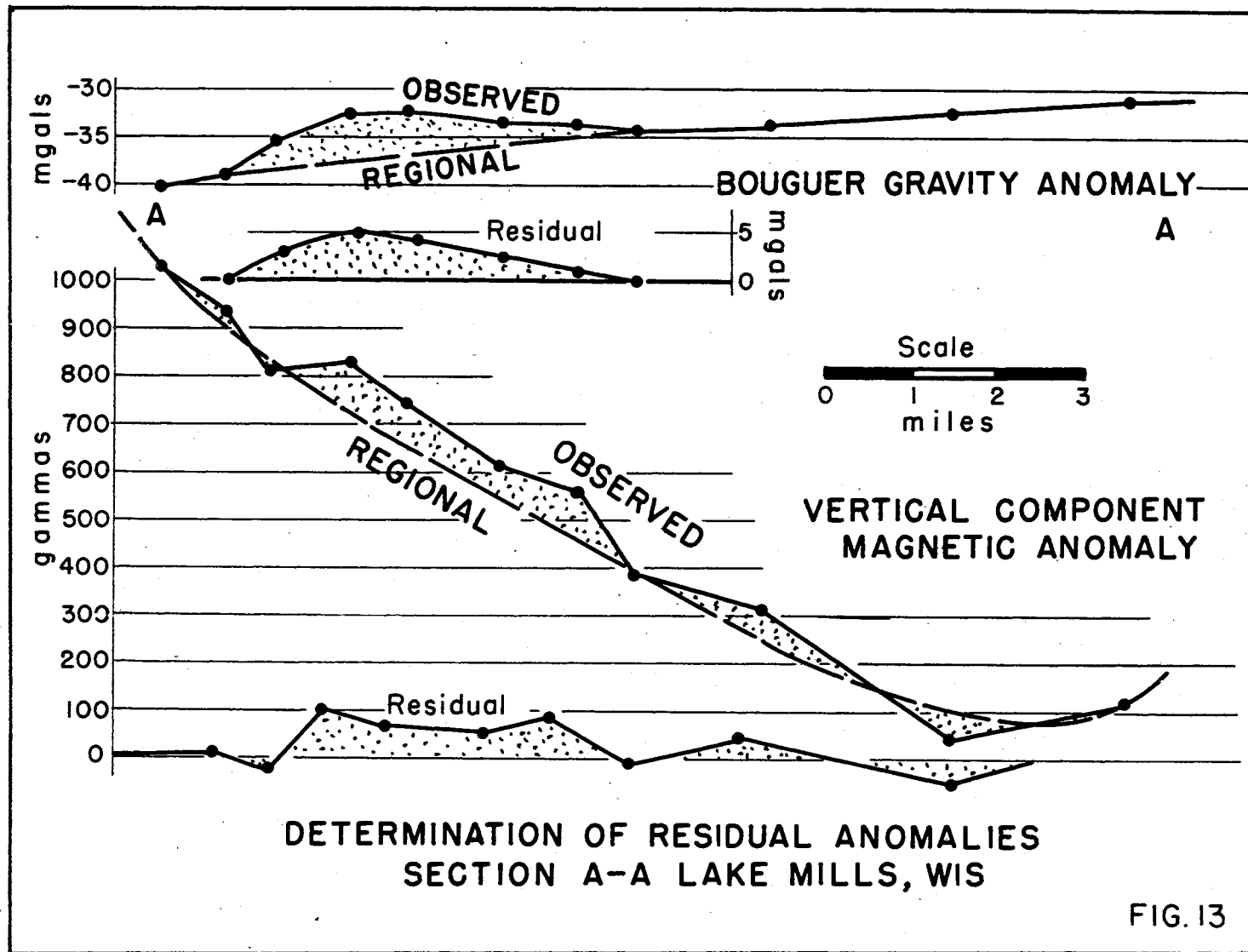
Table of Gravity and Magnetic Anomaly Values
Lake Mills, Wisconsin

Station	Bouguer Gravity	Δz Magnetics	Station	Bouguer Gravity	Δz Magnetics
1	-32.4 mgals	- 40 gammas	36	-39.5 mgals	+ 439 gammas
2	-33.9	- 8	37	-38.1	+ 506
3	-34.3	- 29	38	-38.9	+ 389
4	-34.9	+ 95	39	-38.9	+ 466
5	-38.4	+ 11	40	-40.0	+ 303
6	-39.0	+ 21	41	-35.6	+ 237
7	-37.7	+ 2	42	-38.3	+ 160
8	-37.1	+ 55	43	-39.1	+ 347
9	-32.2	+ 280	44	-36.2	+ 303
10	-33.8	+ 223	45	-33.8	+1182
11	-33.5	+ 302	46	-34.6	+ 747
12	-33.4	+ 290	47	-31.7	+1215
13	-34.9	+ 360	48	-36.1	+ 298
14	-33.3	+1393	49	-34.0	+ 439
15	-34.1	+1511	50	-37.1	+ 303
16	-33.7	+1548	51	-37.8	+ 280
17	-33.8	+1685	52	-38.0	+ 277
18	-40.7	+ 198	53	-38.8	+ 307
19	-39.8	+ 464	54	-39.4	+ 382
20	-38.6	+ 666	55	-38.7	+ 587
21	-36.2	+1203	56	-38.3	+ 604
22	-35.3	+2063	57	-37.4	+ 744
23	-36.4	+1498	58	-37.7	+ 817
24	-36.7	+1500	59	-40.5	+ 810
25	-37.2	+1084	60	-44.1	+ 930
26	-38.7	+ 561	61	-45.1	+1028
27	-38.7	+ 965	62	-37.5	+ 38
28	-41.7	+ 415	63	-36.1	+ 109
29	-41.3	+ 376	64	-36.3	+ 356
30	-41.0	+ 216	65	-37.4	+ 217
31	-41.1	+ 439	66	-35.7	+ 759
32	-42.1	+ 503	67	-35.1	+1136
33	-44.2	+ 564	68	-34.3	+1876
34	-42.4	+ 635	69	-34.5	+1799
35	-38.1	+ 700	70	-34.9	+1788
			71	-34.7	+1870









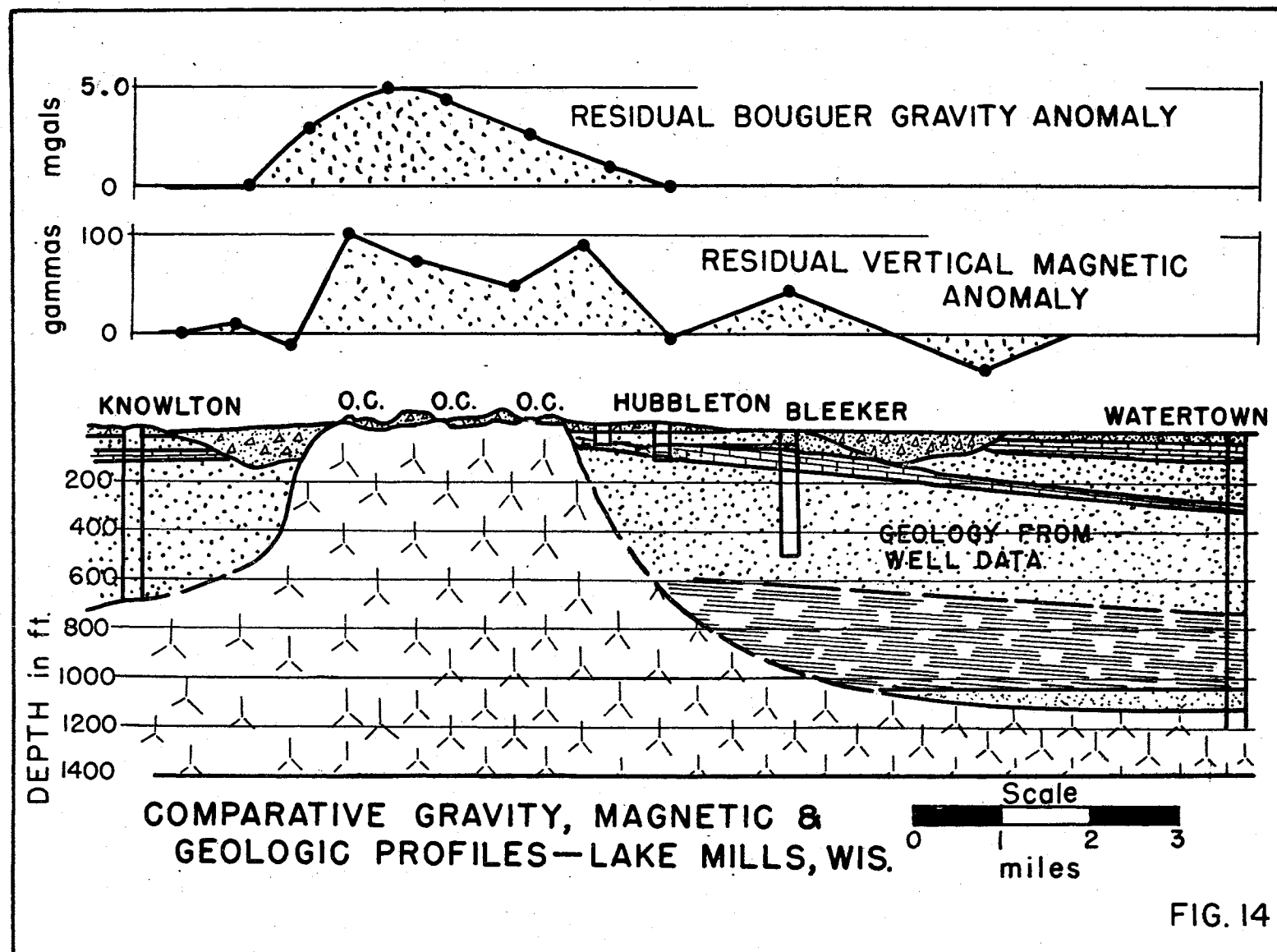
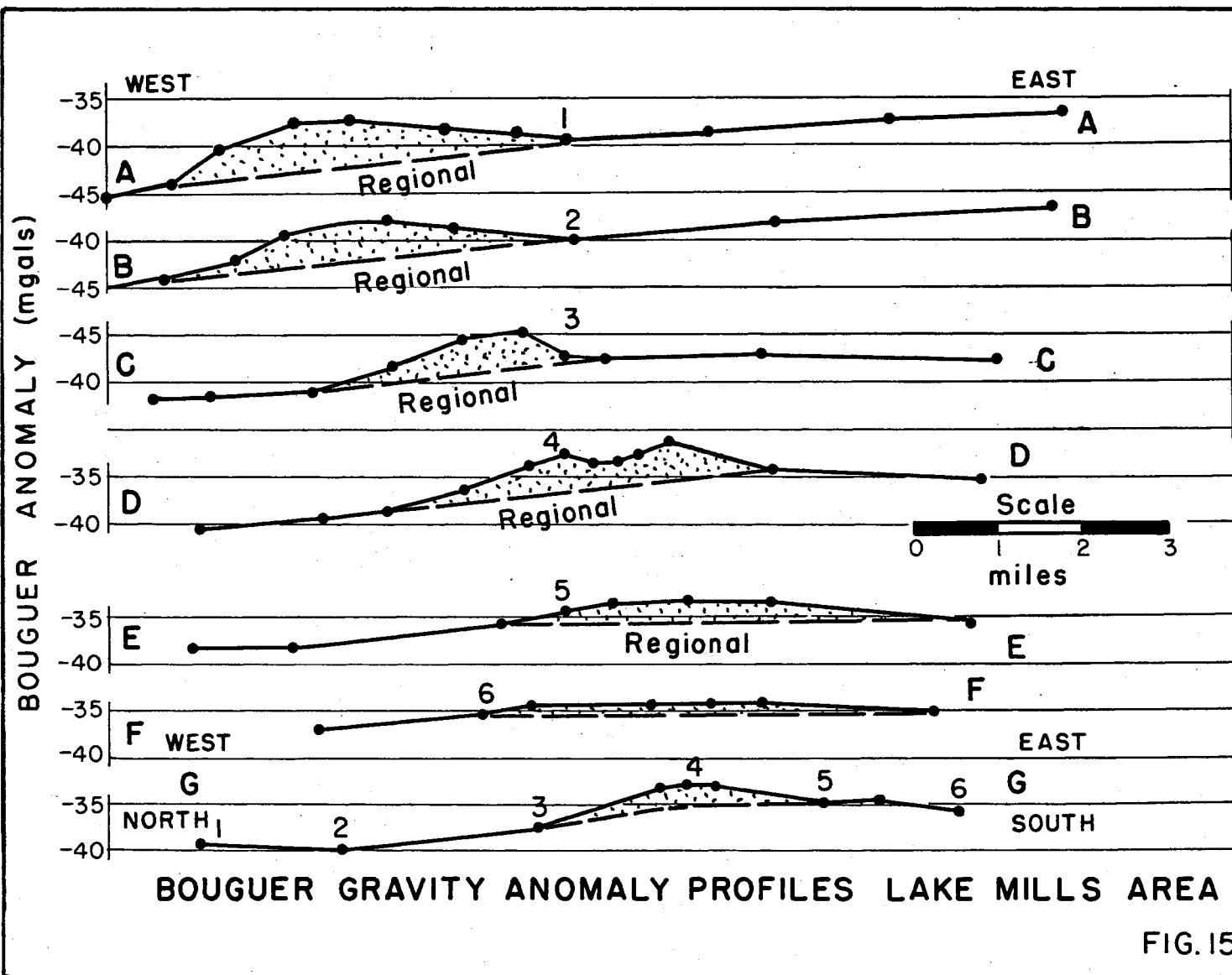
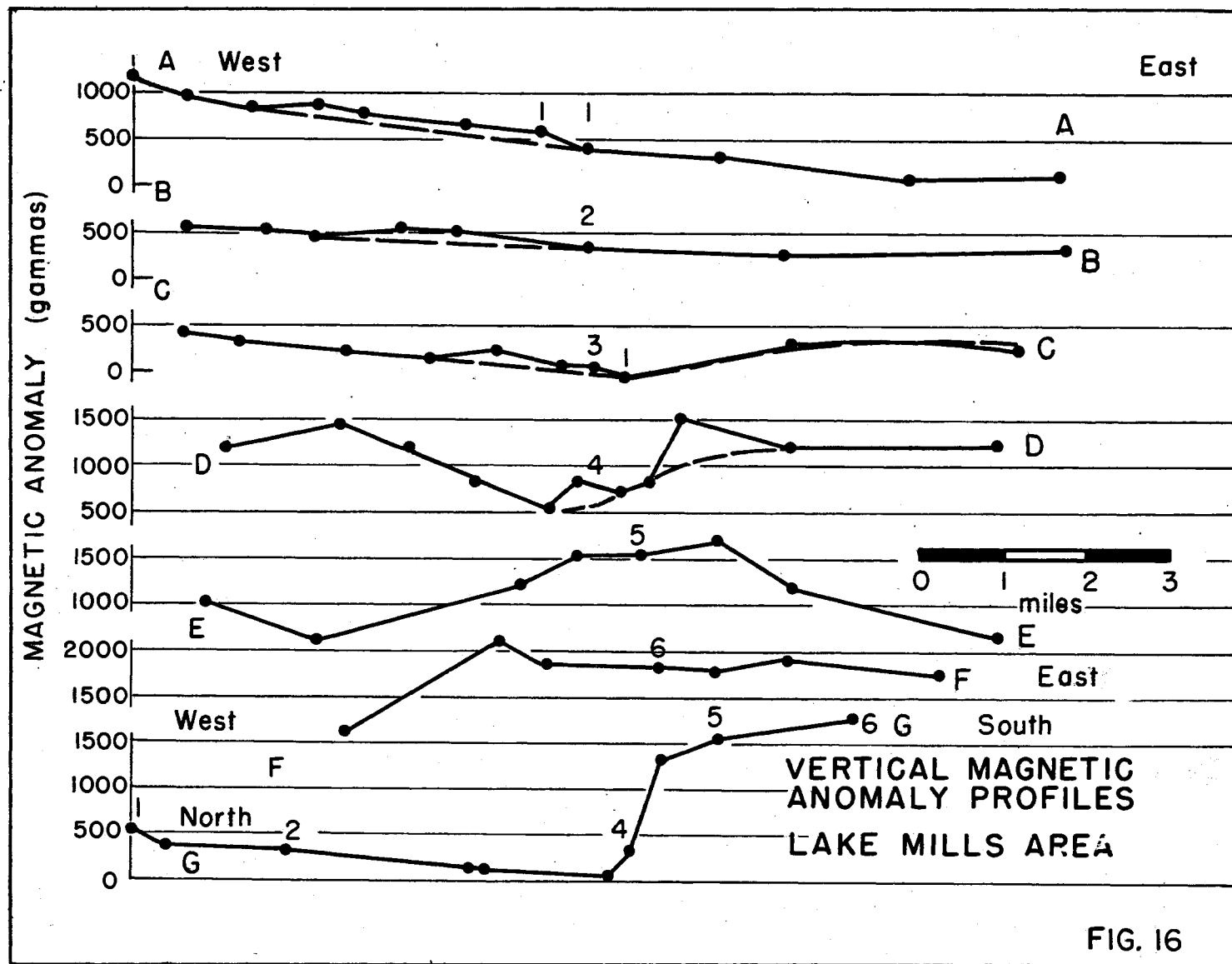


FIG. 14





For example, the North-South magnetic profile, Section G-G, is typical for a fault with the up-throw side to the south. The suggestion of faulting or a change in basement petrology is also indicated to a lesser degree by the gravity anomaly values along traverse G-G; however, without supplementary drilling or seismic data the true significance of this change cannot be definitely stated at this time.

The principal conclusion that may be reached from this study is that buried ridges, which occur at several localities in the state and which restrict the movement of ground water, may be mapped successfully by either gravity or magnetic measurements.

II-1e Concluding Statement on Investigation

It will be noted that this investigation was not a direct search for water but rather a study of the subsurface aquifer, its rock type, depth, lateral uniformity, and vertical extent. Throughout the whole area the water table lay at depths ranging from only a foot or two beneath the surface to ten feet at the well site which was on the highest point of ground. A well located anywhere in the region would have gotten water. The problem was to try and find a location where there would be the best potential water supply in terms of the thickness and extent of the aquifer. A subsidiary problem associated with the investigation was the location of the buried ridge; as this is over 1000 feet in height and three miles in width, it both limits the thickness of the aquifer underlying towns at its crest and restricts the circulation of artesian water to towns on its sides.

II-2 - Antigo, Wisconsin

II-2a General Statement

The area adjacent to Antigo is known as the "flats" and is a glacial outwash plain bordered by terminal moraine. It is an area that is intensively farmed and one in which the Ground Water Division of the U.S. Geological Survey has carried out an extensive ground water survey. As a companion study to this survey, the Geophysics Branch of the U.S. Geological Survey carried out electrical resistivity measurements over much of the area to determine, if possible, the depth of the water table and the thickness of the glacial material which here directly overlies the granite bedrock.

The purpose of the University geophysical study was to test the degree to which various geophysical methods were applicable to ground water problems in areas having similar geologic setting. The earlier work carried out by the U.S. Geological Survey plus local well data would serve as a check upon results.

The program of measurements included a network of 178 gravity and magnetic observations at about one mile intervals covering an area of about 100 square miles around the town of Antigo, and two seismic and resistivity traverses. The latter measurements were made at the same locations so that direct comparisons could be made between the two types of data. One traverse, about a half mile long, was located on the north-west side of town and the other, about one mile long, was located east of the town. The locations of the observation points are shown in Fig. 17.

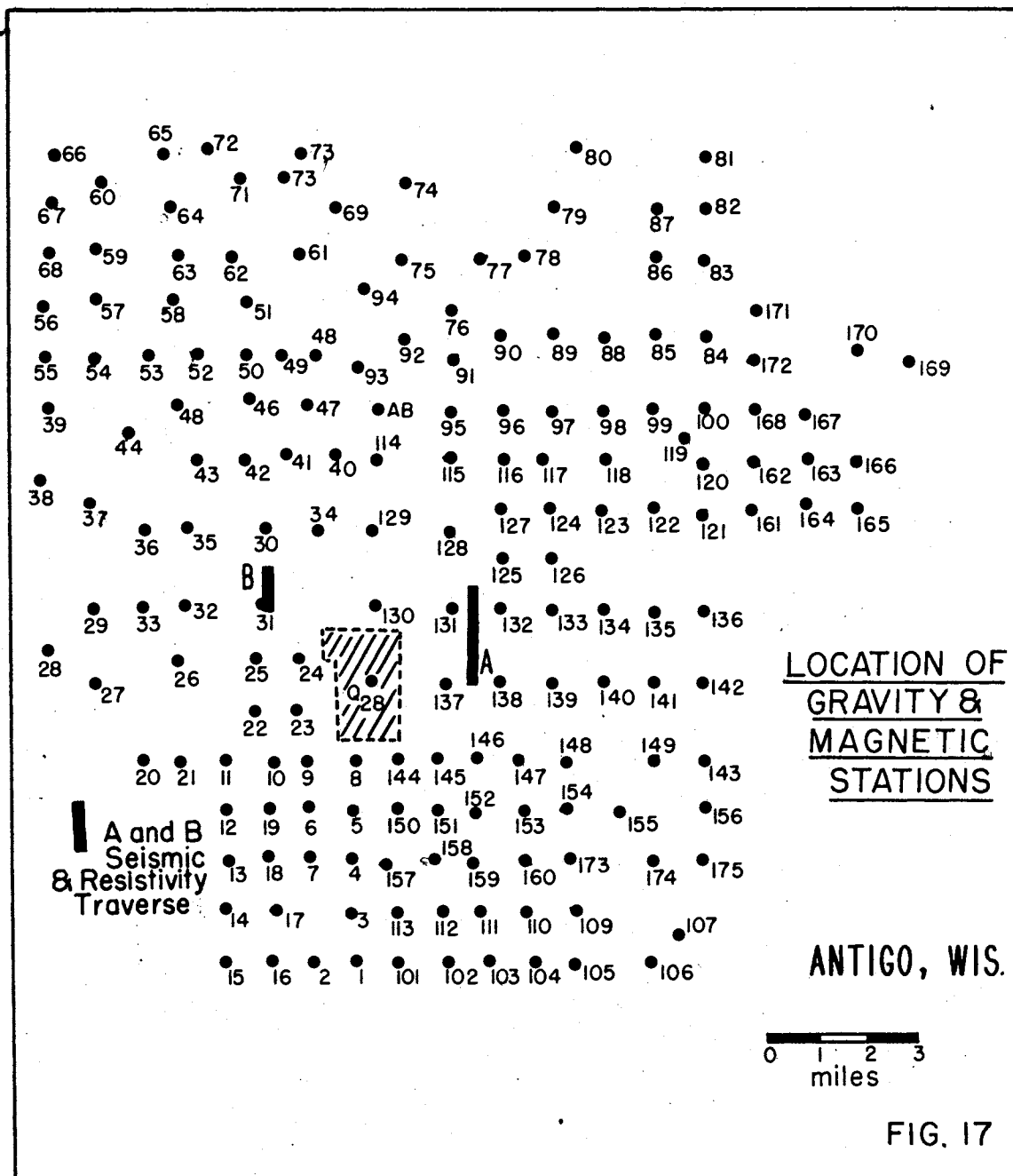
Specific objectives were as follows:

- (1) to determine the degree to which seismic measurements corroborated the electrical resistivity measurements of the U.S. Geological Survey as regards the general depth and relief of the basement rock surface.
- (2) to compare electrical resistivity with seismic results in determining depth to bed rock and water table, using both theoretical and empirical methods of interpreting the electrical resistivity data at sites where the actual depths were known from well log data.
- (3) to see to what degree gravity and magnetic measurements might be applicable for mapping bed rock configuration in the area.

II-2b Seismic Studies

Seismic refraction measurements, using the reverse shooting method described in the Appendix, were used to determine depths to bed rock at thirty locations. Twelve of these determinations were on traverse A-A which was a North-South traverse east of town and about a mile long. Ten determinations were on traverse B-B, which was a traverse west of town and about a half mile long. The balance of the observations were made at the nearby towns of Clintonville, Bryant, and Phlox.

In all areas, three seismic horizons were found. The upper horizon, V_1 , had a velocity varying from 1250 to 3400 ft./sec., and was identified as unsaturated glacial till and probably sand for the most part. The second horizon, V_2 , had a velocity varying from 4500 ft./sec. which was identified as water saturated glacial till and defined the location of water table which was verified by local well data. The third horizon, V_3 , had a velocity varying from 13,800 to 22,080 ft./sec. and was identified as the crystalline bedrock surface.



Pertinent seismic data at each station are shown in Tables 4, 5, and 6 together with the depths determined and available well data. Fig. 18 shows the seismic depth profile along traverse A-A together with that determined by the electrical resistivity measurements. Fig. 19 shows similar data obtained along traverse B-B.

II-2c Electrical Resistivity Studies

The electrical resistivity studies were carried out at 17 sites as depth measurements using a four electrode system set in line at equal distances (Wenner configuration). Non-polarizing, porous pot potential electrodes were used with direct current and potential differences were observed with the current flowing in opposite directions. The electrode spacings used at most sites were 5, 10, 20, 30, 40, 50, 60, 70, 80, 90, 100, 125, and 150 feet. The center point of the spread was maintained constant for all the observations at any one site. The observations were all confined to traverses A-A and B-B except for six sets of measurements which were made at nearby towns; these are the same traverses and sites at which the seismic observations were made. The individual seismic and electrical measurements had common center points so that direct comparisons of results could be made. Traverse A-A to the east of town was about one and a quarter miles long and oriented North-South; on this traverse five sets of measurements were made in line which are designated A-1, A-2, A-3, A-5 and A-6. Traverse B-B to the northwest of town was about one half mile long, and measurements were made at five sites designated B-1, B-2, B-3, B-4, and B-5.

In Fig. 20 the individual observed resistivity profiles along traverse A-A are superimposed for comparison. The results obtained by the U.S. Geological Survey at their station B-4 which lies on this traverse are also included in this figure. All the curves are similar in pattern, although all differ as regards the maximum resistivity value obtained, and the electrode spacing at which the resistivity values peak. Each indicates an increase in resistivity with depth of current penetration as the electrode spacing is increased up to values varying from 20 to 60 feet with a minimum resistivity value at an electrode spacing of about 270 feet.

Five methods of interpretation were tried. Three were empirical methods and two were so-called theoretical methods. These can be identified as the Inflection Point Method, the Two-thirds Inflection Point Method, the Accumulative Plot Method, the Tagg Method and the Longacre (modified Tagg) Method. Descriptions of each are given in the Appendix. For illustrative purposes the data for station A-3 are shown in Fig. 21 as plotted for making a depth interpretation for four of the above methods. The depths obtained by each method are listed in the Table 7, which also gives the seismic depths observed.

Table 4

Seismic Data - Antigo, Wisconsin
Traverse A-A

Station	Apparent Velocity			Depth (feet)		Well Data
	V ₁	V ₂	V ₃	V ₂	V ₃	
A-1a	1428	5270	20400	25	112	
A-1b	1388	5660	16250	27	142	
A-2a	1487	6250	15000	34	112	
A-2b	1580	5560	20400	34	155	
A-3a	1390	6150	21300	31	130	
A-3b	1650	5000	13130	29	114	
A-5a	1470	5550	18750	31	225	
A-5b	1471	5200	-----	---	---	
A-5c	1395	5630	12330	33	158	35*
A-6a	1395	5500	19500	30	189	
A-6b	1250	5380	16500	---	---	
A-6c	1539	5810	26150	35	262	

* Depth of water table indicated in well.

V₁ = unsaturated glacial sand and gravel

V₂ = saturated glacial sand and gravel, average true velocity =
5489 ft./sec.

V₃ = crystalline bedrock (granite), average true velocity =
17,680 ft./sec.

Table 5

Seismic Data - Antigo, Wisconsin
Traverse B-B

Station	Apparent Velocity (ft./sec.)			Depth (feet)	
	V ₁	V ₂	V ₃	V ₂	V ₃
B-1a	3400	-----	11000	-	12
B-1b	3400	-----	16470	-	3
B-1c	-----	-----	16450	-	---
B-2a	1400	5440	24900	3	42
B-2b	1400	5000	20000	3	34
B-3a	1400	6150	17420	2	29
B-3b	1400	5000	20000	2	31
B-4a	1400	5000	19400	5	30
B-4b	1400	5000	18800	3	24
B-5a	1400	8000	15040	4	28
B-5b	1400	5000	20500	4	33

V₁ = unsaturated glacial till

V₂ = saturated glacial till, average true velocity = 5675 ft./sec.

V₃ = crystalline bed rock, (granite) average true velocity = 18028 ft./sec.

Table 6

Seismic Data - Antigo Area, Wisconsin

Station	Apparent Velocity			Depth (feet)		Well Data
	V ₁	V ₂	V ₃	V ₂	V ₃	
Clintonville						
1a	1315	4860	-----	14	---	
2a	1315	4400	-----	10	---	
1b	1315	4280	17950	11	210	215
Bryant						
1a	1614	6330	16670	52	309	60
1b	1111	6600	25700	38	342	
Phlox						
1a	1446	6350	-----	48	49	
1b	1515	6160	-----	---	---	

V₁ = unsaturated glacial till

V₂ = saturated glacial till, average true velocity =
575 ft./sec.

V₃ = crystalline bedrock (granite), average true velocity =
21,200 ft./sec.

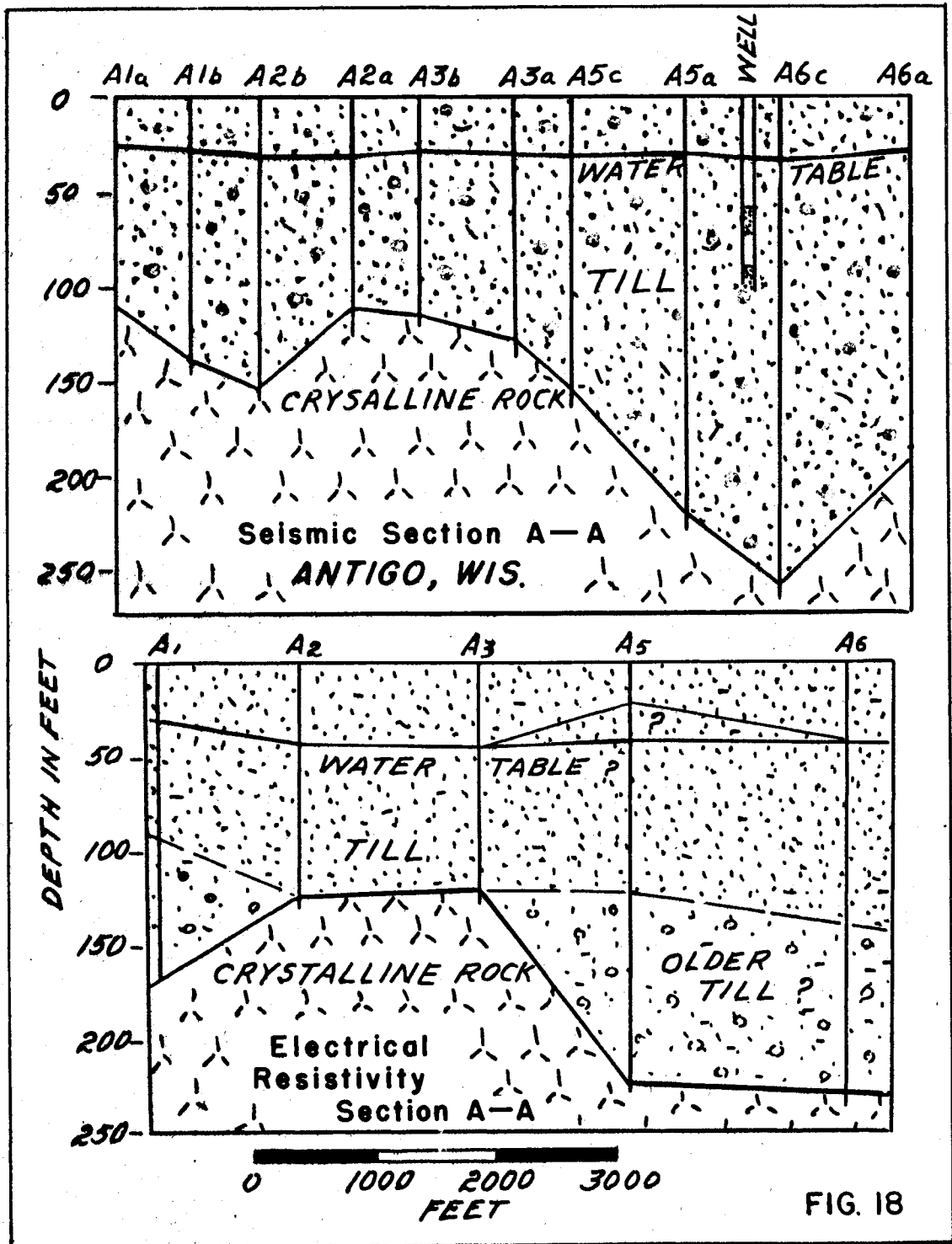
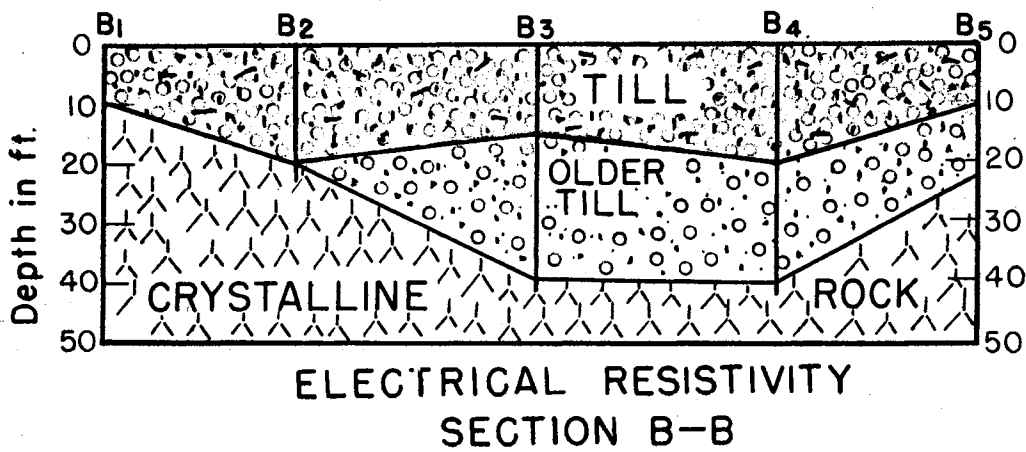
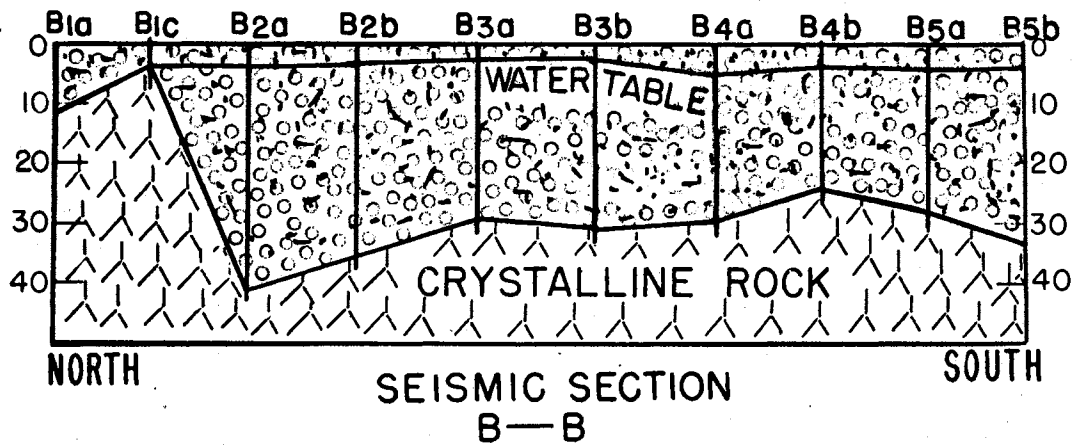


FIG. 18



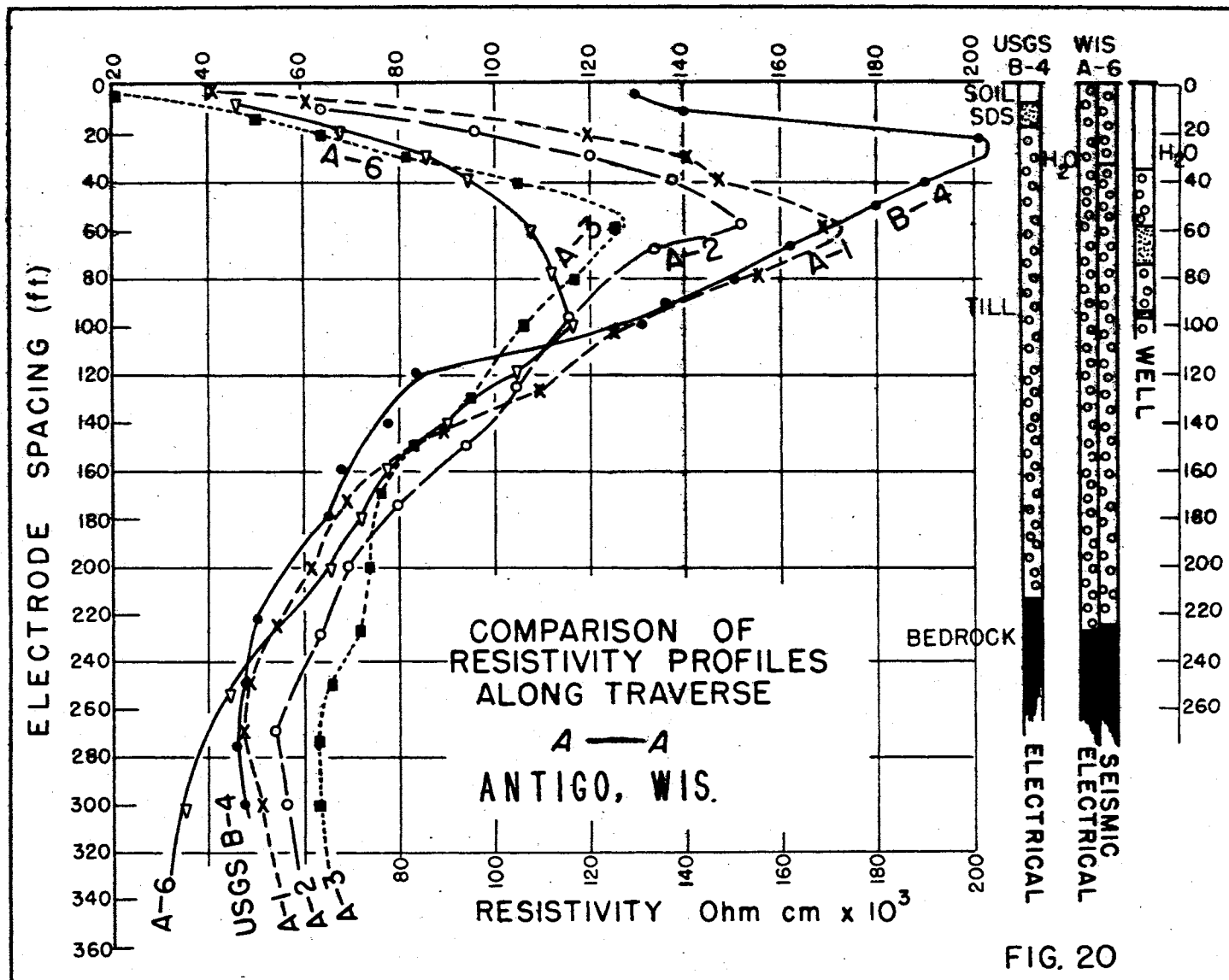
ANTIGO, WIS.

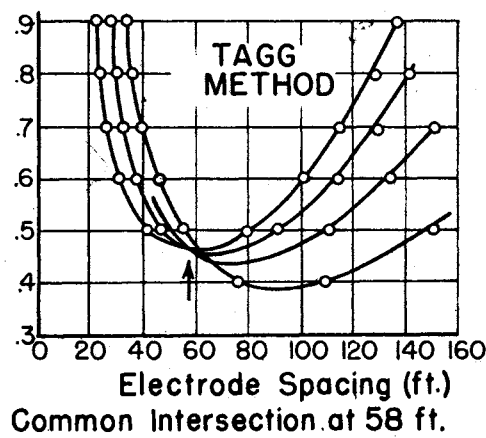
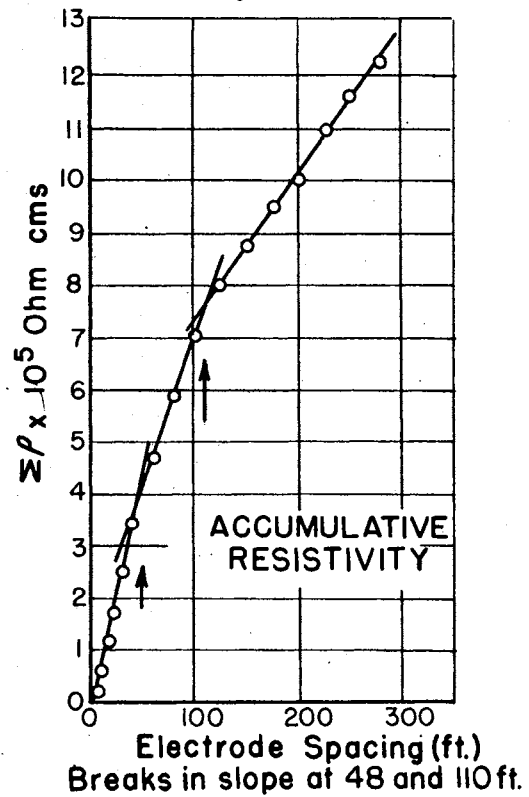
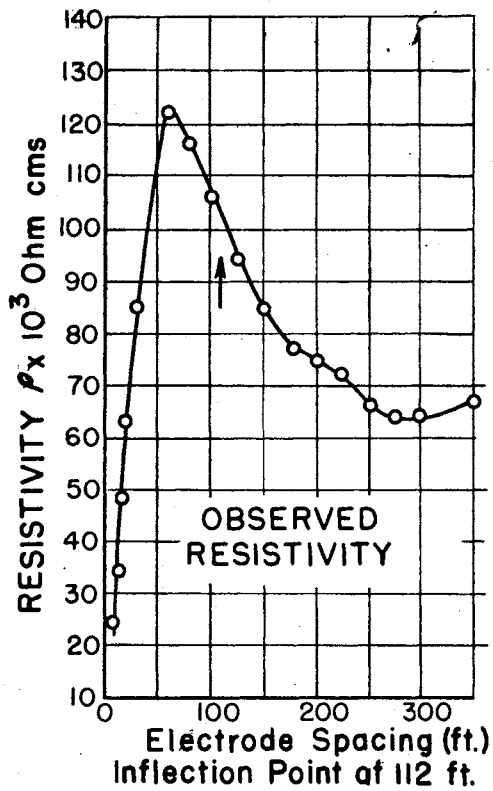
FIG. 19

Table 7

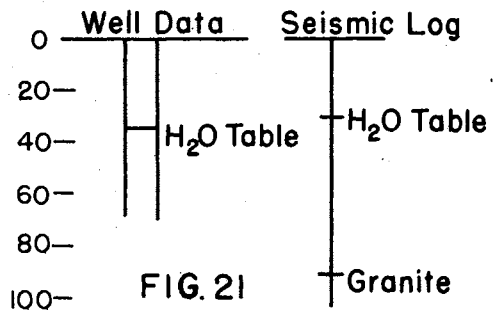
Comparative Interpretations of Resistivity Data and Seismic Data
Antigo Area
Electrode Spacing (feet)

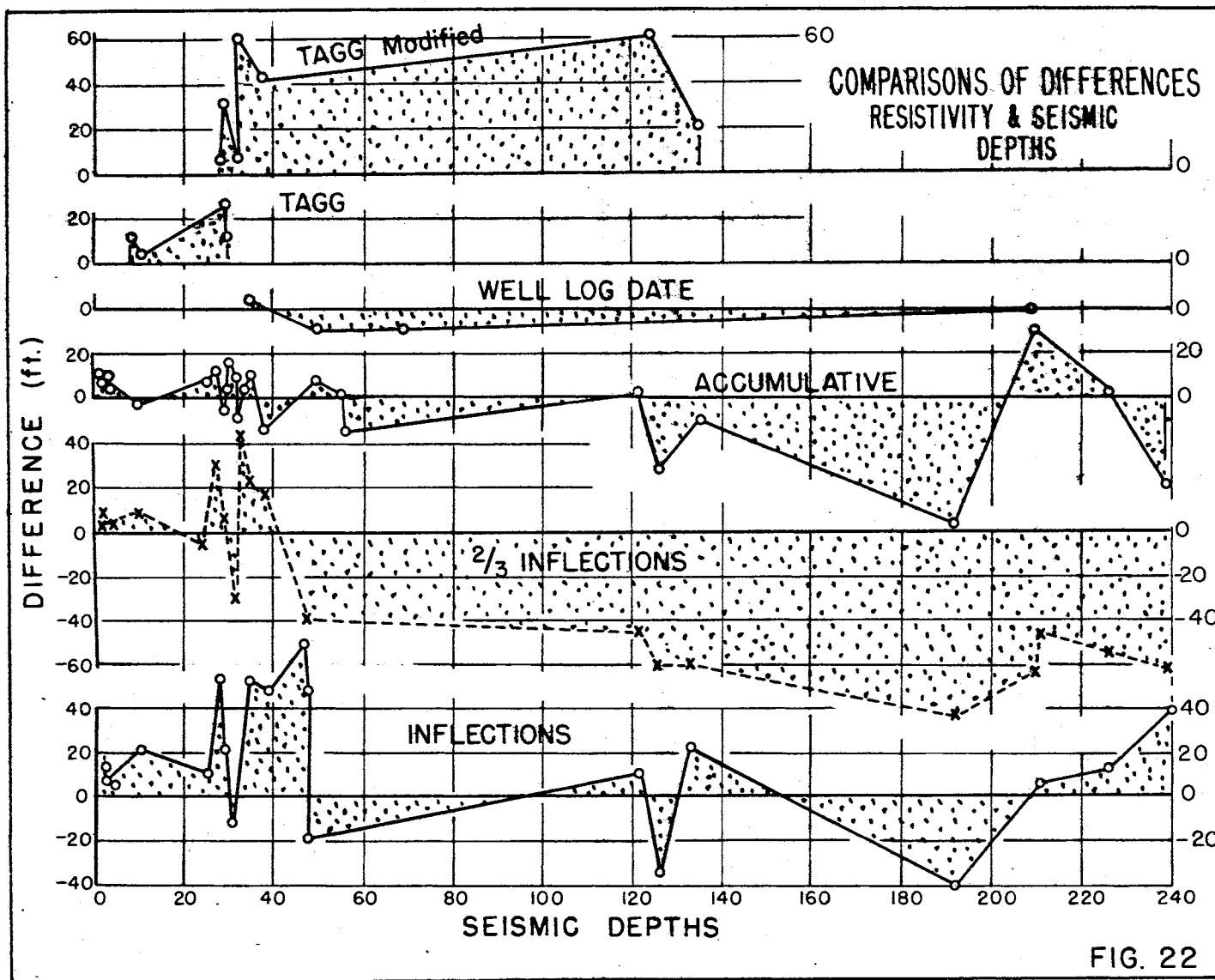
Station	Peaks		Inflection Points		2/3 Inflection Points		Accumulative Slope Breaks			Tagg Crossings		Seismic Depth		Well Data
	Max.	Min.								(1)	(2)	Mean		
A-1	60	265	35	87	23	58	32	91	171	—	65	26	126	—
A-2	60	315	85	110	57	73	45	125	305	—	55	34	133	35
A-3	60	275	112	245	74	165	46	120	310	58	66	30	122	—
A-5	15	350	20	150	14	100	22	42	125	212	—	32	192	—
A-6	100	—	115	240	77	160	42	135	230	—	94	33	226	—
B-1	—	—	110		73		10	20	41	60	28	—	12	—
B-2	12	30	17	90	12	60	20				40	3	38	—
B-3	—	15	12	32	8	21	15	40		42	35	2	30	—
B-4	10	40	20	92	13	62	20	40		—	32	4	27	—
B-5	—	40	12	55	8	37	10	21		—	28	4	30	—
Clinton-ville	55	205	35	90	215	24	60	144	16	60	140	240	—	—
Mattoon-1	15	10	20				10	22		17	—	—	—	—
	32	40												
Mattoon-2	10	17	70	12	53	65	8	35	43	21	30	40	50	—
	60													
Bryant	100	365	150	320	100	214	35	60	160	238	—	52	280	60
White Lake	20	80	55	94	37	63	20	40		—	—	—	—	—
	110													
Phlox-1	70	—	90	165	60	110	15	20	35	140	—	48	—	—
Phlox-2	100	—	18	120	13	80	10	50		—	—	48	—	—





COMPARATIVE
INTERPRETATION PLOTS
SITE 3-A
ANTIGO, WIS.





For comparative purposes the difference from the seismic depths on each basis of interpretation are shown graphically in Fig. 22, and from an inspection of this figure it is seen that the Accumulative Plot Method of interpretation gives the best overall agreement with the seismic data.

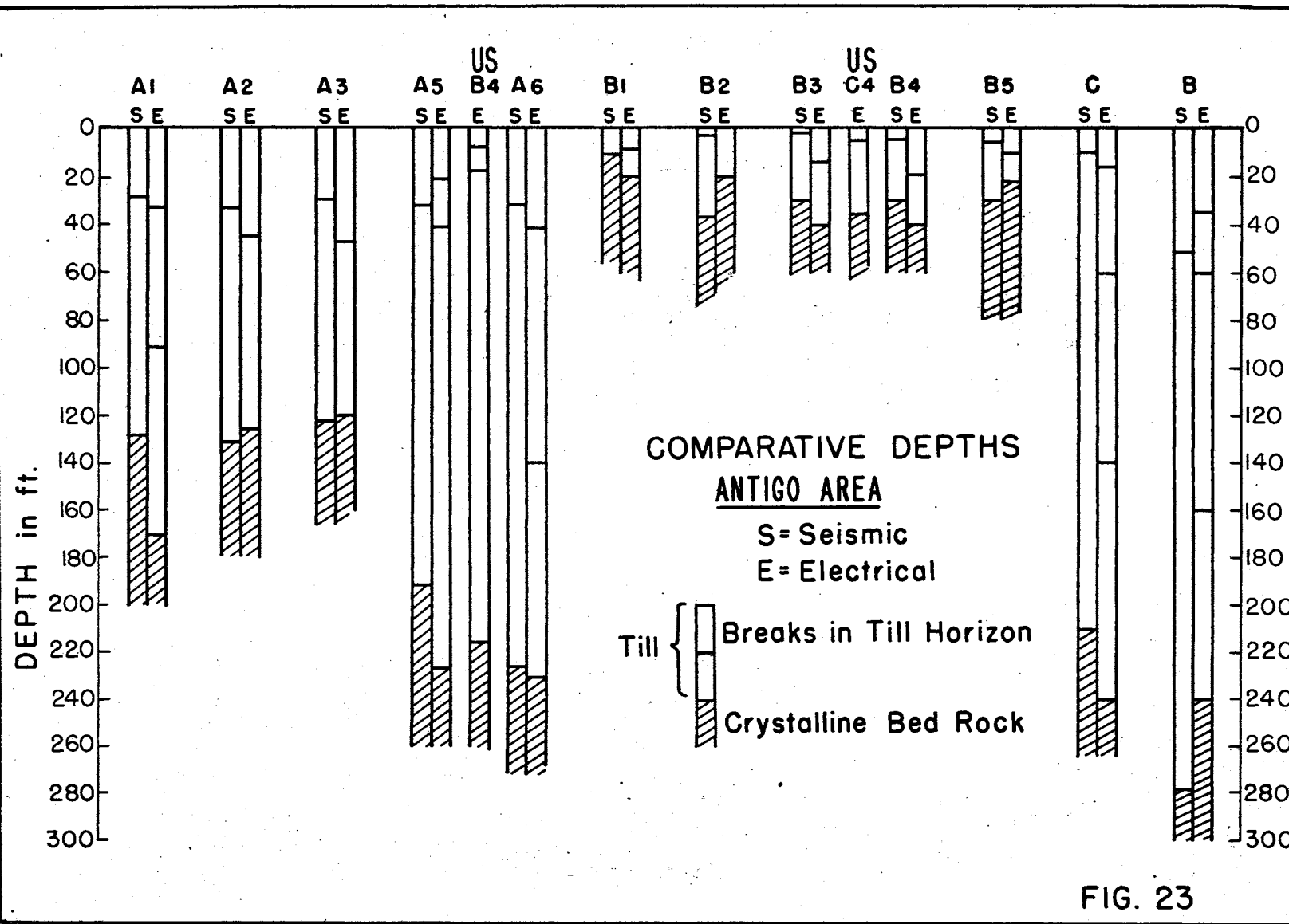
Although it is not possible to compare all of the results of the present work with that done by the U.S. Geological Survey parties, direct comparisons are possible at the U.S.G.S. station B-4 which is on the traverse A-A and station C-4 which is on traverse B-B. The depth values obtained by the U.S. Geological Survey were on the basis of theoretical curve comparisons; those for University of Wisconsin resistivity values are in excellent agreement as regards the depth to the crystalline rock surface and both also agree rather well with the seismically determined depths.

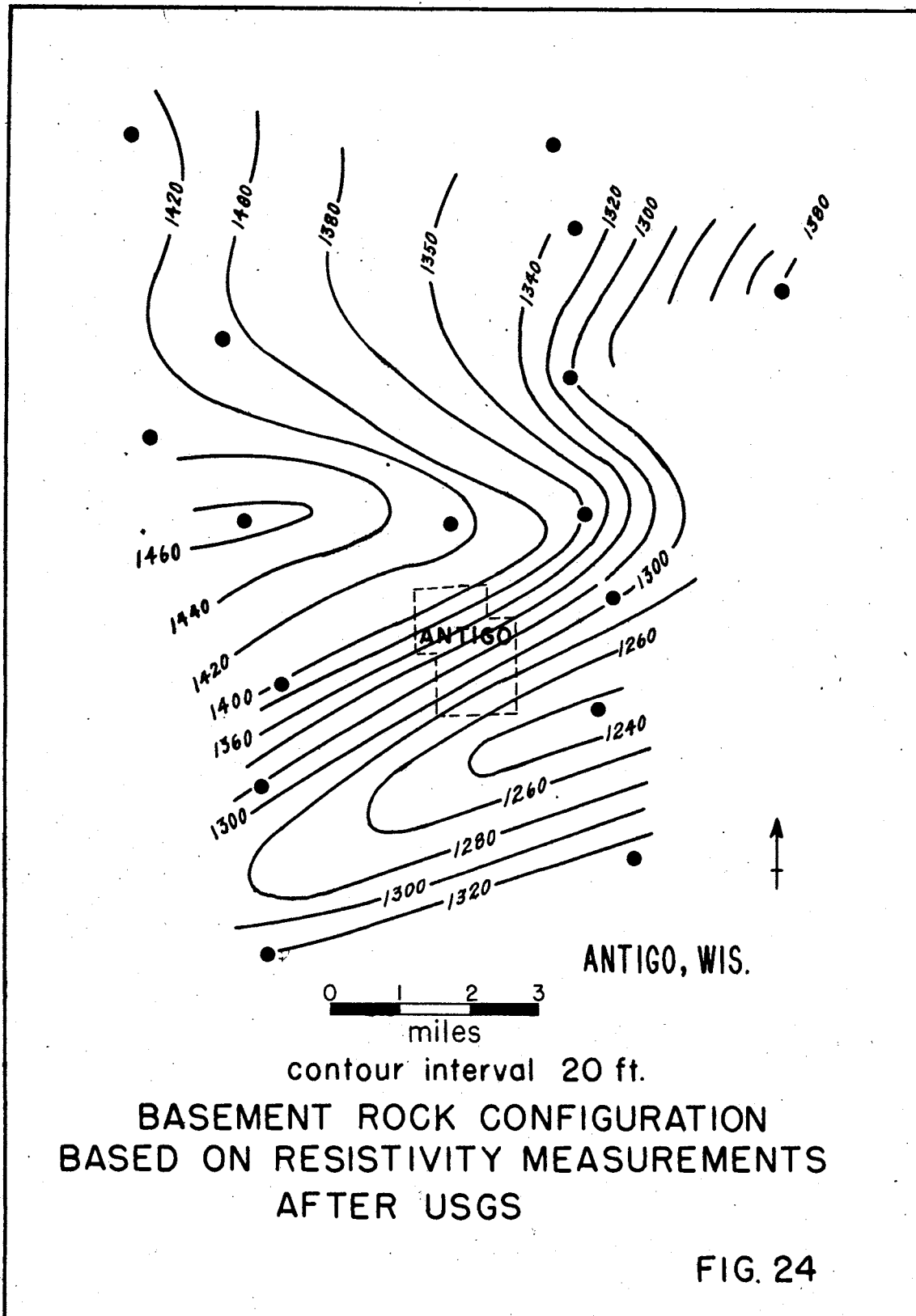
Station	Resistivity Depths		Seismic Depths
	U.S.G.S.	U. of Wis.	U. of Wis.
B-4	220 ft.	225	210
C-4	40	40	30

Above the crystalline rock surface, interpretations differ. The results of the U.S. Geological Survey measurements indicate distinct breaks between soil, sand, and till; at the Wisconsin seismic and resistivity stations only the water table is identified, although other horizons are shown by the resistivity measurements at some of the other sites. Local well data indicate that the water table interpretation is probably correct.

In order to evaluate the general agreement between the seismic and electrical results, a comparative plot was made of the depth to bed rock as obtained at all twelve locations studied. From this plot, Fig. 23, the agreement is seen to be fairly good, and in view of this it appears that either the electrical or seismic method is here applicable to mapping, in gross form, the depth to the crystalline rock surface.

Although the University study did not cover sufficient territory to indicate the relief of the crystalline rock surface on an areal basis, the survey conducted by the U.S. Geological Survey did, and the results of their investigation are shown in Fig. 24. It is evident that the contours of this map would have been somewhat different with closer order control from the large amount of relief indicated by the seismic and resistivity measurements along traverses A-A and B-B, both of which are shorter than the individual station spacing used by the U.S. Geological Survey. See Figs. 18 and 19.





In Table 8, the depths and resistivity values are tabulated at which changes in slope on the accumulative plots occurred denoting a change in resistivity. The seismic depths observed at each site are also given. From an inspection of this table, it is seen that, whereas the seismic values indicated only the depth of the water table and that of the buried crystalline rock surface, the electrical results also showed a horizon above the water table that appears to correlate with the base of the surface outwash sands. The water table also appears to be present and an intermediate horizon in the till is also indicated which might represent an older till. Over part of traverse A-A in addition to the crystalline rock surface, a horizon is shown which lies below the surface of the crystalline rocks. This horizon probably represents an intra-basement change in petrology, possibly associated with the local magnetic anomaly observed in this area.

As there was nothing diagnostic about any of the resistivity values as regards the horizon being depicted, it is very dubious that the results would have been interpreted correctly without the auxiliary seismic data, particularly at those stations where an intra-basement change in resistivity was observed.

II-2d Magnetic Survey

The magnetic observations were carried out with an Askania Schmidt type vertical component magnetometer, having a sensitivity of 31.8 gammas per scale division. The diurnal variation in the earth's field strength during the period of the survey was determined by returning to a base station for repeat observations at approximately three hour intervals. The theoretical changes in magnetic field for change in magnetic latitude were determined from the vertical component magnetic map prepared by the U.S. Coast and Geodetic Survey for 1945 corrected up to the date of the survey. (1950) The anomaly values, the difference between the observed values after corrections for the diurnal change and the theoretical change with location, were plotted and contoured to give the iso-anomaly map shown in Fig. 25.

II-2e Gravity Investigation

The gravity observations were carried out using two gravimeters, a North American constant temperature gravimeter with a sensitivity of 0.21185 mgals per division and a Worden temperature compensated gravimeter with a small dial sensitivity of 0.1583 mgals per scale division. The same sites were occupied as in the magnetic survey, and instrumental drift (change in readings with time) was observed at the same times and stations as were used for determining the magnetic field diurnal variation.

Table 8

Electrode Spacings at Which Layers are Indicated
on Accumulative Basis of Interpretation
Antigo Area
Traverse A-A

Sta.	Depths (feet) Electrode Spacing					Resistivity Values at Depth Points (Ohm Cms x 10 ⁶)					Seismic Depths(ft.)	
	ρ_0	ρ_1	ρ_2	ρ_3	ρ_4	ρ_0	ρ_1	ρ_2	ρ_3	ρ_4	Water Table	Rock
A-1		32	91	171	315		0.53	1.04	1.32	1.6	26	126
A-2		45	100	150	305		0.56	0.91	1.10	1.52	34	133
A-3		40	---	120	310		0.36	---	0.80	1.33	30	122
A-5	22	42	125	212	---	0.7	0.8	1.11	1.27	---	32	192
A-6		42	135	230	---		0.38	0.92	1.21	---	33	226

- ρ_0 ---- not known
 ρ_1 ---- probably water table
 ρ_2 ---- not known, possible older till
 ρ_3 ---- crystalline rock surface
 ρ_4 ---- not known, possible intrusive rock associated with magnetic anomaly

Traverse B-B

Sta.	Depths (feet) Electrode Spacing		Resistivity Values at Depth Points (Ohm cms x 10 ⁶)		Seismic Depths(ft.)	
	ρ_1	ρ_2	ρ_2	ρ_3	Water Table	Rock
B-1	10		0.12		0	12
B-2	20		0.18		3	38
B-3	15	40	0.12	0.22	2	30
B-4	20	40	0.32	0.41	4	27
B-5	10	20	0.35	0.50	4	30

- ρ_1 ---- not known, may be surface sand interface with till
 ρ_2 ---- crystalline rock surface

Table 8 (continued)
Clintonville

Depths (feet) Electrode Spacing				Resistivity Values at Depth Points (Ohm cms x 10 ⁶)				Seismic Depths(ft.)	
ρ_1	ρ_2	ρ_3	ρ_4	ρ_1	ρ_2	ρ_3	ρ_4	Water Table	Rock
16	60	140	240	0.03	0.11	0.176	0.231	11	210

ρ_1 ---- probably water table
 ρ_2 & ρ_3 ---- not known, may be older till or changes in till
 ρ_4 ---- crystalline rock surface

Mattoon

Sta.	Depths (feet) Electrode Spacing			Resistivity Values at Depth Points (Ohm cms x 10 ⁶)			
	ρ_1	ρ_2	ρ_3	ρ_1	ρ_2	ρ_3	
A	10	22	41	0.058	0.132	0.4	no seismic data
B	20	26	40	0.15	0.19	0.51	

ρ_1 ---- unknown, may be base of snad
 ρ_2 ---- water table
 ρ_3 ---- crystalline rock surface

Bryant

Sta.	Depths (feet) Electrode Spacing				Resistivity Values at Depth Points (Ohm cms x 10 ⁶)				Water Table Rock	
	ρ_1	ρ_2	ρ_3	ρ_4	ρ_1	ρ_2	ρ_3	ρ_4		
A	15	65	140	235	0.1	0.65	1.03	1.2	52	280
B	38	60	160	235	0.2	0.5	1.21	1.52	—	—

ρ_1 ---- not known, may be base of sand
 ρ_2 ---- water table
 ρ_3 ---- not known, may be older till
 ρ_4 ---- crystalline rock surface

Table 8 (continued)

White Lake

Depths (feet) Electrode Spacing			Resistivity Values at Depth Points (Ohm cms x 10 ⁶)			
ρ_1	ρ_2	ρ_3	ρ_1	ρ_2	ρ_3	
8	20	40	0.04	0.136	0.22	no seismic data

ρ_1 ---- not known, possible base of sand
 ρ_2 ---- water table (?)
 ρ_3 ---- crystalline rock surface

Phlox

Sta.	Depths (feet) Electrode Spacing			Resistivity Values at Depth Points (Ohm cms x 10 ⁶)			Seismic Depths (ft.)	
	ρ_1	ρ_2	ρ_3	ρ_1	ρ_2	ρ_3	Water Table	Rock
A	12	40	138	0.08	0.28	0.58	48	----
B	20	65	140	0.38	0.20	0.36	—	----

ρ_1 ---- base of sand (?)
 ρ_2 ---- water table
 ρ_3 ---- crystalline rock surface

All results were reduced to give absolute values of gravity on the Potsdam System on the basis of the observed gravity value (980.3681 cm/sec.) at the U.S. Coast and Geodetic Survey gravity base at Science Hall in Madison. Simple Bouguer anomalies were determined at each station as described in the Appendix, and the results plotted and contoured (Fig. 26). The gravity and magnetic anomaly values obtained at each station are given in Table 9.

II-2f Magnetic and Gravity Results

The magnetic results showed local anomalies as large as 2000 gammas, and the gravity results indicated local anomalies as great as 30 mgals. Examination of the gravity anomaly map (Fig. 26) shows a positive anomaly area centered about 8 miles northwest of Antigo which has a radius of approximately 6 miles. In the same area the magnetic anomaly map (Fig. 25) shows a broad magnetic high having a tri-lobate pattern upon which local peaks are superimposed. Similarly another anomalous area involving both sets of data is found which centers about 4 miles southeast of Antigo. Section A-A of Figs. 25 and 26 crosses both areas. A sectional profile along traverse A-A is shown in Fig. 27. Regional trends are seen to be present in both sets of data and these trends have been sketched in to isolate that part of the anomaly due to local near surface causes.

The residual for the northwest magnetic anomaly area is seen to have a smooth, slightly asymmetric profile with 1000 gammas relief, while that for the southeast anomaly area appears to be a composite from two separate sources. Similarly the residual for the northwest gravity anomaly area appears to be a composite resulting from two small mass effects superimposed upon that of a single large mass which is probably related to the same geologic cause as that responsible for the magnetic anomaly. The residual for the southeast gravity anomaly area appears to correlate with the eastern member of a pair of adjacent magnetic anomalies noted in this area. In both sets of data, another anomaly area is indicated to the southeast just beyond the boundaries of the survey.

II-2g Interpretation of Gravity and Magnetic Results

The problem of interpretation here is to decide whether the anomalies are due entirely to changes in rock type at depth or whether a change in the topographic relief of the basement is also involved. In order to evaluate this, certain assumptions have to be made as to the probable shape of the disturbing mass, the kinds of rocks that might be involved, and their depth.

Table 9

Table of Magnetic and Gravity Anomaly Values
Antigo, Wisconsin

Magnetic Values in gammas and Gravity Results in mgals

Anomaly			Anomaly		
Magnetic Gravity			Magnetic Gravity		
Sta.	(gammas)	(mgals)	Sta.	(gammas)	(mgals)
1	524	-78.8	36	58	-60.6
2	662	-78.5	37	233	-59.3
3	886	-78.2	38	237	-54.6
4	1086	-78.2	39	410	-53.1
5	796	-79.7	40	620	-69.3
6	554	-79.2	41	441	-66.1
7	1670	-82.4	42	576	-63.2
8	2204	-80.2	43	1135	-58.4
9	273	-78.7	44	967	-54.7
10	468	-75.5	45	996	-56.2
11	1154	-71.4	46	572	-59.4
12	1498	-76.1	47	477	-66.9
13	1390	-77.5	48	338	-69.1
14	1475	-77.9	49	747	-64.5
15	1253	-78.5	50	874	-59.4
16	1219	-77.9	51	544	-61.2
17	1766	-77.7	52	721	-57.4
18	1876	-77.5	53	965	-53.4
19	1527	-77.6	54	898	-52.1
20	890	-67.9	55	1244	-51.6
21	935	-68.8	56	418	-54.9
22	742	-74.4	57	1058	-55.8
23	873	-77.2	58	574	-54.8
24	718	-76.4	59	597	-55.9
25	561	-75.2	60	508	-61.6
26	575	-69.5	61	186	-72.5
27	467	-66.3	62	581	-60.7
28	479	-65.1	63	1300	-57.8
29	302	-63.7	64	1672	-62.3
30	265	-51.5	65	0	-68.6
31	438	-70.9	66	90	-70.1
32	426	-65.2	67	275	-69.5
33	452	-62.8	68	151	-66.5
34	267	-71.7	69	1312	-69.0
35	190	-61.4	70	492	-71.6

Table 9 (continued)

Sta.	Anomaly	
	Magnetic (gammas)	Gravity (mgals)
71	354	-68.9
72	165	-70.3
73	1266	-66.7
74	1105	-72.7
75	70	-74.0
76	218	-73.3
77	208	-77.8
78	326	-80.6
79	333	-81.8
80	365	-75.4
81	429	-76.1
82	443	-81.1
83	496	-84.3
84	582	-81.2
85	473	-85.4
86	522	-82.7
87	387	-82.0
88	394	-85.9
89	367	-83.6
90	291	-79.1
91	239	-74.6
92	212	-69.8
93	3	-66.8
94	34	-75.5
95	204	-73.7
96	383	-77.8
97	533	-80.7
98	478	-83.9
99	586	-84.4
100	603	-84.9
101	1013	-78.5
102	991	-80.5
103	1047	-79.5
104	1059	-80.8
105	1674	-77.9
106	1932	-68.5
107	1970	-65.9
108	2484	-65.5
109	1374	-79.5
110	1435	-80.3
111	1307	-80.4
112	1191	-79.3

Sta.	Anomaly	
	Magnetic (gammas)	Gravity (mgals)
113	272	-79.8
114	1382	-72.3
115	1387	-74.6
116	634	-77.7
117	1246	-81.1
118	480	-84.0
119	574	-83.9
120	553	-83.0
121	1331	-83.0
122	1297	-84.5
123	506	-84.4
124	601	-82.8
125	435	-77.6
126	558	-83.8
127	444	-76.5
128	566	-75.0
129	837	-73.2
130	684	-76.5
131	852	-71.2
132	868	-81.4
133	1048	-82.6
134	1680	-84.9
135	533	-84.6
136	616	-82.8
137	1278	-81.4
138	1075	-81.9
139	761	-87.2
140	730	-85.4
141	2870	-80.1
142	1298	-80.1
143	530	-77.7
144	1414	-80.2
145	960	-82.1
146	1098	-83.2
147	889	-83.0
148	955	-82.6
149	819	-68.9
150	1066	-79.8
151	1399	-79.5
152	1334	-77.6
153	1396	-80.4
154	1390	-72.4

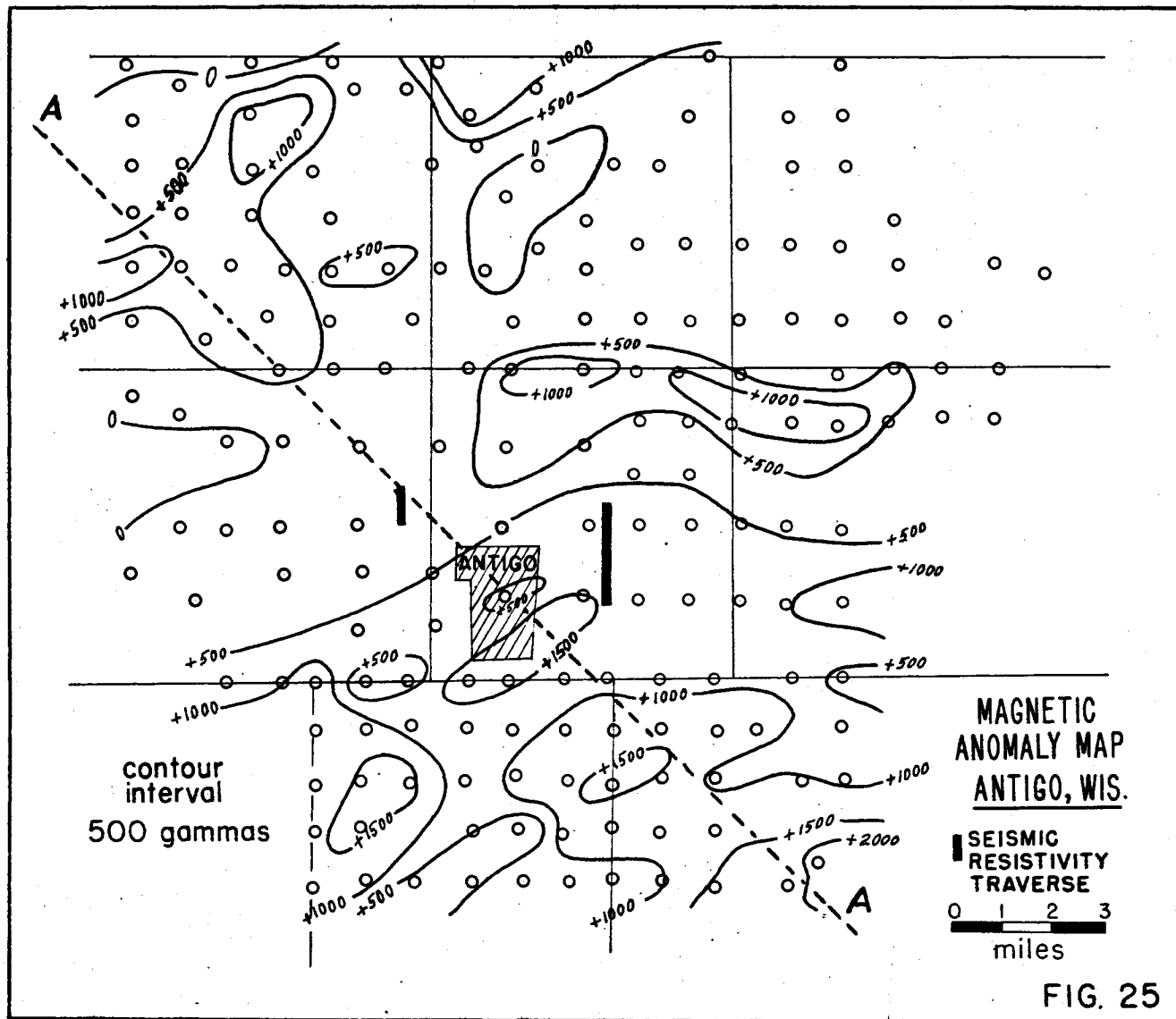
Table 9 (continued)

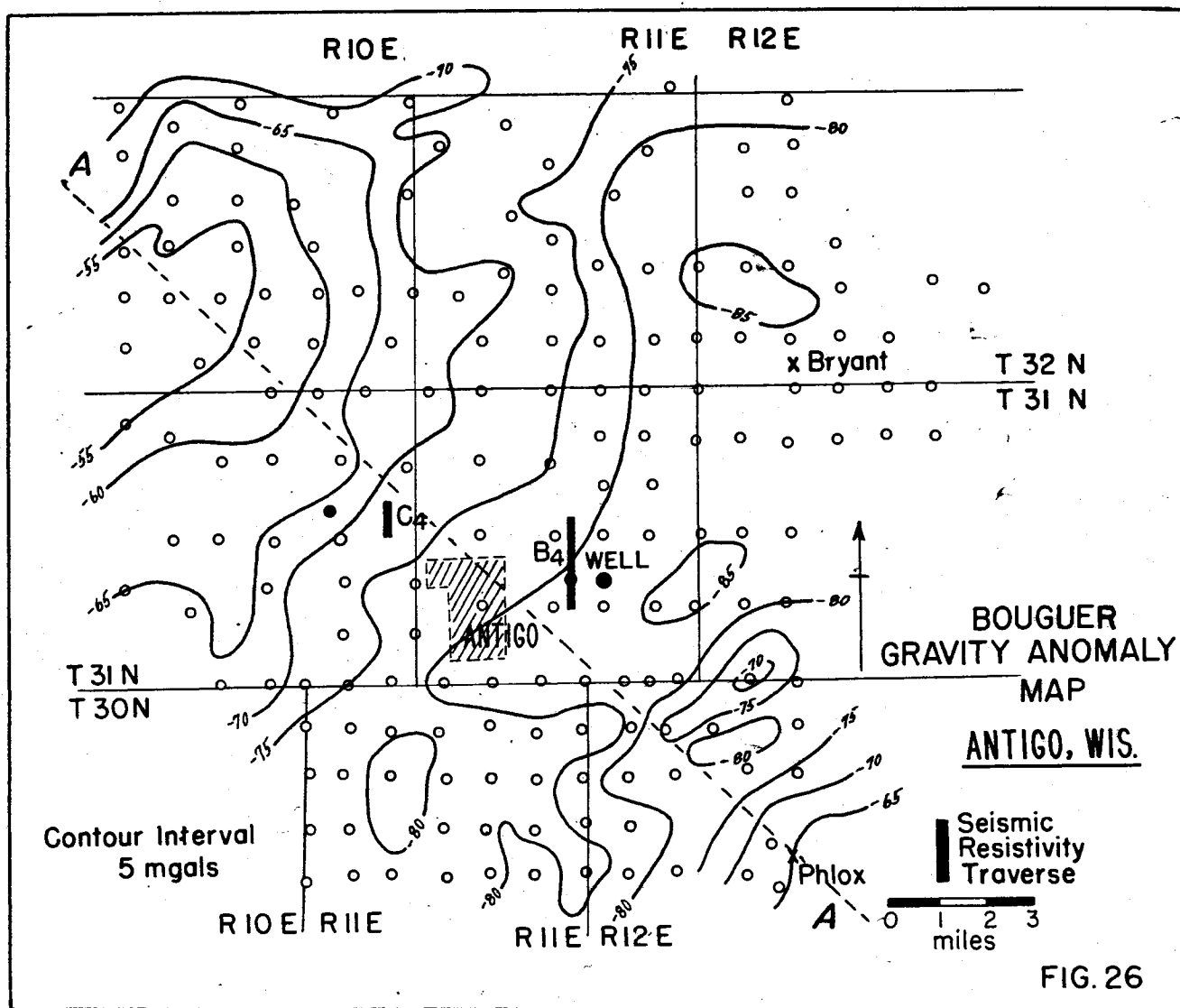
Sta.	Anomaly		Sta.	Anomaly	
	Magnetic (gammas)	Gravity (mgals)		Magnetic (gammas)	Gravity (mgals)
155	1386	-82.3	168	612	-83.0
156	829	-77.8	169	450	-80.5
157	1423	-79.0	170	503	-82.4
158	1528	-79.7	171	649	-83.4
159	1653	-80.7	172	671	-86.3
160	1567	-77.2	173	847	-79.4
161	611	-82.9	174	1325	-77.6
162	631	-82.0	175	956	-74.3
163	578	-82.5			
164	548	-83.8	Q-28	610	-78.0
165	476	-80.6	Y-28	343	-71.7
166	527	-80.5	W-13	206	-70.4
167	607	-82.4			

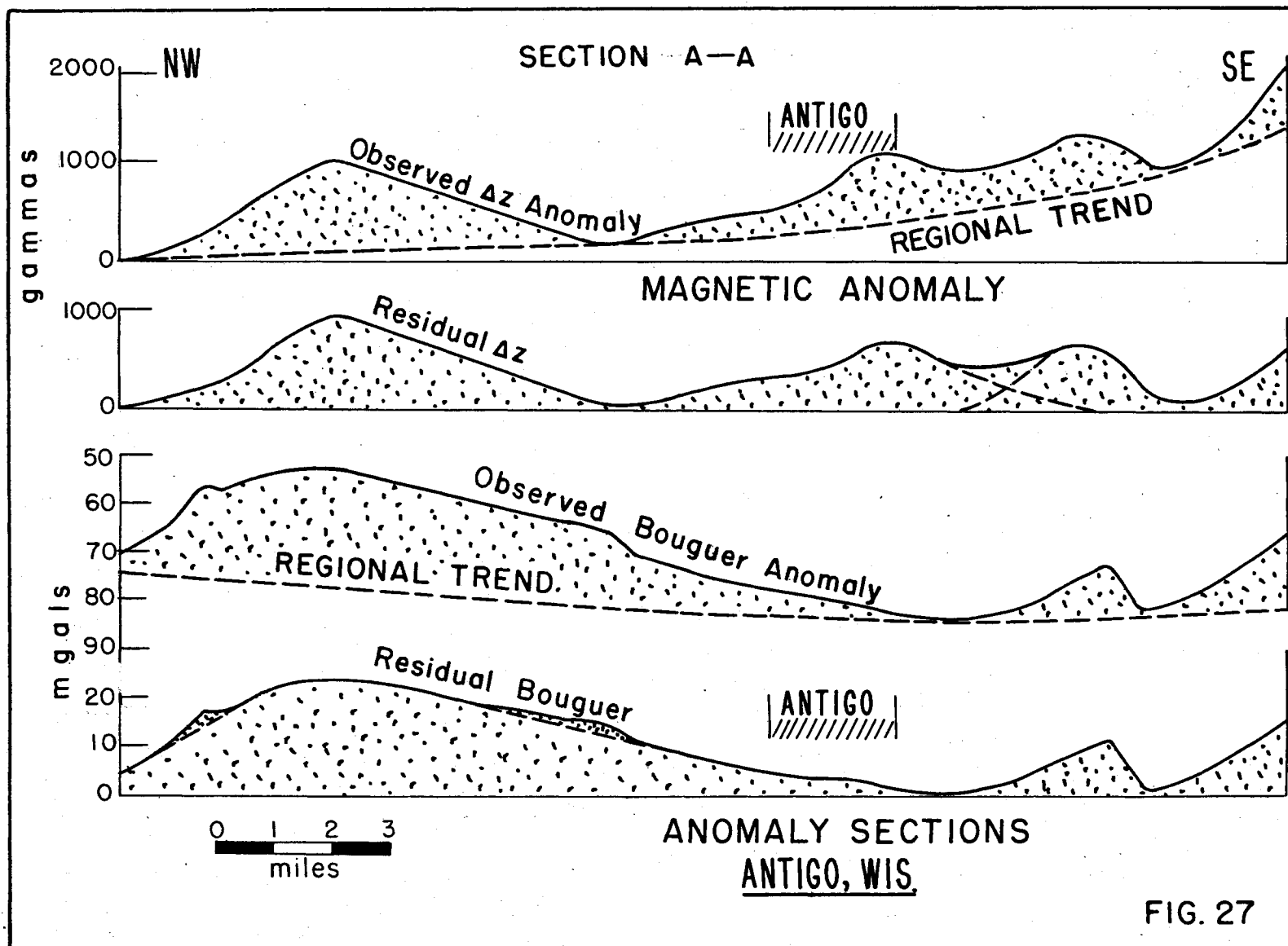
Northern Anomaly Area:

Consider first the northwestern anomaly area shown in Fig. 26. The gravity anomaly pattern is roughly circular in outline suggesting a mass that might have the form of a sphere or a vertical cylinder. The magnetic anomaly pattern on the other hand, is located at the apices of a triangle about three miles on a side. (Fig. 25) Since there is not a corresponding pattern of magnetic "lows" which would indicate the presence of deeper oppositely polarized areas that would be obtained with a vertical cylindrical body, it is probable that the disturbing masses are more or less spherical. On this assumption, then, the depth to the center can be estimated on the basis of the relationship of the width of the anomaly area corresponding to half the amplitude of the anomaly. This "half-width" value defines a maximum depth from which the anomaly can originate.

Consider for the moment only the most northern portion of the magnetic anomaly (top leaf of the tri-lobate pattern) and assume that the gravity anomaly represents the aggregate from three separate but closely spaced rock masses as suggested by the magnetic anomaly pattern. Using the "half-width" values, the depth to the center of a mass giving this local magnetic anomaly of 1000 gammas is approximately 1.4 miles, but on the basis of the much larger gravity anomaly, the depth to the center of the disturbing mass would be 3.2 miles. To resolve this apparent discrepancy, it is necessary to explore by quantitative calculations which appears to be the more reasonable.







As both gravity and magnetic "highs" are obtained, it can be assumed that the anomaly results from the intrusion of a basic rock such as gabbro into granitic rocks. Gabbro has a density varying from 2.9 to 3.0 gm/cm³, while granite gneiss has a density of about 2.65 gm/cm³. Moreover, magnetite, the mineral which accounts for most magnetic anomalies, is generally sparse in granites but nearly always plentiful in gabbro.

Assuming the above two rock types with a density contrast of 0.25 gm/cm³ the gravity data can be analyzed in terms of a sphere.

$$g = \frac{4\pi R^3 \gamma \sigma z}{3r^3}$$

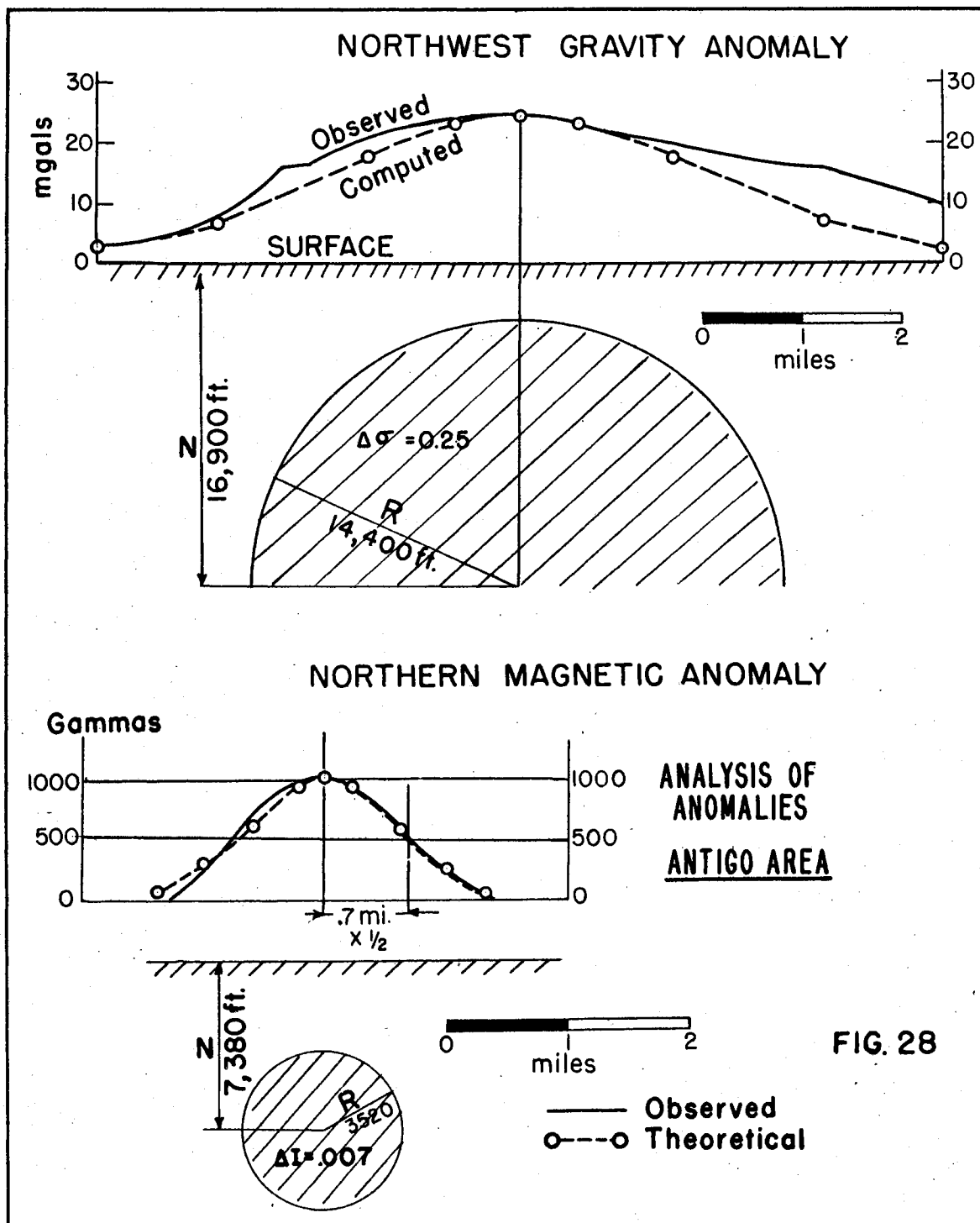
in which γ = the gravitational constant 6.67×10^{-8}
 σ = the density contrast = 0.25 gm/cm³
 z = depth to center = 3.2 miles
 r = distance from center, zero over center
 R = radius

Solving with these values it is found that the peak anomaly of 22 mgals would require a spherical mass having a radius of 14,400 feet (2.7 miles). This would bring the top of such a gabbroic mass within 2500 feet of the surface. However, further computations of the theoretical effects of such a mass, out to distances of 5 miles from the center, show that this interpretation will not satisfy completely the anomaly values away from the center position in that the observed anomaly is broader than that which would result from such a rock mass. See Fig. 28.

Approaching the problem in terms of the northern-most magnetic anomaly of the tri-foliate pattern whose residual profile is shown in Fig. 28, the following expression can be applied for vertical polarization. (As the actual inclination of the earth's field is about 75° in Wisconsin, this assumption is close enough for practical purposes.)

$$V = \frac{4\pi R^3 I}{3z^3} \cdot \frac{2 - (x/z)^2}{[1 + (x/z)^2]^{5/2}}$$

in which V = anomaly (1000 gammas)
 R = radius
 I = polarization contrast
 z = depth to center = 1.4 miles
 x = horizontal distance from the center



If it is assumed that the gabbro has 4 % more magnetite than the granitic gneiss, the polarization can be computed as $I = .04 \times .3H$ where .3 is the magnetic susceptibility of magnetite and H the vertical component of the earth's magnetic field in Wisconsin = 0.6 oersteds. Therefore,

$$I = .04 \times .3 \times .06 = .007 \text{ cgs.}$$

On this basis the radius of the mass giving rise to the observed 1000 gamma anomaly is about 3500 feet. Computing effects at different distances from the center show that such a gabbroic mass with a 4 % magnetite contrast at a depth of 1.4 miles (7380 feet) would have a magnetic effect very closely approximating that observed. See Fig. 28. It is thus seen that, on either basis of interpretation, the top of the disturbing mass would lie more than 2500 feet beneath the surface and hence it is not likely there would be any marked expression of its presence in the relief of the basement rock surface which lies only about 100 feet beneath the surface.

Studying these anomalies further, however, it is found that the gravitational effect of the basic rock mass satisfying the local magnetic anomaly having a radius of 3500 feet and buried at a depth of 7380 feet would be only 2.5 mgals. This is about the amount of gravity excess indicated by the observed anomaly in the flank areas over the theoretical gravity value for the aggregate mass. It therefore appears possible that the tri-foliate peak pattern is related to cupolas on the top of a much larger rock mass whose overall size is best reflected by the gravity anomalies. That this larger mass at depth must have less magnetite than is present in the postulated cupolas is suggested by the fact that if the same polarization contrast was used to compute the magnetic effect of the larger mass satisfying the gravity anomaly as was assumed for the postulated cupola, the resultant magnetic anomaly would be over 3000 gammas. The observed anomaly value for the broad magnetic high, however, is only about 1000 gammas.

In order to reconcile more closely the depths to the top of the postulated basic intrusive rock mass as determined magnetically and gravitationally, a greater density contrast than 0.25 must be assumed since the postulated cupola is at a lower elevation than the postulated parent mass. The use of a density contrast of 0.3 gm/cm^3 assuming 2.95 gm/cm^3 for the density of the gabbro for example, would decrease the radius of the large mass from 14,400 feet to 13,000 feet. This would place the top 3900 feet beneath the surface and be more in agreement with the depth of 3800 feet as determined from the magnetic data. It will be noted this change in density and size of the resultant body will not change the computed theoretical effect. Both conditions will satisfy equally well the observed anomaly.

Other Anomaly Areas:

The failure to obtain a gravity anomaly "high" corresponding to the magnetic "high" in the immediate vicinity of Antigo indicates that, while there is undoubtedly a high concentration of magnetite in the rocks of this area, the general petrologic composition has not changed from that of a granitic type rock. The adjoining gravity and magnetically high area which has a lenticular pattern in both sets of data suggest that here the petrology of the rocks has changed to a more basic type. That the anomaly is not due to a basement rock ridge can be easily demonstrated. On the basis of the seismic depths, it is known that the crystalline rock basement does not lie at a depth greater than 225 feet. Therefore, any basement ridge could not have a height greater than this value. On the basis of the gravity anomaly pattern, the ridge could not be more than a mile in width. Assuming a specific gravity contrast between gabbro and glacial till of 0.8 gm/cm^3 and approximating the ridge as a slab 200 feet thick the gravitational effect would be only 1.9 mgals whereas the observed anomaly is about 12 mgals or about six times as great.

In this area it can only be concluded that gravity and magnetic data are not definitive as regards locating the areas having high or low basement relief. These methods appear most useful here for delimiting areas that may have relief associated with change in petrology. In passing, attention should be called to the fact that granite areas are usually identified as gravity minima and frequently form topographic high points, whereas areas of basic rocks are usually identified as gravity maxima and usually have little topographic relief. This difference in relief results from the differential resistance of the two types of rock to weathering. However, as shown here, the anomalies frequently result from intra-basement masses which may never reach the surface of the crystalline rock complex.

II-2h Conclusion on Study at Antigo

The seismic method appears to be the best of the various geophysical techniques tried in the Antigo area for determining the depth of water table and the underlying rock layers as well as determining the nature of the rock types present. The electrical resistivity measurements, while agreeing as to the amount of the grosser changes in the depth to the crystalline rock surface and in part also the depth of the water table, do not give as good agreement with the available well data as do the seismic measurements. Failure of the resistivity method in this respect can be attributed directly to the lack of a readily applicable theoretical method for analyzing the results obtained.

The analyses of the gravity and magnetic studies showed that the presence of rather large intra-basement rock masses so dominate the gravitational and magnetic field in this area that these methods cannot be readily applied for studying the relief of the underlying crystalline rock surface, or even for delineating the variations in the kinds of crystalline rock which comprise it. On the other hand, the variations in the true seismic velocity values associated with the crystalline rock surface show considerable variation (13,800 - 22,080 ft./sec.) and these can be used for outlining the variations in its petrologic composition.

II-3 - Seismic Investigation at Gresham, Wisconsin

II-3a General Statement

The village of Gresham lies in Shawano County where the till directly overlies the basement crystalline rock surface. In this area the till is the primary aquifer and additional subsurface water can generally be secured only from unpredictable fractures in the underlying crystalline rock surface which is usually described as "granite". No well log data were available but rock outcrops could be seen on the far bank of the stream above the dam north of the village. The problem was to define the area within the village boundaries where the till was thickest and determine if a buried pre-glacial valley was present which might contain sand and gravel and serve as an alternative aquifer.

II-3b Seismic Investigation

Seismic refraction measurements using the reverse shooting technique were employed and depths and velocities were determined at 20 locations. Two seismic horizons were found to be present. The upper horizon had a velocity of about 6200 ft./sec. and was identified as till, and the lower with a velocity of about 19,000 ft./sec. was identified as crystalline rock. The velocity, depth and sea level elevation of each horizon is given in Table 10.

Fig. 29 shows the location of the seismic stations and the bedrock contours based on the seismic depths. An examination of this map indicates that a buried valley is suggested in the northern part of the area studied. The axis of the valley strikes approximately 30° west of North and the center line lies approximately below seismic site 14.

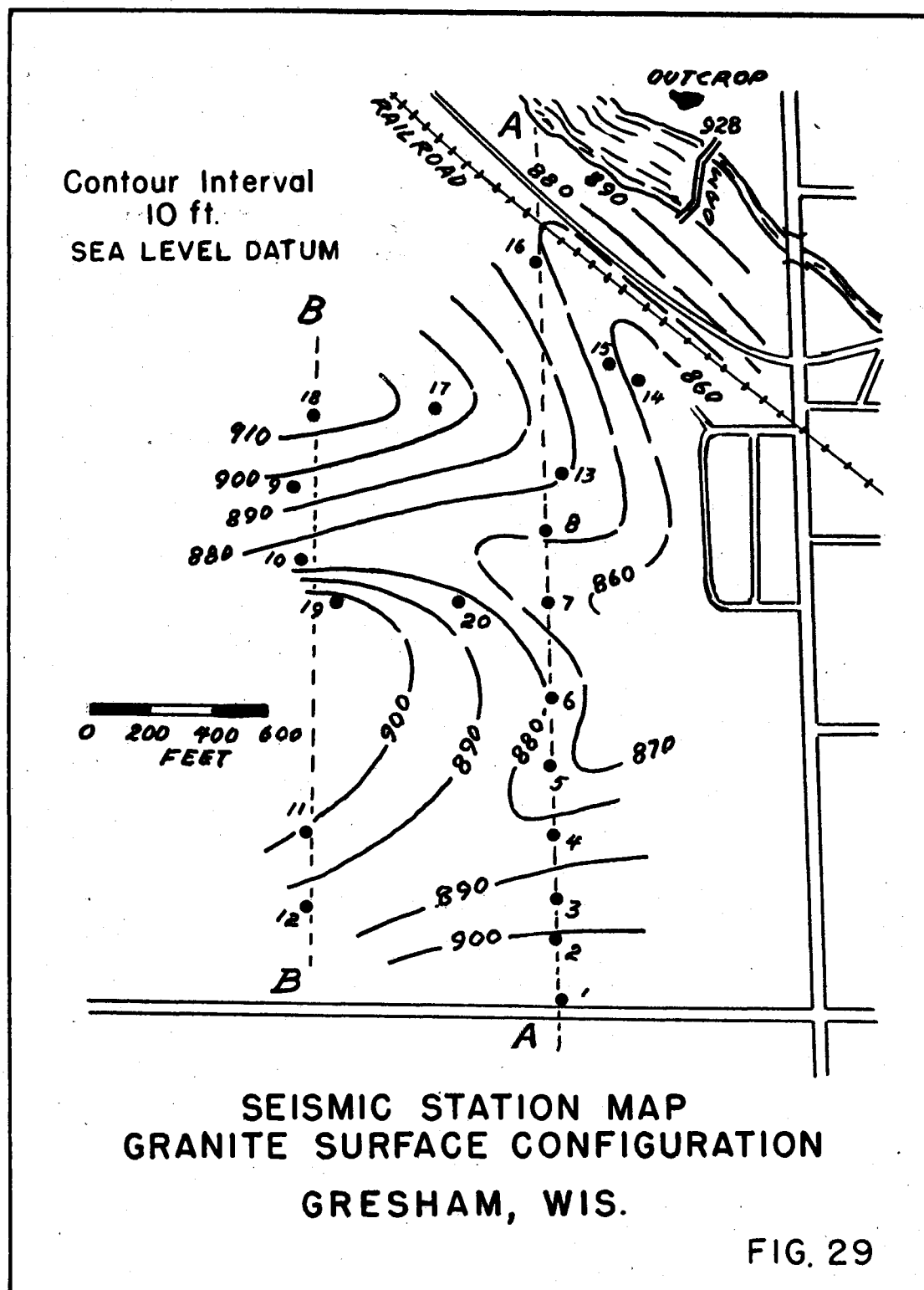
Table 10

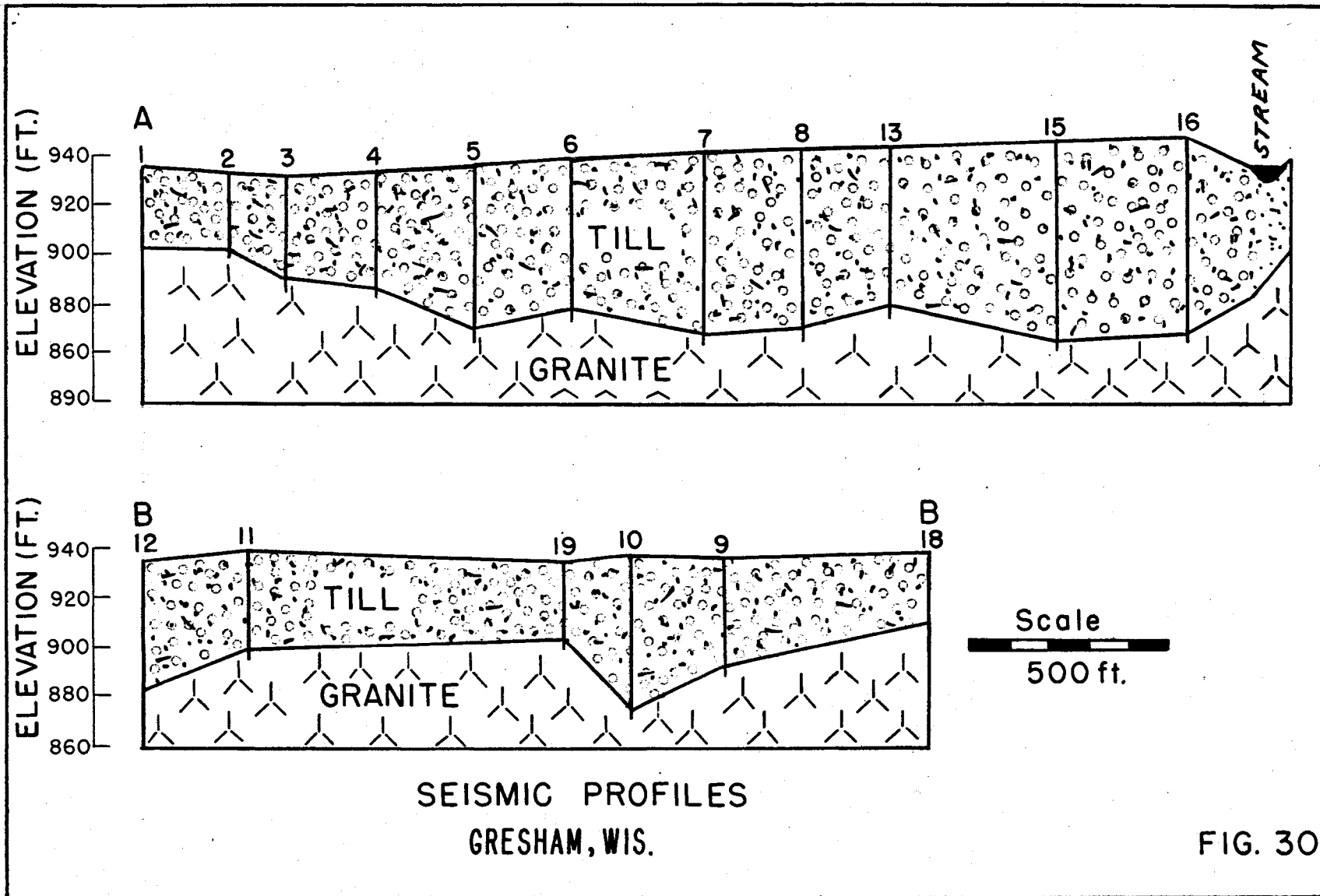
Seismic Data, Gresham, Wisconsin

Station	Apparent Velocity		Depth to Horizon	Sea Level Elevation
	V ₁	V ₂	V ₂	V ₂
1a	5370	21500	33	903
2a	6380	14500	32	902
3b	2000	20000	42	892
4b	6600	20200	50	888
5c	6670	20000	66	872
6c	4830	20000	61	880
7a	6240	20000	76	868
8a	6700	20000	72	872
9e	7350	16400	43	896
10e	6920	20000	63	876
11f	7000	17000	40	899
12f	6690	20000	49	882
13g	4990	10370	63	881
14g	7750	30100	85	856
15h	4375	17630	81	864
16h	4180	20000	80	872
17i	5000	12200	36	907
18i	6670	12500	28	912
19j	5740	16120	31	906
20j	7420	24400	53	885

V₁ = velocity of surface material (glacial till).

V₂ = velocity of V₂ layer, (crystalline rock)
average true velocity = 18,644 ft./sec.





A tributary to this valley is indicated between seismic sites 7 and 8. As seen from this map and profiles A-A and B-B, Fig. 30, the bottom of the main valley lies about 65 feet below the general elevation of the surrounding bed rock surface and it also is about 50 feet below the level of the bottom of the present surface stream valley which lies over its northeast flank. This area should constitute a good site for test drilling from the standpoint of thickness of till aquifer present, possible channel sand aquifer at depth, and recharge from the surface stream. At the time of this report there is no record of any subsequent drilling that might verify the accuracy of this study.

II-4 - Campbellsport, Wisconsin

II-4a General Statement

The town of Campbellsport lies in an area of glacial till underlaid by the Niagara Dolomite. Subsurface water supplies are available from the till, from cavernous structures within the dolomite and from deeper Paleozoic sandstones which constitute artesian aquifers in this area. As the latter are over 2000 feet deep and likely to be saline in this area, the purpose of the investigation was to determine where the thickness of till was greatest in order that it could be exploited more effectively as an aquifer.

The problem, therefore, was to map the configuration of the Niagara Dolomite surface underlying the till. It was also hoped that a buried pre-glacial valley might be located which might contain sands and gravel that would constitute a better aquifer than the till.

II-4b Seismic Investigation

Three areas were chosen by the village authorities for study, and seismic depths were determined at 42 sites using the reverse shooting refraction method. At most of these locations three seismic layers were identified. In Area I, the upper horizon (V_1) had a velocity varying from 1500 ft./sec. to 3000 ft./sec. with a mean of 1700 ft./sec. which was identified as unsaturated glacial till. The second horizon (V_2) had a velocity varying from 4500 ft./sec. to 9000 ft./sec. with a mean of 6000 ft./sec. which was tentatively identified as either an older till layer or weathered dolomite. This layer however was present at only about one third the sites studied in this area. The third horizon (V_3) had a velocity varying from 10,000 ft./sec. to 20,000 ft./sec. with a mean of 12,500 ft./sec. which was identified as the Niagara Dolomite.

In Area II, the correlations were the same as in Area I with the upper horizon (V_1) having a mean velocity of 2000 ft./sec. The second layer (V_2) had a mean velocity of 9500 ft./sec., which horizon was present at about half the sites in the area. The third horizon (V_3) correlated with the Niagara Dolomite with a mean velocity of 14,800 ft./sec. In Area III, all three seismic layers were observed at all the observation points. The layer identified as till, V_1 , had a velocity of 2000 ft./sec. The V_2 horizon identified as older till or weathered dolomite had a mean velocity of 8000 ft./sec. The V_3 horizon, identified as dolomite, had a mean velocity of 16,000 ft./sec.

Because of the lack of well log data, the greatest uncertainty here was in the identification of the V_2 horizon. In view of the wide spread in true velocity values (7000 ft./sec. to 11,700 ft./sec.) it appeared that this horizon varied geologically, or else it represented a differentially weathered layer of the V_3 dolomite horizon. The velocity values themselves suggested a sandstone, but this was not regarded as likely on the basis of the known general geology of the area. The wide spread in the V_3 horizon true velocity values (10,700 ft./sec. to 21,600 ft./sec.) was believed either to reflect cavernous development in the dolomite or else variations in the lithology of the dolomite as might be occasioned by the inclusion of reef facies.

Complete velocity and depth data for all horizons in each area are given in Tables 11, 12, and 13. In Figs. 31, 32, and 33, the elevation data for the V_3 , Niagara Dolomite, horizon are plotted and contoured. In Figs. 34 and 35, sections are drawn along the traverses which show the depth relations of each velocity layer interface to the surface. From these maps and sections it is seen that buried valleys are indicated in the V_3 surface in both Areas I and II but not in Area III. It is also seen that although the V_1 horizon maintains a fairly constant thickness, the V_2 horizon occurs mostly as fill material where there is a depression in the V_3 surface. This strongly suggests the V_2 material is older till, although the velocity values are abnormally high as compared to those obtained elsewhere for this material (5500 ft./sec. to 7500 ft./sec.).

As no subsequent drilling has been undertaken in this area the above interpretation cannot be evaluated, but in any event, the two valleys appear to be the logical sites for test drilling to explore the possibility of developing a shallow ground water supply.

Table 11

Seismic Data at Campbellsport, Wisconsin

Area I

Station	Apparent Velocity			Depth from Surface		Elevation of Surface	
	V ₁	V ₂	V ₃	V ₂	V ₃	V ₂	V ₃
1a	2000	8750	-----	13	---	1024	-----
2a	1670	4740	15000	7	31	1028	1004
3b	1820	4060	11250	4	22	1036	1018
4b	1480	-----	10230	---	14	-----	1022
5c	1250	7400	-----	8	---	1027	-----
6c	-----	-----	-----	---	---	-----	-----
7d	2450	-----	15000	---	11	-----	1025
8d	2000	-----	10000	---	11	-----	1026
9e	1780	-----	12670	---	9	-----	1026
10e	1430	-----	9090	---	8	-----	1028
11f	3100	-----	12500	---	21	-----	1018
12f	1820	8120	11820	9	27	1031	1013
13g	1620	3420	17270	9	51	1038	996
14g	-----	-----	-----	---	---	-----	-----
15h	2040	-----	18000	---	14	-----	1021
16h	2530	7940	20000	12	37	1023	998

- V₁ = glacial till
V₂ = older glacial till, weathered dolomite or sandstone(?)
average true velocity = 6750 ft./sec.
V₃ = Niagara Dolomite, average true velocity =
12,956 ft./sec.

Table 12

Seismic Data at Campbellsport, Wisconsin

Area II

Station	Apparent Velocity			Depth from Surface		Elevation of Surface	
	V ₁	V ₂	V ₃	V ₂	V ₃	V ₂	V ₃
171	6000	10000	18000	16	52	1018	982
181	1970	11760	14280	11	36	1026	1001
19j	2060	8340	19640	7	49	1033	991
20j	1640	7830	13100	7	24	1032	1015
21k	1530	-----	13890	--	10	-----	1034
22k	1450	-----	14250	--	10	-----	1031
231	1450	12440	20520	9	60	1026	975
241	1970	10980	22500	12	70	1027	969
25m	1550	-----	13890	--	9	-----	1024
26m	3550	-----	17240	--	14	-----	1017
27n	4580	-----	15130	--	14	-----	1016
28n	5340	10000	14700	10	24	1020	1006
29o	3280	8480	23640	4	40	1028	992
30o	3620	9910	19830	12	43	1020	989
31p	1690	-----	15130	--	12	-----	1022
32p	2500	-----	14100	--	13	-----	1020

V₁ = glacial till

V₂ = older till, weathered dolomite or sandstone(?)
Average true velocity = 9977.5 ft./sec.

V₃ = Niagara Dolomite, average true velocity =
11,685 ft./sec.

Table 13

Seismic Data at Campbellsport, Wisconsin
Area III

Station	Apparent Velocity			Depth from Surface		Elevation of Surface	
	V ₁	V ₂	V ₃	V ₂	V ₃	V ₂	V ₃
33q	1970	7540	17500	7	39	1040	1008
34q	2030	10870	17740	11	61	1027	977
35r	1970	10200	16670	9	46	1031	994
36r	2600	11210	17740	12	34	1034	1012
37s	2060	7500	15830	8	35	1039	1012
38s	1270	7840	14430	8	52	1042	998
39t	3290	7140	12200	7	36	1050	1021
40t	2570	8870	11760	9	46	1035	998

V₁ = glacial till

V₂ = older till, weathered dolomite, sandstone(?)
Average true velocity = 8862 ft./sec.

V₃ = Niagara Dolomite, average true velocity =
15,487.5 ft./sec.

Table 14

Seismic Data at Campbellsport, Wisconsin
Area IV

Station	Apparent Velocity			Depth from Surface		Elevation of Surface	
	V ₁	V ₂	V ₃	V ₂	V ₃	V ₂	V ₃
41u	6040	-----	19000	---	46	---	900
42u	6360	-----	13710	---	40	---	906

(approx.)

V₁ = water saturated till of older till (?)

V₂ = Niagara Dolomite, average true velocity =
16,350 ft./sec.

SEISMIC STATION MAP AND
CONFIGURATION OF NIAGARA
DOLOMITE SURFACE AREA I

CAMPBELLSPORT, WIS.

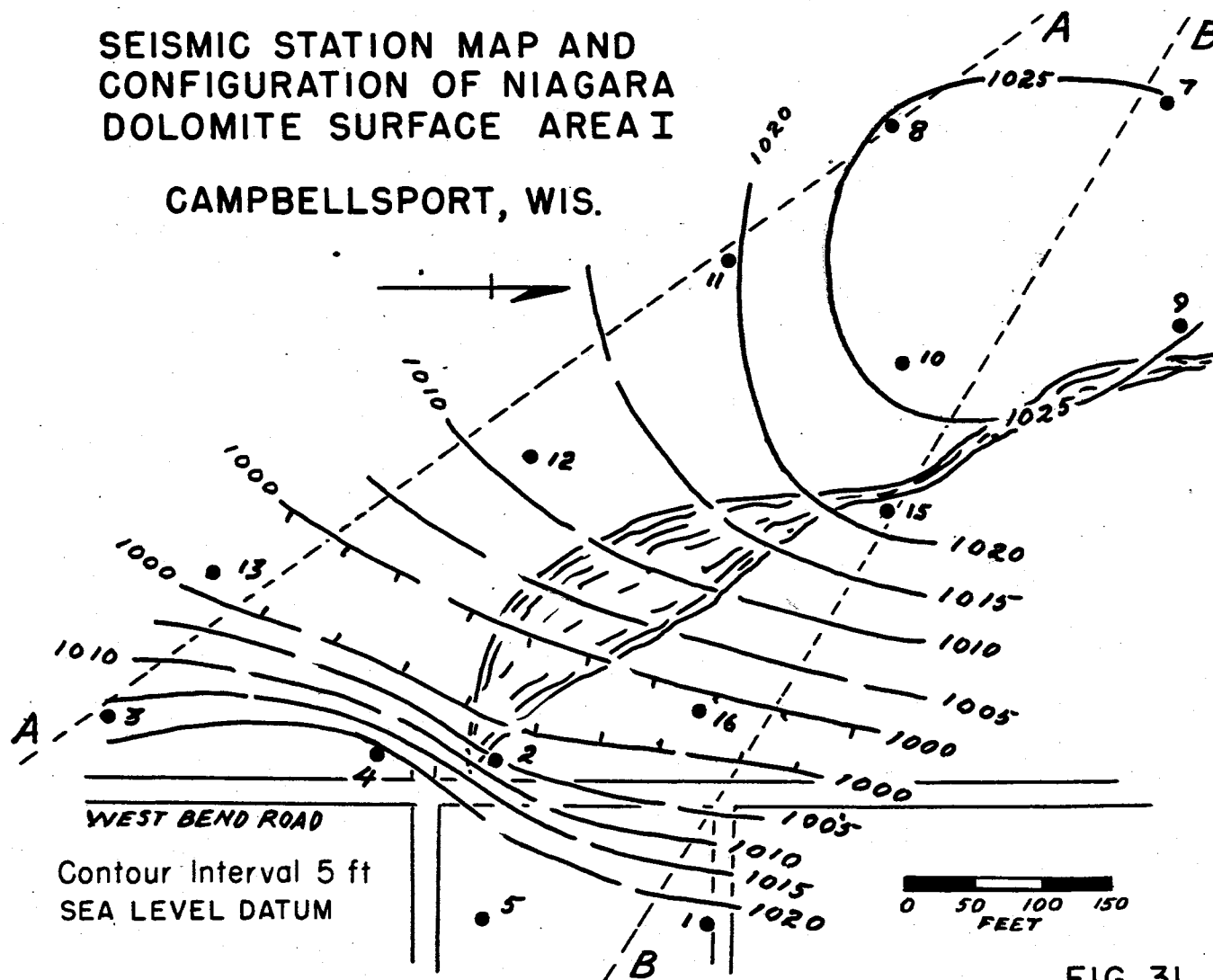


FIG. 31

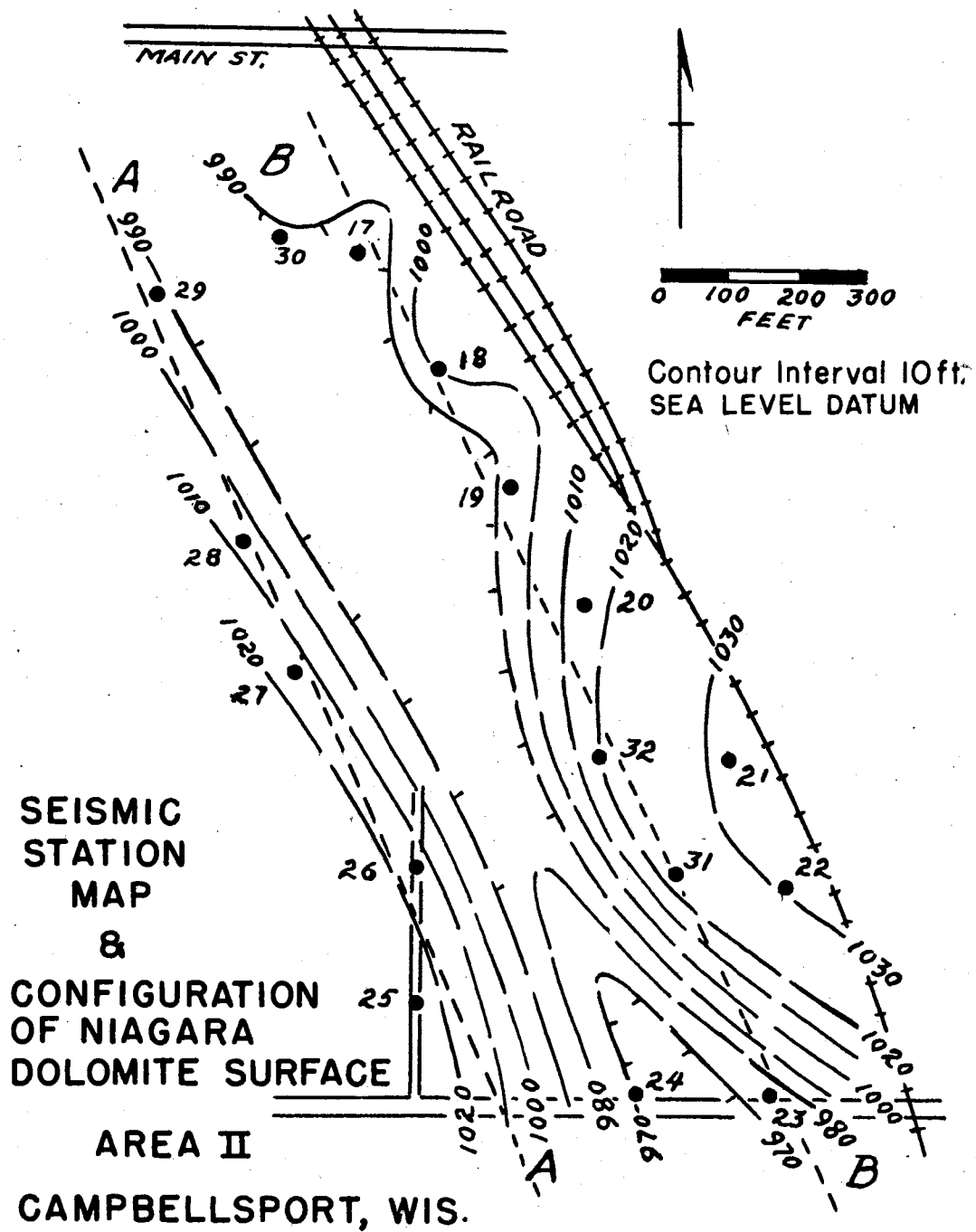
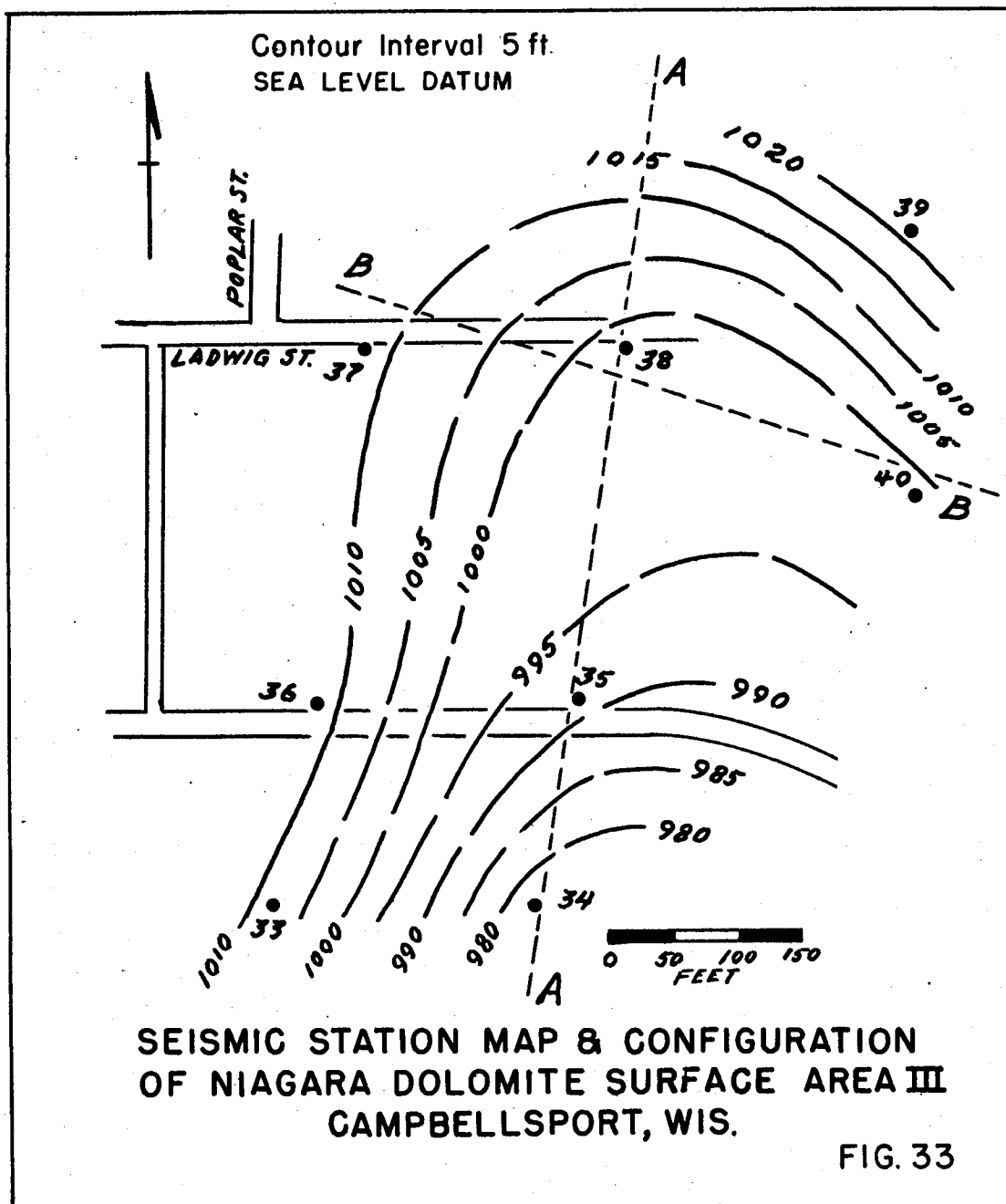
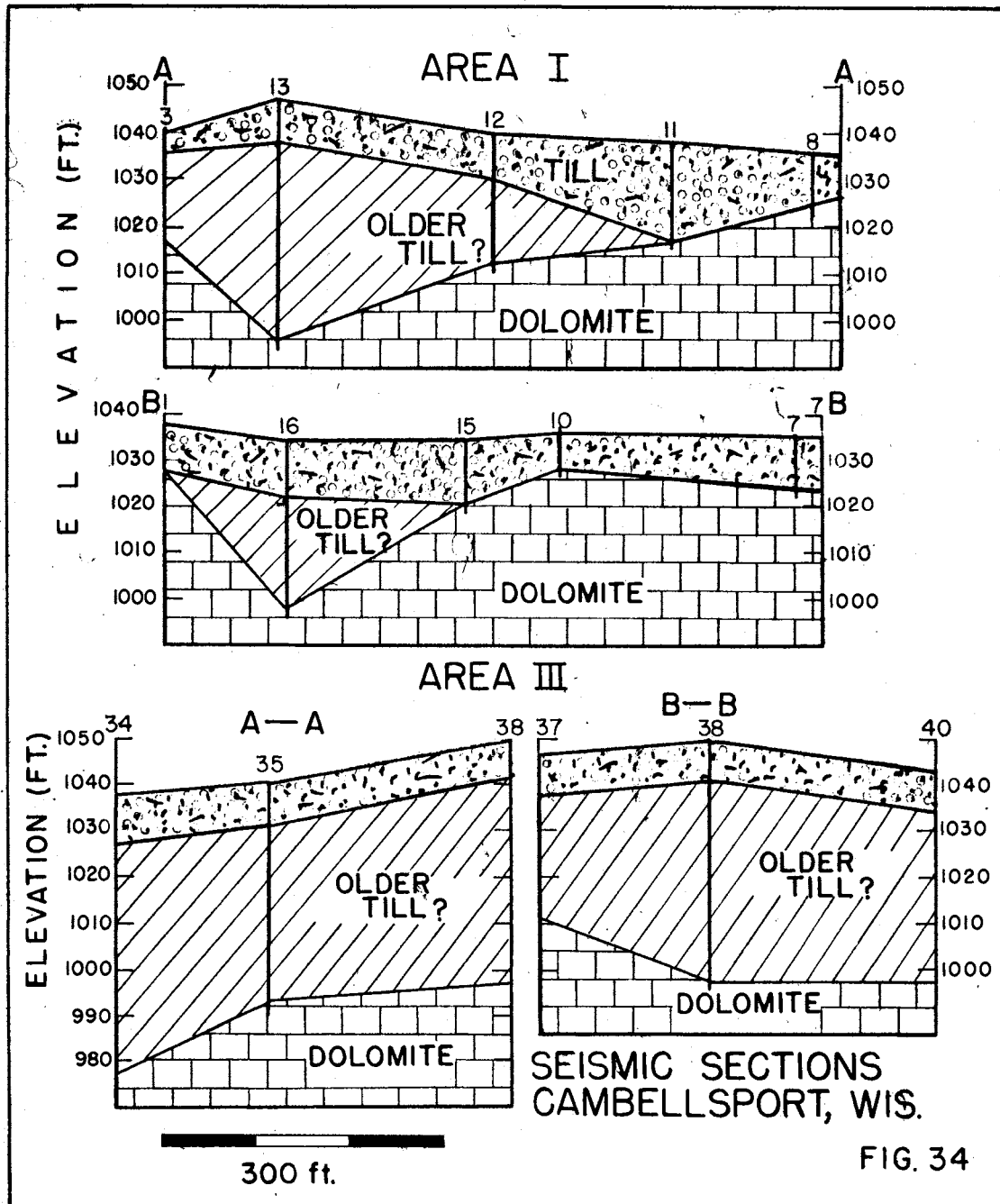
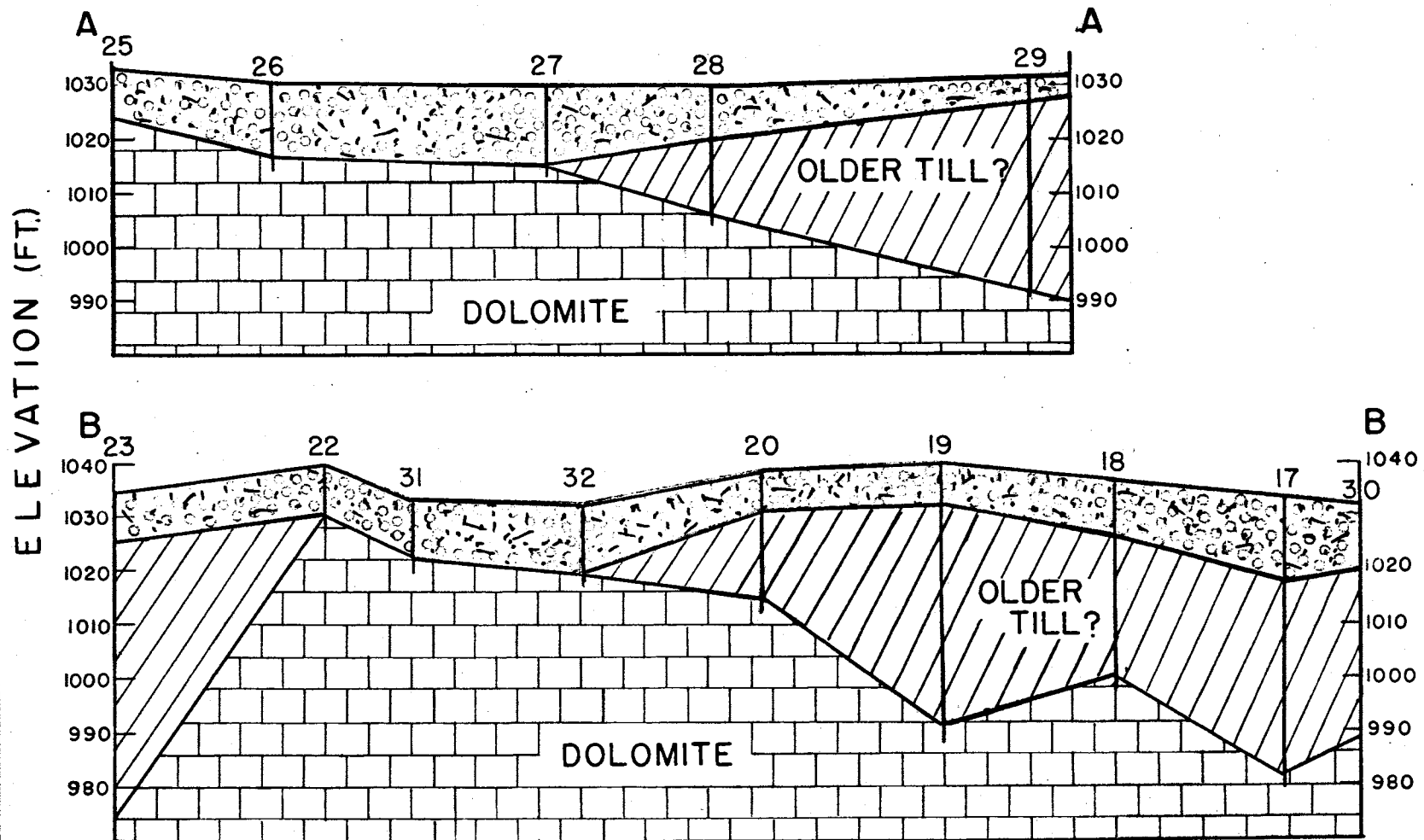


FIG. 32







SCALE
300 ft.

SEISMIC SECTIONS AREA II
CAMBELLSPORT, WIS.

FIG. 35

Two additional measurements were made east of the city dump to check on a postulated fault. These data are summarized in Table 14. These measurements show there is a change of about 100 feet in the elevation of the dolomite in this area from that in the other areas studied. This is also the approximate change in surface elevation between areas. The data, therefore, can be interpreted as supporting the idea of a fault lying between the two areas.

II-5 - Hudson, Wisconsin

II-5a General Statement

The town of Hudson lies on the east bank of the St. Croix River at the foot of a high bluff formed by the Mt. Simon Sandstone and the Eau Claire formations which are topped by glacial drift. The problem here was to locate the depth to water table, the base of the till, and if possible the depth to the pre-Cambrian crystalline rock surface. The area of investigation was one chosen on top of the bluff by the town authorities.

This study was undertaken under very adverse weather circumstances and, as a consequence, was of a limited nature. It was necessary to get a snow plow to clear the lines along which observations were to be made and the temperature during the study averaged about 30° below zero.

II-5b Seismic Investigation

Depths were determined at six sites bracketing the area of a proposed well using the reverse shooting refraction technique. Three seismic velocity horizons were found. The upper horizon (V_1) had a velocity of approximately 1360 ft./sec. and was identified as unsaturated glacial drift. The second horizon (V_2) had a velocity of approximately 5250 ft./sec. and was identified as water table. The third velocity horizon (V_3) had a velocity averaging 8200 ft./sec. and was identified as the underlying sandstone. One long spread was shot in an attempt to determine the depth to the basement surface and although no exact depth was determined, it could be safely said that this surface lay at a depth greater than 400 feet. In Table 15, the pertinent data obtained at each site are given.

The location of the seismic stations and the position of the proposed well are shown in Fig. 36. Schematic contours on the V_3 (sandstone) surface are also shown, and it is seen that a buried valley is indicated between sites 3N and 3S. This valley is shown along traverse A-A in Fig. 37, and it is seen that its axis chances to coincide approximately with the proposed well location where the depth to sandstone, as determined from seismic data, is about 240 feet.

Table 15

Seismic Values, Hudson, Wisconsin

Station	A pparent Velocity			Depth to Surface		Elevation of Surface	
	V ₁	V ₂	V ₃	V ₂	V ₃	V ₂	V ₃
1N	1370	5250	8220	96	218	741	622
1S	1370	5250	8220	98	184	714	655
2N	1354	5230	8100	100	230	734	614
2S	1354	5230	8100	102	185	739	656
3N	1385	5160	8690	97	222	749	624
3S	1385	5160	8690	100	192	742	650

V₁ = unsaturated glacial till

V₂ = water staured glacial till (water table surface)

Average true velocity = 5213 ft./sec.

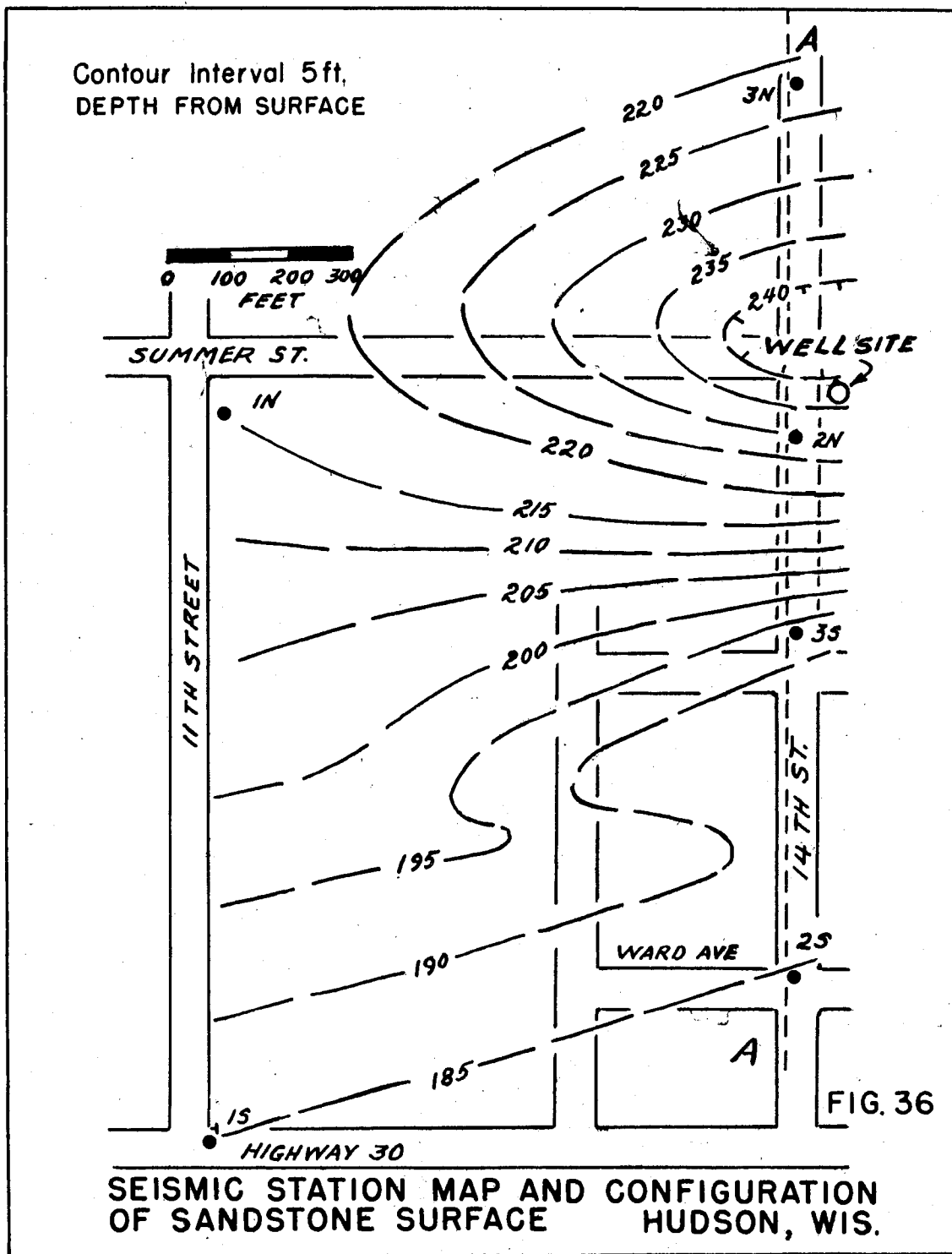
V₃ = sandstone (?) Average true velocity = 8336 ft./sec.

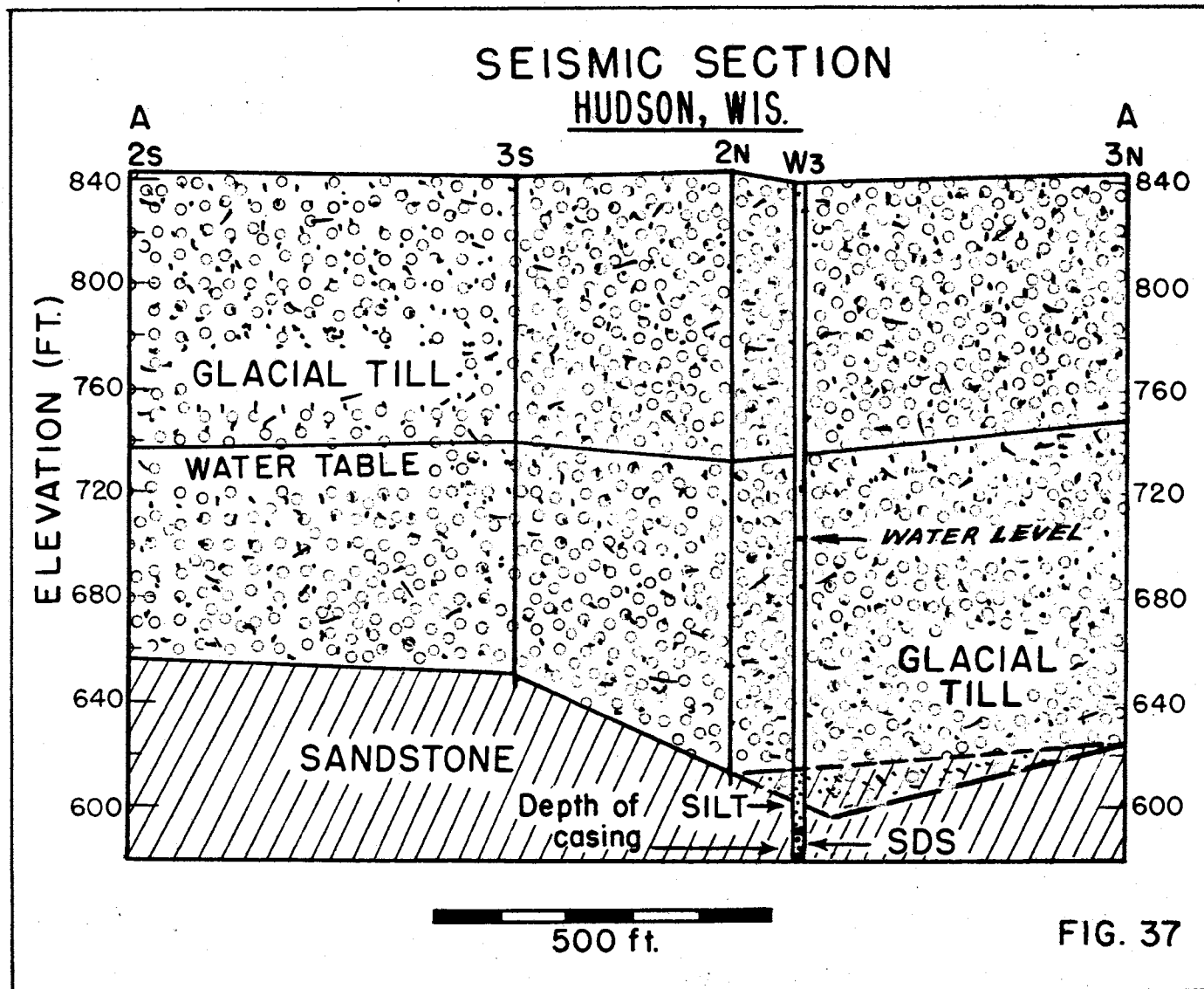
II-5c Evaluation of Results

Two years after the completion of the above study a well was drilled at about the site indicated. The condensed log of the well is as follows:

Glacial Drift	0 - 215 ft.	sand—medium to coarse
	215 - 245	silt, slightly dolomitic (till?)
	245 - 250	gravel and sand
<hr/>		
Eau Claire Formation	250 - 265	siltstone
	265 - 270	sandstone
<hr/>		
Mt. Simon Formation	270 - 375	sandstone
	375 - 385	siltstone
	385 - 480	sandstone
	480 - 490	siltstone
	490 - 530	sandstone
<hr/>		
Pre-Cambrian Basement	530 - 543	shale

Well cased to 257.75 feet. Static water level , 139 feet.





Comparing the results of the driller's log with the seismic data the agreement between the two is fairly good except on depth to water. The calculated seismic data to the top of the sandstone was approximately 240 feet. The well log shows the base of the drift to be at 250 feet. The seismic data showed the basement to lie at a depth greater than 400 feet. The well log shows that basement is not encountered until 530 feet. The depth to water as indicated by the seismic measurements was 100 feet while that in the completed well was 139 feet.

There are three possible explanation for this discrepancy regarding the depth to water: (1) The siltstone horizon acts as an impermeable barrier separating the sandstone aquifer from the drift. As the well is cased through the latter it would be the water level in the sandstone which is reflected in the well. Because the sandstone is exposed in the bluffs, it is free to discharge water, which would lower the piezometric surface in the sandstone while the water level in the drift might be less affected due to a lower hydraulic gradient. (2) If there is free communication between the sandstone and the drift, a frost barrier might have formed in the sub-zero weather preventing leakage from the bluffs and raising water level. (3) The water table may have been lowered during the two years between the investigation and the completion of the well by increased demand, decrease in recharge or a combination of both.

Regardless of the true explanation, there appears to be no reason to doubt that the water levels mapped in the drift were accurate at the time of the survey in 1951. Evidence to support this is as follows:

1. If the water depth was in error by 40 feet, the depth to the sandstone also would have been in error instead of essentially correct.
2. All six sites give depths to the water surface that agree within a few feet. If this surface were not real at the time of the investigation, it is highly unlikely that this would have been the case.

II-6 - Clark County Hospital, Wisconsin

II-6a General Statement

The Clark County Hospital is located in a section of the state where glacial till lies for the most part directly upon the crystalline basement rock surface. Locally thin layers of Cambrian sandstone may intervene, but these are discontinuous and seldom reach 10 feet in thickness. As in all such areas, the till and sandstone constitute the principal subsurface source of water. Here, as at Gresham, the problem was to locate the maximum thickness of sediments above the crystalline rock surface and search for a buried valley which might contain sand and gravel.

II-6b Seismic Investigation

The seismic refraction method was used to establish depths at thirty-six locations using the reverse shooting method and only two seismic horizons were detected. The upper horizon had a mean velocity of about 5000 ft./sec. and was identified as being unconsolidated rock, probably glacial till. The lower horizon had a mean velocity of about 18,000 ft./sec. and was identified as being the basement complex. The velocity values obtained at each site and the computed depths are given in Table 16.

The locations of the seismic stations are shown in Fig. 38. An approximate representation of the basement rock surface was obtained by contouring the seismic depths but since the control is limited, this contour map can only be regarded as suggestive. As a supplement to the above a vertical section along traverse A-A is shown in Fig. 39.

II-6c Evaluation of Results

A buried valley in the area is indicated by Fig. 38 and Fig. 39 but nowhere does there appear to be more than about 80 feet of material above the crystalline rocks. To a limited extent this is checked by the data of the existing well at the hospital which is believed to have encountered the basement surface at a depth of about 62 feet. However, the results of test drilling at 10 sites within the area, some prior to the seismic work and some following it, did not at first appear to substantiate the seismic results. Three test holes indicated till lying directly on the basement rocks, and of the remaining seven, all but two indicated the presence of intervening sandstone. The maximum thickness of sandstone reported was 14 feet, but most of the occurrences were nearer 5 feet.

It was not surprising that the seismic measurements did not indicate the presence of this sandstone as the spacing of the detectors did not permit the detection of such a thin stratigraphic unit. Further, since the velocity of sound in the sandstone (about 7500 ft./sec.) is not greatly different from that in the till, such thin layers would have no appreciable effect other than slightly raising the apparent velocity values of the till. The same effect could be created by an increase in the degree of water saturation of the till with no change of material.

It was surprising that the logs for the test holes reported so little glacial till in contrast to the indications of the seismic measurements.

Table 16

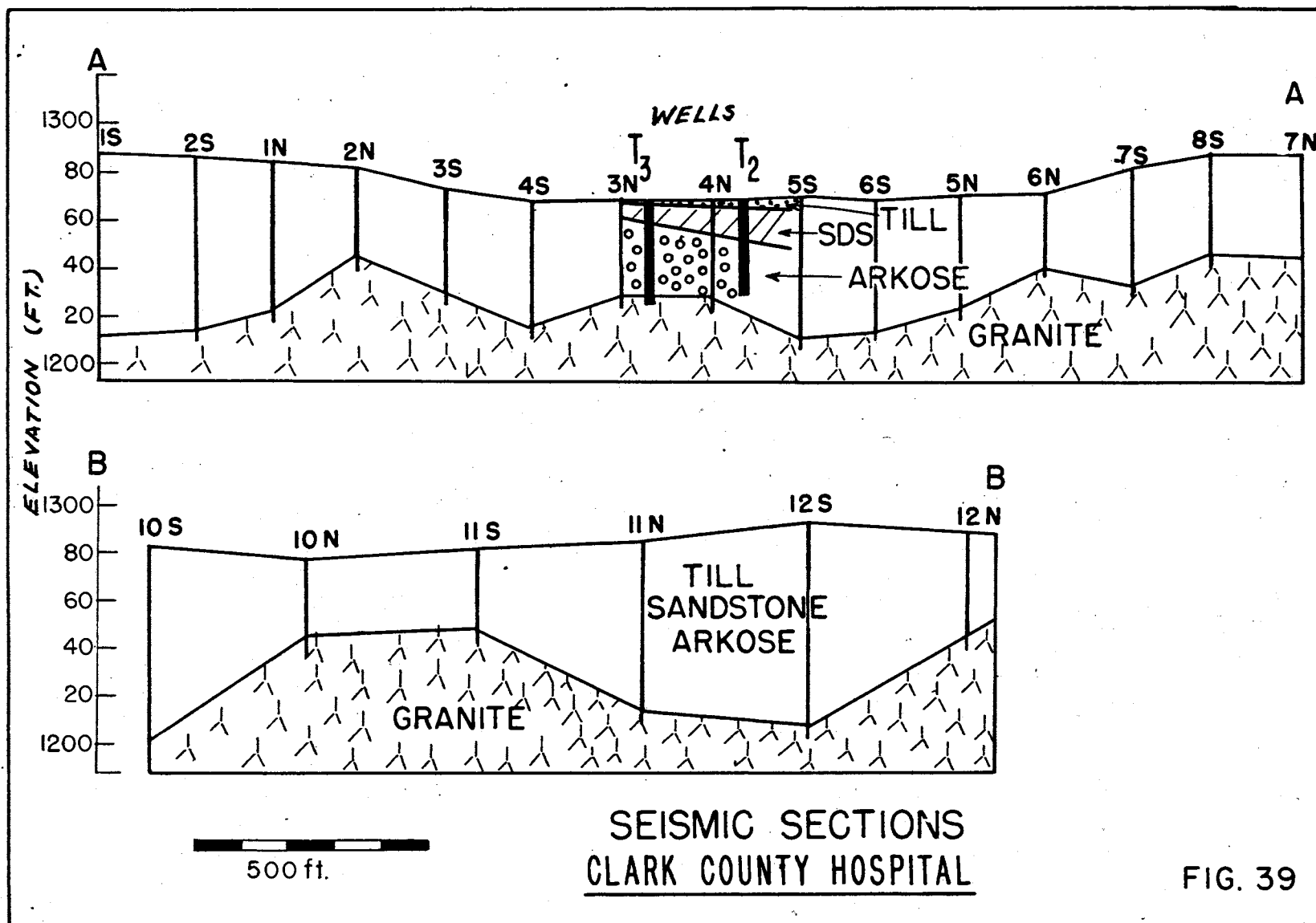
Seismic Data for Clark County Hospital, Wisconsin

Station	Apparent Velocity		Depth to Horizon V ₂	Sea Level Elevation V ₂
	V ₁	V ₂		
1a	5800	17000	77	1211
1b	5800	15600	63	1222
2a	8800	22000	73	1215
2b	4500	13400	39	1244
3a	6200	16000	44	1229
3b	7000	3350	36	1228
4a	6000	29000	50	1217
4b	6200	17400	39	1230
5a	6200	20000	60	1211
5b	5500	18000	51	1222
6a	7700	37000	55	1216
6b	6400	15400	33	1240
7a	5000	14000	44	1234
7b	5200	14000	46	1245
8a	5000	12400	40	1247
8b	5000	22000	65	1229
9a	6100	28800	44	1218
9b	6000	16000	29	1219
10a	5800	24000	83	1200
10b	5600	20000	35	1243
11a	6000	20500	29	1252
11b	5800	21600	69	1216
12a	5000	28000	86	1207
12b	3700	20400	50	1243
13a	5300	16300	15	1238
13b	5300	18400	33	1228
14a	3300	22000	30	1239
14b	4000	28000	53	1220
15a	5700	15200	48	1246
15b	5400	15000	46	1222
16a	3800	14500	40	1243
16b	4700	28000	72	1216
17a	5500	26000	65	1223
17b	4500	16700	73	1213
18a	3800	18000	72	1216
18b	4500	24000	83	1200

V₁ = velocity of surface layer (glacial till and sandstone)

V₂ = velocity of second layer (basement crystalline rock)

Average true velocity = 20555.6 ft./sec.



The average depth was only about ten feet and greatest thickness, twenty-five feet. The bulk of the section above the basement rock appeared to be detrital material derived from granite that had been transported and laid down as an unconsolidated arkose. All of the test holes showed a considerable thickness of this material which is variously described as "decomposed granite", "rewashed granite", "clay", "schist", "granite wash", "quartz pebbles", etc. Since this material would have essentially the same velocity as the overlying sandstone stringers and the glacial till, it was not differentiated by the seismic measurements. The only seismic discontinuity mapped was related to the boundary between this "granite wash" which is frequently characterized by a pebble layer at or near its base, and the "granite" (crystalline rock) surface proper.

From the standpoint of water supply, the decomposed granite would have a considerably higher permeability than the till and would form a more satisfactory aquifer.

Although the location of the test holes was not given by the driller, the approximate positions were given for two new wells, but unfortunately neither of these wells definitely entered the underlying crystalline rock. Well No. 2, described as located 245 feet southeast of Well No. 1, bottomed at 37 feet below the surface at an elevation of 1233 feet in "decomposed granite with much mica". Well No. 3, described as being located 270 feet south of southeast of Well No. 2, terminated at an elevation of 1226 feet in schist or gneiss, decomposed and rewashed granite with rounded quartz pebbles at the base. Although the location of Well No. 1 was not known, it was possible from the surface elevation data and the relative location of Well No. 2 to Well No. 3 to approximate the positions of these wells. The elevation of the (V_2) crystalline rock surface according to the seismic data at positions fitting these given descriptions varies from 1228 to 1235 feet at Well No. 2 and from 1224 to 1230 feet at Well No. 3. As the seismic elevations agree within limits of ± 5 feet with those shown by the wells it may be concluded that the seismic data are valid and define the surface of the crystalline rock.

II-7 - Vesper, Wisconsin

II-7a General Statement

The town of Vesper lies in an area where there is a thin layer of glacial till and sandstone lying directly upon the crystalline basement rock surface. The crystalline rock surface here appears to be rather uneven and granite outcrops at various places around the town. As in Clark County, the problem was to determine locations having the maximum thickness of overlying sediments as these constitute the principal aquifer of the region.

II-7b Seismic Investigation

The seismic refraction reverse shooting technique was used and depth determinations were made at 46 sites. See Fig. 40.

Three velocity layers were found to be present; a surface layer (V_1) with a velocity ranging from 1630 ft./sec. to 6900 ft./sec., identified as glacial till; a second layer (V_2) with a velocity ranging from 6700 to 10,500 ft./sec. identified as Cambrian sandstone; and a third layer (V_3) with a high velocity varying from 13,100 to 20,000 ft./sec. identified as the basement crystalline rock complex having a variable petrologic composition.

In Table 17, the velocity data, depths, and sea level elevations of each layer are given for each seismic site. As the distribution of stations did not permit contouring, the elevation data for the sandstone granite surfaces are listed at each seismic site in Fig. 40. In Fig. 41, vertical sections are shown along the traverses indicated in Fig. 40.

II-7c Discussion of Results

Traverse A-A: This is a SE-NW section paralleling the railroad tracks southeast from Vesper. Sandstone up to 20 feet in thickness is indicated in the southern part of the section, but to the northeast, it is either absent or of such limited thickness it was not detected.

Traverse B-B: This section runs north-south and is along the highway leading to Vesper from the south. Here the crystalline basement rock surface appears to be conformable to the surface topography over much of the traverse. Sandstone occurs to the south of site 6 but none was recorded to the north. This agrees with what is known of the local geology as granite outcrops occur to the north and sandstone outcrops are observed to the south. A maximum thickness of 45 feet of sandstone is indicated at site 10.

Traverse C-C: This traverse runs north-south along County Trunk Highway "C" to the east of Vesper. The seismic data on this section indicate erratic structure but in general, sandstone appeared to be present over most of the traverse with a maximum thickness of nearly 50 feet at site 45.

Traverse D-D: This traverse runs north-south along the east boundary of Range 5-E to the east of Vesper. Sandstone appears to be present north of site 28 with a maximum thickness of 20 feet at site 26.

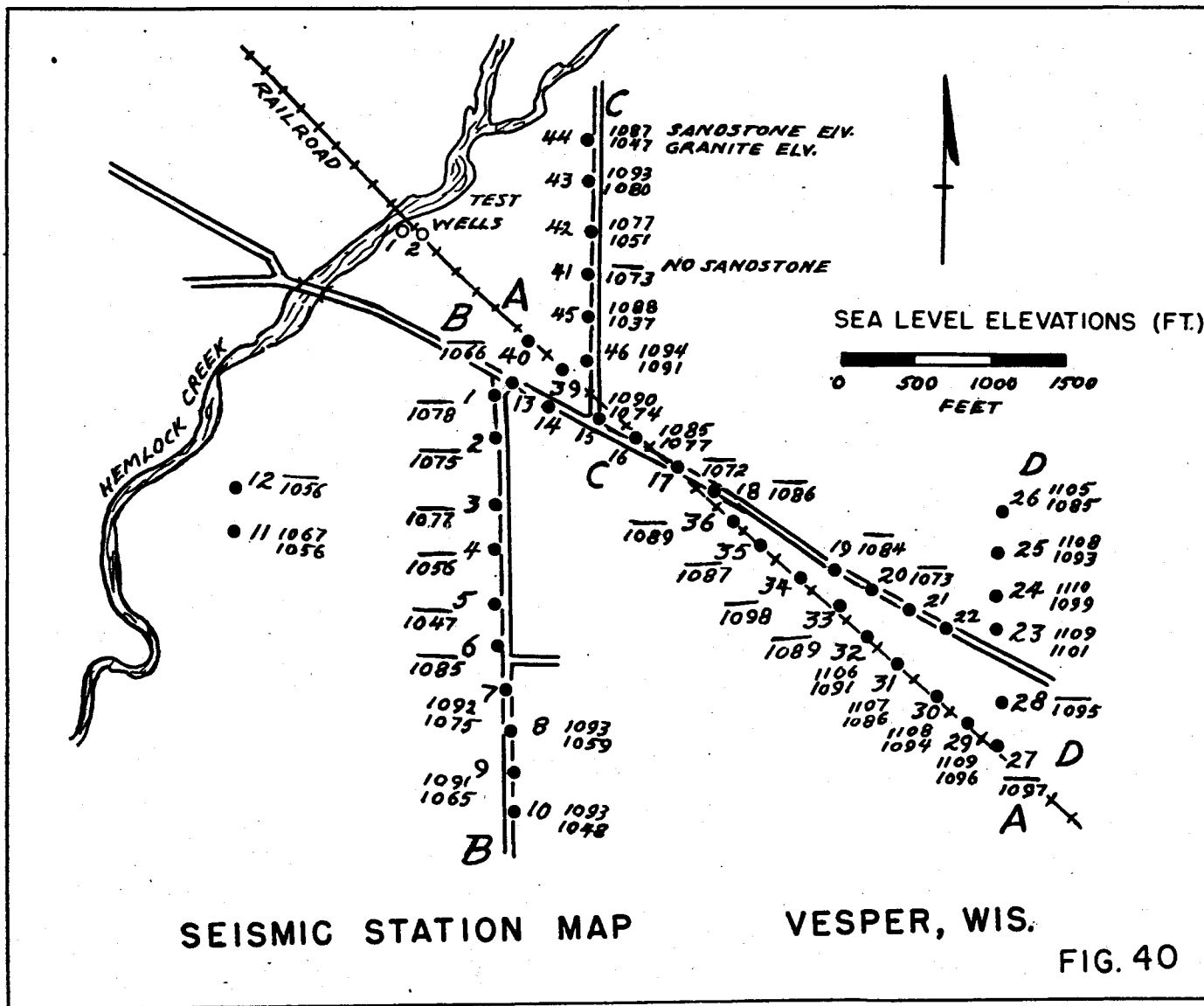


Table 17
Seismic Data, Vesper, Wisconsin

Station	Apparent Velocity			Depth to Horizon		Sea Level Elevation	
	V ₁	V ₂	V ₃	V ₂	V ₃	V ₂	V ₃
1a	5900	-----	17780	---	10	-----	1078
2a	5900	-----	21050	---	13	-----	1075
3b	5900	-----	14550	---	10	-----	1077
4b	5900	-----	23170	---	24	-----	1056
5c	6270	-----	14750	---	38	-----	1047
6c	6280	-----	16250	---	47	-----	1085
7d	3800	8250	15290	6	23	1092	1075
8d	3800	7590	20000	11	45	1093	1059
9e	5110	9860	17890	13	29	1091	1075
10e	3300	8024	23430	12	57	1093	1048
11f	5540	-----	20530	5	17	1067	1055
12f	-----	8560	16670	0	13	-----	1056
13g	4620	-----	15800	---	8	-----	1080
14g	4620	-----	10390	---	7	-----	1085
15h	3360	10530	15000	7	23	1090	1074
16h	3360	10530	19000	14	22	1085	1077
17i	1740	-----	23080	---	28	-----	1072
18i	1520	8330	-----	---	15	-----	1086
19j	4090	-----	14560	---	21	-----	1084
20j	4550	-----	22050	---	34	-----	1073
21k	6170	8730	16460	4	33	1105	1076
22k	6170	10810	21760	3	58	1098	1053
23l	5000	5595	16250	5	13	1109	1101
24l	5000	7333	18750	5	16	1110	1099
25m	6260	9900	15500	11	26	1108	1093
26m	5610	10550	17380	10	30	1105	1085
27n	5710	-----	16660	---	15	-----	1097
28n	6270	-----	20280	---	18	-----	1095
29o	-----	10000	19666	5	19	1109	1094
30o	-----	9850	18095	6	19	1108	1094
31p	-----	6720	16750	5	26	1107	1086
32p	-----	8118	18500	5	19	1106	1091
33q	6240	-----	18000	---	9	-----	1099
34q	6240	-----	19060	---	10	-----	1098
35r	5744	-----	21560	---	19	-----	1087
36r	6730	-----	17630	---	14	-----	1089
37s	-----						
38s	Records Ruined						
39t	6250	-----	12140	---	18	-----	1073
40t	6250	-----	20580	---	24	-----	1066

Table 17 (continued)

Station	Apparent Velocity			Depth to Horizon		Sea Level Elevation	
	V ₁	V ₂	V ₃	V ₂	V ₃	V ₂	V ₃
41u	5000	-----	15600	—	22	-----	1073
42u	3859	11610	21560	17	43	1078	1052
43v	6900	9558	16950	4	17	1093	1080
44v	6900	9642	19290	10	50	1087	1047
45w	-----	8061	27350	5	56	1088	1037
46w	-----	8060	14070	3	6	1094	1091

V₁ = glacial till

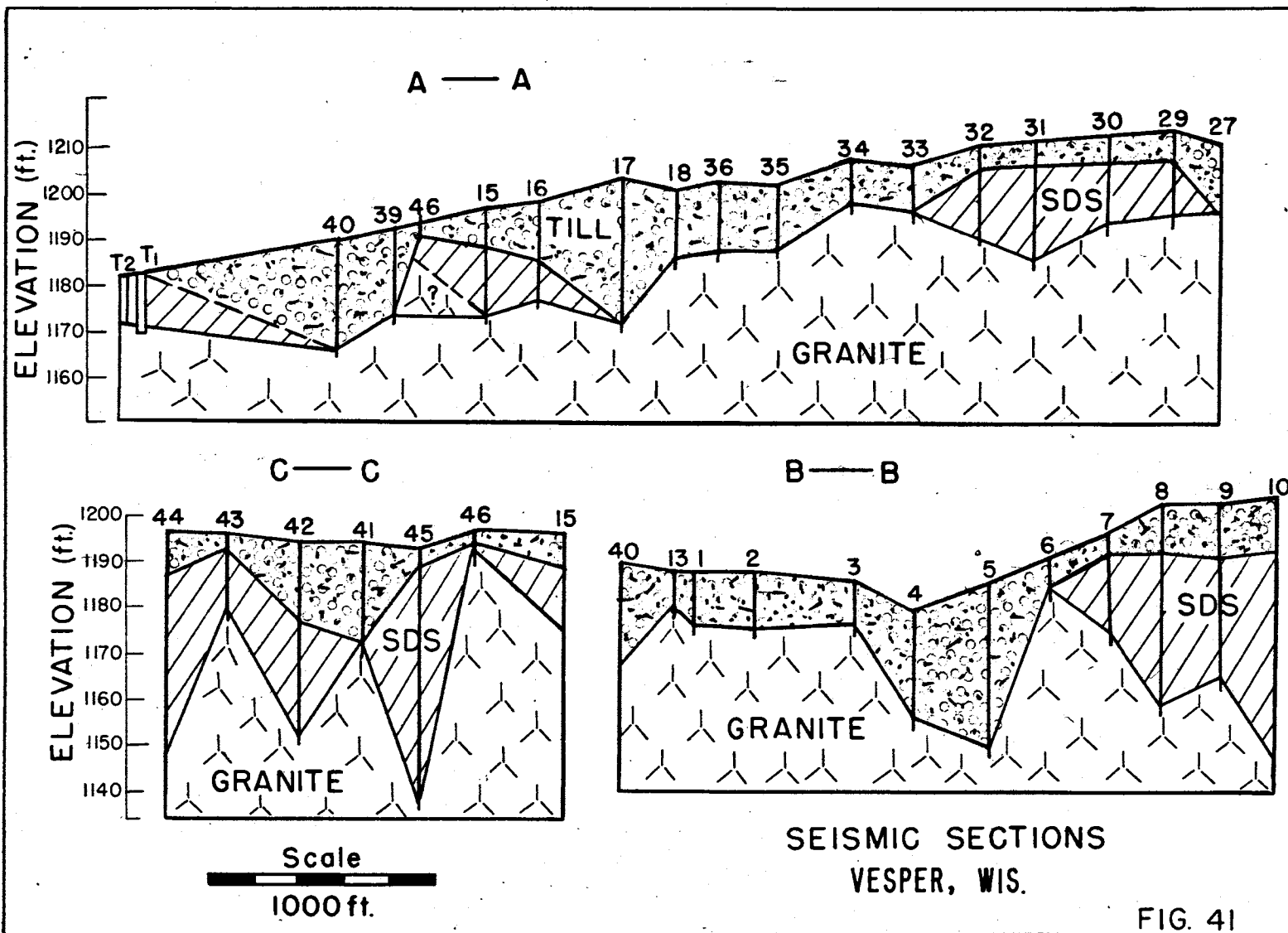
V₂ = Cambrian sandstone, the average true velocity = 9080 ft./sec.

V₃ = crystalline rock complex, the average true velocity = 17547.4 ft./sec.

In general, the surface geology, as well as fragmentary well data gathered from the local inhabitants appear to substantiate the seismic results. After the completion of this investigation, the logs for two test holes drilled in the area became available. These are shown in Fig. 40 as Test Hole I and Test Hole II. Test Hole I showed 10 feet of sandstone overlying weathered igneous rock, apparently basaltic lava flows or basic injection gneiss. Test Hole II showed 12 feet of sandstone overlying the same material. At neither location was there more than 2 feet of glacial till. The extensive thickness of weathered basic rock encountered at Test Hole I was of particular geologic interest; drilling was continued to a depth of 141 feet, and from 12 feet down no fresh rock was encountered. A summary of this log is as follows:

2 - 12 feet sandstone
 12 - 20 feet dark red-gray clay
 20 - 30 feet decomposed basic rock
 30 - 55 feet red-gray clay
 55 - 65 feet decomposed basic rock
 65 - 70 feet decomposed chloritic basic rock
 70 - 80 feet dark gray clay
 80 - 127 feet decomposed basic igneous rock
 127 - 132 feet dark red-gray clay
 132 - 141 feet decomposed basic igneous rock

As this material apparently had weathered in place without subsequent transportation, it is presumed that a large part of the area may be underlain by a similar thick section of weathered basic igneous rock; however, it is evident from the surface granite outcrops, that it does not underlie all of the area. As only a minor amount of water was encountered in Test Hole I, this material cannot be regarded as an aquifer, and the high velocity values associated with the basement everywhere throughout the area further confirm the idea that the material has a low porosity.



II-8 - Greenwood, Clark County, Wisconsin

II-8a General Statement

The town of Greenwood lies in the same general area as the Clark County Hospital previously considered. It was known from existing well records that sandstone, and possibly unconsolidated detrital granitic material, lay between the glacial till and the crystalline rock basement. Test holes and wells showed a variation from 6 to 104 feet to crystalline rock indicating considerable relief on the "granite" surface. The problem was to contour this surface and determine where the greatest thickness of sandstone was present.

II-8b Seismic Investigation

The seismic refraction reverse shooting technique was used and depths determined at 52 locations. Three different velocity horizons were mapped. Over part of the area, the upper layer (V_1) was characterized by a velocity varying from 1600 to 3950 ft./sec. and was identified as unsaturated glacial till. In other parts of the area the surface velocity layer had a velocity varying from 4015 to 6430 ft./sec. and was tentatively identified as water saturated till. The second layer (V_2) had a velocity varying from 6630 ft./sec. to 9800 ft./sec. and was identified as being probably sandstone. The third layer (V_3) characterized by velocities ranging from 13,820 to 23,700 ft./sec. was identified as the basement complex of crystalline rocks.

II-8c Discussion of Results

The travel-time plots showed considerable irregularities in the basement surface, with marked time delay offsets as would be occasioned by abrupt changes in depth between the shooting points. Although allowances were made for these offsets in making the depth calculations, there was no guarantee that they were all handled in a manner that would give a true representation of subsurface conditions. This was brought out very strongly by subsequent drilling. At two stations in particular, 6N and 17S, the difference between the subsurface structure portrayed by the seismic results and that obtained by drilling was so radically different that, in addition to re-examining all of the data and recalculating values, a field party was sent back to make auxiliary field measurements to resolve the discrepancies. The results of these additional measurements and the re-examination of the original data using alternative interpretations wherever more than one interpretation appeared possible, showed depth differences of 20 feet or more at 3 of the 52 stations and at 9 others differences of 10 feet or less were obtained.

In every case the difference involved the depth to the basement crystalline rock surface and not that to the overlying sandstone.

At station 6N the results should have been rejected since the offsets in the V_3 travel-time graph were so complex that an infinite velocity was indicated. The original depth calculated here was based on a mean velocity for the V_3 horizon, and this assumption resulted in a discrepancy of 71 feet in the depth to the basement rocks. The depth to the sandstone at this site, on the other hand, checked within 3 feet of that obtained by drilling. At station 17S, which was also checked by drilling, the sandstone while present at one end of a spread, was missing at the other end. As the surface layer was saturated till having a velocity greater than 5000 ft./sec. it was difficult to decide whether the sandstone was present or actually missing here as at other sites. If the sandstone showed up well on the reverse end of the spread, the tendency was to assume it was probably also present at the other end even though very thin. Of ten such cases, it was fairly definite in six cases that the sandstone was missing. In the other four cases the data were indeterminate and as a consequence it was assumed the sandstone was present though thin. Station 17S was one of these and the test well drilled here showed that the assumption was in error and that no sandstone was present. Since this error in interpretation also affected the calculated depth to crystalline rock surface, it was not surprising that the seismic data failed to check the well log information. However, recalculation on the basis of the sandstone not being present gave agreement with the well data to within 6 feet as to the depth of the granite. Under the original interpretation there was a disagreement of 47 feet.

It is thus seen that the results at Greenwood were complicated by two geologic situations which it was not always possible to evaluate properly from the seismic results. Re-evaluation of all the data with these probable sources of error in mind resulted in changes from 6 to 18 feet at 7 sites and changes of 20 feet or more at 3 sites. Two of the latter as has been indicated were at locations that were selected for test drilling. In one respect this was unfortunate; in another respect it was most fortunate in that it focused attention upon a situation not commonly encountered but which was critical at Greenwood, and which had not been fully appreciated at the time of the original computations.

Depth determinations were carried out at four additional sites on the return trip and the results of these measurements are included in Table 18 with those of the original investigation. Table 19 gives the results of recalculation on the basis of alternate interpretations at stations where it appeared that differences in results of more than 5 feet in depth would be obtained. It should be borne in mind however that there is nothing to indicate that the alternate interpretations are preferable to the ones first determined except in the two locations, 6N and 17S, where subsequent drilling proved the original interpretation to be in error.

Table 18

Seismic Data, Greenwood, Clark County, Wisconsin

Station	Apparent Velocity			Depth to Horizon		Sea Level Elevation	
	V ₁	V ₂	V ₃	V ₂	V ₃	V ₂	V ₃
1N	4970	8450	25000	11	61	1095	1045
1S	3330	7470	12750	15	56	1082	1041
2N	5090	8020	20000	16	55	1059	1018
2S	5090	6620	14820	—	40	—	1023
3N	6570	—	11940	—	38	—	1023
3S	5170	—	25810	—	23	—	1024
4N	6210	—	14290	—	23	—	1018
4S	6650	—	17170	—	35	—	1002
5N	5750	8060	13560	8	30	1036	1014
5S	4000	14090	32000	—	18	—	1021
6N	3960	9370	—	13	109	1054	958
6S	4070	7270	17500	9	63	1042	988
7N	4870	—	18870	—	14	—	1068
7S	3980	—	12200	—	21	—	1057
8N	—	8140	24250	5	21	1040	1024
8S	3260	—	21280	—	17	—	1025
9N	4020	—	16540	—	17	—	1050
9S	4030	—	16070	—	8	—	1043
10N	2580	8240	20600	14	67	1068	1015
10S	3360	—	11360	—	19	—	1055
11N	2120	6960	18370	12	88	1085	1009
11S	2490	9760	15040	17	46	1069	1040
12N	1670	6630	16600	16	46	1070	1040
12S	2220	—	13380	—	17	—	1055
13N	—	7430	15960	5	41	1055	1019
13S	—	7840	15080	5	20	1041	1026
14N	4970	—	15450	—	15	—	1025
14S	4530	—	16260	—	16	—	1021
15N	5090	—	20000	—	14	—	1020
15S	4950	—	21980	—	24	—	1012
16N	2530	5990	16670	13	53	1065	1025
16S	2110	7810	16600	14	46	1054	1022
17N	3950	11020	36830	13	69	1045	989
17S	3911	6260	22730	5	77	1036	964
18N	2480	9800	16670	18	72	1063	1009
18S	2960	—	19900	—	29	—	1048
19N	1600	—	23120	—	22	—	1021
19S	1600	—	12120	—	7	—	1049
20N	2510	—	26500	—	24	—	1021
20S	2510	—	14600	—	12	—	1038

Table 18 (continued)

Station	Apparent Velocity			Depth to Horizon		Sea Level Elevation	
	V ₁	V ₂	V ₃	V ₂	V ₃	V ₂	V ₃
21N	2450	7010	15150	13	61	1045	997
21S	2450	6460	16340	6	67	1056	995
22N	2840	6650	9300	12	33	1056	1035
22S	2840	8350	9880	4	23	1068	1049
23N	3360	-----	13250	---	16	-----	1058
23S	4040	-----	15450	---	18	-----	1062
24N	2500	8200	17940	7	56	1073	1024
24S	2500	8640	21740	14	67	1070	1017
25N	-----	8160	18000	---	21	-----	-----
25S	-----	6700	17800	---	21	-----	-----
26N	1880	-----	12960	39	146	-----	-----
26S	1940	9450	20000	28	120	-----	-----

V₁ = glacial till

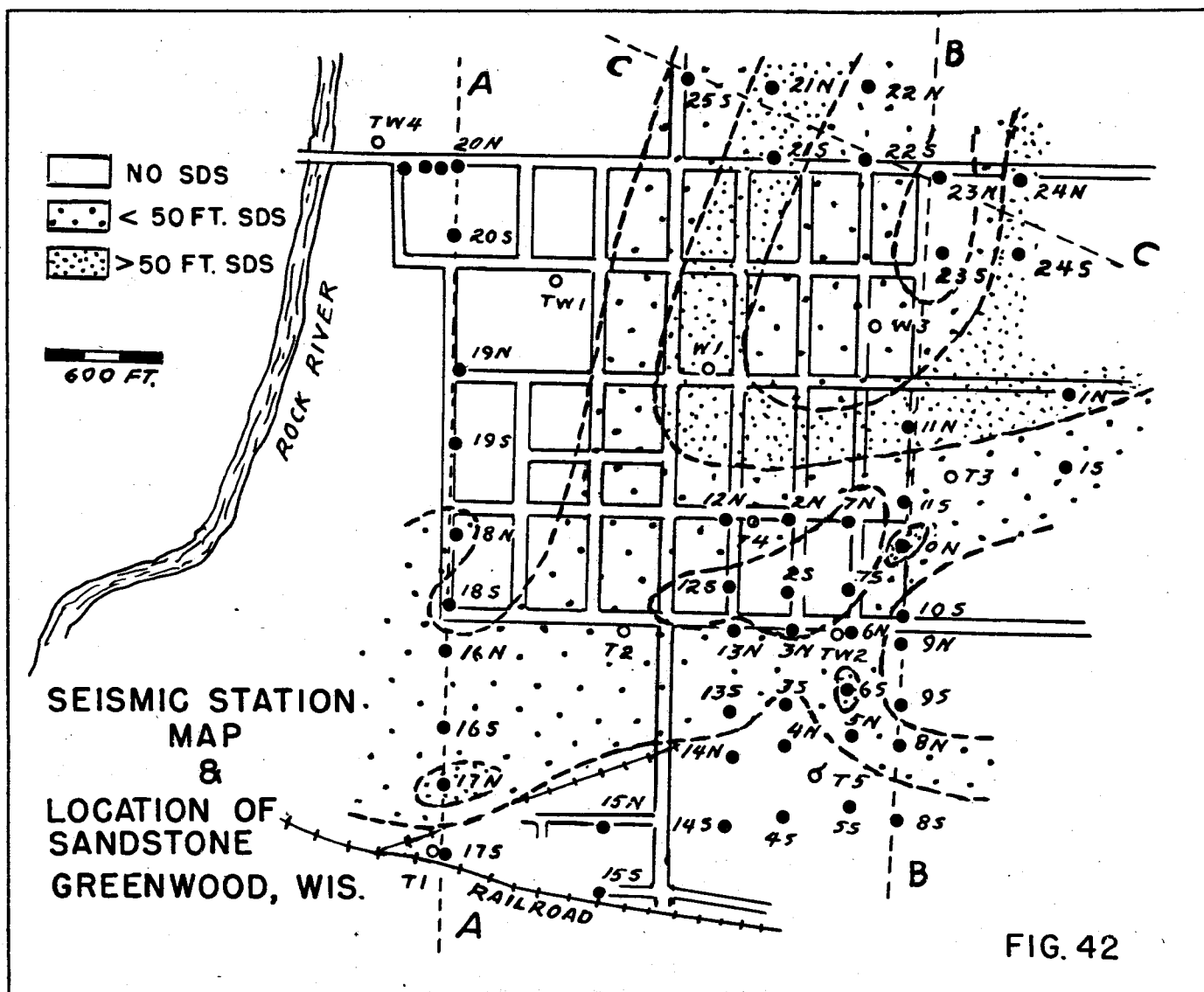
V₂ = Cambrian sandstone, the average true velocity = 7792 ft./sec.

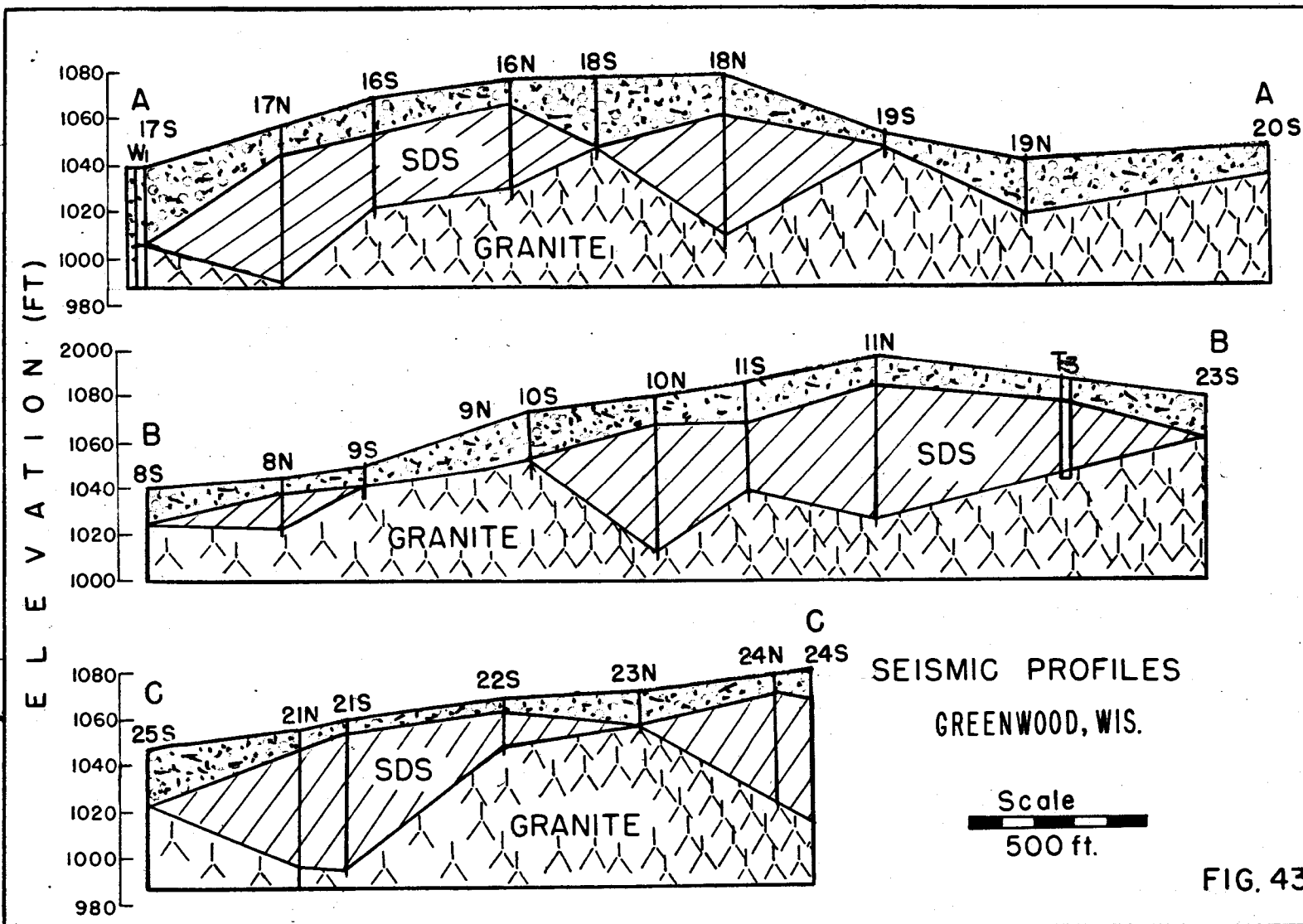
V₃ = crystalline complex, the average true velocity = 16,910 ft./sec.

Table 19

Seismic Stations with Alternate Values

Station	Original Depth		Alternate Depth	
	V ₂	V ₃	V ₂	V ₃
6N	13	104	13	Indeterminate
6S	9	63	12	40
11N	12	88	12	71
11S	17	46	16	56
16N	13	53	13	47
16S	14	46	12	58
17N	13	71	12	87
17S	5	77	---	36
18N	18	72	18	62
22S	4	23	4	37





The location of all the seismic stations, wells and test holes are shown in Fig. 42; areas where sandstone is absent are indicated as are areas where more than 50 feet of sandstone is present. Fig. 43 shows the relation of the till, sandstone, and basement rock surfaces to the ground surface in vertical sections along traverses across the area.

II-8d Evaluation of Results

Although considerable space has been devoted to a discussion of the locations in which appreciable errors in results were discovered, and their cause, attention should also be called to the fact that good agreement between the seismic data and drill hole data was also obtained. It has already been pointed out that an alternative interpretation of the seismic data equally as valid as the one first adopted would have reduced the discrepancy at site 17S from 47 feet to 6 feet, and that the depth to sandstone at site 6S was verified within 3 feet by the drilling although the depth to basement was appreciably in error. At Test Well No. 3 located about 500 feet northeast of seismic site 11S, the drill hole data substantiated the seismically determined depths to the sandstone to within 7 feet, and to the crystalline basement to within 4 feet. Similarly a test hole between seismic sites 2N and 12N and about 200 feet from each corroborated the seismically determined depth to sandstone in that area to within 5 feet. Test hole 5, which lies about half way between seismic sites 4N and 5S and about 400 feet from each corroborated there was no sandstone in this area as indicated seismically and verified within 3 feet the seismically determined depths to the crystalline rock complex. Test Hole No. 4 at the northwest edge of town and located about 200 feet northwest of the two short seismic spreads established to aid in locating a water main likewise corroborated there was no sandstone in that area, and agreed with the seismically determined depth to the basement complex within 3 feet.

Although there were other wells in the area, in particular the main town well which showed 104 feet of section above the basement complex, there were no seismic stations close enough (within about 800 feet) to permit valid comparisons with the seismic results.

A summary table of the agreement obtained at all wells located within 500 feet of any seismic station is given in Table 20. From this table it is seen that the average degree of agreement between the seismic and well log data without regard to sign is 4 feet if the original data for 17S and 6N are omitted as representing abnormal situations. This degree of agreement is more in line with that obtained elsewhere.

Table 20

Comparison of Well and Seismic Depths
Greenwood, Clark County, Wisconsin

Well	Seismic Station	Distance from Well	Elevation of sandstone		Basement	
			Well	Seismic	Well	Seismic
Test No. 4	1W Auxiliary	200 ft. SE	----	----	1024	1027
Well No. 3	11S Interpretation 1	400 ft. SW	1062	1069	1036	1040
	11S Interpretation 2		1062	1070	1036	1030
Test No. 5	4N	400 ft. NW	----	----	1020	1018
	5S	400 ft. SE	----	----	1020	1021
Well No. 2	6N Interpretation 1	At Site	1051	1054	1029	958
	6N Interpretation 2	At Site	1051	1054	1029	Indeterminate
Test No. X	12N	250 ft. NW	1066	1070	----	----
Well No. 1	17S Interpretation 1	40 ft. W	----	5	1011	964
	17S Interpretation 2		----	----	1011	1005

This investigation, outside of those conducted for engineering and mining purposes, is probably the one most thoroughly tested by subsequent drilling. The investigation also involved one of the most difficult problem areas that had been studied up to the time of this survey. Thanks to the extensive drill hole testing program carried out by the town of Greenwood the nature of the problems encountered are now understood. However it cannot be said that in view of this understanding, unambiguous interpretations would now be possible in this same type of an area. Fortunately such areas are the exception rather than the rule, and as indicated here at Greenwood even in a complex area the seismic method is applicable to a study of most of the area.

II-9 - University of Wisconsin, Willows Athletic Field
Madison, Wisconsin

II-9a General Statement

The Willows Athletic Field lies at the head of University Bay on Lake Mendota on a low, flat area that was formerly lake bottom. Little was known of the subsurface geology other than that lake alluvium and glacial till overlaid Cambrian sandstone at depth. The problem was to ascertain the subsurface geology so that it could be decided whether it would be best to sink a well as a source of water supply, or to run in a pipeline and use city water. The general location of the area and the available geologic information from outcrops and well logs in the vicinity are shown in Fig. 44.

II-9b Seismic Investigation

The seismic refraction method of reverse profile shooting was used to establish depths at 13 locations which are shown on the map of Fig. 45. Three distinct velocity layers were found to be present. The upper surface velocity layer (V_1) had a velocity varying from 3500 ft./sec. to 5500 ft./sec. and was identified as glacial till and lake sediments having varying degrees of water saturation. Below this was an intermediate velocity layer (V_2) which had a velocity of about 7000 ft./sec. This layer was only found at about half the sites. The identity of this material was questionable and it was tentatively identified as an older till. Throughout the area a deep high speed layer (V_3) was found which was characterized by a velocity of about 9000 ft./sec. and was identified as the sandstone bedrock.

The velocity depth values and sea level elevation of each horizon are tabulated in Table 21. A contour map showing the configuration of the sandstone surface is included in Fig. 45.

II-9c Discussion of Results

It is seen from the contour map that a well defined buried valley, incised in the sandstone surface, cuts diagonally across the area. The relief indicated on this surface is 126 feet. The greatest depth was at location 4W and the shallowest at 2W. To bring this out more clearly vertical sections were drawn along traverses A-A and B-B of Fig. 46. From these sections it is also seen that the intermediate velocity layer occurs only in the valley area.

To check the nature of the V_3 high speed horizon identified as sandstone, a test hole was drilled at site 2W where the depth to the V_3 horizon was shown by the seismic data to be 13 feet below the surface. Water Table was encountered at 9 feet and a hard sandstone at 13 feet which could only be penetrated with difficulty using a hand auger. This verified both the nature of the material and the seismic depth at this location.

That the valley outlined by the seismic work is probably a tributary to a larger valley to the west of the area is indicated by the well at the Post Farm, City Well No. 6 and outcrops of bedrock seen at the surface. City Well No. 6 showed 45 feet of drift overlying sandstone, whereas the Post Farm well indicated 255 feet of drift overlying sandstone. See Fig. 44. As the surface elevation of both wells is very nearly the same, there seems little reason to doubt that the relief shown on the sandstone surface by the seismic data to the east is real.

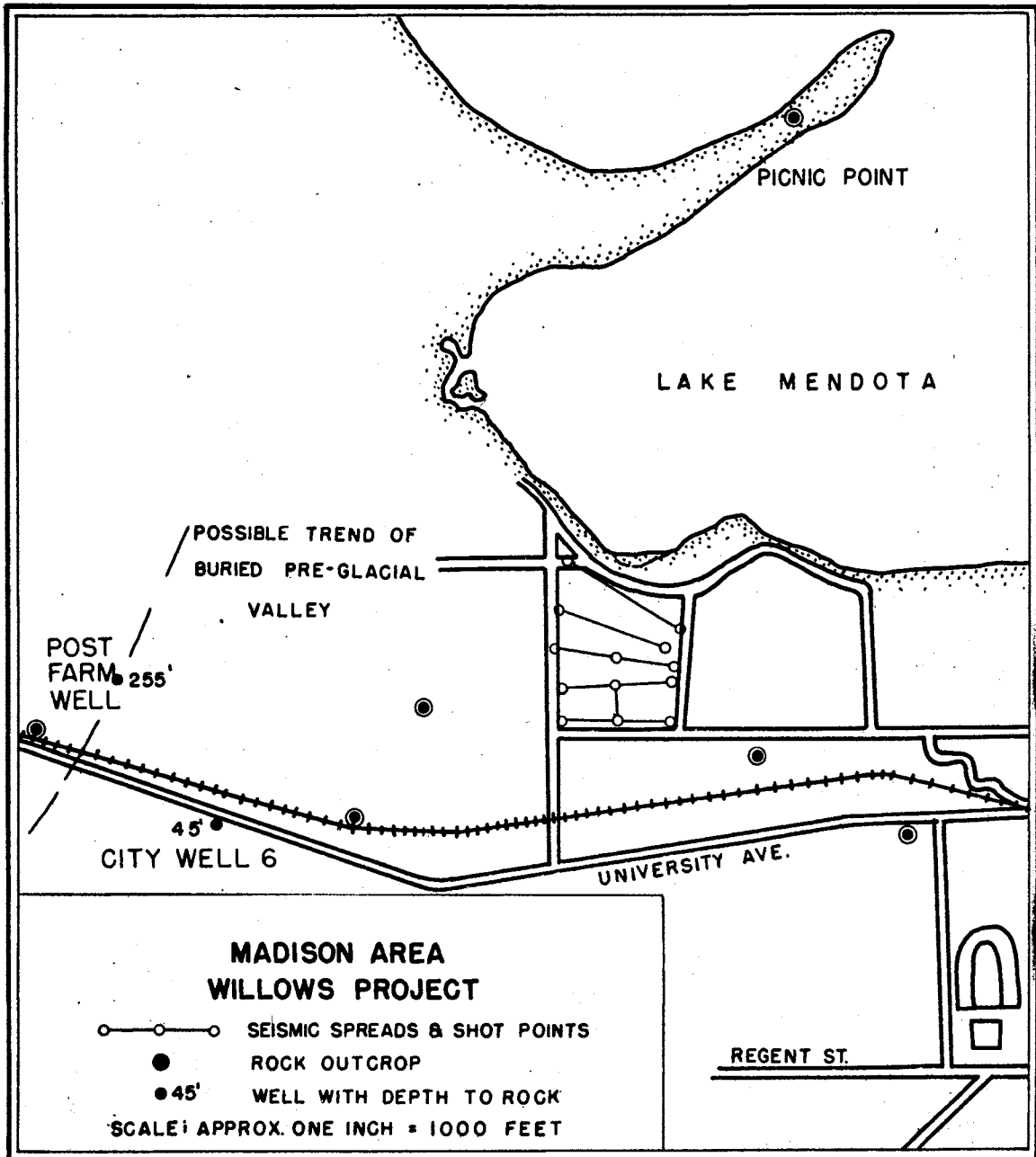
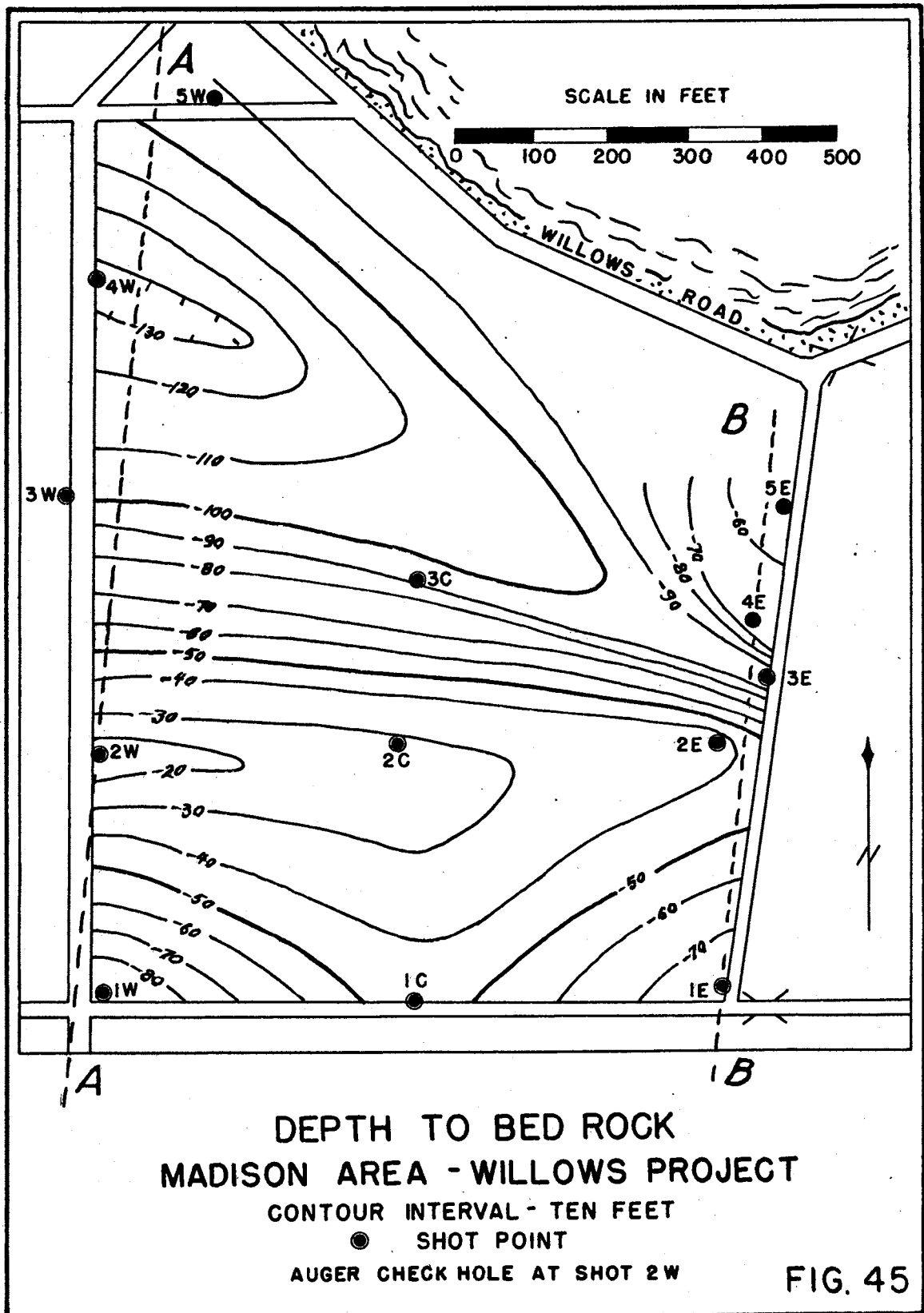


FIG. 44



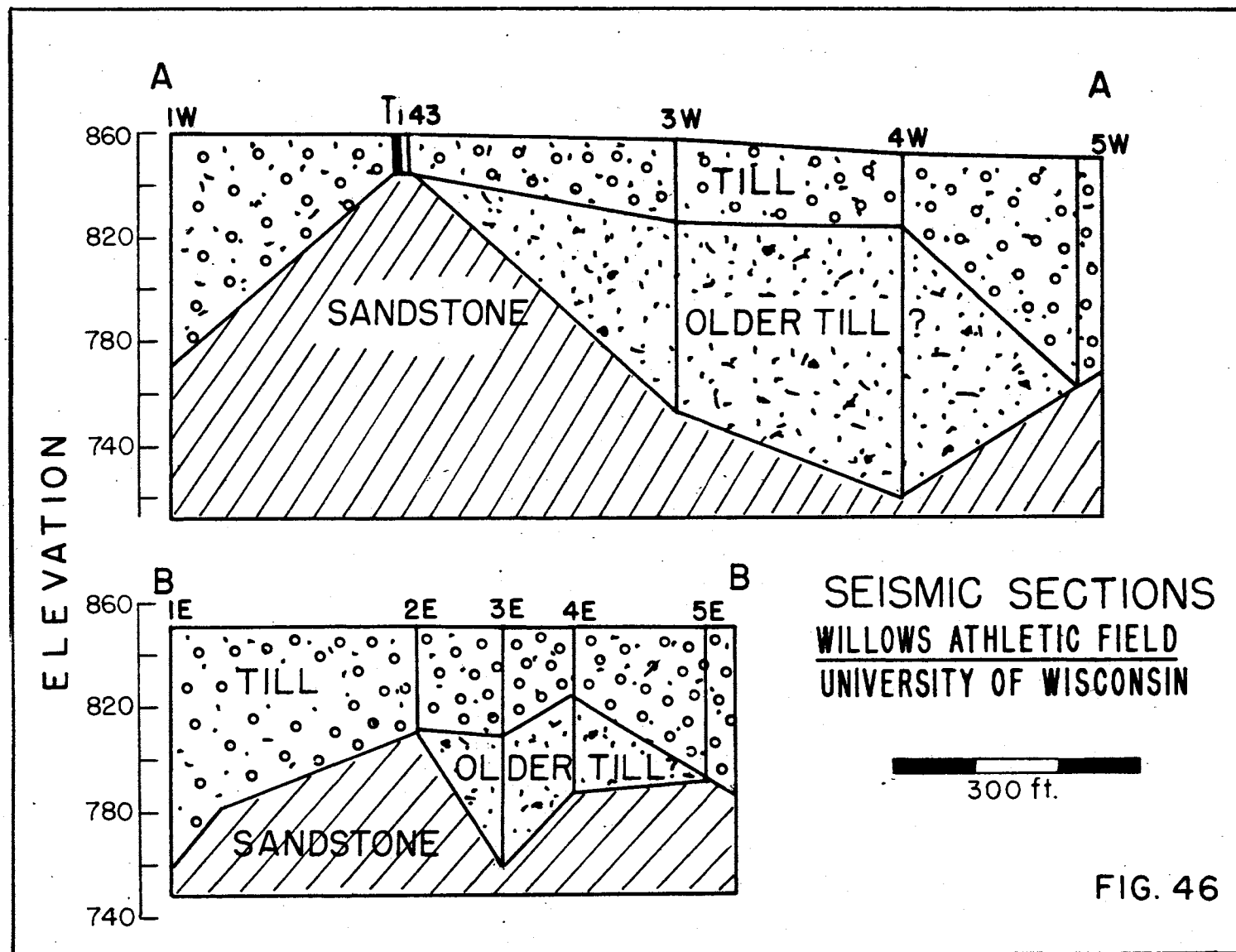


Table 21

Seismic Data

Willows Athletic Field, University of Wisconsin

Station	Apparent Velocity			Depth to Horizon		Sea Level Elevation	
	V ₁	V ₂	V ₃	V ₂	V ₃	V ₂	V ₃
1W	6250	----	9550	---	92	---	768
1E	6250	----	9550	---	78	---	775
1C	5740	----	8980	---	42	---	812
2E	3550	----	9200	---	38	---	812
2W	3550	----	9200	---	13	---	846
2C	4200	----	8820	---	27	---	822
3W	4210	7400	9530	31	102	827	756
3E	4210	7400	9530	41	92	799	758
3C	4680	7300	9500	19	96	833	756
4E	3760	6100	8770	27	63	815	788
4W	3760	6100	8770	28	133	825	720
5E	5650	----	8280	---	58	---	762
5W	5650	----	8280	---	87	---	762

V₁ = glacial till and lake alluvium

V₂ = possible older till, the average true velocity = 6860 ft./sec.

V₃ = sandstone, the average true velocity = 9066 ft./sec.

II-10 - Elkhorn, Wisconsin

II-10a General Statement

Elkhorn lies in an area where a relatively thick section of glacial till (150-230 ft.) overlies shale and dolomite. The aquifer is the till as neither the underlying Richmond Formation nor the deeper limestone of the Galena Formation afford a source of water. This was shown by City Well No. 4 which was drilled to a depth of 1648 feet and encountered essentially no water beneath the base of the till at 227 feet. A buried pre-glacial valley system is known to occur several miles to the west of town and the problem was to determine whether a tributary extended into this area which, if filled with sand and gravel, would constitute a better aquifer than the till.

II-10b Seismic Investigation

Seismic refraction reconnaissance measurements were carried out at 10 locations in the area using the reverse shooting refraction method. The results of these measurements showed two seismic layers; a surface layer (V_1) having a velocity varying from 6900 ft./sec. to 8280 ft./sec. which was identified as glacial till, and a second layer (V_2) having a velocity varying from 13,200 ft./sec. to 24,300 ft./sec. which was identified as shales and dolomites of the Richmond Formation. The locations of the seismic stations and the city wells are shown in Fig. 47. The pertinent data for each seismic station are given in Table 22. Profile sections along the three traverses indicated in Fig. 47 are shown in Figs. 48 and 49. Contours on the surface of the Richmond Formation are included.

II-10c Discussion of Seismic Results

The seismic study here was disappointing as no subsurface bedrock valley was indicated in the town area. On the contrary, there were indications of a broad ridge beneath the town with about 40 feet relief. The greatest thickness of till found was about 280 feet and occurred on the south side of town.

As the town was obtaining its water supply from a sand and gravel lens lying within the till that occurred at depths between 20 and 160 feet, it was decided to see if the lateral extent of this lens could be determined using electrical resistivity measurements. If it was sufficiently large a second well might be located in it without affecting the yield of the existing well.

II-10d Electrical Resistivity Investigation

Three different electrode spacings for constant depth profiling were used with a Wenner configuration. (See Appendix for description of this configuration and the traverse method of measurement.) Assuming that the effective depth of penetration is approximately two thirds that of the surface electrode separation, two series of measurements were run along a traverse where the seismic depths indicated the greatest thickness of till; on one series the electrode spacing was 90 feet and on the other it was 130 feet. In the other areas, traverses were run with electrode spacings of 50 and 130 feet. These electrode intervals were adopted on the basis of the depths over which sand and gravel were observed in Well No. 4, 20 to 160 feet. By measuring resistivity values down to two fixed depths on a series of traverses crossing the area,

Table 22

Seismic Data, Elkhorn, Wisconsin

Station	Apparent Velocity V_1	Apparent Velocity V_2	Depth to Horizon V_2	Sea Level Elevation V_2
1a	6460	12700	208	813
2a	6460	13750	220	797
3b	7200	14390	257	760
4b	7200	12300	232	777
5c	7100	13120	202	804
6c	7100	15400	264	742
7d	7100	24750	283	702
8d	7100	24000	269	726
9e	8260	19220	244	736
10e	8260	18740	232	733

V_1 = saturated glacial till

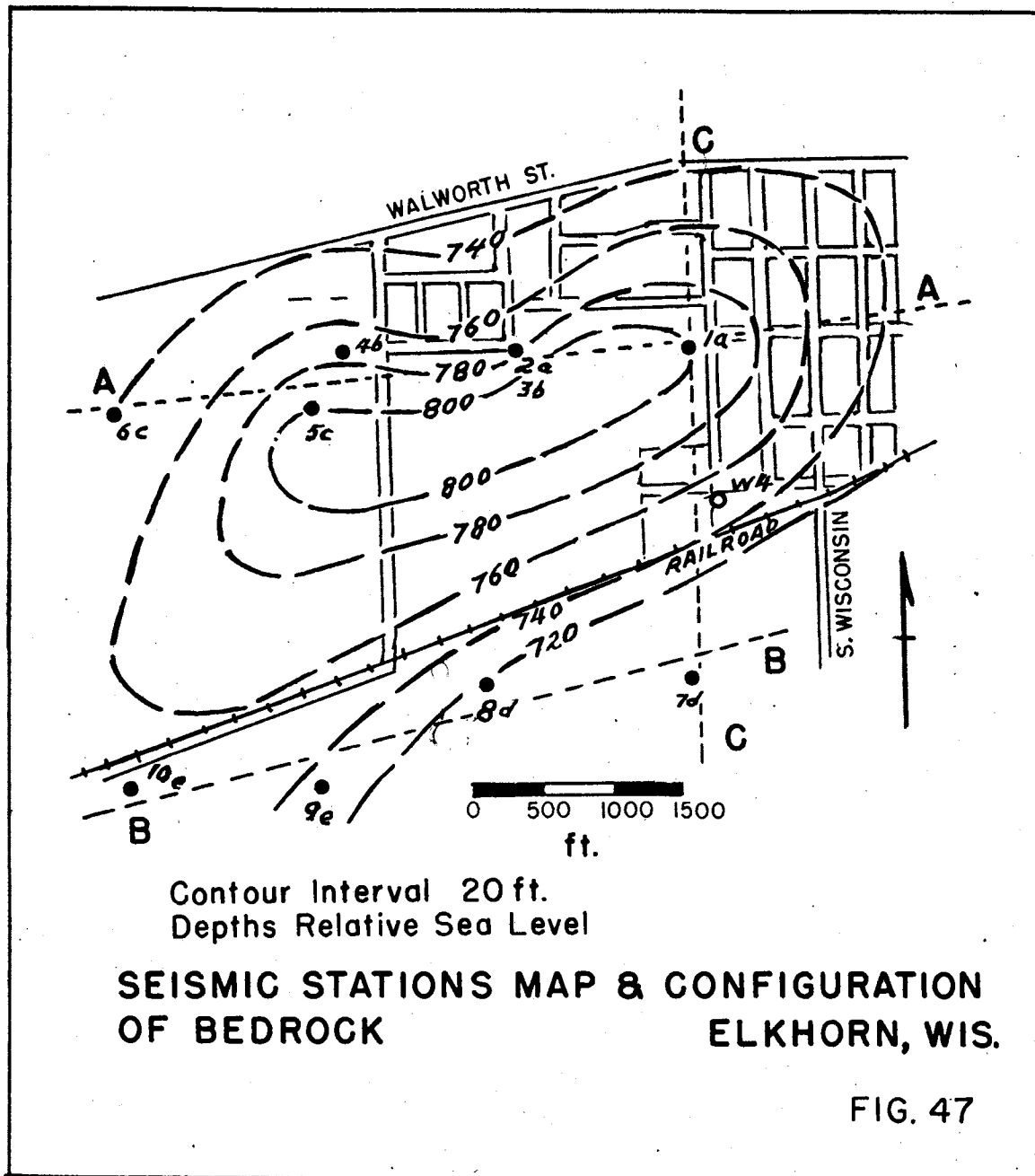
V_2 = Richmond shale and dolomite, the average true velocity = 16,812 ft./sec.

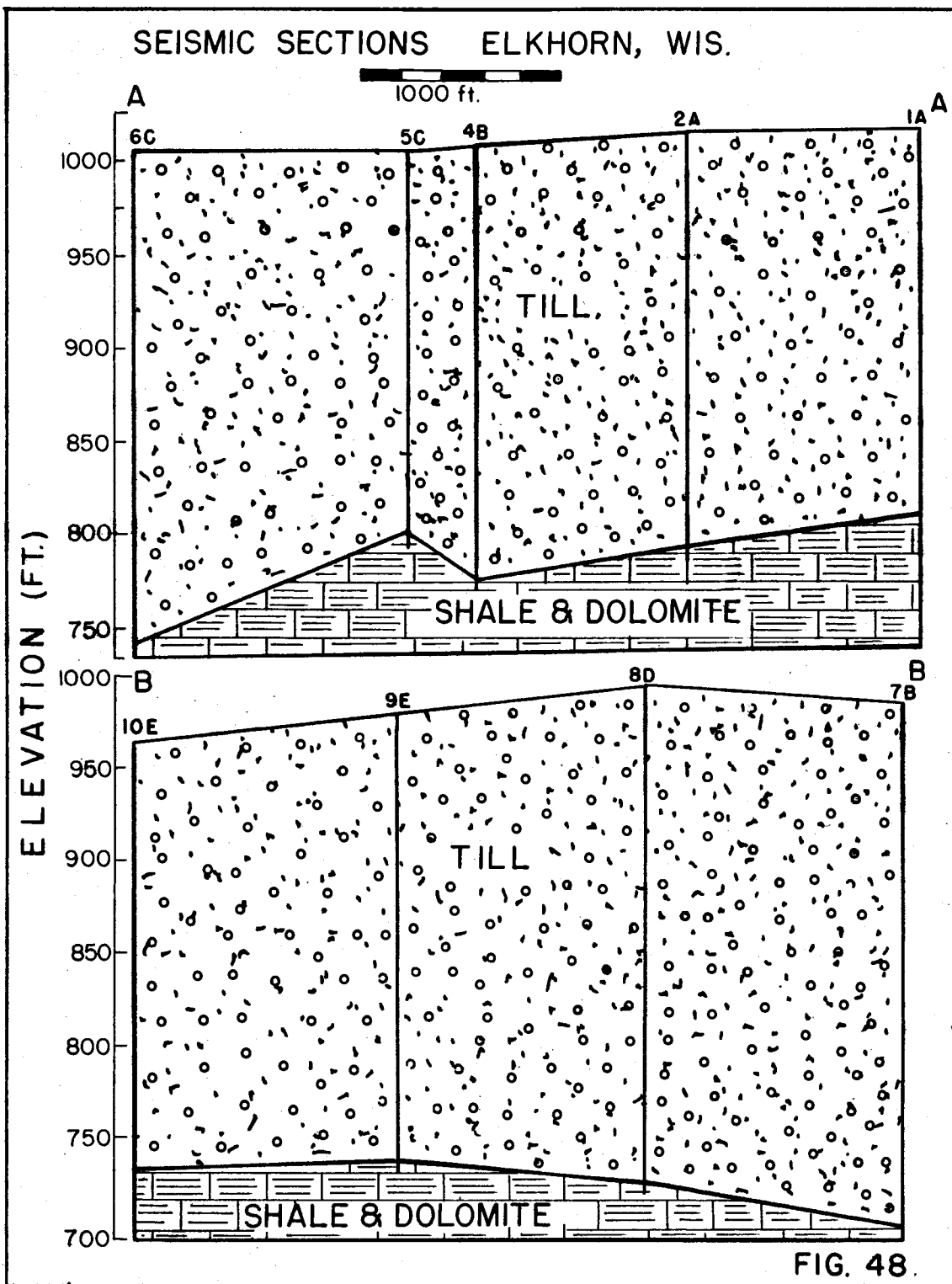
it was hoped not only to define the lateral boundaries of the sand and gravel in the till but also to get some idea as to whether a uniform thickness was maintained. The locations of the resistivity traverses are shown in Fig. 50.

II-10e Electrical Resistivity Results

The resistivity values obtained for both electrode spacings used on each traverse are listed in Table 23. These values were plotted at the location of the center points of the electrodes spread at each location and were contoured as shown in Fig. 50. In Figs. 51, 52 and 53, resistivity profiles are drawn along each traverse.

It is seen from the profiles and contour map that there is a pronounced resistivity "high" whose axis lies in the vicinity of Well No. 4. This "high" is about 1000 feet wide and its axis strikes about 60° east of north. Since a similar pattern is shown with both the 50 and 130 foot electrode intervals, there seems little doubt that the same geologic factor is influencing both sets of measurements which bracket a 80 foot depth interval. The sand and gravel layer observed in Well No. 4 which extends from 20 to 160 feet is believed to be the explanation for this high resistivity area. As the resistivity values get progressively smaller to the southwest, the postulated lens of sand and gravel either thins out or plunges downward in this direction.





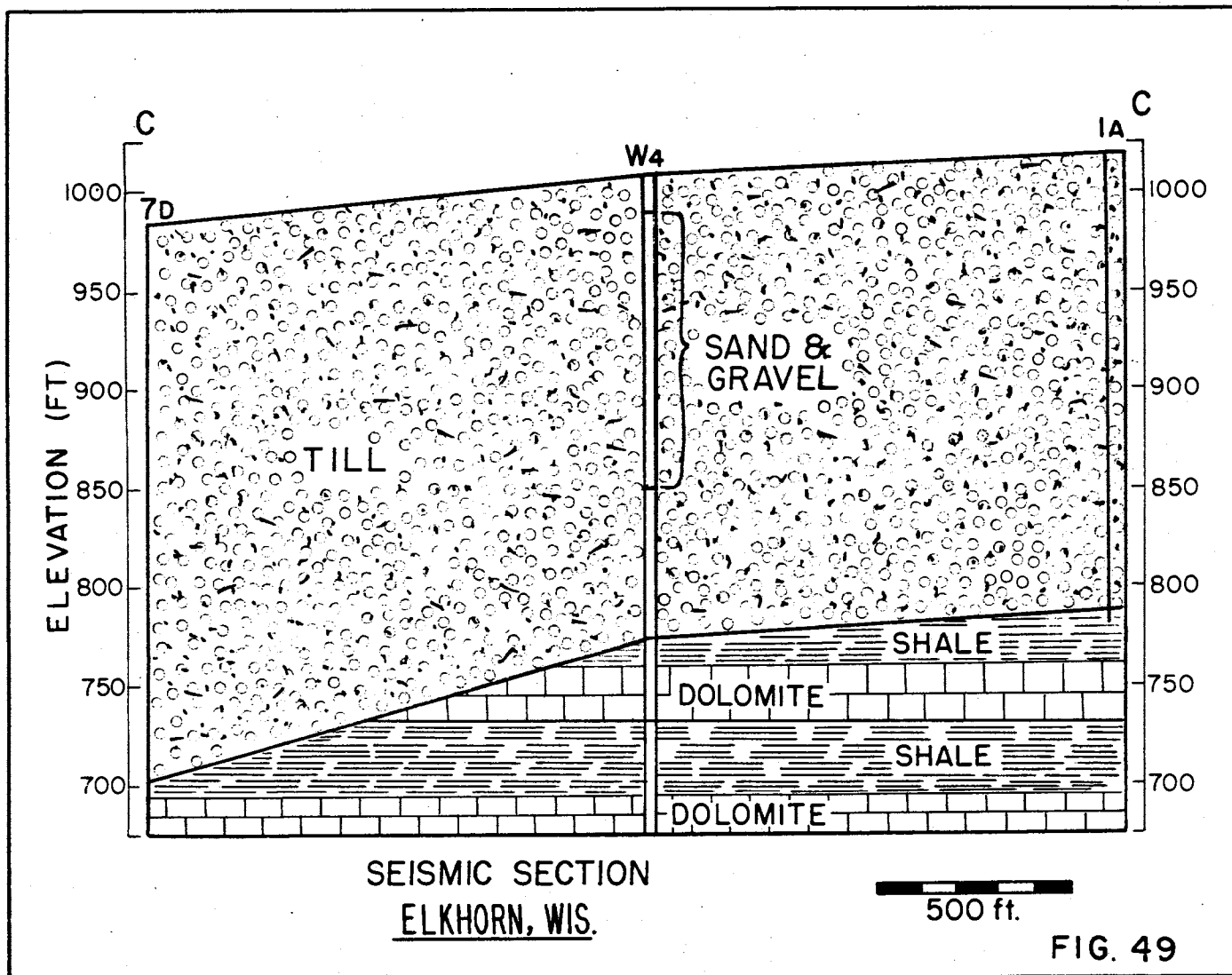


Table 23

Resistivity Values, Elkhorn Wisconsin

Line A---N-S line SE $\frac{1}{4}$ of Sec. 1, T 2N, R 17E

North End Station	Resistivity (90 ft. Spacing)	Ohm Centimeters (1300 ft. Spacing)
1	12290	10210
2	10450	11700
3	12100	10020
4	12000	11720
5	11680	12100
6	11300	11300
7	12200	11650
8	14050	15500
9	14520	14600
10	13920	17030
11	16580	15690
12	11700	15340

Line B---N-S in center N $\frac{1}{2}$ of Sec. 1, T 2N, R 17E

South End Station	Resistivity (50 ft. Spacing)	Ohm Centimeters (130 ft. Spacing)
1	12840	12850
2	14500	21480
3	15180	21670
4	16500	15810
5	14480	13020
6	9560	9260
7	9070	9800
8	8340	7840
9	8760	6980

Line C---N-S line in SW $\frac{1}{4}$ of Sec.1, T 2N, R 17E

North End Station	Resistivity (50 ft. Spacing)	Ohm Centimeters (130 ft. Spacing)
1	12955	14663
2	13941	14314
3	10753	13692
4	12700	11450
5	14371	12345
6	13041	13469

Table 23 (continued)

Line D---E-W line in $S\frac{1}{2}$ of $S\frac{1}{2}$ of Sec.1, T 2N, R 17E

End of Line A Station	Resistivity (50 ft. Spacing)	Ohm Centimeters (130 ft. Spacing)
1	12450	12700
2	12480	13950
3	13100	14010
4	14000	12920
5	12800	12920
6	10430	10620
7	11490	11400
8	11310	11270
9	14270	13680
10	13100	11900
11	11100	13690

Line E---E-W line in $N\frac{1}{2}$ of Sec.1, T 2N, R 17E

East End Station	Resistivity (50 ft. Spacing)	Ohm Centimeters (130 ft. Spacing)
1	17045	11080
2	18000	14060
3	16660	13395
4	11680	12075
5	14360	12780
6	12780	11800
7	11203	9385
8	8140	8340
9	11250	9660
10	10005	9040

Table 23 (continued)

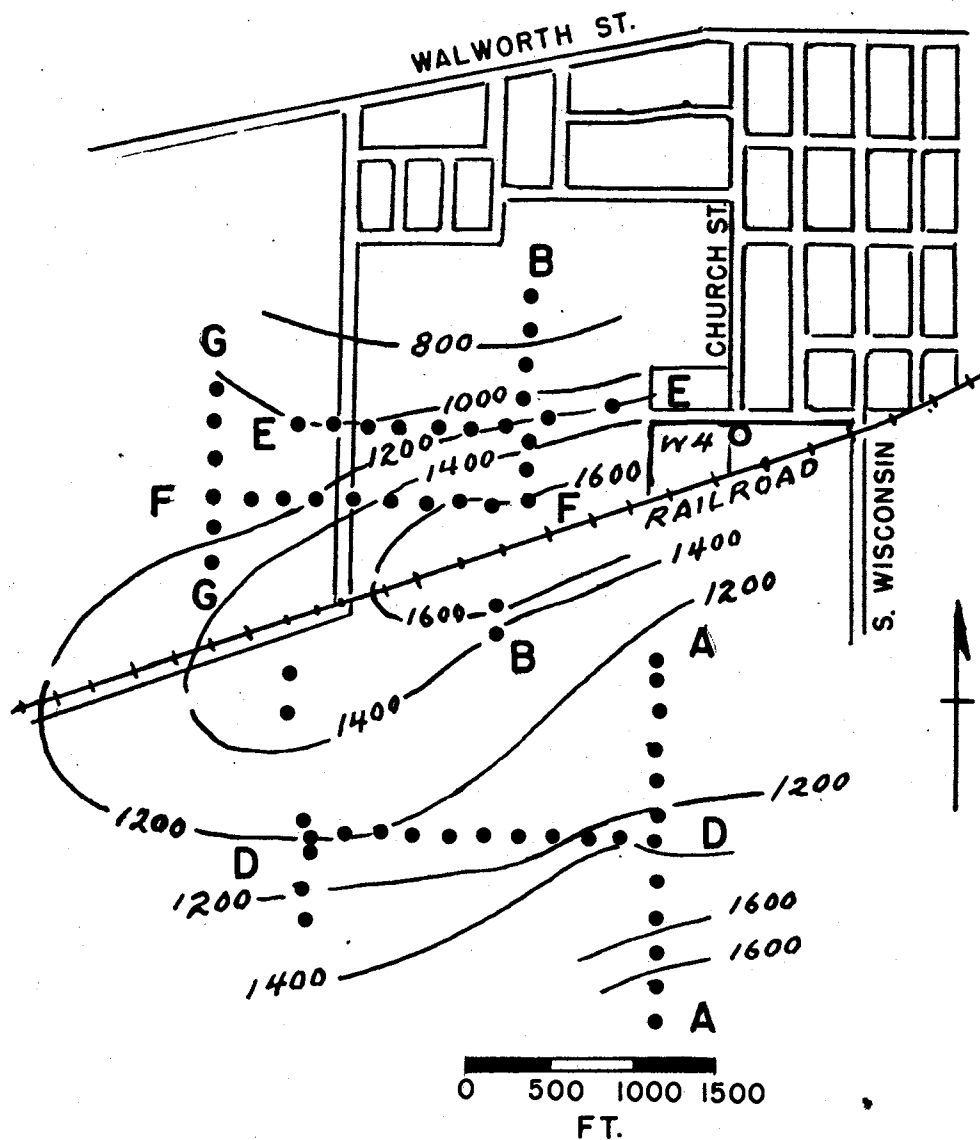
Line F---E-W line in N $\frac{1}{2}$ of Sec. 1, T 2N, R 17E

East End Station	Resistivity (50 ft. Spacing)	Ohm Centimeters (130 ft. Spacing)
1	15035	15350
2	13980	15195
3	14600	16180
4	14750	15610
5	13900	15290
6	14800	12370
7	13120	12920
8	11680	11475
9	11970	11950
10	11680	11250

Line G---N-S line in NW $\frac{1}{4}$ of Sec.1, T 2N, R 17E

South End Station	Resistivity (50 ft. Spacing)	Ohm Centimeters (130 ft. Spacing)
1	13120	13700
2	12060	11975
3	11970	11525
4	11970	10980
5	11970	10510
6	10085	10850

South of the railroad the resistivity pattern suggests much greater irregularities in the till than is found to the north of the railroad. At the north edge of the area the sharp negative resistivity gradient observed is probably related to an abrupt termination of the sand and gravel in that direction. Whether this is related to the bedrock ridge revealed by the seismic data, whose crest lies in about the area of marked change in resistivity, cannot be deduced on the basis of present data, though such a situation would give a logical explanation for the observed change in the resistivity values.

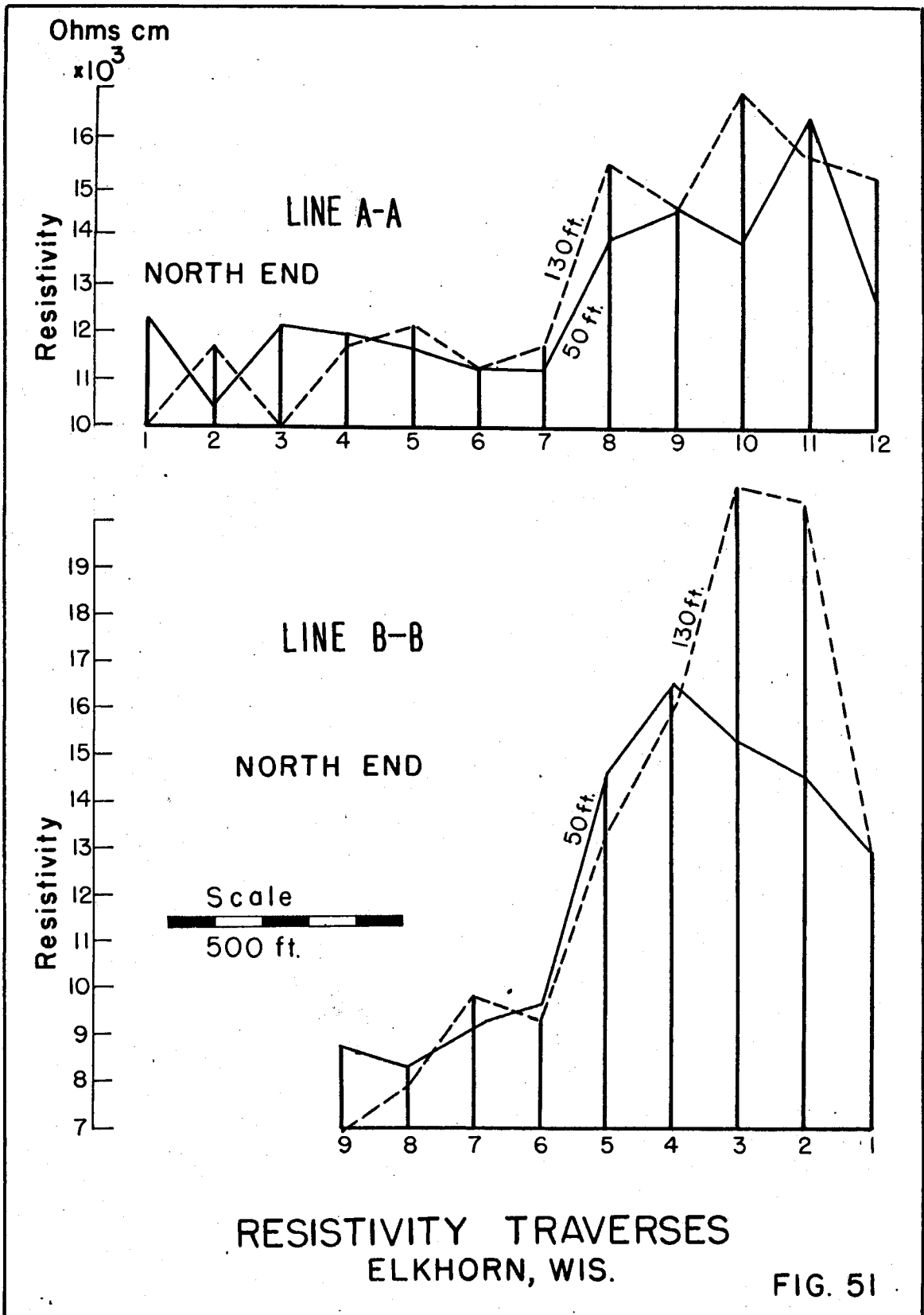


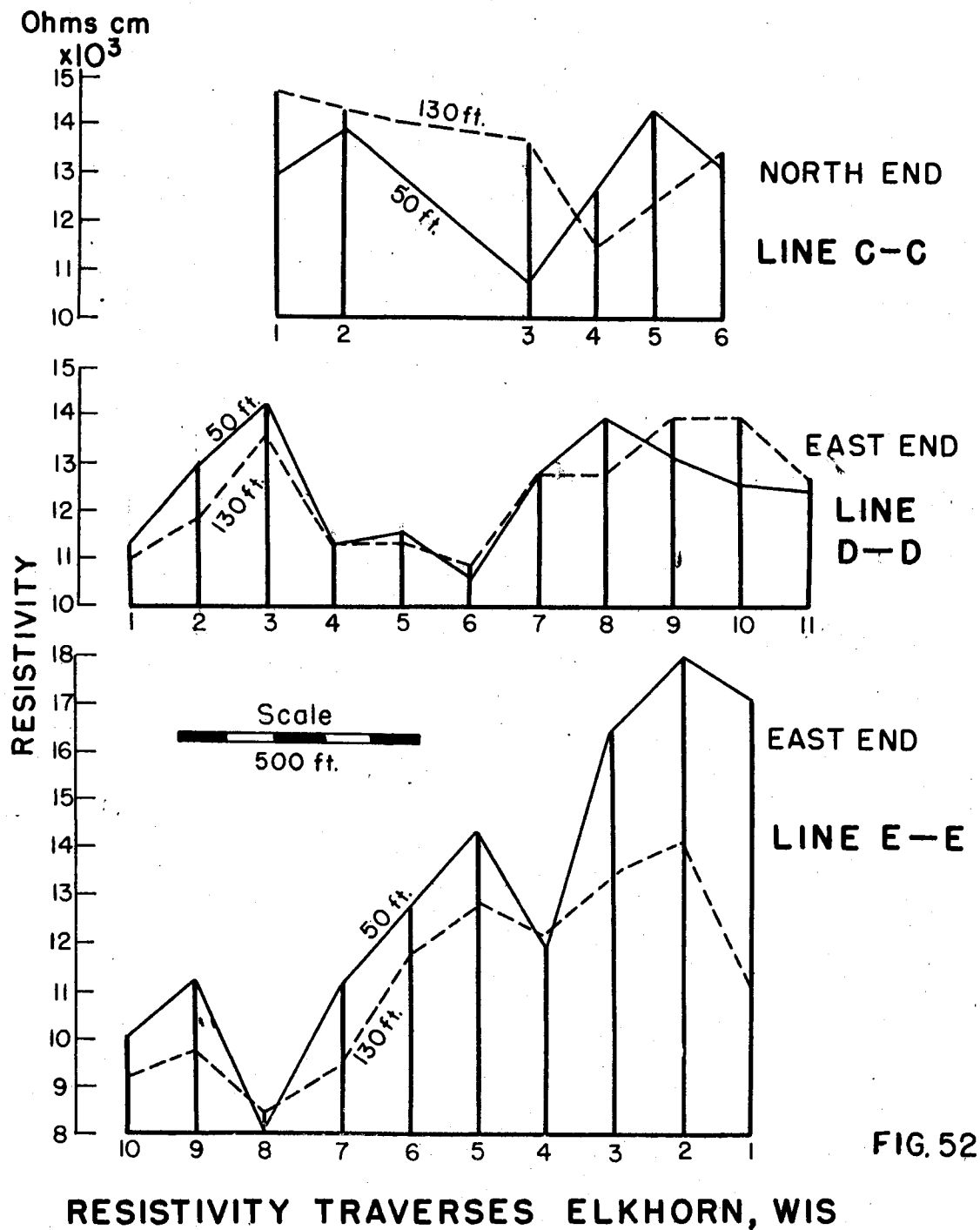
Contours Based on 130 ft. Electrode Spacing
Contour Intervals 200 Ohms-cms

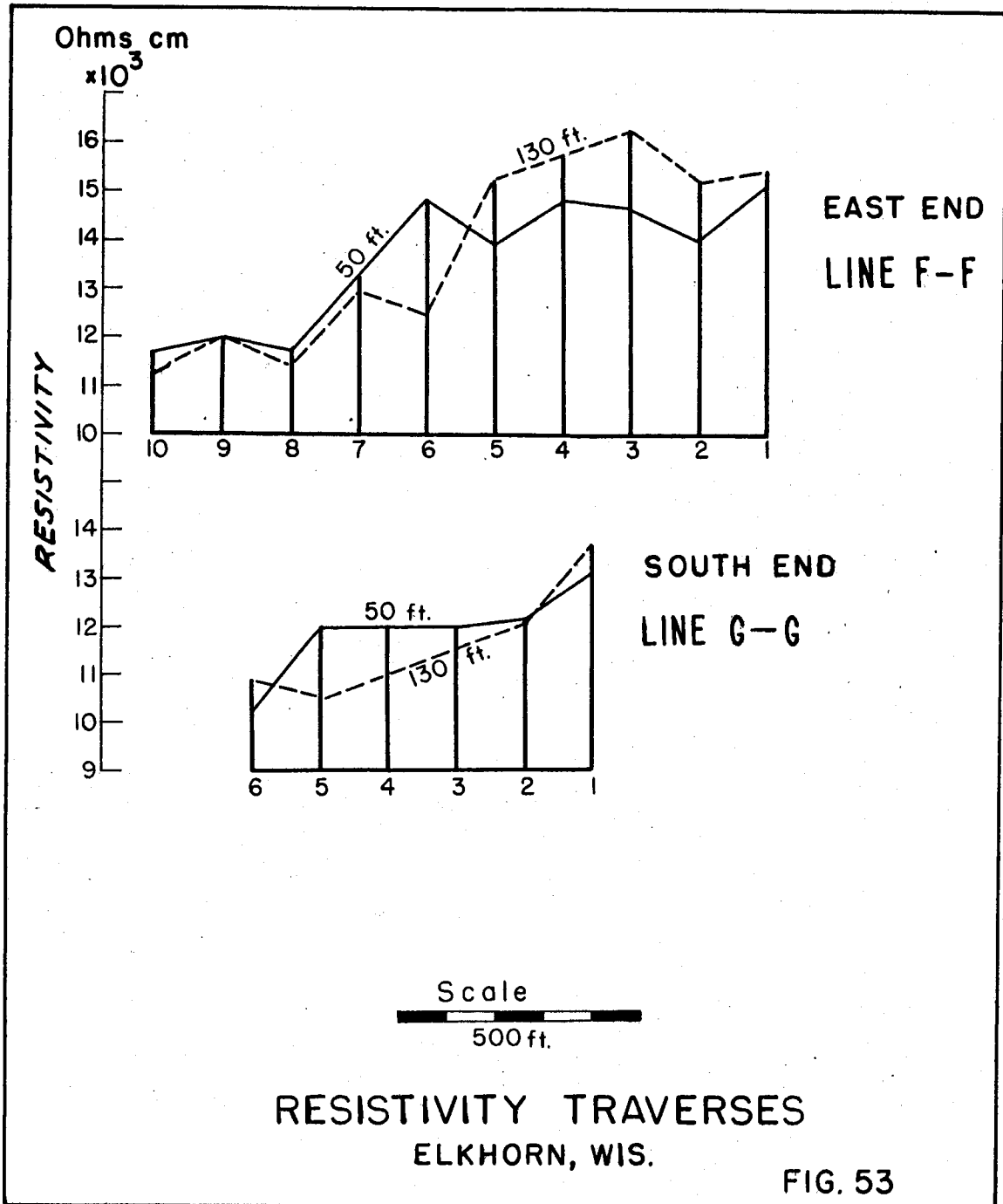
ELECTRICAL RESISTIVITY STATIONS & AREA OF HIGH RESISTIVITY

ELKHORN, WIS.

FIG. 50







II-11 - Neillsville, Wisconsin

II-11a General Statement

Neillsville is in a portion of the state where glacial till is underlaid by Cambrian sandstone and granite. The purpose of the geophysical measurements was in the nature of a test and reconnaissance. The area had been previously studied using electrical resistivity depth measurements by the U.S. Geological Survey and a well had been drilled at what appeared to be a favorable site. The well data, however, failed to corroborate the depth to granite indicated by the geophysical measurement, and the lack of agreement was over 100 feet. As the electrical depth measurements at Antigo, Wisconsin (See Section II-2) had agreed in gross measure with both the seismic refraction depth measurements and well data, the seismic measurement at Neillsville was proposed to see if the driller had struck a large granite boulder in the drift and not true basement rock.

II-11b Seismic Investigation

Seismic refraction measurements were made at three sites in the Neillsville area. Site 1 was at the location of the well where the depth to granite differed so radically from that indicated by the electrical measurements. Sites 2 and 3 were selected by the town engineer as potential areas for locating a new water well. The general locations of the measurements are shown in Fig. 54.

At site 1, reverse seismic refraction measurements were made with the shot located at the well in each case. At the other two sites the measurements were open ended. The data obtained in each area are given in Table 24.

Table 24

Seismic Data, Neillsville, Wisconsin

Site	Apparent Velocity			Depth (feet)		Depth from well at Site 1
	V ₁	V ₂	V ₃	V ₂	V ₃	
1a	2160	6780	20350	13	60	0-10 till
1b	2080	8760	17760	13	58	10-47 sandstone
2	4060	8910	18000	16	89	47 granite
3	2860	9410	19000	68	235	

V₁ = surface till

V₂ = sandstone

V₃ = crystalline basement rock (granite)

II-11c Remarks on Test

The seismic tests substantiated the well data on the depth of basement rock at site 1, and in addition indicated that site 3 might be the best location for a well from the standpoint of thickness of potential aquifer. In Fig. 54, the thickness of sandstone indicated at each site is given at the respective locations. As surface elevations were not available for each site, it is not known whether an actual bedrock valley also occurs in the area of site 3 or not.

II-12 - Marshfield, Wisconsin

II-12a General Statement

The city of Marshfield lies in a section of the state where for the most part glacial till lies directly upon the pre-Cambrian crystalline rock surface. Locally there are some thin layers of Cambrian sandstone, but in general it is the till that serves as an aquifer. The thickness of material above the crystalline rocks is quite variable but seldom exceeds 50 feet except where there are buried valleys incised in the crystalline rock surface.

As a program of test well exploration for additional water for the city had failed after drilling approximately 50 test wells, the U.S. Geological Survey undertook an electrical resistivity survey in the area to study the depth of the underlying "granite" surface in the hope of finding a buried valley with associated gravels that would serve as an aquifer. This program was successful both in locating a well-defined buried valley which contained a thick section of gravel yielding abundant water. Because many of the buried glacial valleys in Wisconsin are filled with relatively impermeable till rather than sand and gravel, the full significance of locating the valley could not be appreciated until a test well had been drilled penetrating it. This well showed 16 feet of drift followed by 49 feet of coarse gravel and sand underlaid by granite.

II-12b Gravity and Magnetic Study

As the position of the buried valley was now known, it was decided to see if it could have been located using gravity and magnetic measurements. Accordingly, 41 sets of observations were made in sections 28 and 33 of T 26N, R 3E with a station spacing of about 0.2 miles. In these sections the resistivity measurements indicate that the buried valley strikes northeast-southwest diagonally across section 28 and then north-south in section 33. Some of the stations were located on the perimeter of the area with a station spacing of about one mile

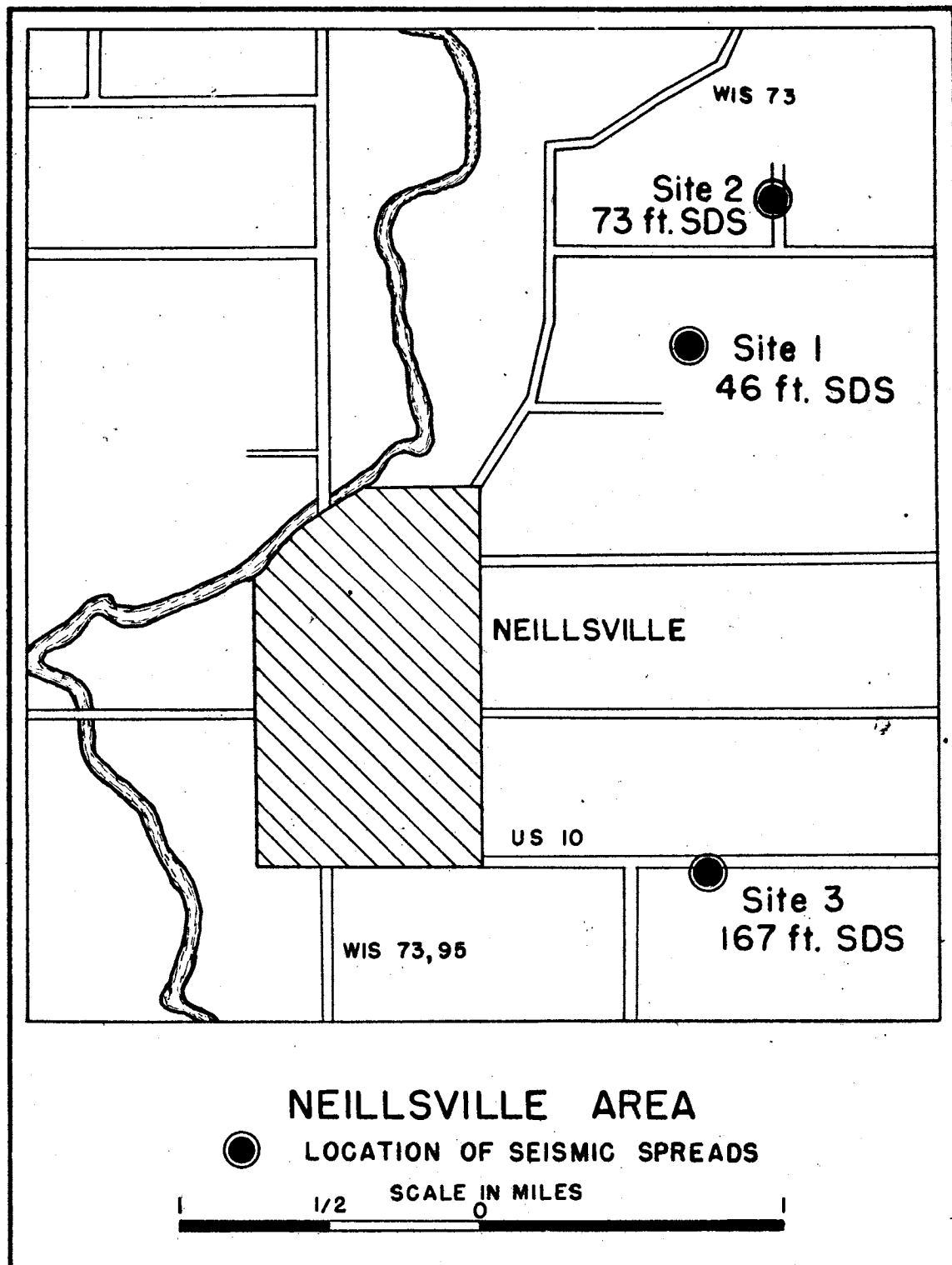


FIG. 54

for regional control. Fig. 55 shows the location of the gravity and magnetic stations in relation to the position of the valley as mapped on the basis of the resistivity measurements and test wells.

The anomaly values are tabulated in Table 25 and Figs. 56a and 57 show Bouguer Anomaly and magnetic anomaly maps of the area respectively.

From Fig. 56a, it is seen that the regional gravity gradient is so pronounced that the effect of the buried valley is almost completely masked. The only indication of its presence is a negative re-entrant in the contours indicating a local deficiency in mass. The magnetic anomaly map, on the other hand, shows a well-defined magnetic "low" crossing the area which appears to be associated with the valley. This "low", while parallel in general trend to the valley as indicated in Fig. 55, appears to be displaced both to the west and south; however, there seems to be little reason to doubt that it is related to the valley.

In order to study the gravity values further, the regional gradient was subtracted from the gravity anomaly map of Fig. 56a and the resultant residual values contoured to outline a north-south area of minimum gravity values having about 1 mgal relief. This residual map, while not giving any great detail, does agree in general location and trend with the known valley. See Fig. 56b

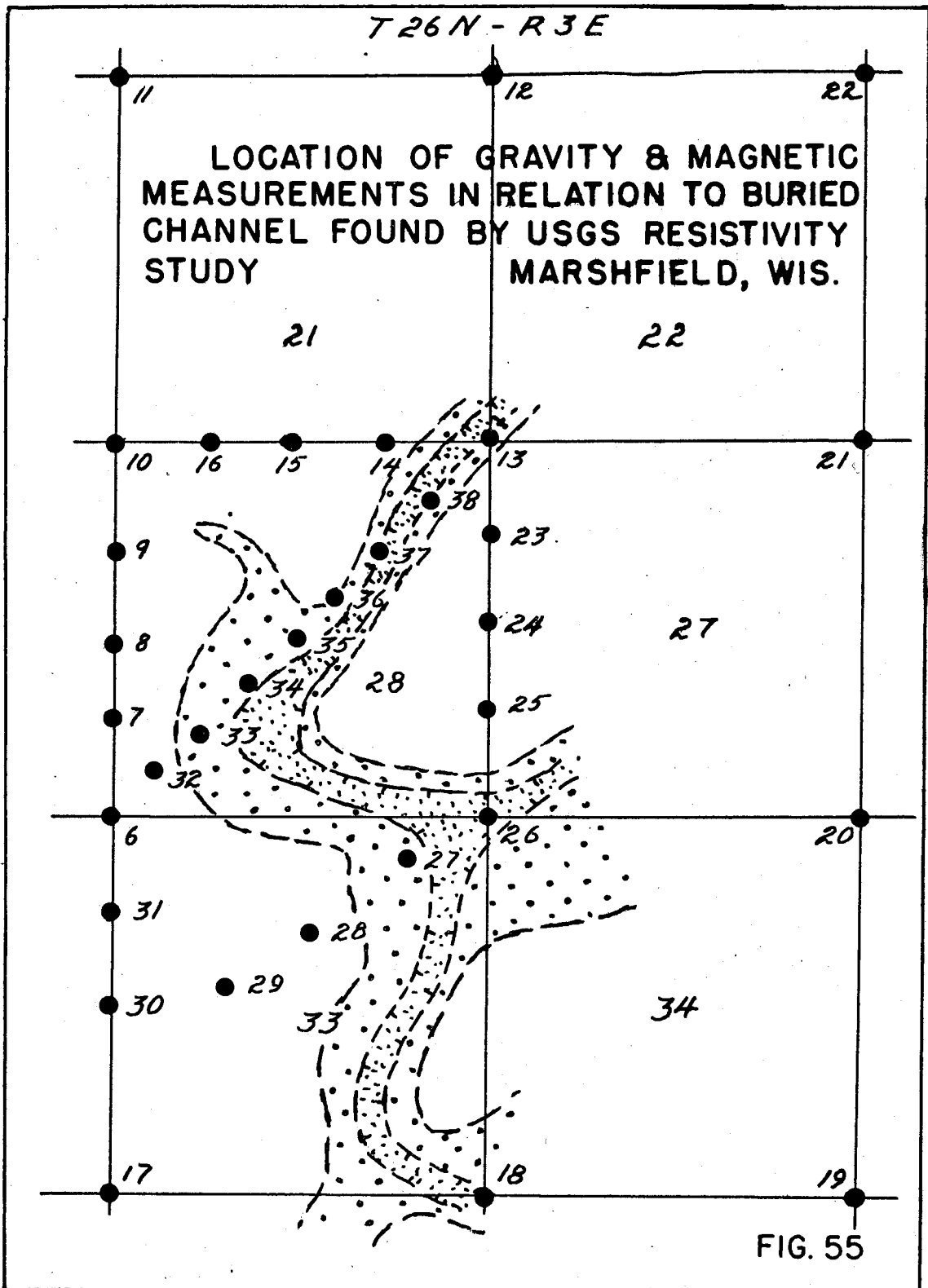
It therefore appears that both gravity and magnetic measurements can be used to outline buried valleys. However, it is fortuitous that a valley as small as that of Marshfield which is about 0.3 miles wide and less than 100 feet in depth shows up so distinctly in these measurements. The density differential indicated between the crystalline rock and the gravels present is about 1 gm/cm^3 which is rather high. Likewise the change in magnetic susceptibility indicated between the gravels and the crystalline rocks is large. In another area where the valley is filled with "normal" glacial drift or the bedrock material different, the anomalies might be considerably smaller.

Table 25

Gravity and Magnetic Anomaly Values

Marshfield, Wisconsin

<u>Station</u>	<u>Bouguer Gravity (mgals)</u>	<u>Magnetic (gammas)</u>	<u>Station</u>	<u>Bouguer Gravity (mgals)</u>	<u>Magnetic (gammas)</u>
2	-78.31	100	21	-72.96	59
3	-81.74	87	22	-78.68	123
4	-75.21	90	23	-75.93	127
5	-72.33	108	24	-76.09	42
6	-76.32	91	25	-76.61	93
7	-75.41	54	26	-77.30	92
8	-74.70	77	27	-77.95	121
9	-73.33	123	28	-77.80	38
10	-72.20	119	29	-77.73	61
11	-68.73	130	30	-77.79	24
12	-70.44	300	31	-77.11	173
13	-73.88	59	32	-75.73	22
14	-73.86	42	33	-76.48	21
15	-73.66	95	34	-76.52	-66
16	-73.02	134	35	-76.26	35
17	-78.28	68	36	-75.80	20
18	-78.72	83	37	-75.15	77
19	-77.13	71	38	-74.83	85
20	-75.93	232			



MARSHFIELD, WIS.
OBSERVED BOUGUER ANOMALY

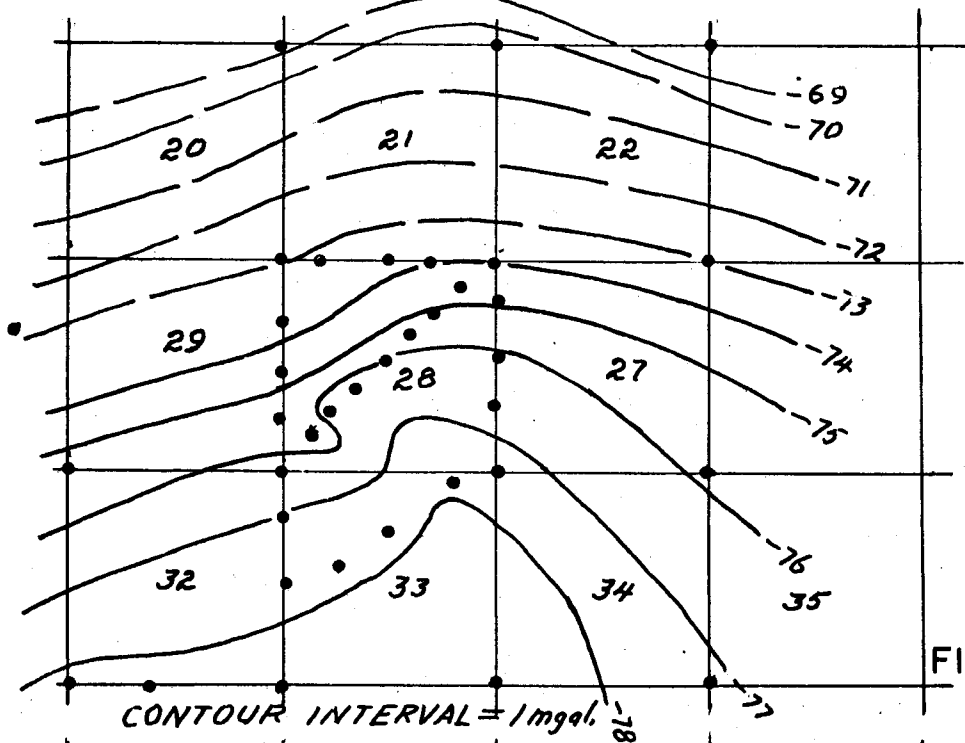


FIG. 56a

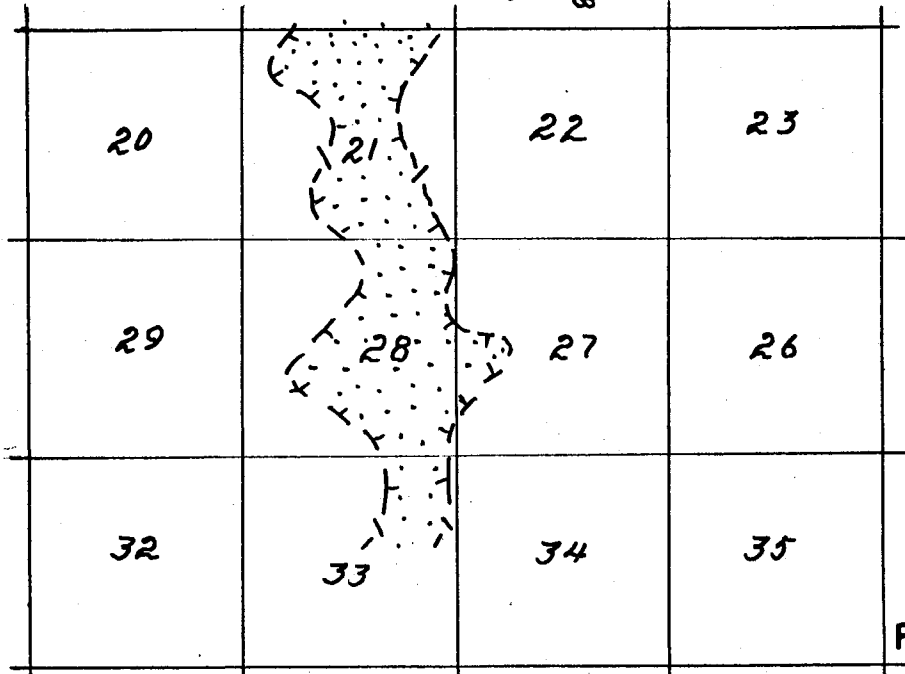
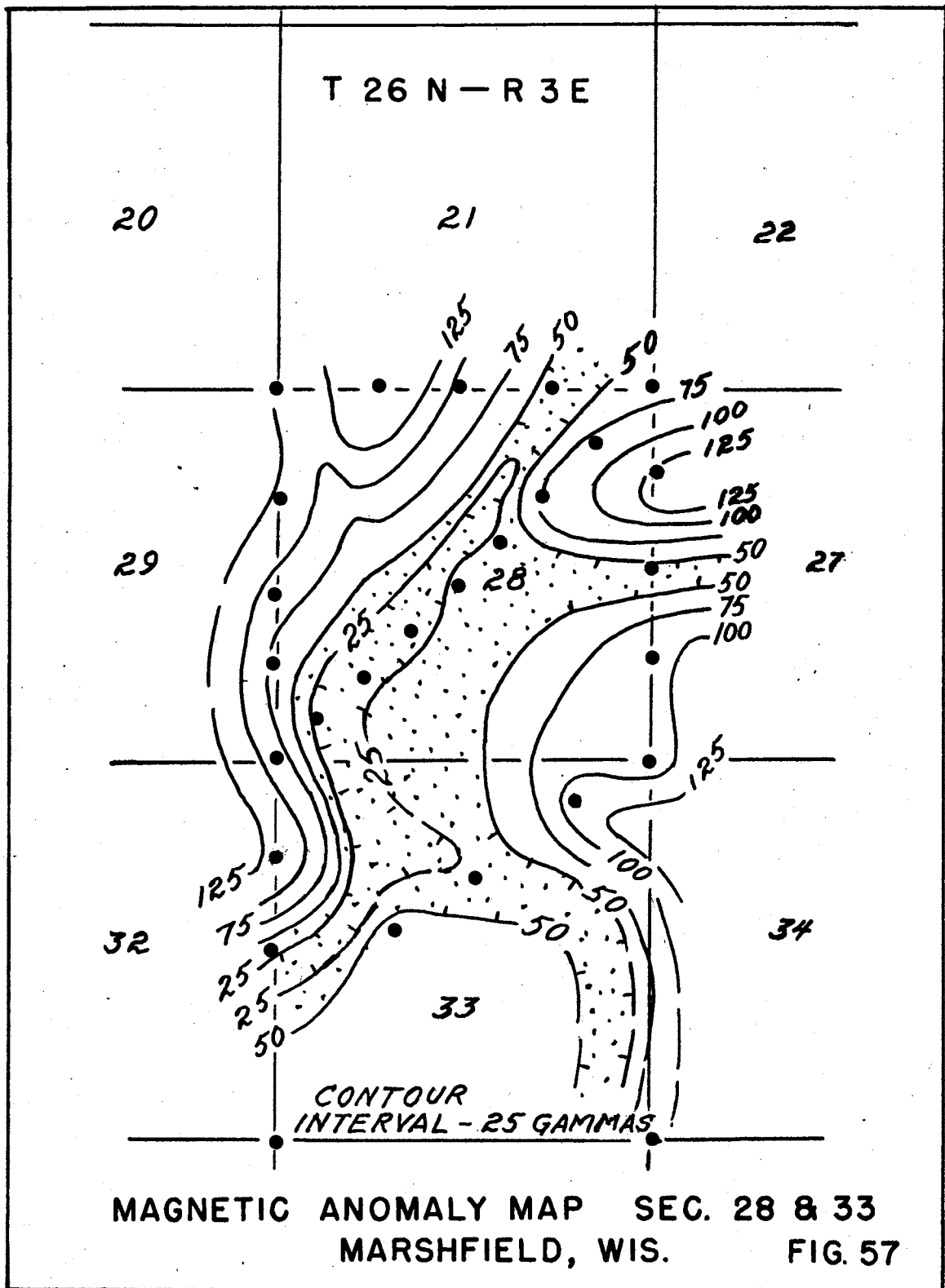


FIG. 56b

RESIDUAL BOUGUER ANOMALY



Part III

Subsurface Engineering Studies

III-1 - General Statement

Engineering applications of geophysics can be divided into the following categories:

- (1) Materials exploration, the location of sand, gravel or rock for construction purposes.
- (2) Foundation studies, the determination of the subsurface geology at the sites for buildings, dams or bridges.
- (3) Route investigations, the location of the most economical route for roads, railroads or canals.
- (4) Structure studies, the testing of models or actual structures from the standpoint of design or specifications.

Investigations in the first three categories are included in this report.

III-2 - Lower Paint River Dam Diversion Canal Crystal Falls, Michigan

III-2a General Statement

The Lower Paint River Dam is part of the hydro-electric development of the Wisconsin-Michigan Power Co., and is located just across the Wisconsin-Michigan State line near the town of Crystal Falls. The geology of the area is simple with glacial till overlying granite bedrock. The geophysical investigation was carried out to determine the depth to bedrock along the route of a proposed diversion canal, about 7000 feet in length, between the dam and Peavey Pond. Preliminary drilling had shown that the depth to the underlying granite varied from a few feet to over 20 feet and that the rock surface was very irregular with abrupt changes in relief up to 15 feet.

III-2b Seismic Investigation

Depth measurements were made at sixty-two locations using the reverse shooting seismic refraction method, and three seismic velocity horizons were found to be present. The upper horizon (V_1) which had a velocity varying between 1500 and 2200 ft./sec. was identified as unsaturated glacial till. The second horizon (V_2) with a velocity varying from 5000 to 5600 ft./sec. was identified as saturated glacial till (water table), and in the swamp areas formed the surface layer. The third horizon (V_3) had a velocity varying between 11,000 and 20,000 ft./sec. and was identified as the crystalline rock surface having a variable petrologic composition.

The seismic depths and elevations are tabulated in Table 26. The location of the points of depth measurement are shown in Fig. 58 along with contours on the "granite" surface. In Figs. 59 and 60, depth profiles along the proposed route of the canal are shown.

III-2c Evaluation of Results

At the time of the seismic survey, a few test holes had been drilled along the proposed center line of the canal, and it was in part because of the highly irregular results shown by the drill data that the University was asked to make a study of the route. The agreement between the seismic data and the drill hole logs varied considerably, but as most of the tests were near the dam in an area with marked irregularities in the bedrock surface, no conclusion was reached regarding the overall accuracy of the survey. However, on the basis of the accuracy achieved on other seismic investigations, it was decided to re-route the canal in part and modify the design so as to raise the bottom 7 feet in order to avoid rock.

After the construction work was completed, it was possible to secure a better evaluation of the seismic results from both the engineer's records of where rock was encountered and rod sounding of the proximity of bedrock to the canal bottom. It was found that where the seismic measurements were made in line with the canal the agreement was good. Where seismic spreads were far apart (500 feet or more) the rock surface irregularities were such that straight line extrapolation of depths between seismic stations was not justified. Where the seismic measurements were made at right angles to the canal the degree of irregularity of the bedrock surface was frequently correct but the actual location of the irregularity was not. These relations can best be seen from the comparative profiles shown in Fig. 61 for sections along the center line of the completed canal corresponding to sections AA and CC of Fig. 58.

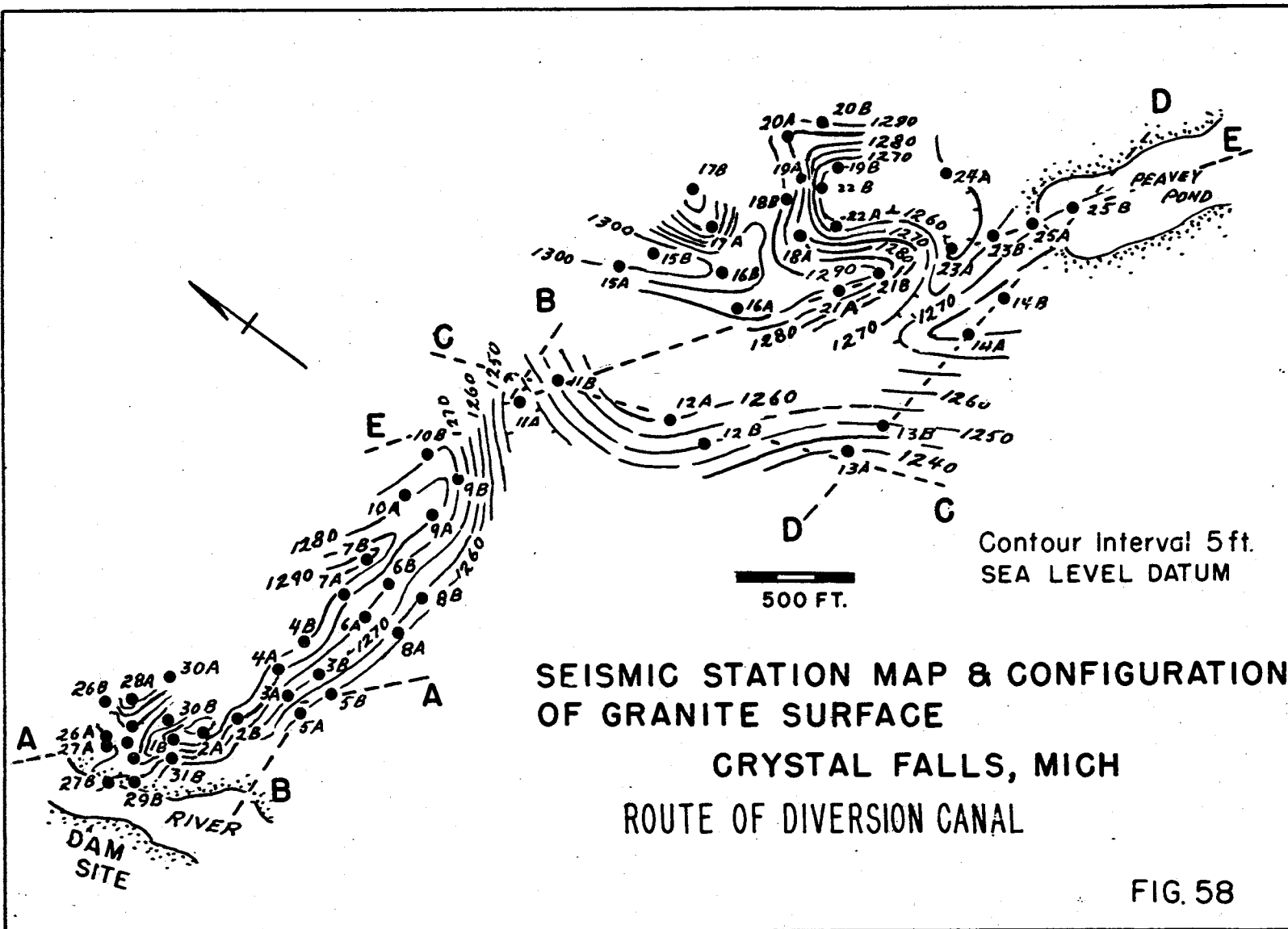
Table 26

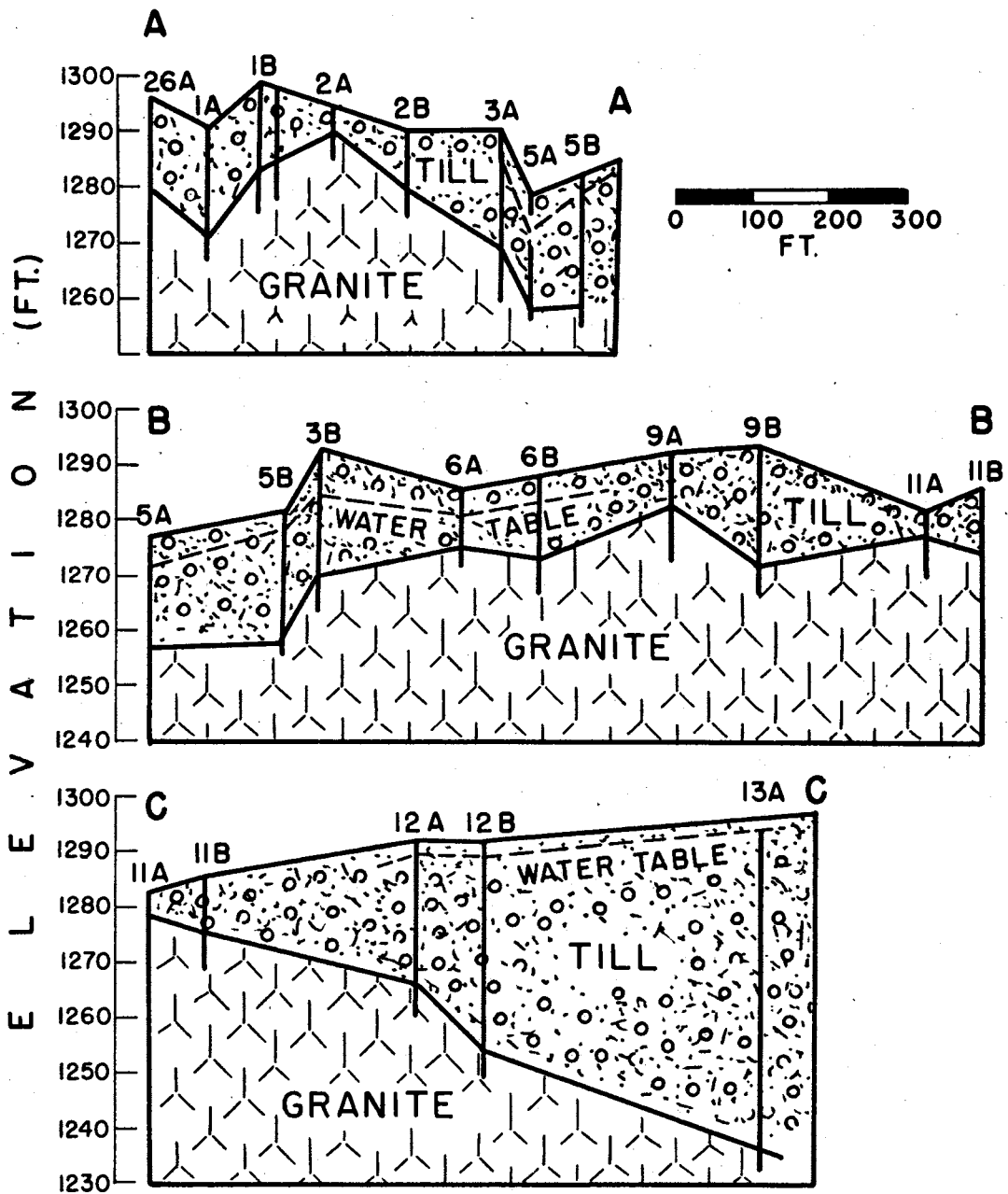
Seismic Data, Lower Paint River Dam Diversion Canal
Crystal Falls, Michigan

Elevations Relative Sea Level

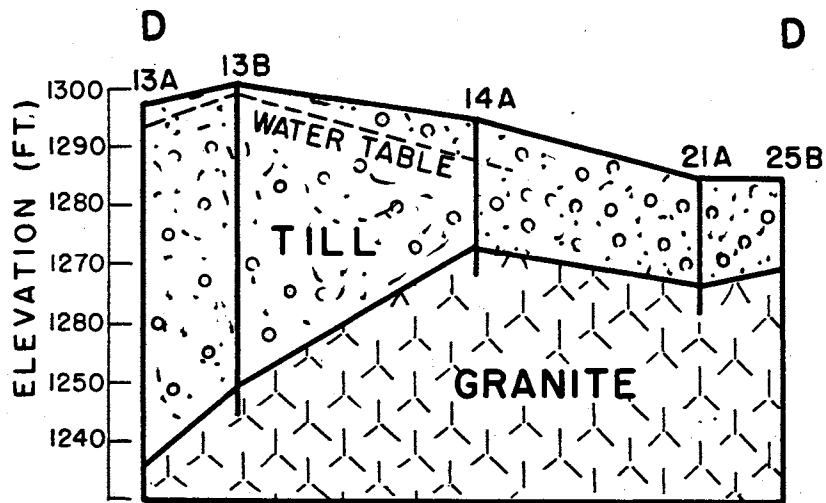
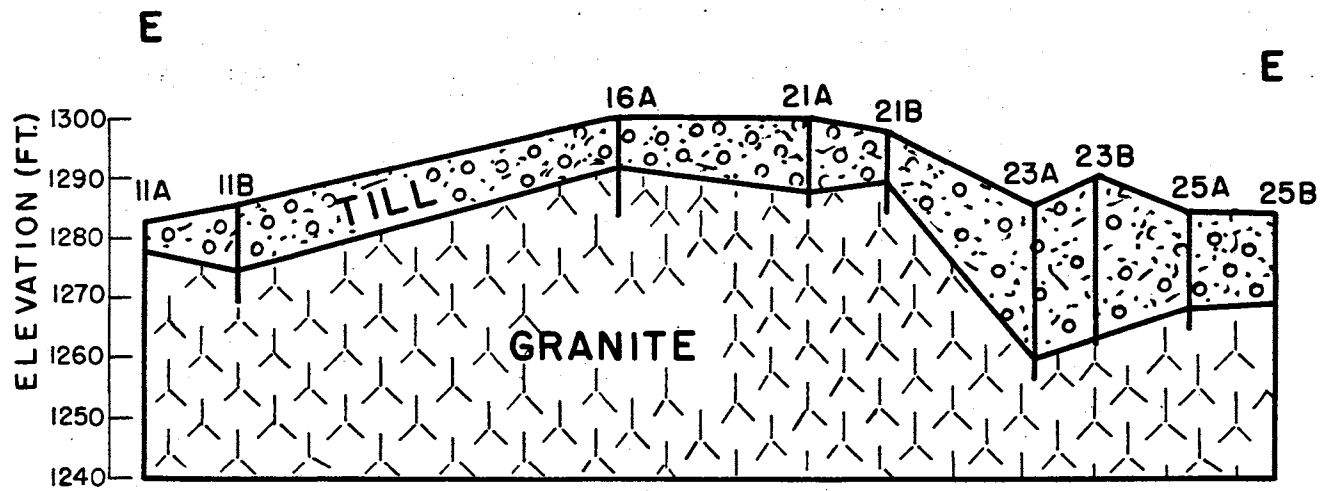
Station	Ground Level	Water Table	Rock Surface	Station	Ground Level	Water Table	Rock Surface
1A	1291	----	1271	16B	1307	----	1297
1B	1299	----	1285	17A	1304	1298	1273
2A	1295	----	1290	17B	1307	1298	1266
2B	1290	----	1280	18A	1313	1300	1278
3A	1291	1286	1271	18B	1301	----	1290
3B	1294	1285	1271	19A	1296	----	1288
4A	1303	1300	1281	19B	1291	----	1269
4B	1304	1301	1286	20A	1296	----	1285
5A	1278	1272	1258	20B	1298	----	1291
5B	1282	1280	1258	21A	1303	----	1288
6A	1287	1282	1276	21B	1299	----	1289
6B	1289	1284	1274	22A	1298	1287	1261
7A	1297	----	1281	22B	1293	1288	1253
7B	1304	----	1293	23A	1289	1288	1260
8A	1283	1276	1262	23B	1291	1290	1265
8B	1288	1282	1266	24A	1285	----	1257
9A	1293	----	1283	25A	1286	----	1269
9B	1284	----	1274	25B	1286	----	1270
10A	1299	1293	1277	26A	1296	1292	1279
10B	1295	1291	1273	26B	1315	1294	1268
11A	1283	----	1278	27A	1296	1290	1280
11B	1287	----	1276	27B	1275	----	1274
12A	1293	1290	1266	28A	1310	1300	1250
12B	1292	1290	1255	28B	1284	----	1280
13A	1298	1295	1237	29A	1304	----	1274
13B	1303	1299	1251	29B	1275	----	1274
14A	1295	1287	1278	30A	1316	1311	1264
15A	1315	----	1297	30B	1304	1299	1283
15B	1319	----	1311	31A	1304	1295	1283
16A	1304	----	1292	31B	1274	----	1271

The general consensus of opinion of the engineers in charge of the project was that the work was successful and had resulted in saving several thousands of dollars.





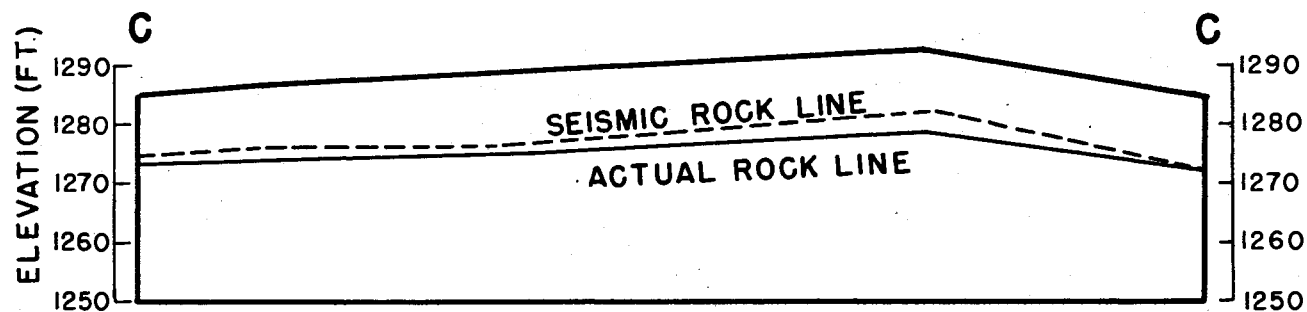
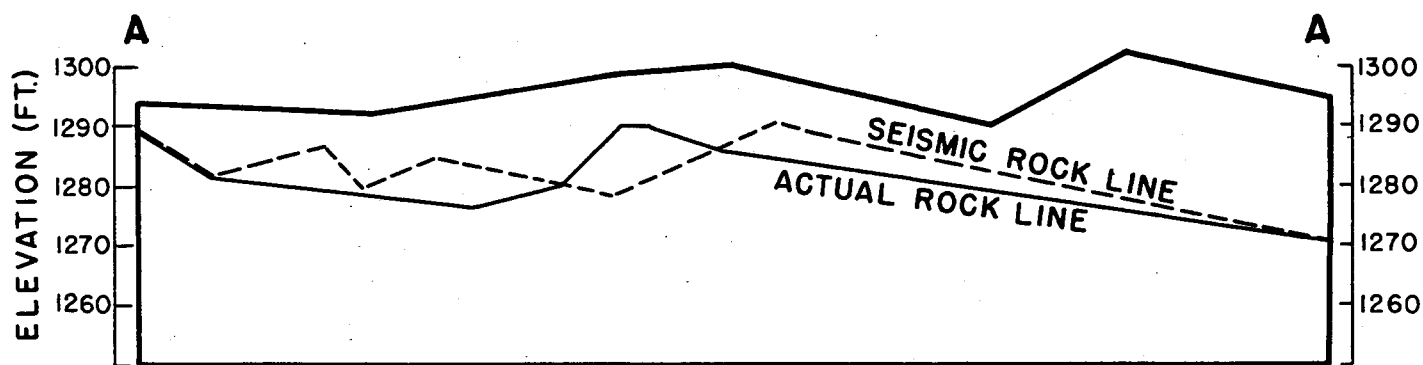
SEISMIC SECTIONS DIVERSION CANAL
CRYSTAL FALLS, MICH. FIG. 59



0 100 200 300
FT.

**SEISMIC SECTION
DIVERSION CANAL
CRYSTAL FALLS, MICH.**

FIG. 60



COMPARISON OF SEISMIC & ACTUAL DEPTHS TO
BEDROCK ALONG CENTER LINE OF CANAL

CRYSTAL FALLS, MICH.

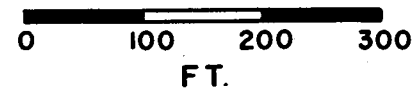


FIG. 61

III-3 - Wisconsin Dells, Wisconsin
Subsurface Materials Investigations

III-3a General Statement

The purpose of this investigations was to ascertain the degree to which sands and gravels could be differentiated from glacial till on the basis of seismic velocity determinations and electrical resistivity measurements. The area studied was north of Wisconsin Dells and immediately adjacent to the glacial terminal moraine. A supplementary study was also made north of Madison in two gravel pits near the village of Burke.

Measurements were carried out first at seven sites in a large gravel pit where the materials could be identified and correlated with the geophysical results. Further observations were made at six sites on the till behind the moraine and at four sites on the outwash sand deposits in front of the moraine. As these observations were for the determination of typical resistivity and velocity values only, the seismic spread was limited to 200 feet and the resistivity electrode intervals to 1000 feet. As twelve seismic detectors were used in line over the 200 foot spread, the velocity values are well established.

III-3b Seismic Investigation

In all of the locations, except two in the gravel pit, there appeared to be a low velocity surface layer, tentatively identified as weathered glacial till in which the average velocity was about 1350 ft./sec. Similar velocity values were also noted for the surface layer over the moraine and the outwash plain.

The velocity values observed over known gravel both at Wisconsin Dells and Burke, varied from 2240 to 3040 ft./sec. with an average value of about 2660 ft./sec. The spread in values observed over the outwash sands in front of the moraine was greater than that observed over the gravels and it was indeterminate whether these sands could be differentiated from till or gravel. The till behind the moraine was characterized by velocity values varying from 1650 to 2620 ft./sec. with an average value of 1990 ft./sec.

On the basis of these results it would appear that gravel or a mixture of sand and gravel might well be differentiated from till so long as both materials were unsaturated and above water table. As the effect of complete saturation is to raise the apparent velocity to a value approximating that of sound in water (about 5000 ft./sec.), it is obvious that both materials would have essentially the same velocity below water table.

In Table 27 the observed velocity values are given along with the depth of the weathered surface layer as determined from the seismic measurements in the test areas.

A series of velocity determinations were carried out at twenty-seven other sites along the edge of the moraine as an extension of this study and their general locations are indicated in Fig. 62. At all of the sites a low velocity surface layer of about 1350 ft./sec. was observed. The actual values ranged from 1010 ft./sec. to 1780 ft./sec. At fourteen locations the velocity values observed immediately below the surface layer were in the range 2440 ft./sec. to 3420 ft./sec. The material here was tentatively identified as gravel or a combination of sand and gravel. At nine locations the velocity values observed below the surface layer were in the range of 1700 to 2000 ft./sec. and the material was classified as probable till. The velocity values beneath the surface layer at the other sites were in the range of 2000 to 2200 ft./sec. and the nature of the material was indeterminate. These data are summarized in Table 28.

III-3c Resistivity Studies

Resistivity measurements were also carried out in the test area at essentially the same sites as the seismic measurements were made. The Wenner electrode configuration was used with electrode spacing of 20, 40, 60, 80, and 100 feet. Average resistivity values for each of the above electrode spacings were determined with current flowing in opposite directions.

The results of these measurements in the test area are summarized in Table 29, and shown graphically in Fig. 63. At four of the sites in the gravel pit area the resistivity values increased systematically with increase in electrode spacing. It is significant that at each of these sites the overburden of soil had not been stripped off the underlying gravel. The results at the two locations on exposed gravel, sites G-1 and G-5, are markedly different in that at these locations the resistivity values obtained with both the short and long electrode spacings are consistently high.

Somewhat similar relations are observed over the till with results at four sites showing an increase in values as the electrode spacing is increased and those at two sites, T₁ and T₃, remaining essentially constant, although values are significantly lower than those in the gravel pit. The values were more variable on the outwash plain, although significantly higher, than in the other two areas. Despite the variability in values the change in resistivity with increase in electrode spacing was very similar.

Table 27a

Seismic Results in Test Areas
Wisconsin Dells, Wisconsin

Station	Seismic Velocities			Depth of Layers	
	V ₁	V ₂	V ₃	V ₂	V ₃
Gravel Pit					
G-1	-----	2100	-----	20	--
G-2	1600	2952	-----	9	--
G-3	1300	2842	-----	5	--
G-4	1340	2239	-----	6	--
G-5	1720	3014	-----	4	--
G-6	-----	2440	3750*1	--	12
G-7	1800	3040	-----	5	--
Outwash Plain					
O-1	1360	-----	-----	35	--
O-2	1321	1832	-----	19	--
O-3	1324	3020	-----	36	--
O-4	1223	-----	5470*2	--	46
Moraine					
T-1	1250	2160	-----	21	--
T-2	1890	-----	-----	30	--
T-3	1433	2000	-----	28	--
T-4	1400	2620	-----	2	--
T-5	1400	1650	3368*1	3	31
T-6	1647	-----	-----	30	--

V₁ = weathered glacial till but may include sand in outwash plain area.

V₂ = area of gravel pit = gravel

*1 = clay or older till (?)

*2 = water table (?)

Table 27b

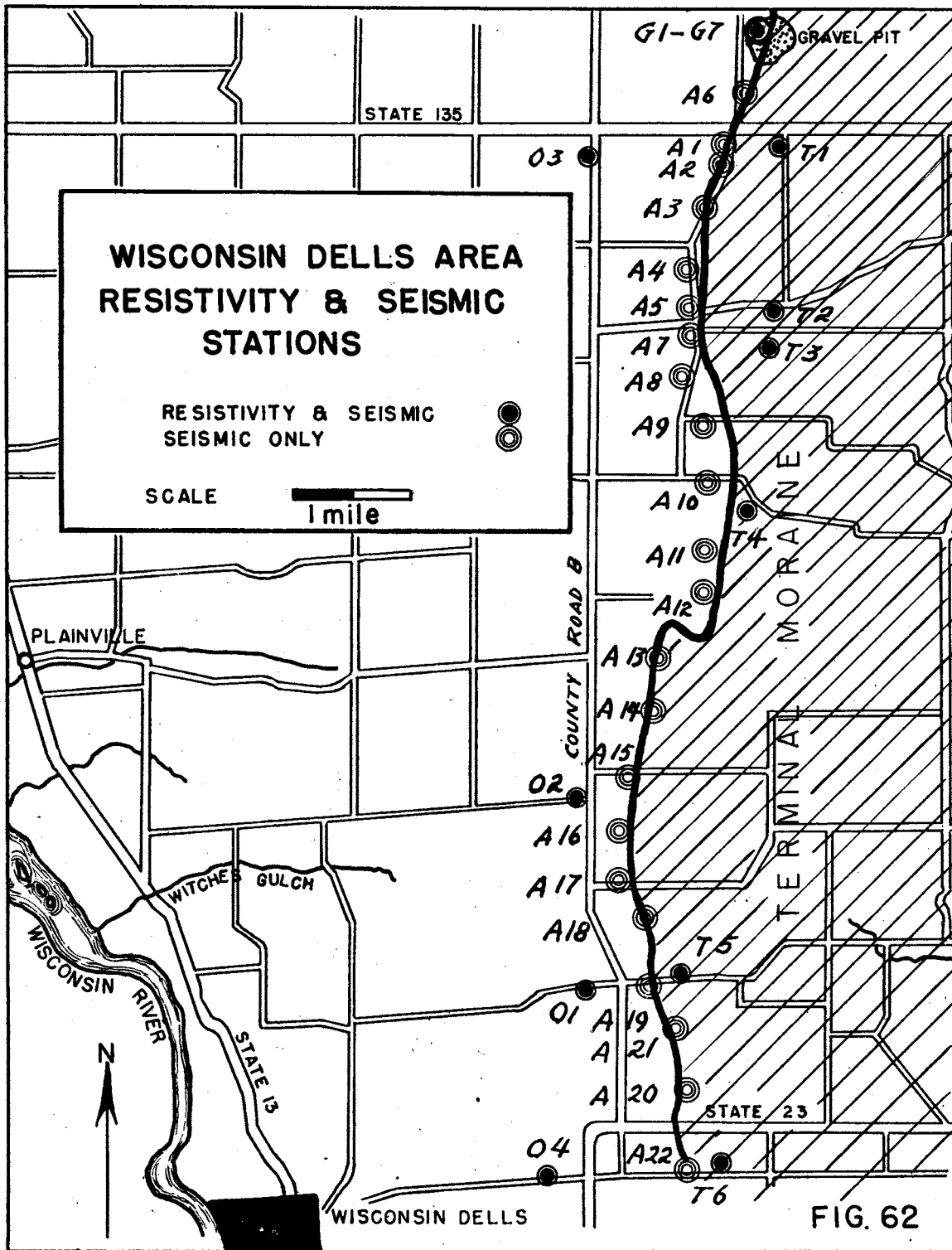
Observations near Burke, Wisconsin

Station	V ₁	V ₂	V ₃	V ₂	V ₃
1	1290	-----	4520	--	20
2	1780	2330	5600	4	30
3	-----	1960	8400	0	32

V₁ = weathered till

V₂ = sand and gravel

V₃ = water table at sites 1 and 2, bedrock at site 3



Seismic Values, Wisconsin Dells Area

Station	Seismic Velocities			Depth of layers		Material Identification at Depth
	V ₁	V ₂	V ₃	V ₂	V ₃	
A-1	1540	3300	----	7	---	gravel
A-2	1300	2187	----	5	---	?
A-3	1500	2045	----	4	---	?
A-4	1040	1818	----	4	---	till
A-5	1340	2820	----	7	---	gravel
A-5 ¹	1000	2440	----	4	---	gravel
A-6	1200	2528	----	5	---	gravel
A-7	1340	1572	----	4	---	till
A-8	1400	1730	----	6	---	till
A-9	1200	2890	----	5	---	gravel
A-9 ¹	1700	2990	----	14	---	gravel
A-10	1060	1700	2315	3	18	gravel
A-11	----	2010	3165	5	---	gravel
A-11 ¹	1760	----	----	-	---	till
A-12	1040	1908	----	1	---	till
A-13	1440	2015	----	6	---	till
A-14	1200	2000	----	4	---	till
A-15	1014	2192	----	4	---	?
A-16	1700	2440	----	7	---	gravel
A-17	1040	1850	----	5	---	till
A-18	1780	2530	----	18	---	granite
A-18 ¹	1525	----	----	-	---	till
A-19	1710	----	----	-	---	till
A-20	1460	2150	----	3	---	?
A-21	1360	2762	----	4	---	gravel
A-21 ¹	1100	2440	----	3	---	gravel
A-22	1410	3470	----	5	---	gravel

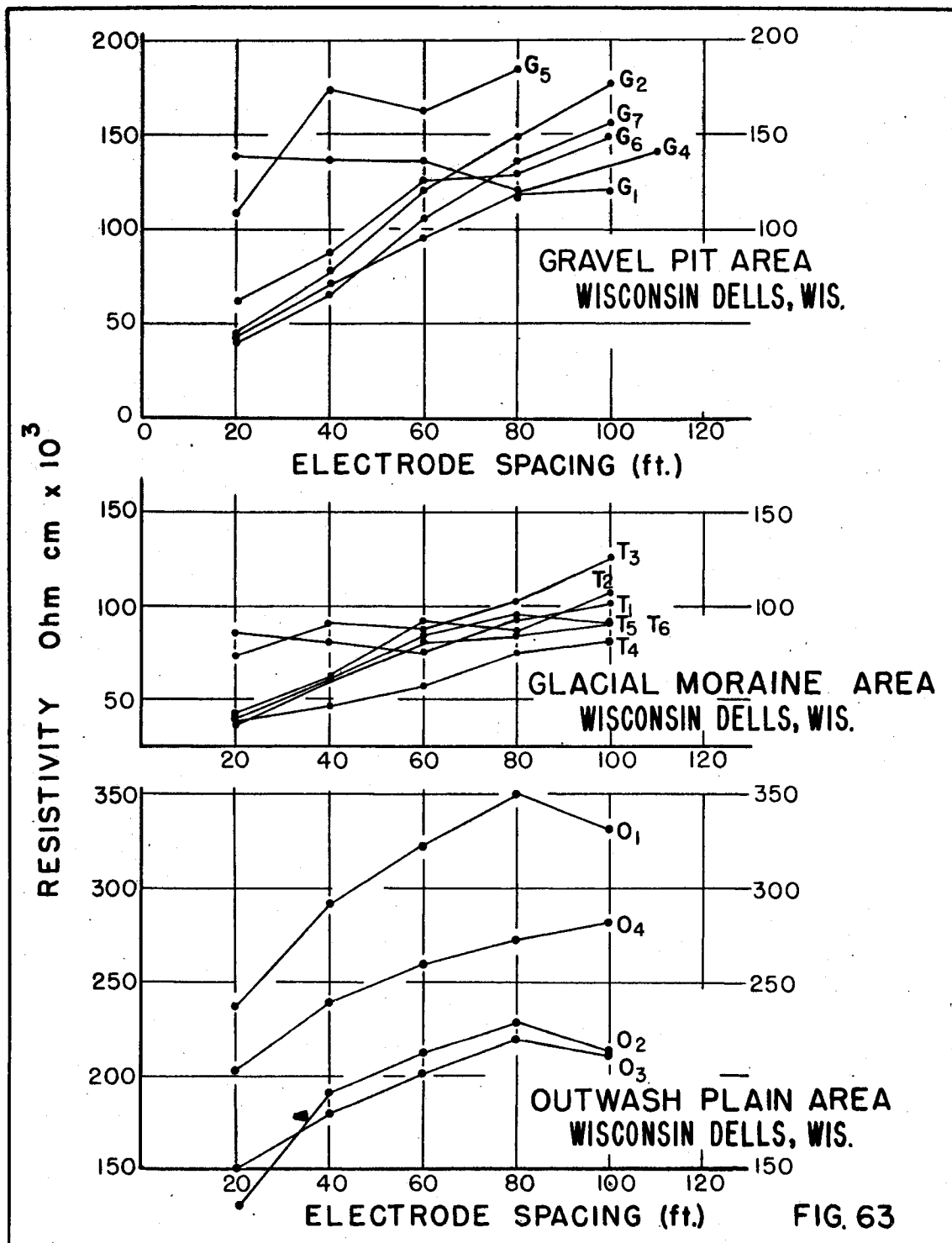
Table 29

Resistivity Values

Wisconsin Dells, Wisconsin

Site	20 ft.	40 ft.	60.ft.	80 ft.	100 ft.
	Ohm cm x 10 ³				
Gravel Area					
G-1	139.0	137.0	136.0	117.0	122.0
G-2	49.2	78.4	123.0	150.0	178.0
G-3	44.4	72.3	97.6	120.0	141.0
G-4	109.0	175.0	169.0	184.0	-----
G-5	60.0	87.2	125.0	130.0	150.0
G-6	41.7	67.3	109.0	137.0	156.0
Moraine Area					
T-1	83.5	80.2	77.9	93.2	103.0
T-2	41.3	65.1	92.7	87.3	109.0
T-3	75.3	85.1	88.2	102.0	126.0
T-4	38.6	46.9	58.4	76.4	82.0
T-5	41.7	64.2	81.8	87.3	90.2
T-6	36.4	61.7	87.8	93.3	90.3
Outwash Plain					
O-1	237.5	291.0	322.0	350.0	331.0
O-2	116.7	180.0	214.5	228.0	188.5
O-3	150.5	182.5	202.0	221.5	219.0
O-4	201.2	239.5	261.5	273.5	281.5

From these comparisons it appeared that on a relative basis at least sand could be differentiated from till on the basis of the higher resistivity values, and the steeper resistivity gradient obtained with increase in electrode spacing.



III-4 - Argyle, Wisconsin, Yellowstone River Dam Site

III-4a General Statement

The Yellowstone River flows through an area of Paleozoic rocks in southern Wisconsin, and at a site about five miles northwest of Argyle a dam was planned by the Wisconsin State Conservation Department. The valley walls at the proposed dam site are composed of St. Peter sandstone capped with Galena limestone and rise about 60 feet above the valley floor. The purpose of the geophysical investigation was to determine the thickness of alluvium along the center line of the dam, and the depth of the Lower Magnesian dolomite, which lies below the St. Peter sandstone. The dolomite is frequently cavernous and if occurring near the surface, might cause excessive leakage beneath the dam.

III-4b Seismic Investigation

Depth determinations were made using the reverse refraction shooting method at 10 sites; four were along the center line of the proposed dam and the balance were in the area of the proposed spillway.

Four distinct velocity horizons were found. The upper horizon (V_1) had a velocity ranging from 1380 to 1860 ft./sec. and was identified as unsaturated alluvium. The second horizon (V_2) had a velocity varying from 3050 to 5670 ft./sec. and was identified as partially to completely saturated alluvium; this horizon constituted the surface layer over part of the area. The third horizon (V_3) had a velocity varying from 7700 to 9600 ft./sec. and was identified as the St. Peter sandstone. The deepest horizon (V_4) which was determined, had a velocity varying from 13,600 to 15,800 ft./sec. and was identified as the Lower Magnesian dolomite. The velocity and depth values for each site are given in Table 30.

Table 30
Seismic Data at Yellowstone River Dam Site

Station	Seismic Velocities			Depth of Layers	
	1	2	3	1	3
1N	3080	8330	15080	25	83
1S	4950	11000	16500	25	98
2W	5670	7460	-----	19	80
2E	4910	9690	-----	22	80
3W	3960	9740	-----	25	50
3E	3960	7000	12500	22	54
4	3800	6750	-----	20	55
5S	1380	9260	-----	21	79
5C	1860	7730	15000	21	125
5N	3830	7710	12230	26	138

V_1 = surface alluvium
 V_2 = St. Peter sandstone, average true velocity 8460 ft./sec.
 V_3 = Lower Magnesian dolomite, average true velocity 14,700 ft./sec.

The location of the depth measurements are shown in Fig. 64 which also includes depth profiles constructed along the center line of the proposed dam and spillway.

III-4c Evaluation of Results

In addition to the seismic measurements, auger holes were put down at ten locations along the center line of the dam. Three of these were at seismic stations and in each case the auger indicated a depth of alluvium nearly 8 feet less than that was indicated by the seismic measurements. The reason for this discrepancy is not definitely known but there are two possible explanations.

(1) The surface of the St. Peter sandstone is weathered in this locality. The weathered layer would have a velocity similar to that of alluvium, hence the seismic depth would be that for the fresh rock which would be deeper than that of the actual geologic boundary.

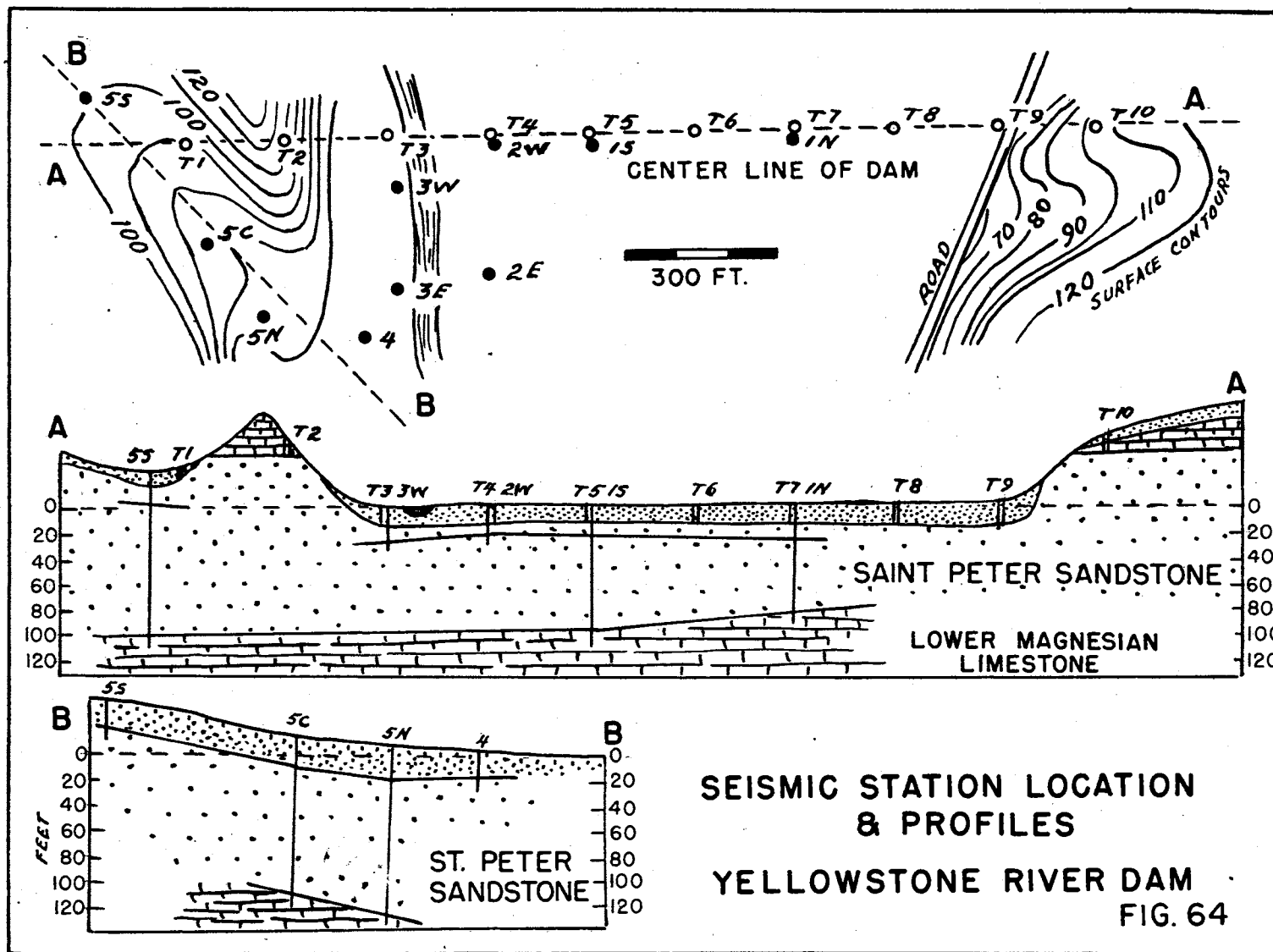
(2) Layers of hard pan are not uncommon in alluvium. In this case such a layer could be interpreted as being the underlying sandstone.

As the dam finally built was of earth fill construction with no excavation to bedrock, it is not known which of the above explanations is correct. No drilling was carried out to test the accuracy of the seismic measurements as to the depth of the Lower Magnesian dolomite which appears to be at depths greater than 50 feet below the valley floor throughout the area.

III-5 - Madison, Wisconsin Second Point Nuclear Accelerator Site

III-5a General Statement

Second Point, known also as Breeze Point, lies on the south shore of Lake Mendota and was selected as a possible site for the location of a new laboratory and nuclear accelerator. A requirement for the proposed structure was that the foundation extend to bedrock, as the settling tolerance for the accelerator was extremely small. The area is covered by glacial drift and no specific information was available regarding the depth to bedrock except from scattered rock outcrops along the lake and the log of a well about a half mile away; the latter showed a depth of 98 feet. A map of the pre-glacial surface of the Madison area did indicate that bedrock formed a hill under the area, but the data upon which this map was based could not be found.



As specific information regarding the elevation of bedrock was required within two days, only a limited number of seismic depth measurements were made.

III-5b Seismic Investigation

Measurements were made using the reverse shooting refraction method at the six locations shown in Fig. 65. Three seismic horizons were found to be present at all of the locations and at two sites four horizons were mapped. The upper horizon (V_1) had a velocity of approximately 1700 ft./sec. and was identified as unsaturated glacial till. The second horizon (V_2) had a velocity of about 4000 ft./sec. and was tentatively identified, on the basis of the velocity values, either as older till or water table. On the basis of the subsurface map referred to, the elevation of this horizon correlated it with the Madison sandstone. The third horizon (V_3) which had a velocity of approximately 7300 ft./sec. was similarly identified on the basis of the velocity value as sandstone, but on the basis of the map it correlated with the Mendota limestone or the Jordan sandstone if present. The deepest horizon (V_4) had a velocity averaging about 12,000 ft./sec. and on the basis of the velocity value was believed to be limestone. The discrepancy between the subsurface geology indicated by the map and the seismic velocities could not be resolved as there was no time to carry out further field studies. On the basis of the known soft character of the Madison sandstone and the fact that it would probably be above water table if present as mapped, it was decided that it might have a velocity as low as 4000 ft./sec. and the section was correlated as indicated in Table 31.

Table 31

Seismic Data at Second Point

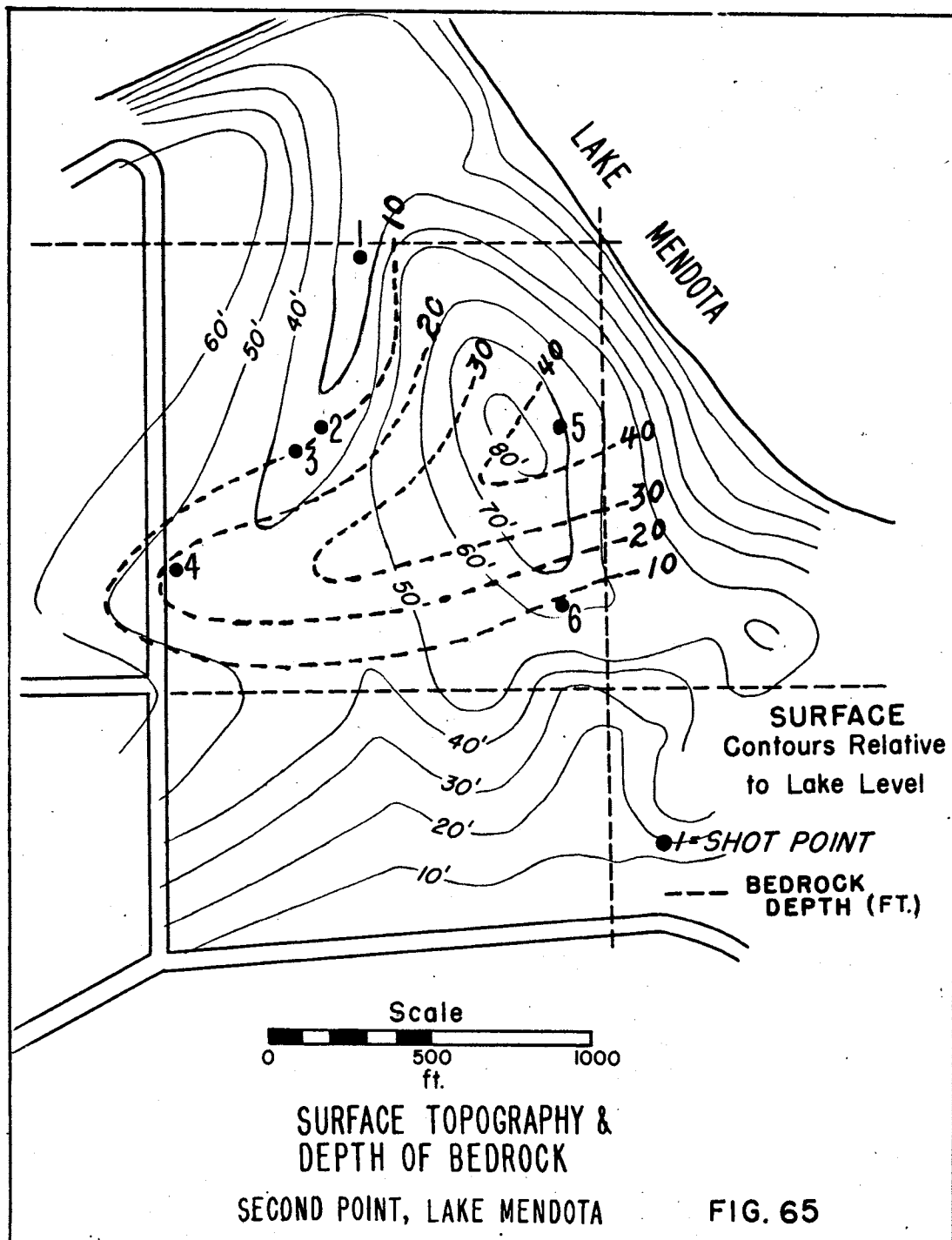
Site	Elv.	Apparent Velocities			Depth of Layers		Elv.	Rel. Lake
	Rel. Lake	V_1	V_2	V_3	V_2	V_3	V_2	V_3
1	25	1420	3335	7350	- 7	-31	+18	- 6
2	32	1470	5530	6900	- 9	-21	+23	+ 4
3	35	1510	4270	6600	-11	-30	+24	+ 5
4	47	1650	5000	8500	-22	-40	+25	+ 7
5	72	2175	3850	8340	-42	-98	+30	-26
6	63	1516	3050	5660	- 8	-71	+55	- 8

V_1 = unsaturated till

V_2 = Madison sandstone (?)

V_3 = Jordan sandstone (?)

V_4 = at sites 1 and 2 only, Mendota limestone = 12,000 ft./sec.



It was however recognized that this correlation might be in error because the first horizon was poorly defined in each case. (See Fig. 66) An alternate interpretation could be put on the data whereby the two upper, low velocity layers would be combined into a single layer. The effect of this difference in interpreting the travel-time data on the calculated depth of bedrock is brought out in Table 32.

Table 32

Alternate Interpretation of the Seismic Data
Second Point

Site	Elv.	Apparent Velocities		Depth V_2	Elv.
	Rel. Lake	V_1	V_2		Rel. Lake V_3
1	25	2500	7350	-18	+ 7
2	32	2000	6900	-13	+ 9
3	35	2000	6600	-20	+15
4	47	1650	8600	-23	+24
5	72	2170	7550	-65	+ 7
6	63	3500	5770	-64	+ 9

V_1 = surface till

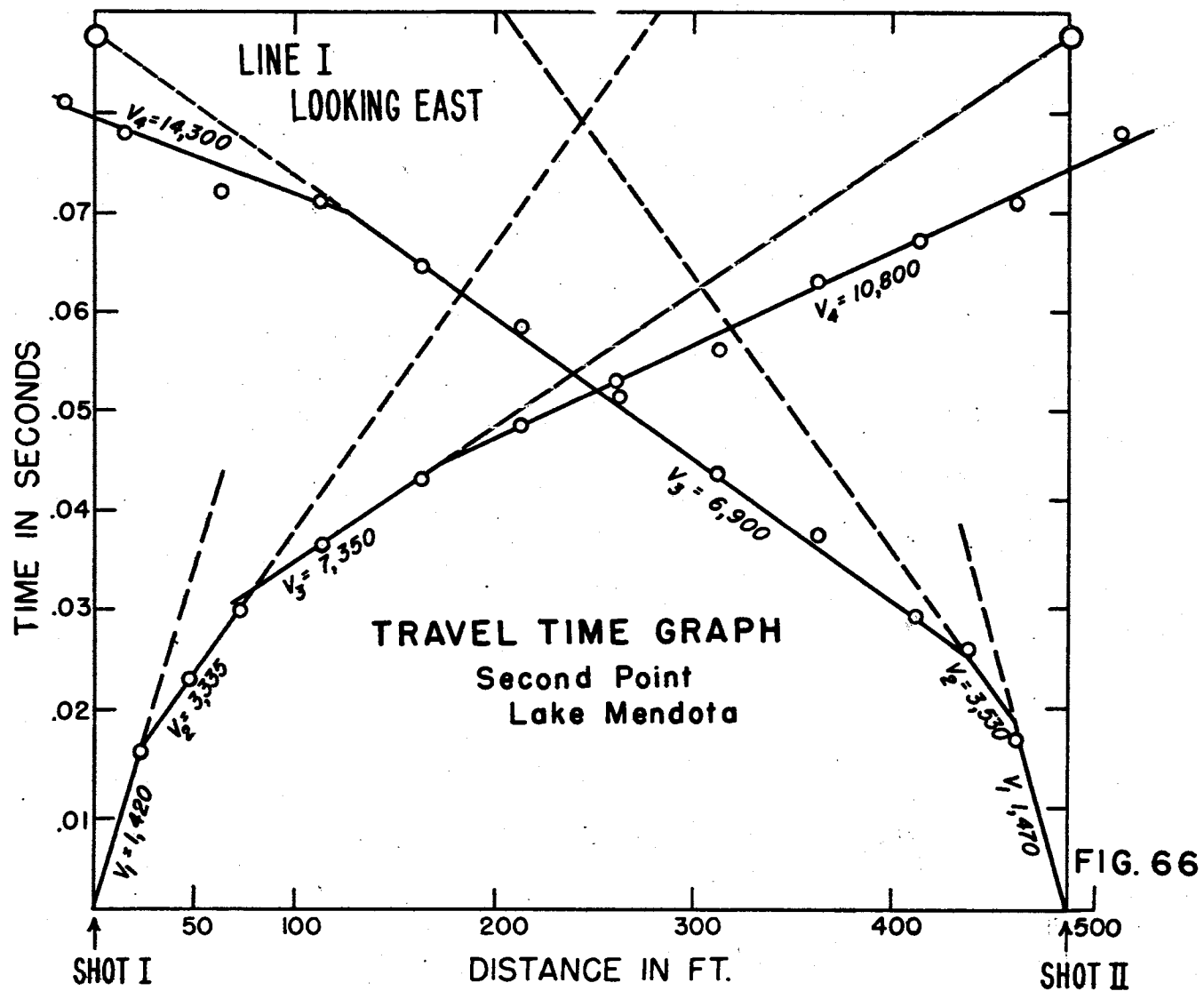
V_2 = Madison sandstone

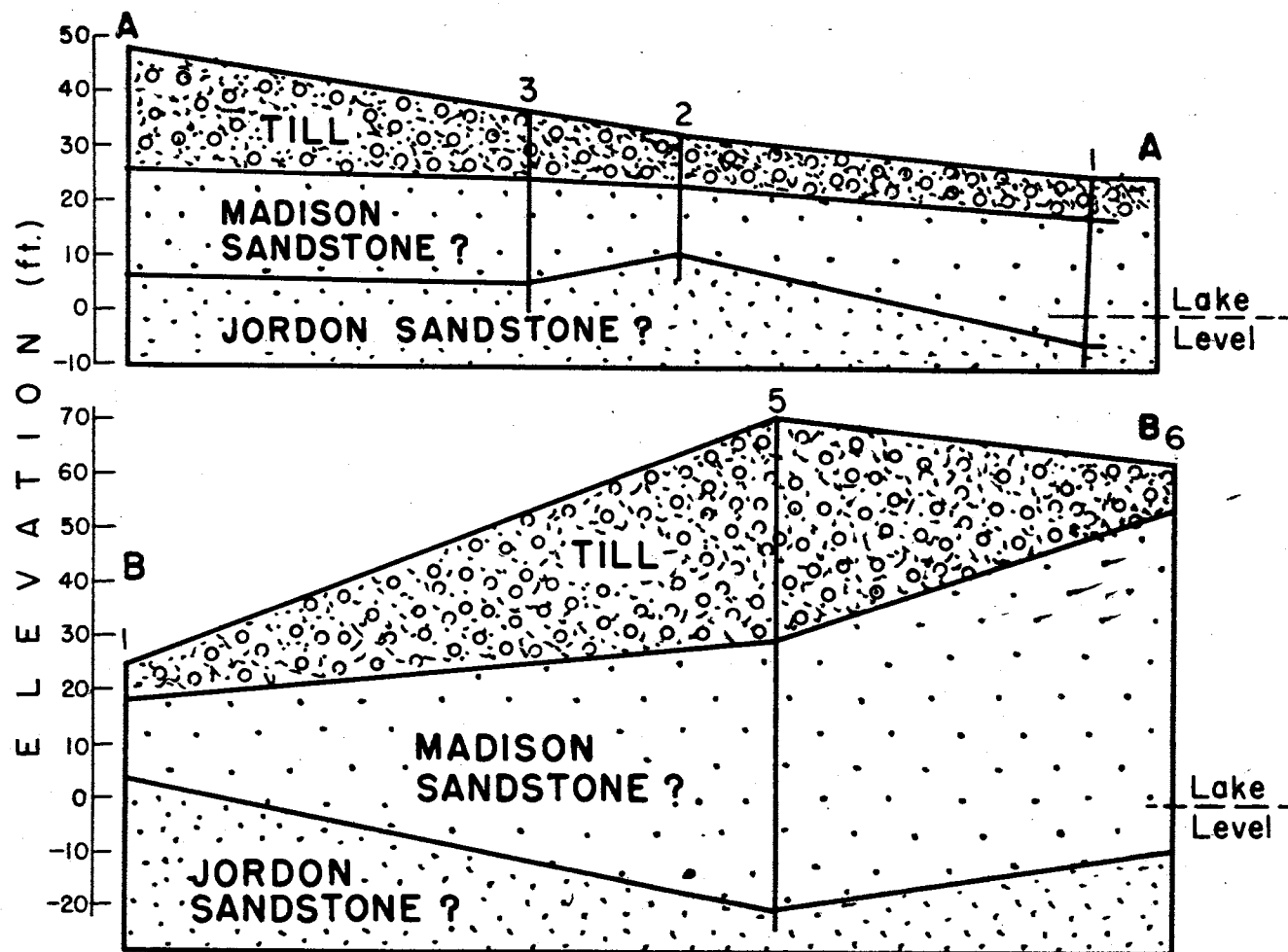
V_3 = at sites 1 and 2 only, Mendota limestone = 12,000 ft./sec.

It was not resolved which of the above interpretations was the more correct until later, when close order seismic work showed that the original interpretation as shown in Fig. 66 was correct. Table 32 has been retained to show the effect of this potential source of error on the results.

An auger hole was put down at site 2 to test the geologic interpretation of the data and sandstone was encountered at 9 feet. This was the calculated depth to the 4000 ft./sec. (V_2) horizon that had been correlated with the Madison sandstone. The interpretation of the data therefore was correct although the velocity is abnormally low for a sandstone.

In Fig. 65 contours showing the depth to the bedrock surface (V_2) horizon are shown and depth profiles along traverses A-A and B-B are presented in Fig. 67.





SEISMIC PROFILES, SECOND POINT LAKE MENDOTA

FIG. 67

III-6 - Madison, Wisconsin
Hydraulics Building
University of Wisconsin

III-6a General Statement

Science Hall, the site of the University seismograph pier, was found to be no longer suitable for teleseismic recording of earthquakes because the glacial till, on which the pier rests, was picking up traffic vibrations to such an extent that the only quiet periods were between 01:00 and 05:00 in the morning. In an effort to locate a bedrock site the Hydraulics Laboratory, which has an elevation about 80 feet lower than Science Hall, was selected as a place that might have bedrock within a few feet of the surface. A reverse seismic refraction depth measurement was made along the shore of Lake Mendota just west of the Laboratory to see if this was the case.

III-6b Results of Seismic Measurement

Two seismic velocity horizons were found to be present. The upper horizon (V_1) had a velocity of about 5300 ft./sec. and was identified as water saturated glacial till. The lower horizon (V_2) had a velocity of about 9000 ft./sec. and was identified as the underlying sandstone. The pertinent data are summarized in Table 33.

Table 33

Seismic Results, Hydraulics Laboratory

Site	Apparent Velocities		Depth V_2	
	V_1	V_2		
1	5145	8150	110 ft.	(east end)
2	5691	9900	72 ft.	(west end)

V_1 = water saturated till
 V_2 = sandstone

As the depths indicated are well below any practical level for a pier to bedrock, it was concluded that the seismograph station would have to be moved to some other area.

III-7 - Cave of the Mounds Gravity Study

III-7a General Statement

Although caves are natural phenomena which are familiarly exploited as tourist attractions they may also have a very vital bearing upon the foundations of engineering structures and leakage from reservoirs. In addition they are becoming increasingly important as a means of protecting vital industry and storing records in times of war.

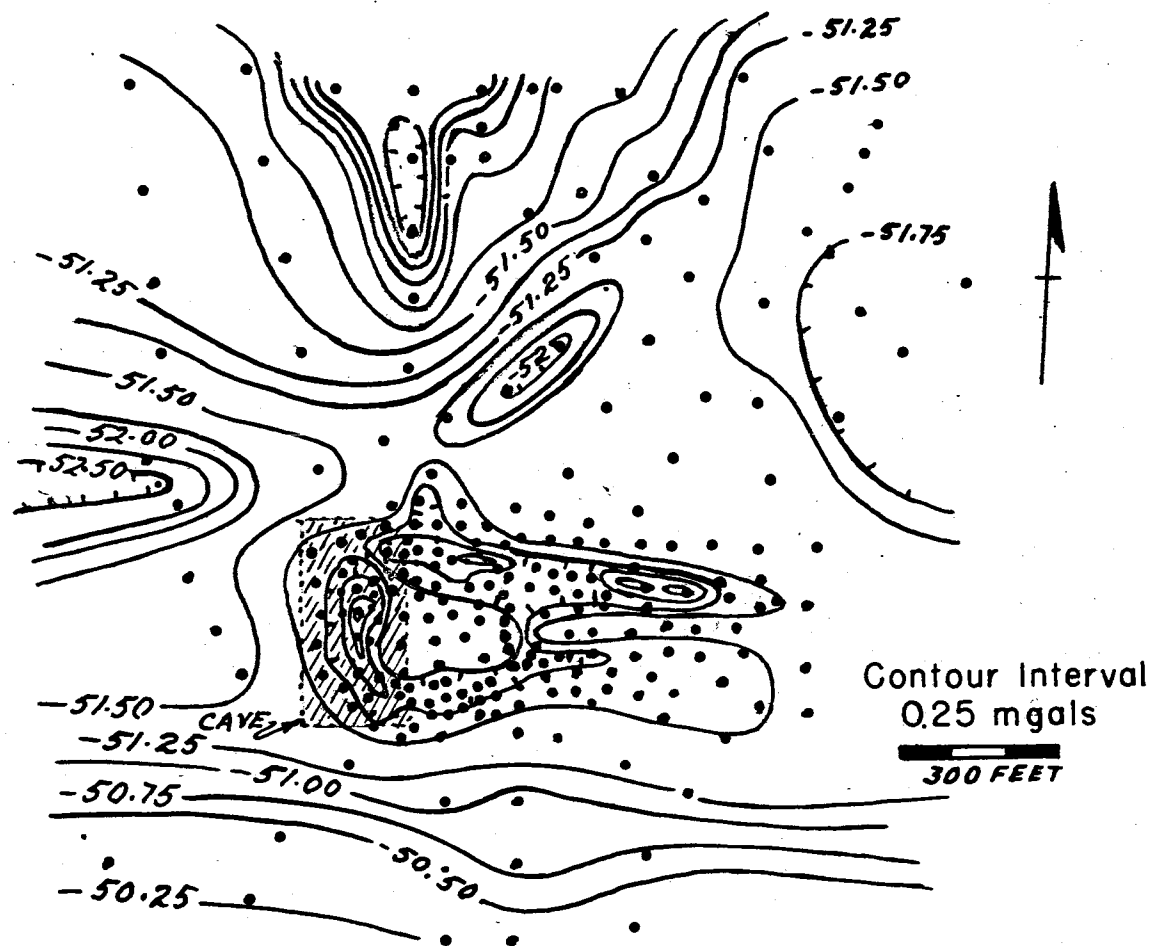
The present investigation was undertaken to find out if caves could be successfully located by using gravity observations. The area chosen embraced about 4.5 square miles near Blue Mounds in Dane County and included the Cave of the Mounds. This cave extends about 400 feet in a north-south direction with a short easterly extension at the northern end. The cross-section varies approximately from 10 by 25 feet to 50 by 25 feet.

III-7b Gravity Survey

Two hundred and seventy-nine gravity stations were established in the area with approximately two-thirds of them concentrated over the area of the cave. The density of the limestones in that area is approximately 2.71 gm/cm^3 which figure also represents the density contrast.

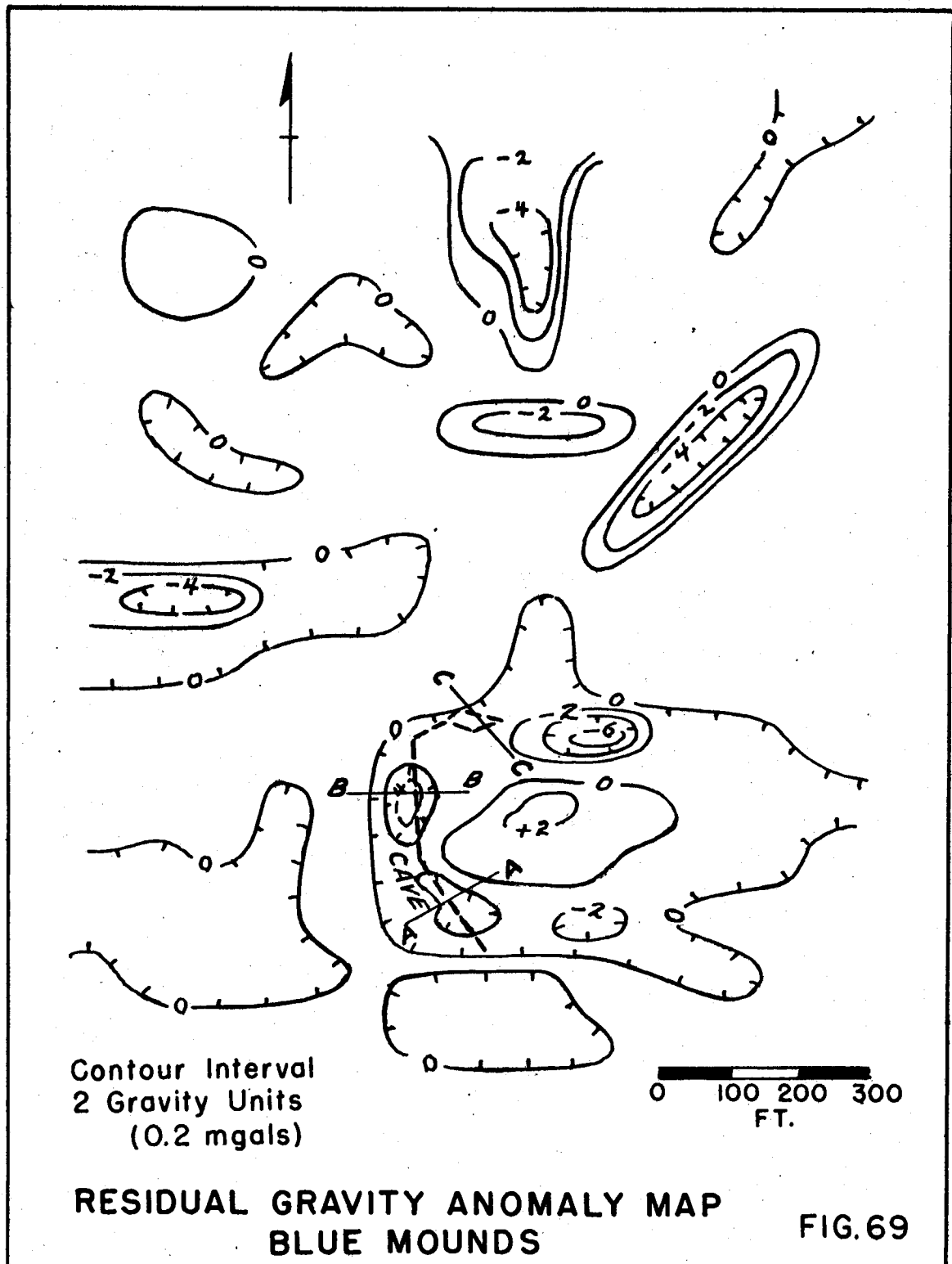
The gravity readings were reduced to give Bouguer anomalies and a contoured iso-anomaly map of the area is shown in Fig. 68. This map shows that a well-defined gravity minimum is associated with the known cave, and several other gravity minima suggest other caves in the area. These relations are brought out more strongly by the residual gravity map (Fig. 69) which was prepared using a grid averaging system for removing the regional effect.

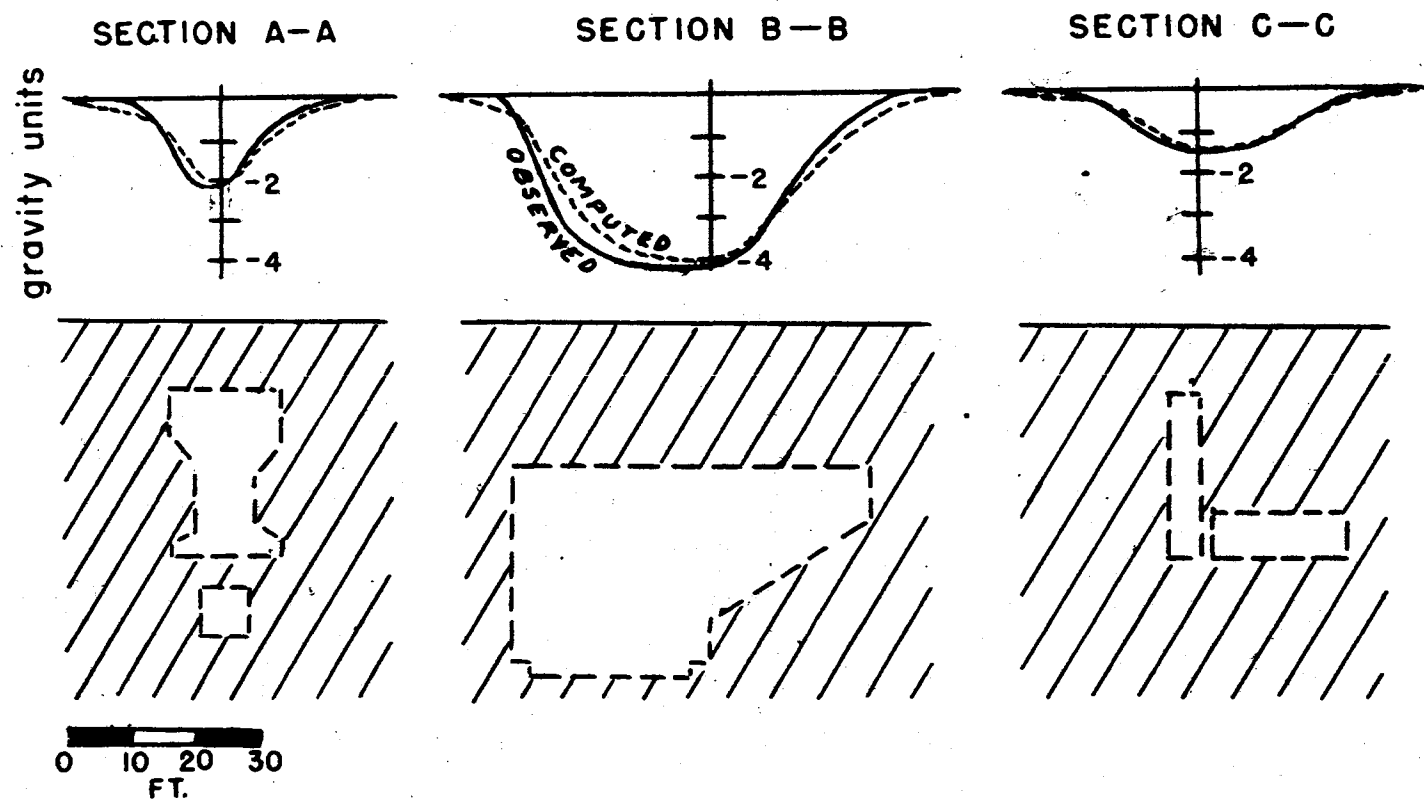
In order to compare the residual anomalies on this map with those that would be expected, measured sections were taken in the cave at A-A, B-B, and C-C, and the theoretical gravitational effect of the cave at each section computed. These are compared with the observed residual values in Fig. 70. The agreement is very close and shows that the method is applicable for this type of study.



BOUGUER GRAVITY ANOMALY MAP
BLUE MOUNDS AREA, WIS.

FIG. 68.





COMPARISON OF OBSERVED & COMPUTED GRAVITY
PROFILES
CAVE OF THE MOUNDS

FIG. 70

III-8 - Oshkosh, Wisconsin
Gravel Pit Extension

III-8a General Statement

Oshkosh is located in the eastern part of the state in an area where glacial drift lies directly upon Paleozoic limestone. The problem here was to determine what adjacent land should be purchased for the further development of an established gravel pit located in the drift. The sand and gravel occurs as sheet-like deposits interbedded with till and that area having the greatest thickness of drift above the limestone was sought as being the most desirable. Had this been a limestone quarry the problem would have been the reverse, as the area having the least amount of stripping would have been the one looked for.

The seismic refraction method of reverse shooting was used and depths were determined at 29 sites. The locations of these sites in relation to the existing sand and gravel pit are shown in Fig. 71.

III-8b Seismic Results

Two distinct seismic horizons were found to be present. The upper horizon (V_1) had a velocity varying from 1500 to 3500 ft./sec. which was identified as unsaturated glacial till composed of clay, sand and gravel. The lower horizon (V_2) had a velocity which averaged about 16,000 ft./sec. which was identified as the underlying limestone. The seismic depth data for each site are listed in Table 34. The variations in thickness of drift over the limestone are indicated by the contours in Fig. 71 which show the depth to the limestone. This is also brought out by the profile sections of Fig. 72.

Inspection of these figures shows that to the north of the present gravel pit the depth of drift decreases from about 40 feet to 10 feet; however the change in thickness does not appear to be uniform and a buried limestone ridge is indicated which strikes across the area in a northwest-southeast direction.

In a limited way the above indications are substantiated by test trenching which encountered limestone at 10 feet where limestone is shown by the seismic measurements to be at a depth of 12 feet.

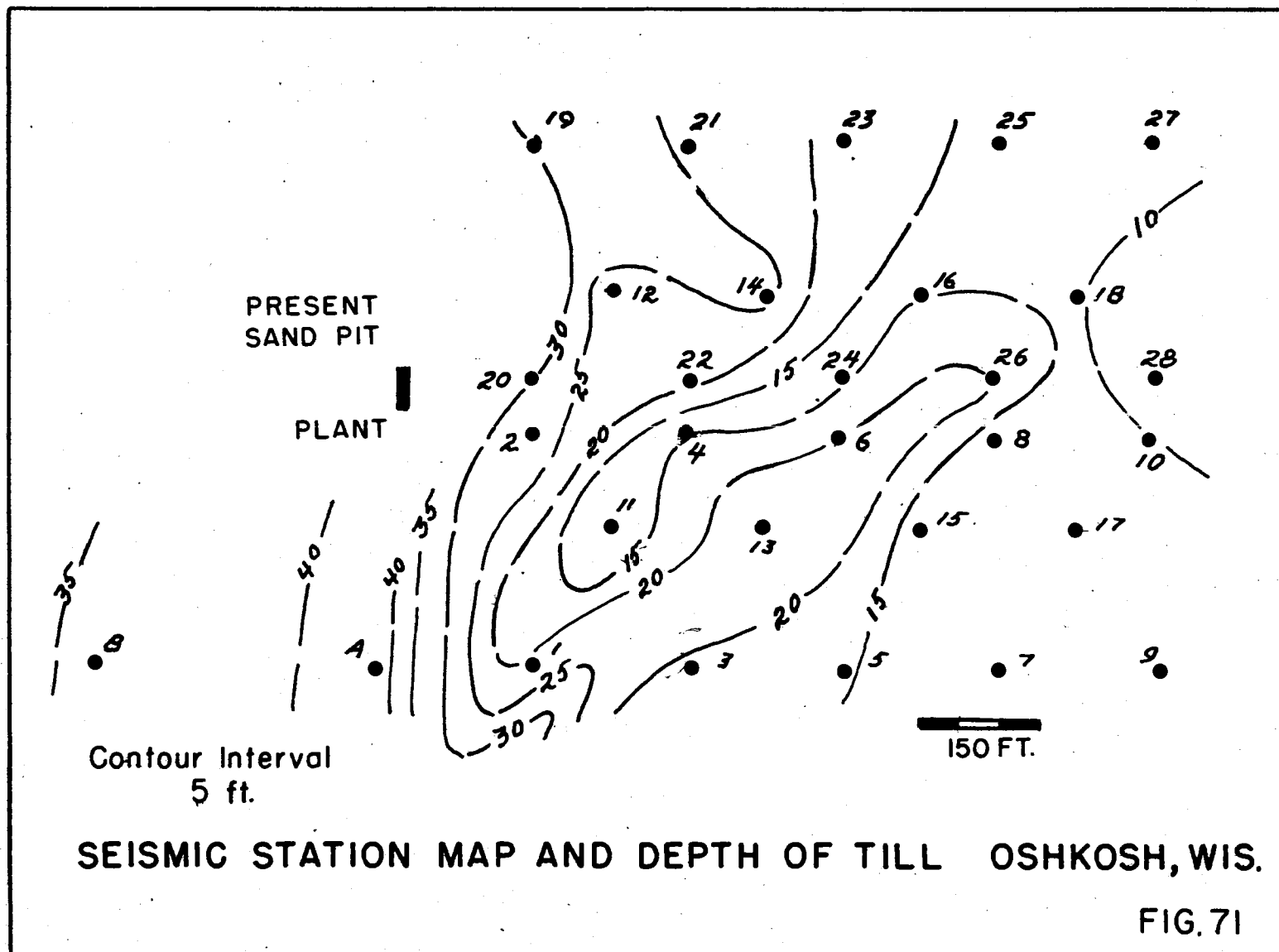


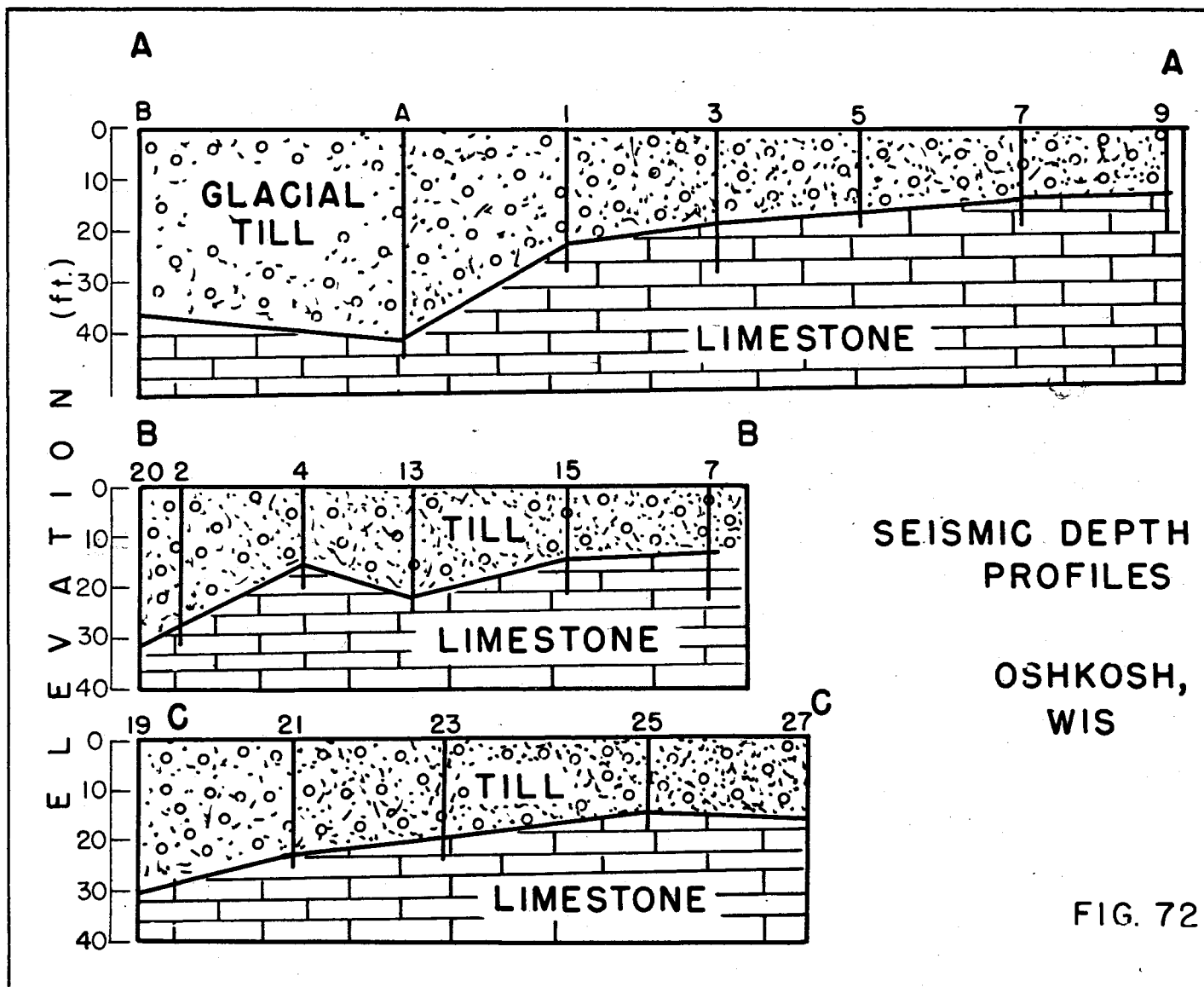
Table 34

Seismic Results, Oshkosh, Wisconsin

Station	Apparent Velocities		Depth of Layers V ₂
	V ₁	V ₂	
B	2710	15400	36
A	3410	23900	41
1	4090	14300	22
2	3670	14200	27
3	5000	14500	18
4	1430	21700	15
5	4150	19600	16
6	5550	24000	20
7	2720	12800	13
8	1930	11100	11
9	2630	16670	12
10	-----	-----	--
11	2780	50000	11
12	2040	9250	22
13	1750	12500	22
14	2290	18700	26
15	1800	12000	13
16	1670	14600	15
17	2720	13000	11
18	2080	12400	11
19	2370	16700	30
20	3460	13600	31
21	2250	16230	22
22	2190	18320	21
23	1900	20000	19
24	2710	12500	14
25W	2000	12400	14
26E	2760	17500	20
27	2000	16820	15
28	2750	12500	8

V₁ = glacial till

V₂ = limestone, average true velocity 16,100 ft./sec.



III-9 - Milwaukee Harbor
Thickness of the Lake Bottom Sediment

III-9a General Statement

Test measurements were made off Milwaukee Harbor as a preliminary to carrying out a seismic refraction study in the off-shore area of the Atlantic Coastal Plain.

Two, 38 foot picket boats were made available by the U.S. Coast Guard and three reversed seismic refraction profiles were shot in depths of water ranging from 55 feet to about 100 feet. The locations of the measurements in relation to the Milwaukee Harbor entrance are shown in Fig. 73.

III-9b Seismic Results

Two distinct velocity layers were observed beneath the bottom. The upper layer (V_1) had a velocity of about 6300 ft./sec. which, on the basis of chart notations as to the type of bottom, was water saturated sand. The lower layer had a velocity of about 17,000 ft./sec. and was tentatively identified as limestone, probably the "cement rock" of the Milwaukee Formation but possibly underlying Niagara dolomite, which also outcrops along much of the Milwaukee lake shore.

In addition to these refraction measurements, reflections were obtained from a third horizon which, on the basis of the depth, would appear to be the Niagara Formation if the bedrock surface is correctly identified as being the Milwaukee Formation. In computing the reflection depths, mean velocities were estimated from a graph of the square of the travel-time versus the square of the distance. The depth was then determined from the equation:

$$h = \frac{\sqrt{V^2 t^2 - x^2}}{2}$$

in which h = depth
 V = travel time
 x = distance from shot point to receiving point.

The results are summarized in Table 35.

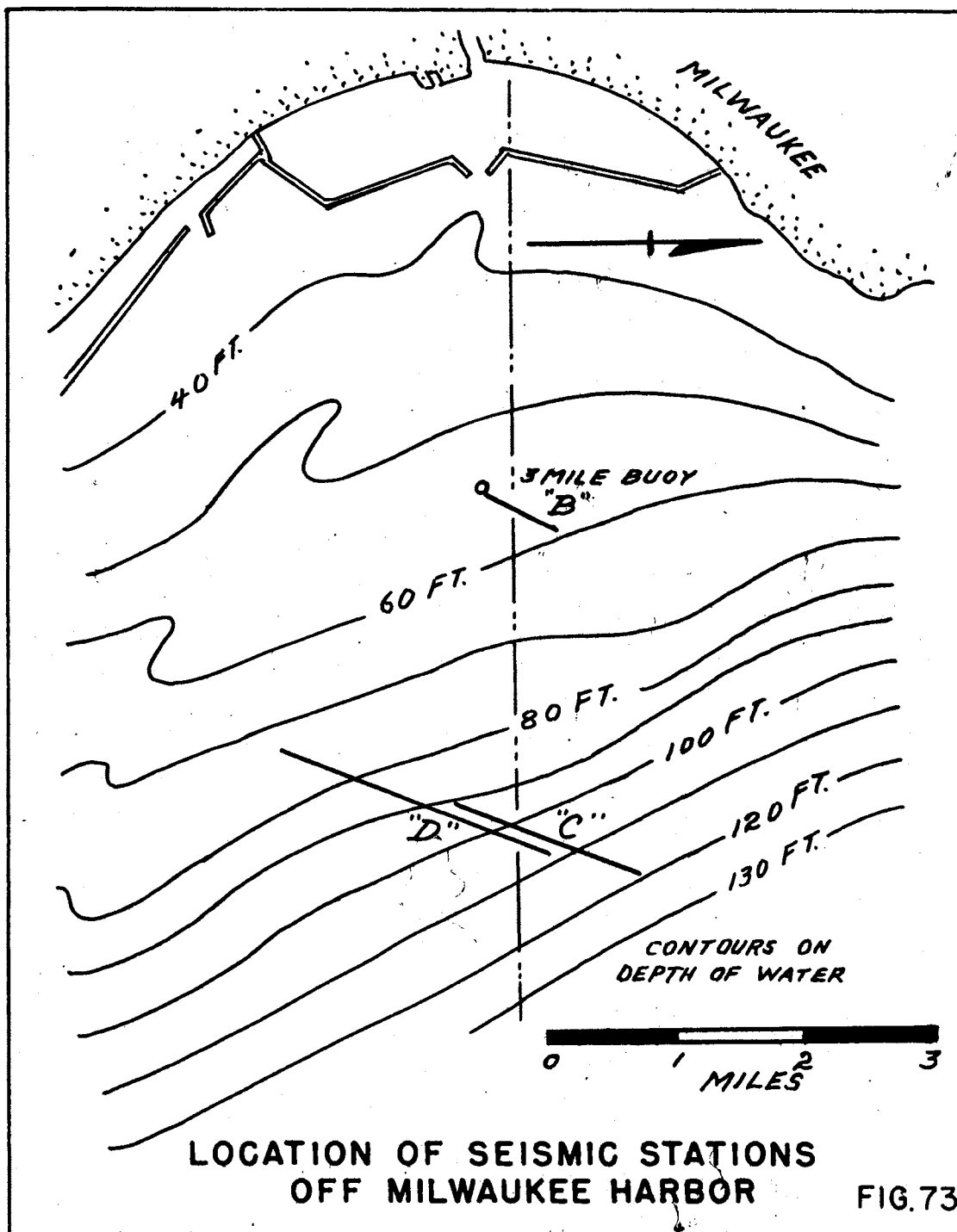


Table 35
Seismic Results, Milwaukee Harbor

Refraction Measurements

Station	Shot Location	Apparent Velocities			Depth from Lake Surface	
		V ₂	V ₂	V ₃	V ₂	V ₃
B	surface	4700	6296	16440	57	88
CN	surface	4700	6333	17000	105	229
CN	bottom	4700	6087	17770	105	243
CS	surface	4700	6333	18235	95	229
DN	surface	4700	6260	17270	95	231
DS	bottom	4700	6280	17400	95	231

V₂ = lake sediments unconsolidated

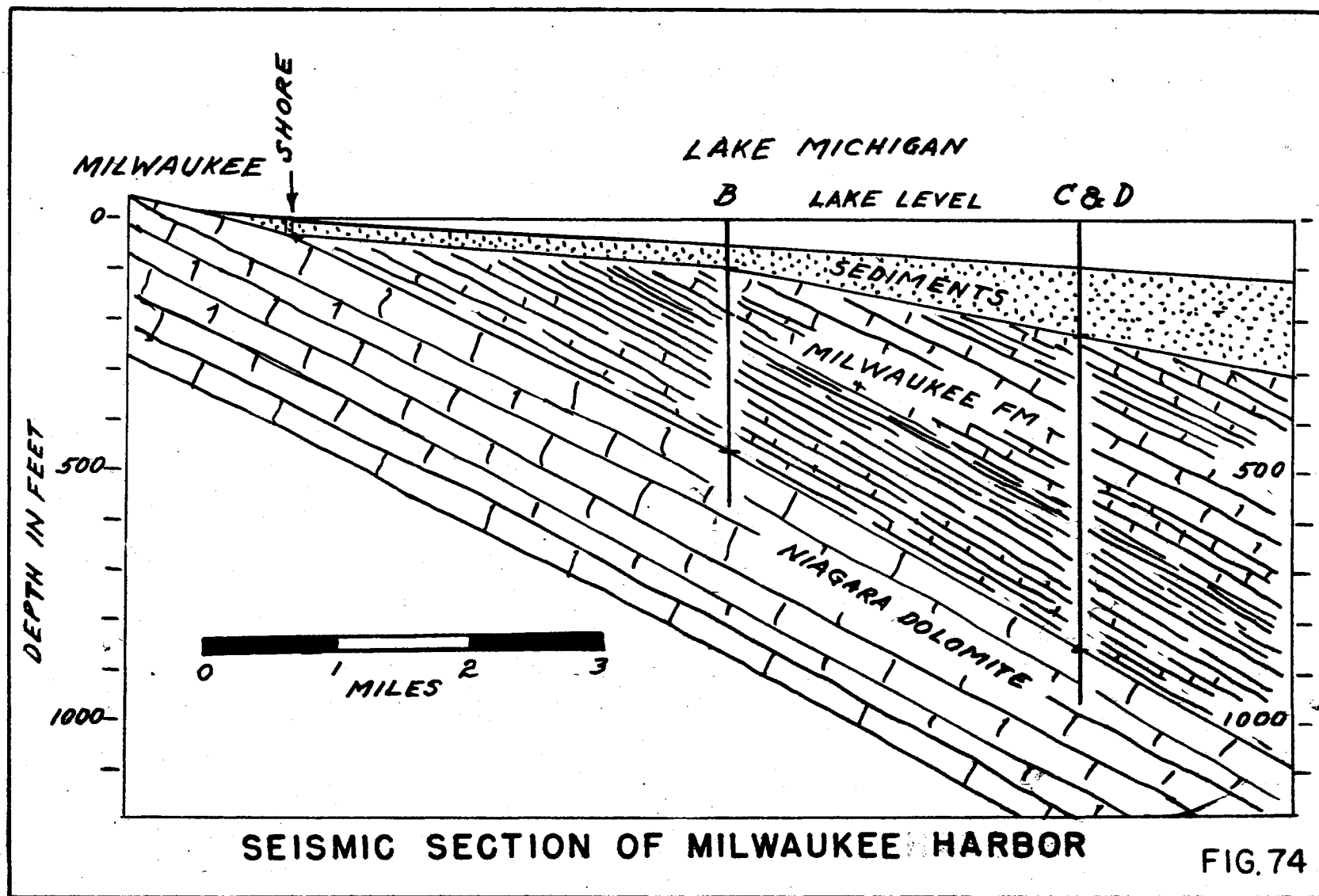
V₃ = Milwaukee Formation (limestone and shale)

Reflection Measurements

Station	Shot Location	Mean Velocity	Depth from Lake Surface
			V ₄
B	surface	13,270 ft./sec.	475
CN	surface	11,400 ft./sec.	846

V₄ = Niagara dolomite (?)

It is seen from the above table that the sediments range from 31 feet in thickness at station B, which is three miles off the harbor entrance, to 134 feet, three and one half miles offshore. This represents an increase in the thickness of sediments of 103 feet or a thickening of 29 feet to the mile. In identifying the V₃ horizon as the Milwaukee Formation, the reflections at stations B and C were used as a guide along with the known thickness of local formations from well data. This reflection came from a depth of about 390 feet beneath the bedrock surface at station B and 615 feet at station C. By projecting these various surfaces (V₃ and V₄) back towards the shore, it is seen that both surfaces intercept at about the shoreline. This relation is to be expected because the Milwaukee Formation is truncated by erosion to give a feather edge at Milwaukee with its outcrop limited to the area immediately adjacent to the lake shore. See Fig. 74.



As the seismic spreads were oriented roughly perpendicular to the section of Fig. 74, it was possible to determine the slope of the bed-rock surface (top of the Milwaukee Formation) in a direction slightly east of north, and it was found that the component of dip in this direction is roughly $1\frac{1}{2}^{\circ}$.

On the basis of these measurements it appears that the seismic method is applicable to the study of sedimentation and silting in harbors and reservoirs and can also be used for studying the fundamental geologic structure beneath the Great Lakes.

Part IV

Mineral Deposit Studies

IV-1 - General Statement

Although the application of geophysics to subsurface studies received its initial impetus from mineral exploration investigations, most of the methods soon fell into disrepute and in large measure were abandoned by the mining companies until relatively recently. This lack of confidence in geophysical measurement can be attributed principally to three causes. (1) The methods were developed primarily by physicists who, for the most part, had little understanding of the complex geologic parameters associated with many mineral occurrences that would limit the application of the measurements. As a consequence, there were many investigations attempted that were foredoomed to failure. (2) Most geologists and mining engineers, instead of cooperating and working with the physicists, adopted the attitude that it was up to the physicists to demonstrate that they could produce positive results without the benefit of any geologic information. Many otherwise successful investigations failed because of the lack of key geologic information that was deliberately withheld. (3) As with all new scientific innovations that are only partially understood by the public, there were a group of unscrupulous entrepreneurs who rushed in to exploit the gullibility of the mining profession.

It has only been because of the successful application of geophysics to petroleum exploration and the fact that the major oil companies have assumed a leading role in developing more advanced exploration methods, that the mining profession is again considering geophysics as a tool for exploration and development. However, the geology of most mineral deposits is far more complex than that associated with those of oil and the uncertainties will always be large. Further, as nearly every mining district constitutes a unique situation, there will always have to be some blind exploratory work, and a certain percentage of failures is inevitable.

The following geophysical studies are limited to mineral exploration problems pertinent to Wisconsin, but they are varied enough to show many of the difficulties and limitations to be expected in using geophysics in the search for ore deposits.

IV-2 - Geophysical Studies over Iron Formation

IV-2a General Statement

Iron ore production in the Lake Superior Region has progressed to the point that exhaustion of present known high grade deposits can be forecast, and a great deal of attention has been focused on Wisconsin as representing an area that might have high grade reserves that have not yet been exploited.

Most of the state is covered by glacial drift and it is only from dip needle measurements that much of the geology of the area has been deduced. A major problem though is to distinguish between magnetic anomalies related to changes in petrology and those related to iron formation, especially as hematite, which is the principal ore, is non-magnetic.

In order to ascertain what geophysical methods might be applicable to locating possible iron reserves in Wisconsin, several series of geophysical investigations were carried out in the various iron districts of the Lake Superior region. The areas studied, and the methods used, were as follows:

Vermillion Range of Minnesota	Gravity studies in conjunction with existing magnetic data
Mesabi Range of Minnesota	Seismic and electrical studies
Gogebic Range of Wisconsin	Gravity, seismic, and electromagnetic studies in conjunction with existing magnetic data
Baraboo Area of Wisconsin	Magnetic and gravity studies

The detailed data and the exact locations of the studies reported are not given because of the economic significance of the results to the companies directly concerned who cooperated in making these investigations. The results presented are believed to be representative examples for particular geologic situations which occur in each of the areas investigated.

IV-3 - Vermillion Range, Minnesota

IV-3a General Description

In the Vermillion district the Soudan Iron Formation occurs as steeply dipping lenses of ferruginous cherts infolded in the volcanic Ely greenstone which is overlaid by the sedimentary Knife Lake Series.

Intrusive granites are present in the area which may account for the metamorphism of much of the iron formation.

Pronounced magnetic anomalies are commonly associated with the iron formation although where the mineralization is chiefly hematite, as at Ely, no anomaly may be associated with the ore. Gravity studies were carried out at three separate localities of known iron occurrence, and samples were collected for density determinations. The density values obtained are given in Table 36.

Table 36

Density Values, Vermillion Range

Material	No. of Samples	Spread in Values	Average
Greenstone	6	2.80-3.21 gm/cm ³	3.00 gm/cm ³
Iron Formation			
oxidized, leached, porous chert	1		2.61
coarse, black jasper	1		3.88
hematite "hard" ore	2	4.34-4.82	4.58
Knife Lake Series	4	2.70-2.85	2.77
Granite	3	2.65-2.68	2.67

The significant density contrast is that between the greenstone and the iron ore, and from Table 36 it is seen that the density of the ore-bearing iron formation is, on the average, at least 0.5 gm/cm³ greater than that of the greenstone. The actual contrast at any one place will, of course, depend upon the relative amount of oxidation of the ore that has taken place. As most of the ore in this area is "hard" blue hematite rather than "soft" earthy oxidized hematite, gravity methods should be useful for mapping the occurrence of this ore.

IV-3b Gravity Studies

All of the gravity studies were carried out with Worden gravimeters with a sensitivity ranging from 0.01 to 0.1 mgals per scale division. In each area a series of gravity traverses were made across known occurrences of iron formation with a station spacing varying from 40 to 200 feet. All readings were reduced to give simple Bouguer anomalies, which were regarded as adequate for the study being made.

IV-3b₁ Area A

Earlier dip needle work in this area showed a change in dip of 75° in crossing the iron formation which is about 600 feet wide; and aero-magnetic work conducted at an elevation of 1000 feet showed an anomaly of about

5000 gammas. The gravity study, which consisted of observations at about 40 to 50 foot intervals, indicated a local gravity anomaly centered over the iron formation which rises about + 1.7 mgals above the regional trend as seen from Fig. 75. Similar results were noted on all the traverses, and the results shown can be regarded as representative of the area. The results of the earlier magnetic measurements have also been included for comparative purposes. The displacement in the magnetic anomaly is caused by the inclination of the earth's magnetic field and the difference in elevation at which the observations were made relative to the elevation of the upper induced magnetic pole in the steeply dipping iron formation.

IV-3b₂ Area B

In this area, a test gravity profile was run along a traverse which included the so-called Ely trough, from which iron ore has been produced to a depth of about 3000 feet. As aero-magnetic data are available for the area, they have been included in this study for comparative purposes. Relationships that are of particular interest here are: (1) the effect on the magnetic anomaly values of relatively small amounts of magnetite in non-commercial iron deposits and (2) the relatively small but consistent gravity anomalies associated with areas of workable iron ore.

The traverse crosses a section of greenstone which contains iron formation at two locations and the whole is infolded in granitic rocks. One of the iron occurrences is in the Ely trough where the iron is in the form of "hard" blue hematite. At the other location, the iron formation consists of thin layers of finely disseminated magnetite in slate and chert, and is of non-commercial grade. It is seen from Fig. 76 and Fig. 77 that small local gravity anomalies occur over the outcrop area of iron formation in each case, but, whereas a magnetic anomaly of 9000 gammas is indicated over the area of low grade magnetite ore, no magnetic anomaly at all is indicated in the area of the high grade hematite ore body.

The large regional gravitational anomaly gradients appear here to be related to the thickness of greenstone in the surrounding granite, and this regional effect has to be removed in order to isolate the weaker anomaly values associated with the iron formation. The residual value in each case is seen to be about 0.5 mgal.

IV-3b₃ Area C

This area lies in Lake County, Minnesota. Traverses were run crossing four known outcrop areas of iron formation in greenstone.

COMPARATIVE MAGNETIC GRAVITY PROFILES—VERMILLION DISTRICT, MINN

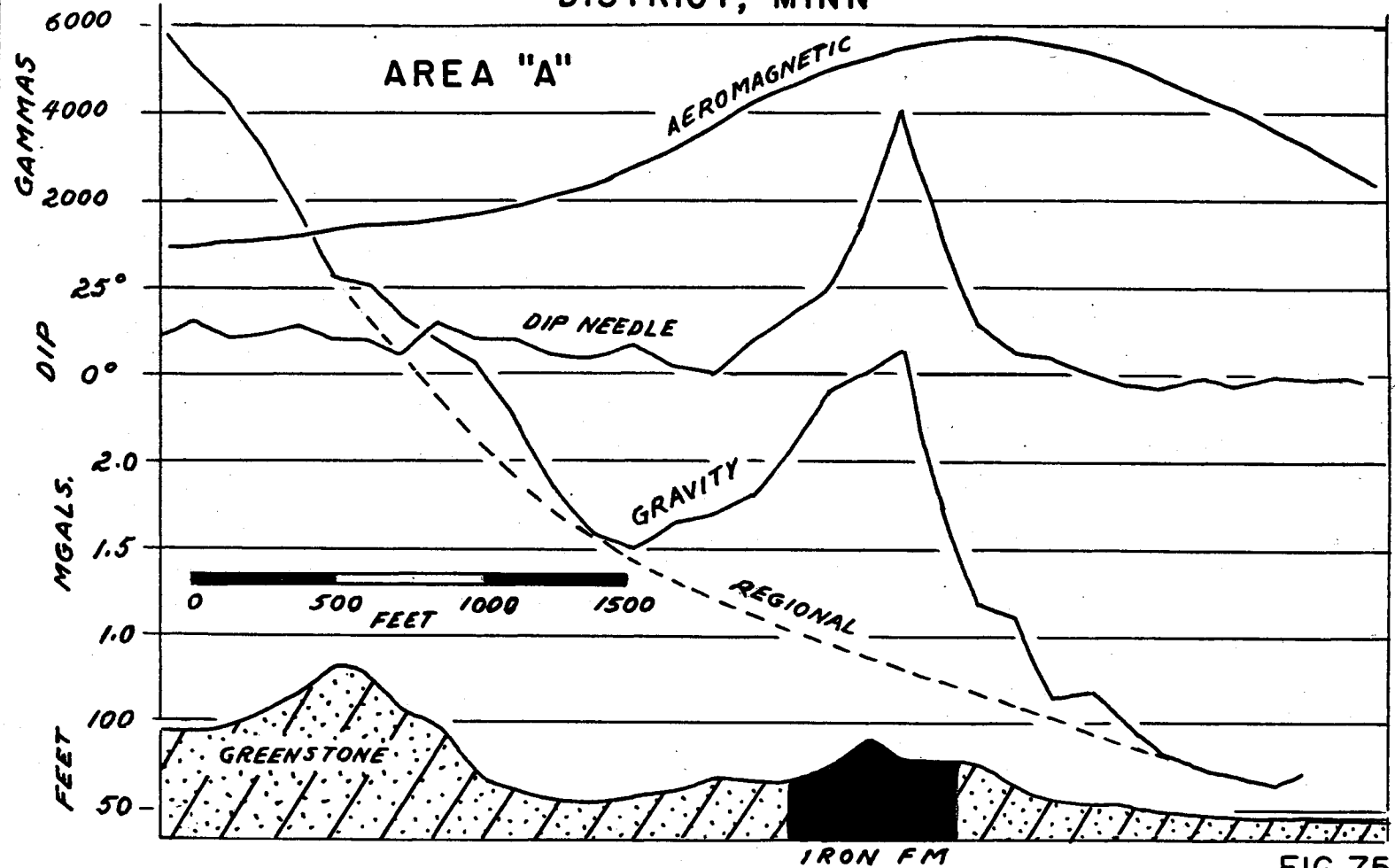
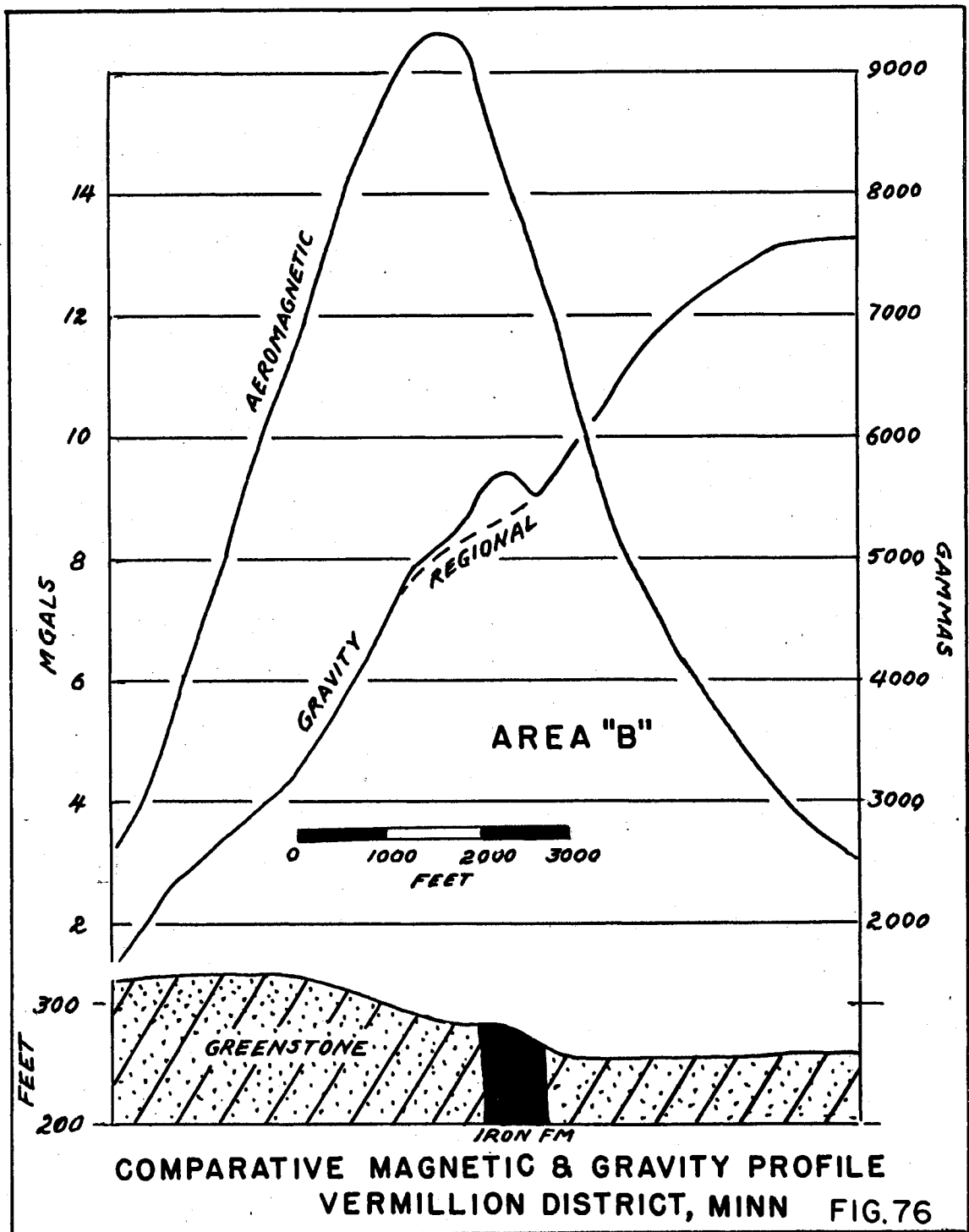
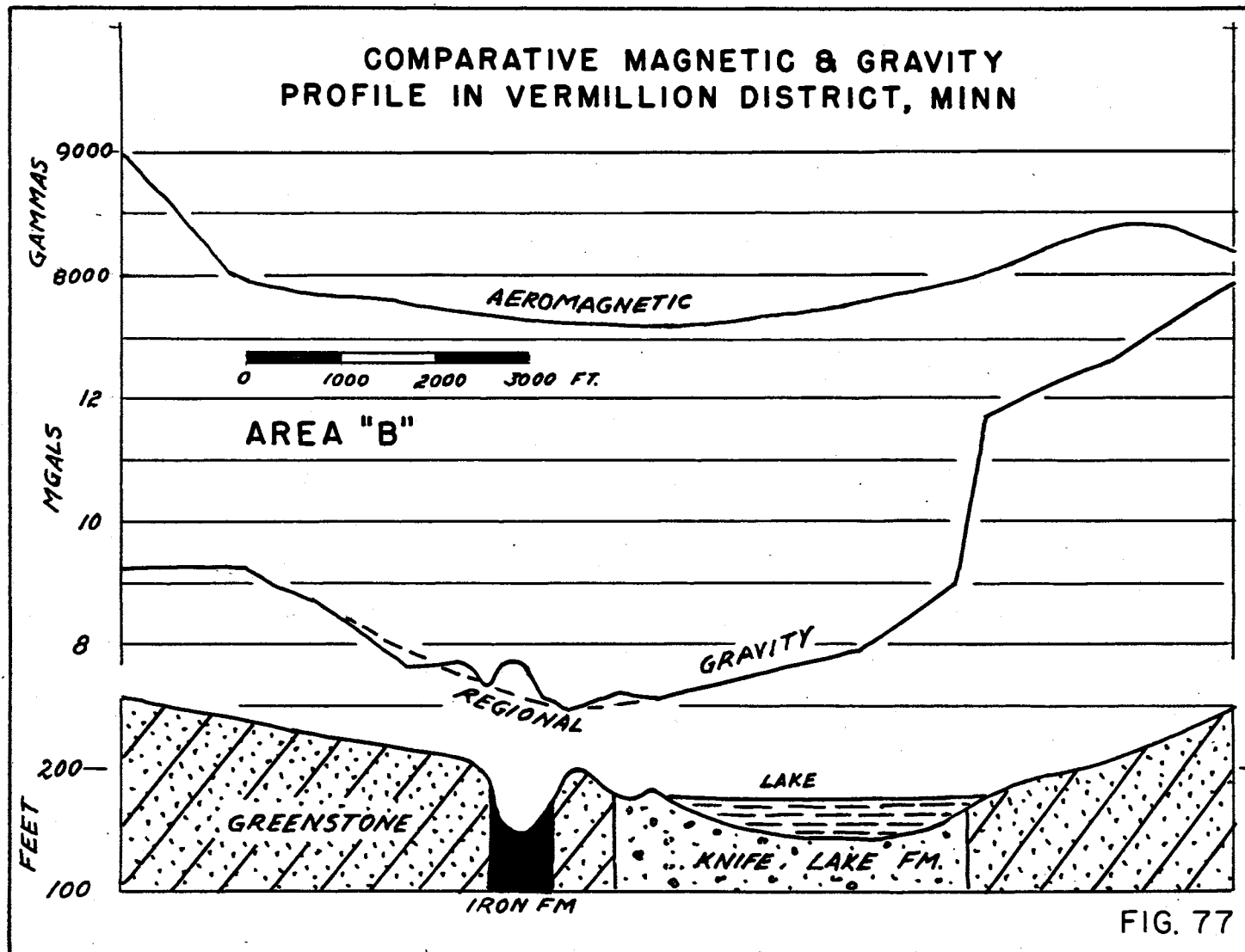


FIG. 75





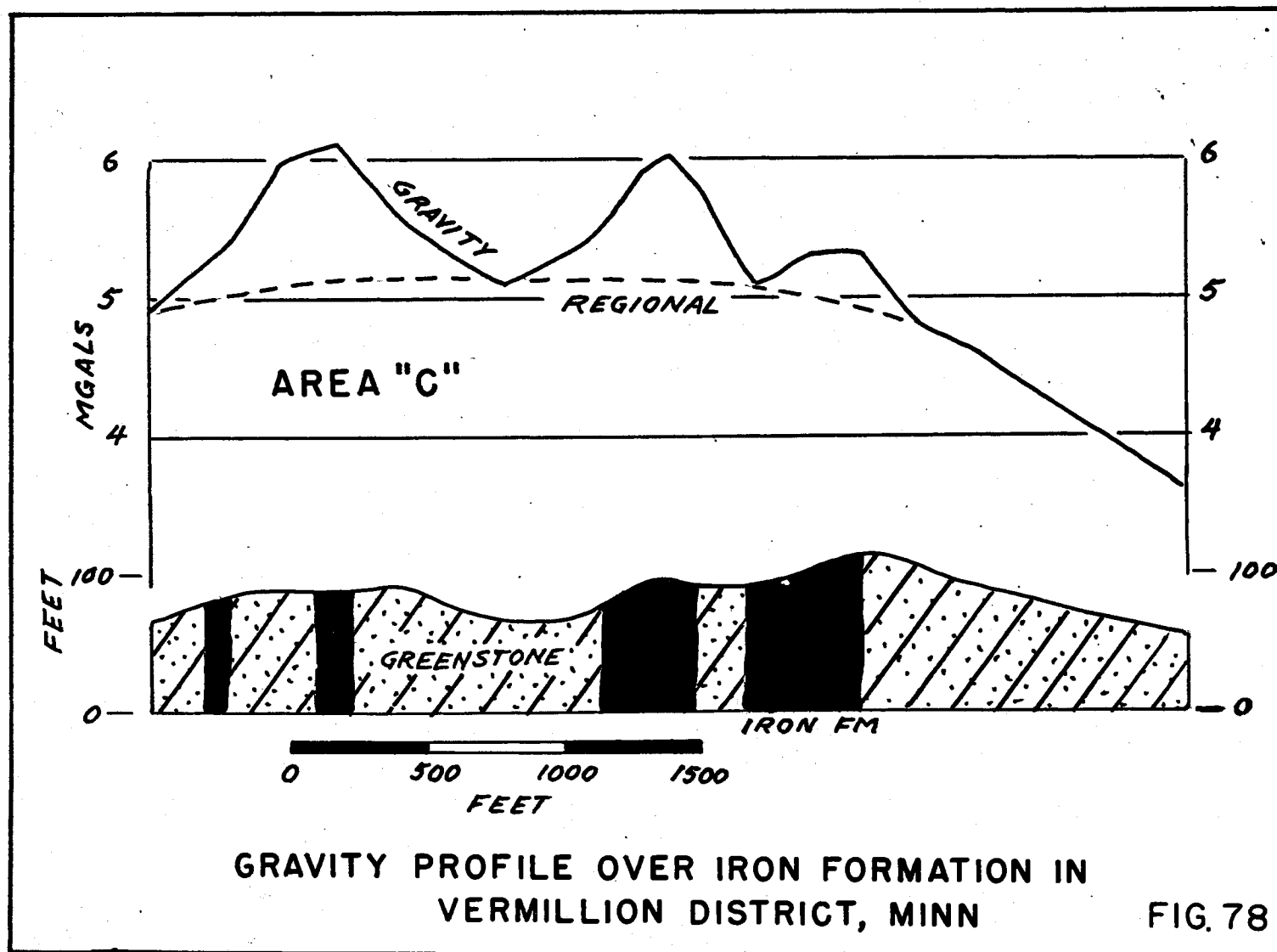


Fig. 78 shows three local gravity anomaly "highs" in association with these iron occurrences, and the residual anomaly values vary between 0.3 and 1.0 mgals. The failure to obtain an anomaly over all four of the outcrop areas is probably related to the fact that there are actually only three areas of iron formation present. From an inspection of Fig. 78, it is seen that the anomaly width actually includes both of the reported iron occurrences in the area where the direct correlation between the gravity anomaly peaks and iron occurrence is missing. As no "saddle" is indicated in the anomaly peak it would seem that the entire area between the two iron occurrences is mineralized.

IV-3c Conclusion on Vermillion Range Studies

Gravity anomalies appear to be associated with both hematite and magnetite in this area. Strong regional gravity gradients tend to mask the local anomalies associated with the iron formation but these can be successfully, and easily, removed in order to isolate the residual gravity values associated with the iron formation. The magnitude of the residual values in general appears to be sufficiently large, greater than 0.5 mgal, so that terrain corrections are only required in areas of very marked relief. The magnetic anomalies, by contrast, are confined to only those iron occurrences having magnetite associated with them. As the magnitude of the magnetic anomalies are governed not only by the percent of magnetite present but also such other factors as the geometry and attitude of the iron bearing body in the earth's field. Low grade non-commercial iron occurrences frequently have larger magnetic anomalies associated with them than higher grade deposits with the same type of mineralization. As the iron formation occurs as relatively narrow bands, detailed traverses are required with geophysical observations at no more than 100 foot intervals.

IV-4 - Gogebic Range, Wisconsin

IV-4a General Statement

The Gogebic iron range is located in northern Wisconsin and Michigan. It is composed of a narrow belt of sedimentary pre-Cambrian rocks of upper Huronian age which strike parallel to that of the axis of Lake Superior. The Ironwood Formation which is the most important member of the series economically, consists of about 650 feet of coarse-grained ferruginous chert interbedded with fine-grained cherty iron carbonate. On the basis of this variation in lithology, the formation is divided into five main subdivisions. These formations can be separated both on the basis of lithology, and on the basis of their average densities as shown in Table 37.

Table 37

Divisions of Ironwood Formation

Stratigraphic Divisions	Lithologic Descriptions	Density gm/cm ³
Anvil	Ferruginous chert	3.37
Pence	Cherty iron carbonate	3.08
Norrie	Ferruginous chert	3.35
Yale	Cherty iron carbonate	3.10
Plymouth	Ferruginous chert	3.43

The adjacent slates, taken as a whole, have a density approximating 2.7 gm/cm³ except for the basal portion of the overlying Tyler formation. The gravity method should therefore be applicable to trace the iron formation which for the most part is buried beneath a cover of Pleistocene glacial till.

This picture of the local geology, although valid for the eastern part of the range near Hurley, is complicated to the west by the presence of a gabbro laccolith which is in contact with the Ironwood formation near Mineral Lake. The gabbro and the nearby Keweenaw basic lava flows both exert a strong regional gravitational effect in the area. As was shown in the Vermillion District, though, the gravitational effect of such bodies which tend to mask that of the iron formation, can be removed successfully so that the iron formation can be traced.

It is observed that the coarse textured chert usually has magnetite and "hard" blue hematite in association with it, while the fine-grained chert is associated only with iron carbonate. As the coarse-grained chert is predominant, the formation as a whole should have a high magnetic susceptibility. This is indicated to be the case by the results of the early dip needle and sun compass surveys made over the area. Variations in dip of up to 70°, and declination changes of over 170°, were observed in crossing the iron formation.

In the course of the present study, several regional traverses were run using gravity and seismic refraction measurements which in general followed the lines of earlier magnetic measurements. The seismic measurements were made primarily to determine the thickness of the overlying glacial drift. It was also hoped that the various pre-Cambrian rock types beneath the glacial deposits might be characterized by velocity values distinctive enough to permit the formations to be differentiated on this basis. Although true velocity variations from 13,000 to 25,000 ft./sec. were observed for the pre-Cambrian rocks, it was not possible to establish any rigid correlation as outcrop and drill hole data were

too scarce to permit adequate calibration. The specific seismic information obtained at each observation site will not be listed here as the measurements are being included in a more comprehensive study of the area. The depth results however are incorporated in the profiles shown.

In addition to the above measurements, two electro-magnetic traverses were also made across the Ironwood Formation near Upson to see if this method could be used to map the location of the formation.

IV-4b Lake Namekagon-Mellen Area

Comparative dip needle and Bouguer gravity anomaly values and their relation to the underlying geology, along two of the lines of measurement, one near Lake Namekagon and one near Mellen, Wisconsin, are given in Figs. 79a and 79b. Both traverses show appreciable magnetic and residual gravity anomalies defining the location of the iron formation whose depth, as indicated by the seismic measurements, varies from only a few feet to over 200 feet beneath the surface. The residual gravity anomaly on the Lake Namekagon traverse is about 2.0 mgals, and on the Mellen traverse, it is slightly over 5.0 mgals. The associated dip needle anomalies are 72° and 63° respectively. Either basis of exploration, therefore, appears to be adequate for tracing the iron formation in this area although the magnetic values give much the greater anomalies; however, it should be noted that the magnetic anomaly picture observed here is not characteristic of the entire Gogebic Range. At the eastern end of the range the magnetic anomaly pattern is not as pronounced as that shown in Figs. 79a and 79b. The transition observed in anomaly pattern from one end of the range to the other is shown in Fig. 80.

IV-4c Upson Area, Wisconsin, Electro-magnetic Study

IV-4c₁ General Statement

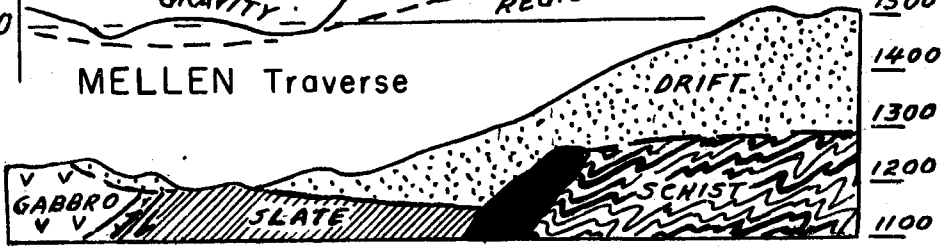
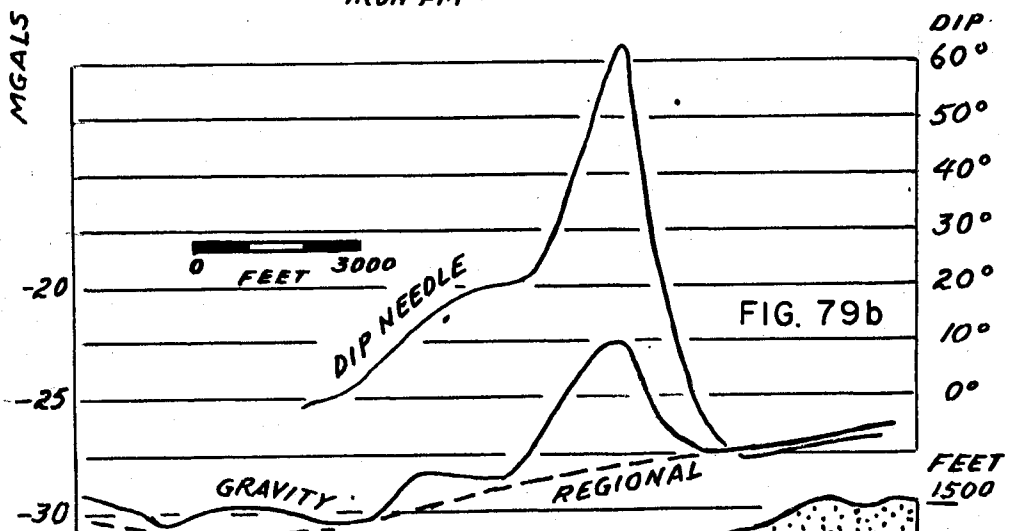
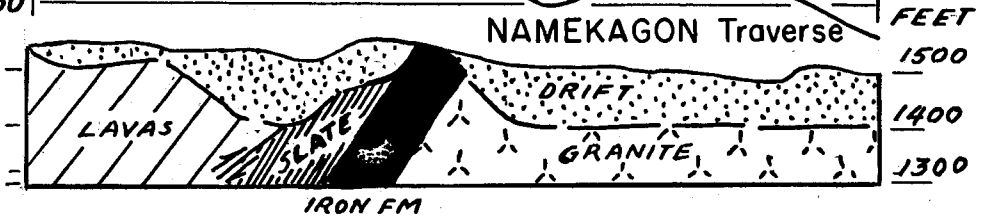
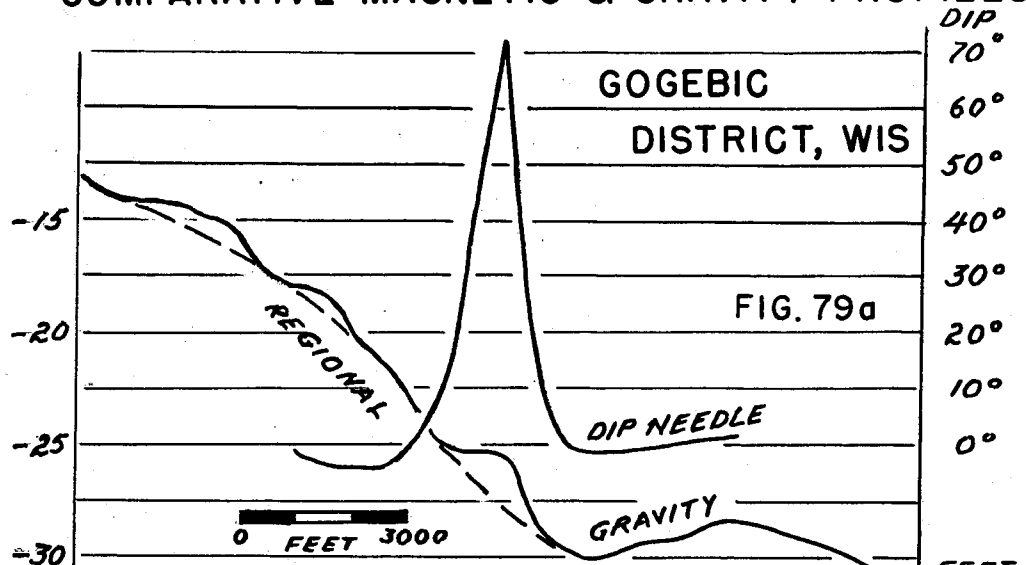
Electromagnetic traverses were conducted near Upson as part of the general study of the Gogebic Range.

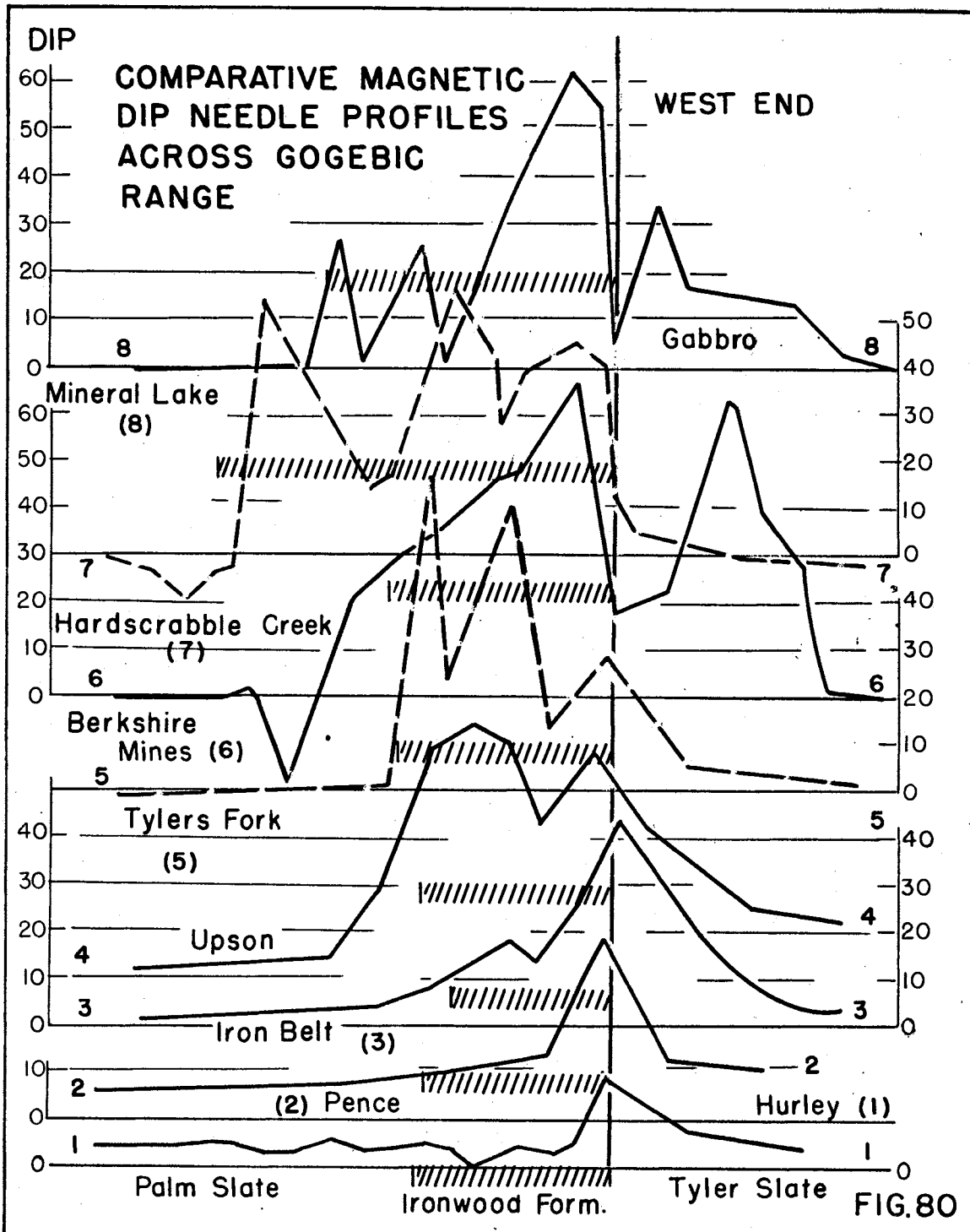
Upson lies in T 45N, R 1W, Iron County, and the Ironwood Formation, as inferred from magnetic measurements, runs just south of the town and strikes approximately 60° West of North. Two electro-magnetic traverses were established here, one running north-south and the other east-west across the iron formation.

IV-4c₂ Electro-magnetic Study

A vertical sending coil, that was energized with a 2000 cycle per second alternating current, was used in these measurements.

COMPARATIVE MAGNETIC & GRAVITY PROFILES





This was oriented in the plane of direction of the receiving search coil, and observations were made following the procedure outlined in the Appendix for "in line" measurements. On the east-west traverse, which was 4700 feet long, coil separations of 30, 100, 300 and 400 feet were used to determine how significant the separations were in depicting the subsurface geology. Observations were made at 100 foot intervals except for the 300 foot coil spacing on which observations were made at 50 foot intervals. As the area here was not characterized by rough topography, misorientation effects are not regarded as significant and the observed dips can all be regarded as real.

With a 50 foot spacing between coils, the primary field completely masked any contributing effect from conductors at depth. As the spacing was increased, the dips increased as shown in Fig. 81. There was little change in values or pattern when the spacing was 300 feet and 400 feet, and dips as high as 50° were recorded.

A similar anomaly pattern of dips was obtained on the north-south traverse using a 300 foot coil separation, although the values observed were only about half those found on the east-west traverse. The cause of the alternating "highs" and "lows" observed on these two traverses is not definitely known. One pronounced "high" appears to be associated with the iron formation, as indicated in Figs. 81 and 82. The other "highs", covering a more extensive area, all occur over the area underlaid by the Tyler slate series. This series is known to have some magnetite and hematite associated with it as was shown by the density studies and the magnetic dip needle profiles in Fig. 80. As the electro-magnetic "highs" are related to this mineralization, it appears that this method may be used to trace the iron bearing formation.

IV-5 - Baraboo Syncline Wisconsin

IV-5a General Statement

Iron formation, in the form of ferruginous slate and cherty dolomite, occurs in the Freedom formation which is near the top of a pre-Cambrian sedimentary sequence in the Baraboo syncline. Although this formation is everywhere buried beneath later Cambrian and Pleistocene sediments, drill hole data show that the iron is in the form of hematite and iron carbonate and that the iron bearing section is about 500 feet thick. Although no mining operations have been carried out in recent years, soft hematite was mined in the past at three different locations along the axis of the syncline. Early magnetic dip needle surveys carried out over the area showed no pronounced magnetic anomalies as would be expected with this type of iron ore; exploration was therefore based almost entirely on drilling. However, it was felt that it might be possible to outline the boundaries of the primary iron formation with the more sensitive vertical component magnetometer and gravity meters.

COMPARATIVE MAGNETIC & ELECTRO-MAGNETIC MEASUREMENTS IRON FORMATION UPSON, WIS.

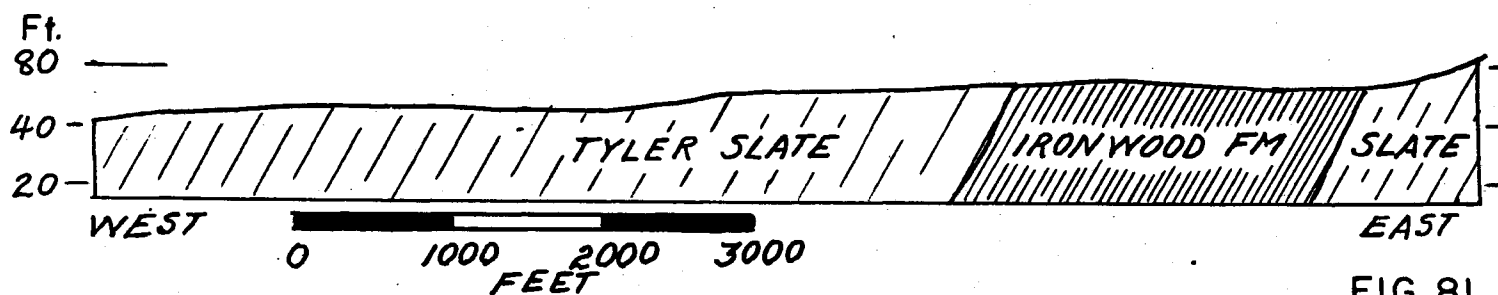
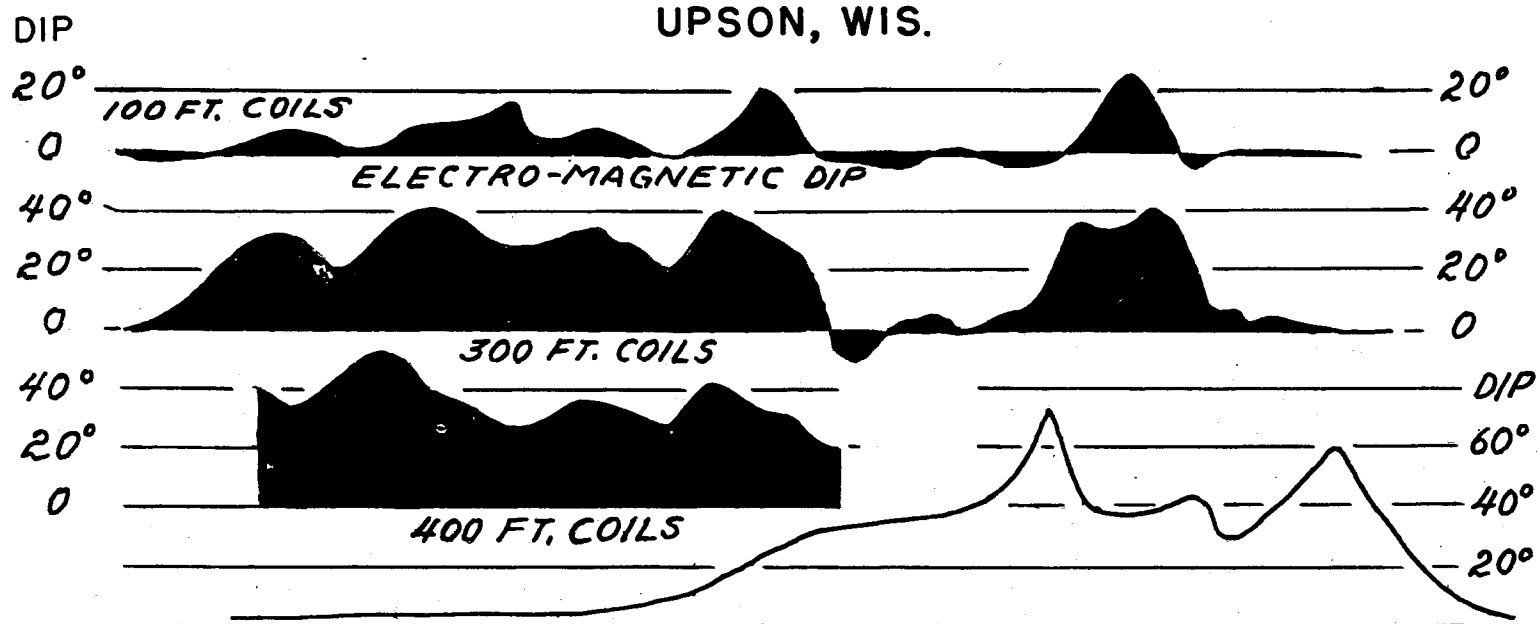


FIG. 81

COMPARATIVE MAGNETIC & ELECTRO-MAGNETIC MEASUREMENTS IRON FORMATION UPSON, WISCONSIN

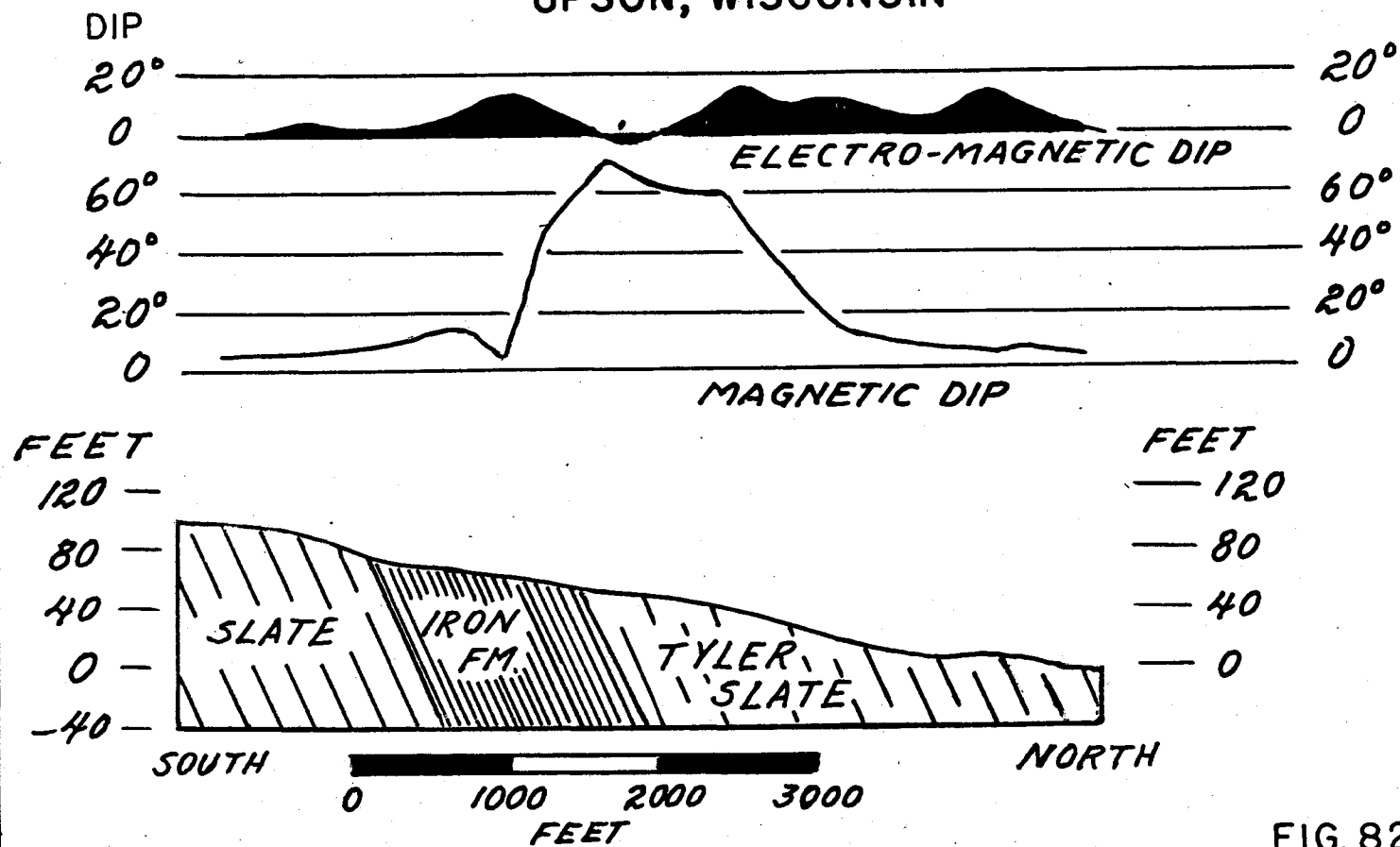
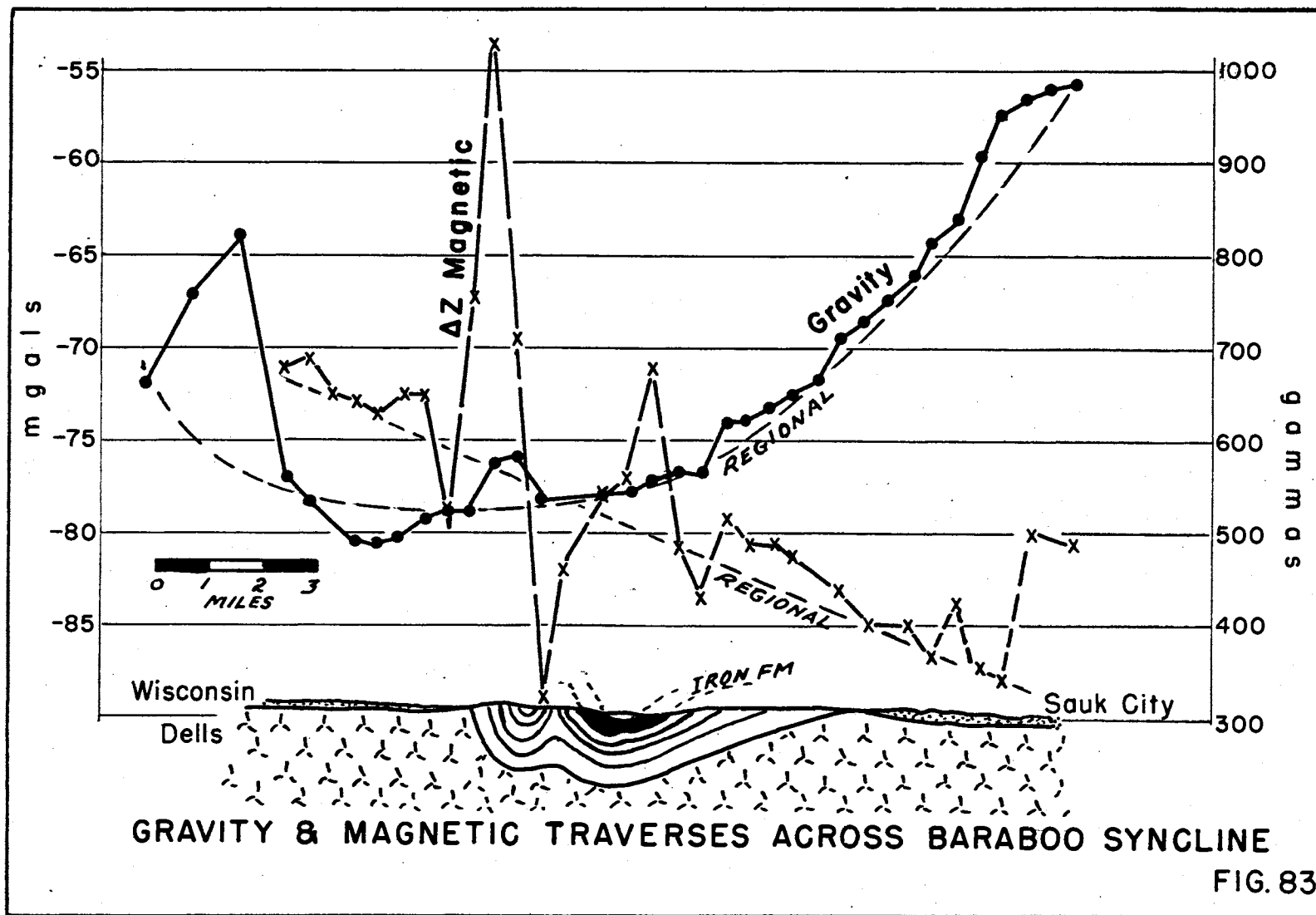


FIG. 82



IV-5b Gravity and Magnetic Study

Fig. 83 shows the gravity and magnetic anomaly values obtained along a traverse across the strike of the syncline between Wisconsin Dells and Sauk City.

Very strong regional gradients are seen to be present in both sets of data, but pronounced local anomalies occur in three places. The most striking of these is over the north limb of the syncline which is mapped as quartzite. Here the residual magnetic anomaly is of the order of 500 gammas and the residual gravity anomaly is about 3.0 mgals. The second anomaly area occurs over the central portion of the syncline where the iron bearing Freedom formation is known to occur. Although there is a residual magnetic anomaly of about 250 gammas in this vicinity, there is no pronounced gravity anomaly. The third anomaly area is over the south flank of the syncline, mapped as quartzite, where the residual gravity anomaly is about 1.0 mgal and the residual magnetic anomaly is about 50 gammas.

Although iron formation has not been reported within or below the basal Baraboo quartzite, these observations suggest that such a layer might be present. It is also possible that the tight fold shown on the north flank of the syncline in Fig. 83 may have iron formation enfolded within the quartzite. An alternative explanation is that the quartzite has been overthrust onto the iron formation. Correct interpretation of the structure is rendered difficult by its complexity and the cover of more recent sediments.

Although the above deductions appear to be logical and substantiated by the data, more extensive studies on the syncline as a whole show that most of the northern magnetic "high" actually occurs beyond the boundary of the syncline. There is therefore considerable doubt as to the validity of the above interpretations and until more work is done, no conclusion can be reached other than it appears possible to map the iron formation in the central part of the syncline by magnetic method. The flanking gravity and magnetic "highs" may be related to an entirely separate and as yet unexplored occurrence of iron formation.

IV-5c Magnetic Investigation at the Illinois Mine

As part of the above investigation, several detailed magnetic traverses were established over the old Illinois Mine with stations at about 100 foot intervals. The results of these measurements suggest that a magnetic minimum of about 100 gammas follows the position of the known ore body which is oxidized soft hematite rather closely. The magnetic susceptibility measurements carried out on the ore and the unoxidized ferruginous slate of the Freedom formation indicate that this relation is to be expected. The susceptibility of the ore was 0.0 and that of the ferruginous slate 19.0×10^{-4} cgs.

Several pronounced one station anomalies, having both a positive and negative sign, were observed in this area, but these are attributed to steel casing or other iron material associated with the mine workings.

IV-6 Mesabi Range, Minnesota

IV-6a General Statement

The iron ores of the Mesabi Range are "soft" ores oxidized from primary ferruginous cherts known as taconites. Investigations were made to see if the thickness of the glacial drift overlying the ore could be determined by seismic or electrical measurements, or, failing that, to see if the depth of the underlying taconite could be established.

Measurements were carried out in five different areas on the Mesabi Range. In each area there were diamond drill hole data which permitted the geophysical results to be evaluated accurately in terms of the sub-surface geology.

IV-6b Seismic Studies

The reverse refraction seismic method was used to determine depths along a traverse about a quarter mile long in each area. Measurements were also made in outcrop areas to establish characteristic velocities for each rock type believed to be present so that formations encountered at depth could be identified. These latter data are summarized in Table 38.

Table 38

Characteristic Velocity Values Mesabi Range, Minnesota

Material	Velocity
Glacial drift (unsaturated)	3300 ft./sec.
Boulder clay (saturated)	5490 ft./sec.
Oxidized ore (soft)	3850 ft./sec.
Upper cherty taconite	4650 ft./sec.
Lower cherty taconite	20800 ft./sec.

From an inspection of Table 38, it is seen that it would not be possible to differentiate the iron ore from till below the water table as the water-saturated sediments have a velocity of about 5000 ft./sec.

It would be problematical whether ore above the water table could be differentiated from drift and impossible if the overlying drift contained much boulder clay. Therefore, it was recognized at the outset that the only information likely to be obtained from seismic work would be the depth of the lower cherty taconite, and possibly the depth of boulder clay if it occurred as discrete layers in the till.

The results for this part of the study have been divided on the basis of the individual areas studied.

IV-6b₁ Area 1

The seismic measurements in this area consisted of three reversed profiles and two open ended measurements. The results are summarized in Table 39.

Table 39

Seismic results, Area 1

Station	Apparent Velocities				Depth of layers			Drill Depth
	V ₁	V ₂	V ₃	V ₄	V ₂	V ₃	V ₄	to taconite V ₄
1A	3150	-----	6660	10600	--	119	238	235
1B	3150	-----	-----	-----	--	---	---	235
1D	3600	-----	7770	-----	--	119	---	280
2S	3060	-----	7800	-----	--	118	---	280
2N	3480	-----	7400	-----	--	119	---	230
3S	3220	4610	6950	-----	45	120	---	305
3N	2070	4130	7030	-----	26	134	---	210
4	3680	-----	8180	-----	--	125	---	210
5	3400	-----	6660	-----	--	120	---	195

V₁ = Glacial drift

V₂ = Older till in drift (?) water table (?) Average true velocity = 4350 ft./sec.

V₃ = Boulder clay, Average true velocity = 7300 ft./sec.

V₄ = Taconite

In identifying the velocity horizons given in Table 39, both the drill hole data nearest each site and the outcrop velocity measurements in Table 38 were used; however, identification of the V₃ horizon was made on the basis of surface exposures in the side of an open pit mine where the boulder clay occurs at a depth of 120 feet. The observed velocity for this clay however averaged about 7300 ft./sec. rather than 5500 ft./sec. which was indicated by the outcrop velocity measurement.

Except for the taconite surface which was defined only at location A₁, this was the deepest horizon mapped. As the boulder clay appears to occur as a layer, a perched water table is to be expected with unsaturated drift and ore beneath it. As a consequence the depth of the deeper taconite horizon is apt to be in error because of the resulting downward refraction. The decrease in velocity with depth under such conditions cannot be recognized, and calculated depth values will be too great. This condition, however, did not appear to be present at location A₁ where the depth to the taconite agreed within 3 feet of that indicated by the drill data.

The locations of the seismic stations relative to the drill holes, and a comparative depth profile based upon the two sets of data, are shown in Fig. 84.

IV-6b₂ Area 2

In this area, two seismic traverses were run at approximately right angles to each other. Two reverse profiles were shot along a north-south line and one reverse profile along an east-west line. The V₃ horizon which averaged about 6000 ft./sec. was tentatively identified as the boulder clay. The V₄ horizon on the basis of the high velocity values appeared to be the taconite. Unfortunately, there were no drill hole data here to permit an evaluation of the results which are summarized in Table 40. The depth profiles based on these data are shown in Fig. 85.

Table 40

Seismic Results, Area 2

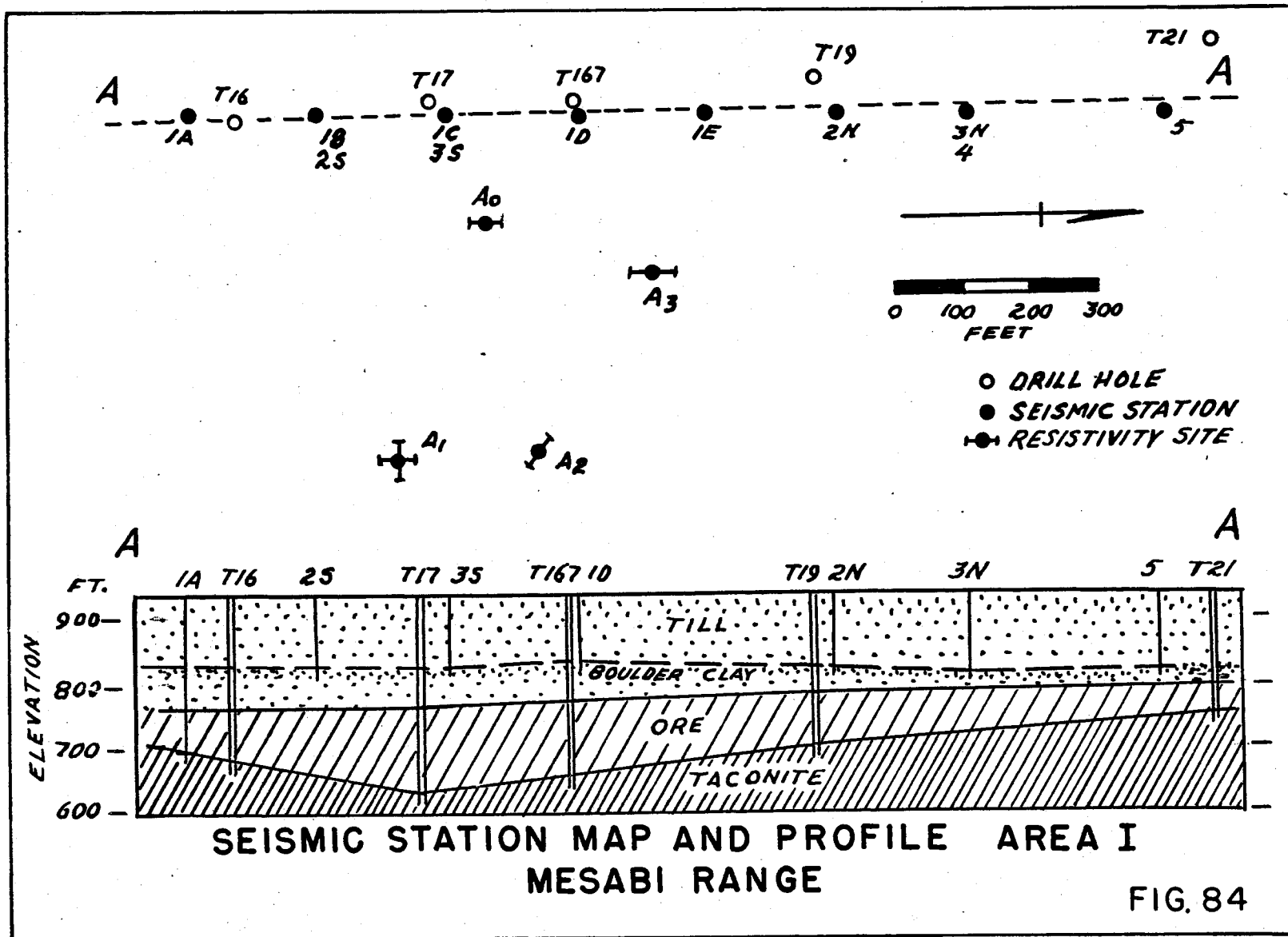
Station	Apparent Velocity				Depth of Layers		
	V ₁	V ₂	V ₃	V ₄	V ₂	V ₃	V ₄
1S	3770	----	5500	-----	---	132	---
1N	2270	4420	-----	-----	24	---	---
2S	4025	-----	5980	-----	---	173	---
2N	2770	-----	6860	-----	---	76	---
3E	3480	-----	-----	10450	---	---	174
3W	3970	-----	-----	12000	---	---	217
4W	-----	-----	-----	11200	---	---	---

V₁ = unsaturated till

V₂ = older till (?) water table (?)

V₃ = boulder clay (?) Average true velocity = 6370 ft./sec.

V₄ = taconite, average true velocity = 11,200 ft./sec.



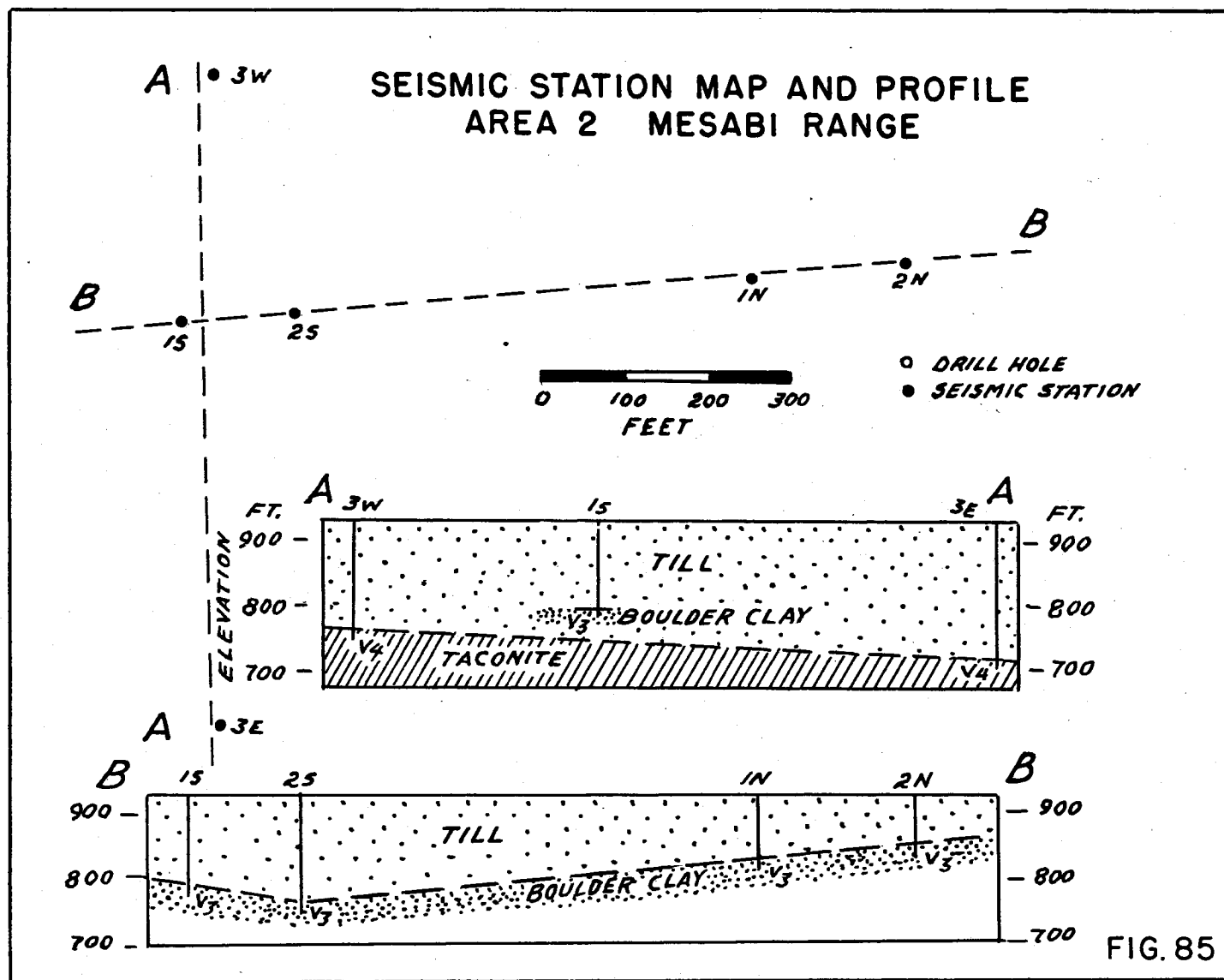


FIG. 85

IV-6b₃ Area 3

Four reverse refraction profiles were shot in this area. At four of the shot points, water table was observed to be close to the surface which is verified by the seismic velocity values for the surface layer at these locations being somewhat greater than 5000 ft./sec. Three seismic horizons were defined which, on the basis of the velocity values, were correlated with the surface till, water table and the taconite. The correlation of the depth of the seismic horizons with the geologic formations shown by the drill hole data, although consistently poor except at sites 1N and 2S, suggested the ore horizon was mapped at 2N and 3S. The departures were not of a random nature, and it is seen that for both the ore and taconite surfaces a deeper conformable surface is indicated. This suggests that over most of the area there is a perched water table with unsaturated material beneath it which, as explained above, would result in too great a depth being calculated. The seismic data are summarized in Table 41, and the depth profile comparing the seismic and drill hole depths is shown in Fig. 86.

Table 41

Seismic Results, Area 3

Station	Apparent Velocity				Depth of Layers			Drill Depth
	V ₁	V ₂	V ₃	V ₄	V ₂	V ₃	V ₄	to Taconite
1S	---	5380	---	17300	---	---	286	120
1N	2890	---	---	14200	---	---	176	180
2S	3220	---	---	8500	---	---	98	105
2N	2017	---	4250	7240	---	85	280	165
3S	3330	---	6930	14300	---	88	259	155
3N	---	6000	---	11000	---	---	257	---
4S	---	5210	---	26000	---	---	231	140
4N	---	5350	---	15200	---	---	145	---

V₁ = glacial drift (saturated in part)

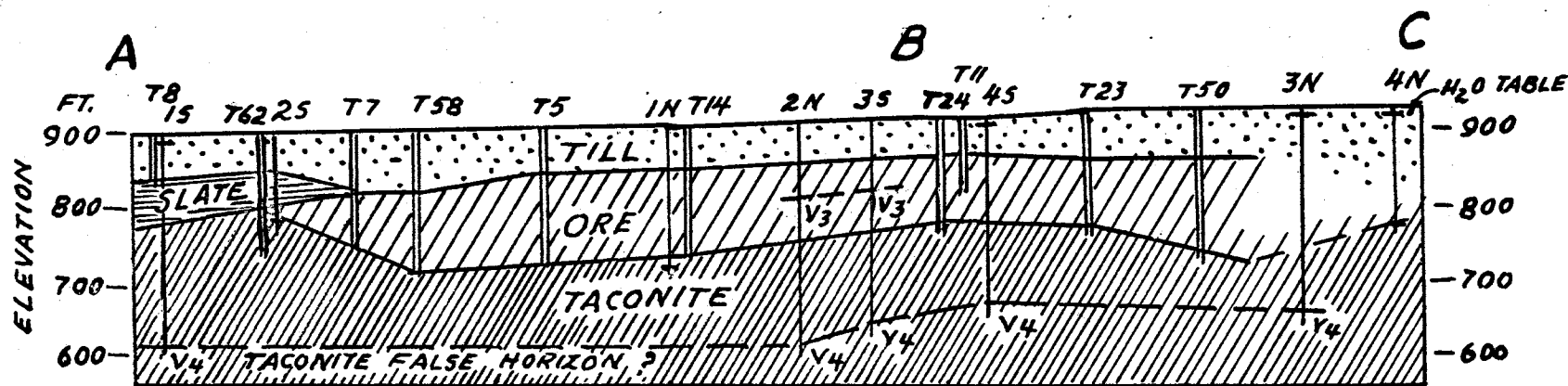
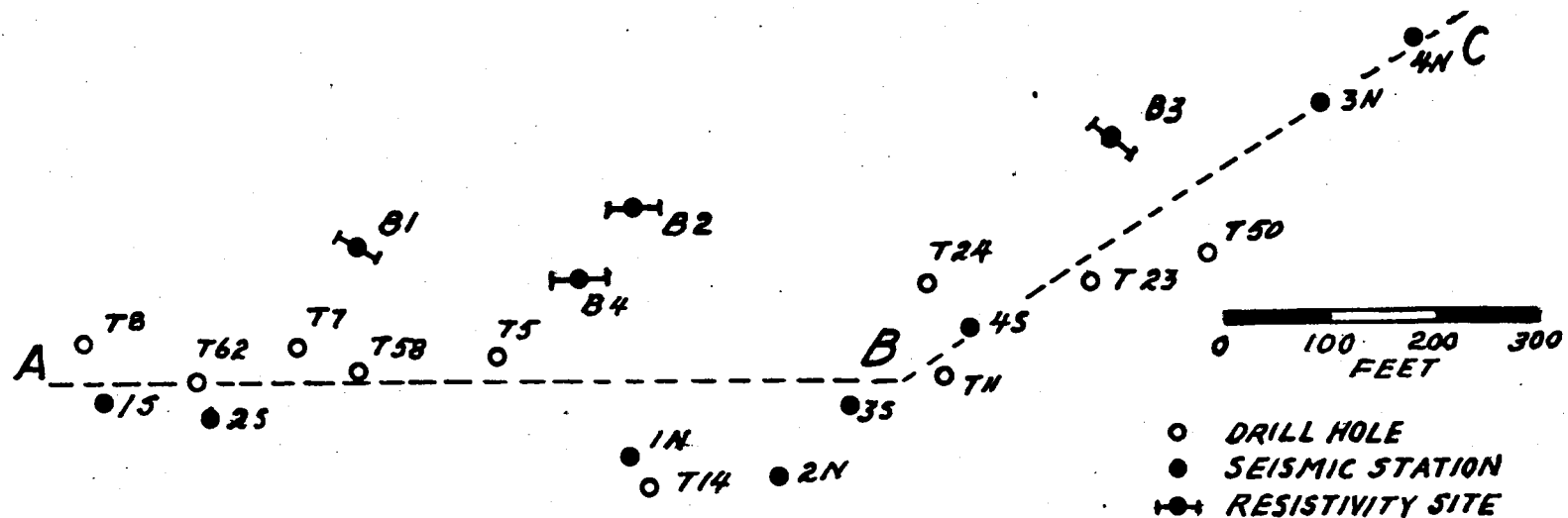
V₂ = water table (?)

V₃ = ore (?) or water table (?)

V₄ = taconite, average true velocity = 14,000 ft./sec.

IV-6b₄ Area 4

The drift cover here was very thin compared to the other areas investigated. Three profiles were established and the data are summarized in Table 42. The comparative depth profiles are shown in Fig. 87 and it is seen that the seismic data agree fairly well with the drill hole logs.



SEISMIC STATION MAP AND PROFILE
AREA 3 MESABI RANGE

FIG. 86

SEISMIC STATION MAP & PROFILE AREA 4 MESABI RANGE

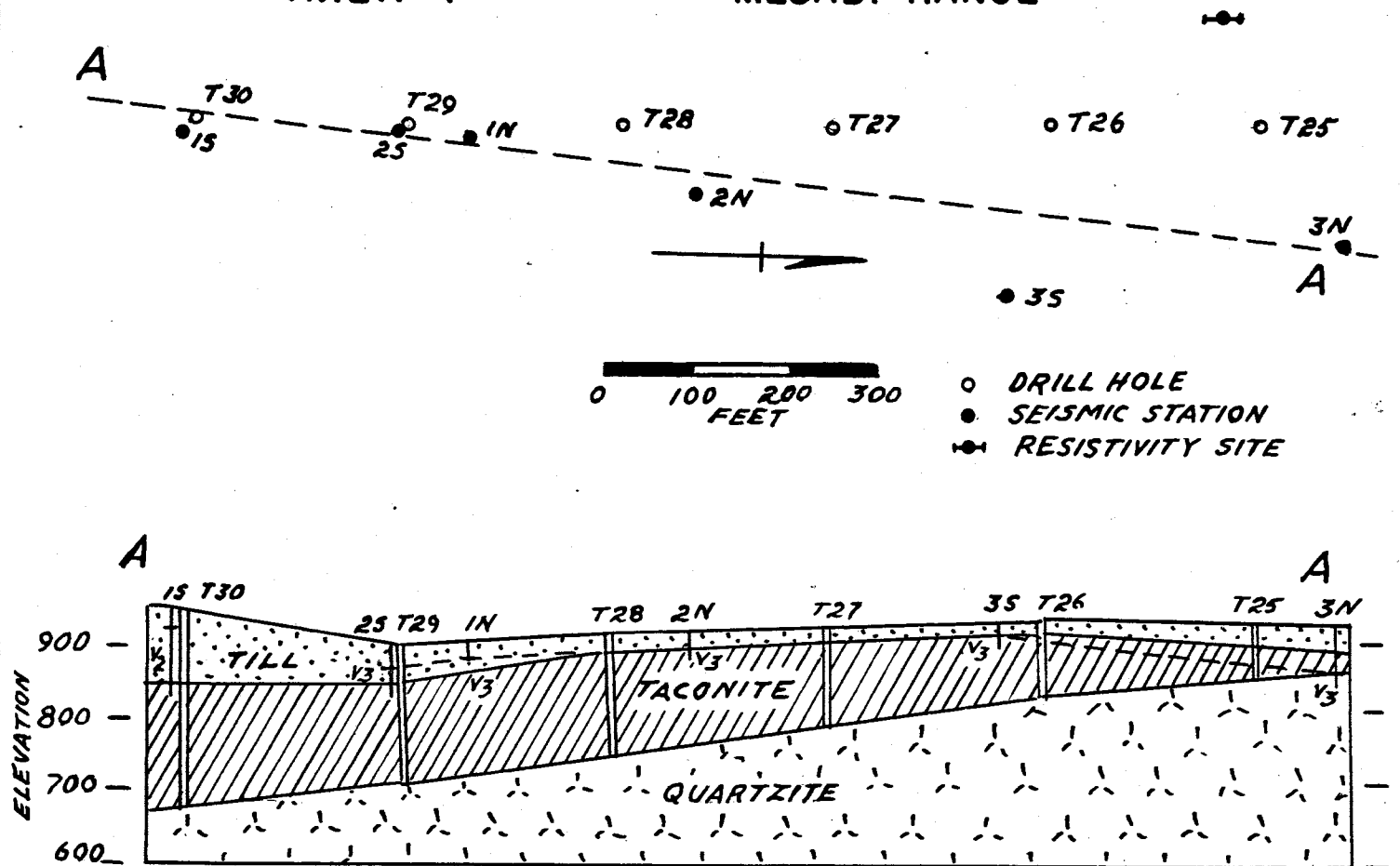


FIG. 87

Table 42

Seismic Results, Area 4

Station	Apparent Velocity			Depth of layers		Drill Depth to Taconite
	V ₁	V ₂	V ₃	V ₂	V ₃	
1S	4510	6930	-----	24	---	95
1N	3240	-----	10300	---	20	30
2S	1760	-----	20500	---	27	45
2N	2810	-----	19400	---	23	22
3S	2420	-----	11100	---	22	20
3N	3710	-----	13000	---	62	25, 60*

* quartzite

V₁ = unsaturated glacial till

V₂ = boulder clay (?)

V₃ = taconite, average true velocity = 16,050 ft./sec.

IV-6b₅ Area 5

Three reverse refraction profiles were established in this area. The subsurface geology, while perhaps more complicated than that at the other sites studied, was on the whole fairly well delineated by the seismic work except at site 1E. The seismic results are tabulated in Table 43, and Fig. 88 shows a profile comparing the seismic and drill hole data

Table 43

Seismic Results, Area 5

Station	Apparent Velocity			Depth of Layers		Drill Depth to Taconite
	V ₁	V ₂	V ₃	V ₂	V ₃	
1W	5510	-----	9680	---	127	135
1E	5260	-----	16500	---	240	170
2W	5560	-----	13000	---	149	170
2E	5890	8830	12500	96	209	205
3W	4550	-----	28600	---	221	210
3E	-----	8320	24700	---	221	227

V₁ = saturated glacial drift

V₂ = unknown horizon in upper taconite

V₃ = lower taconite, average true velocity = 14,725 ft./sec.

SEISMIC STATION MAP PROFILE AREA 5 MESABI RANGE

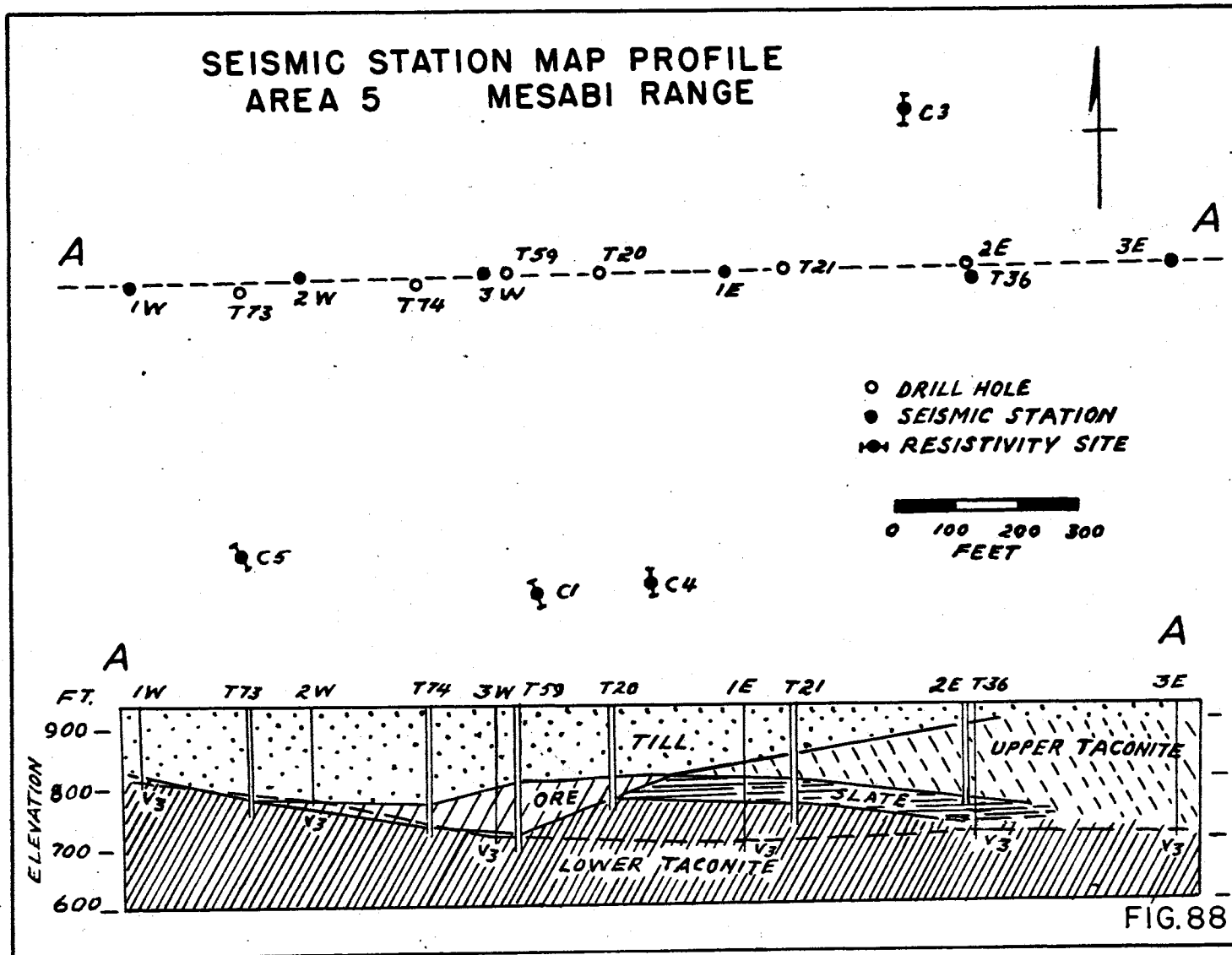


FIG.88

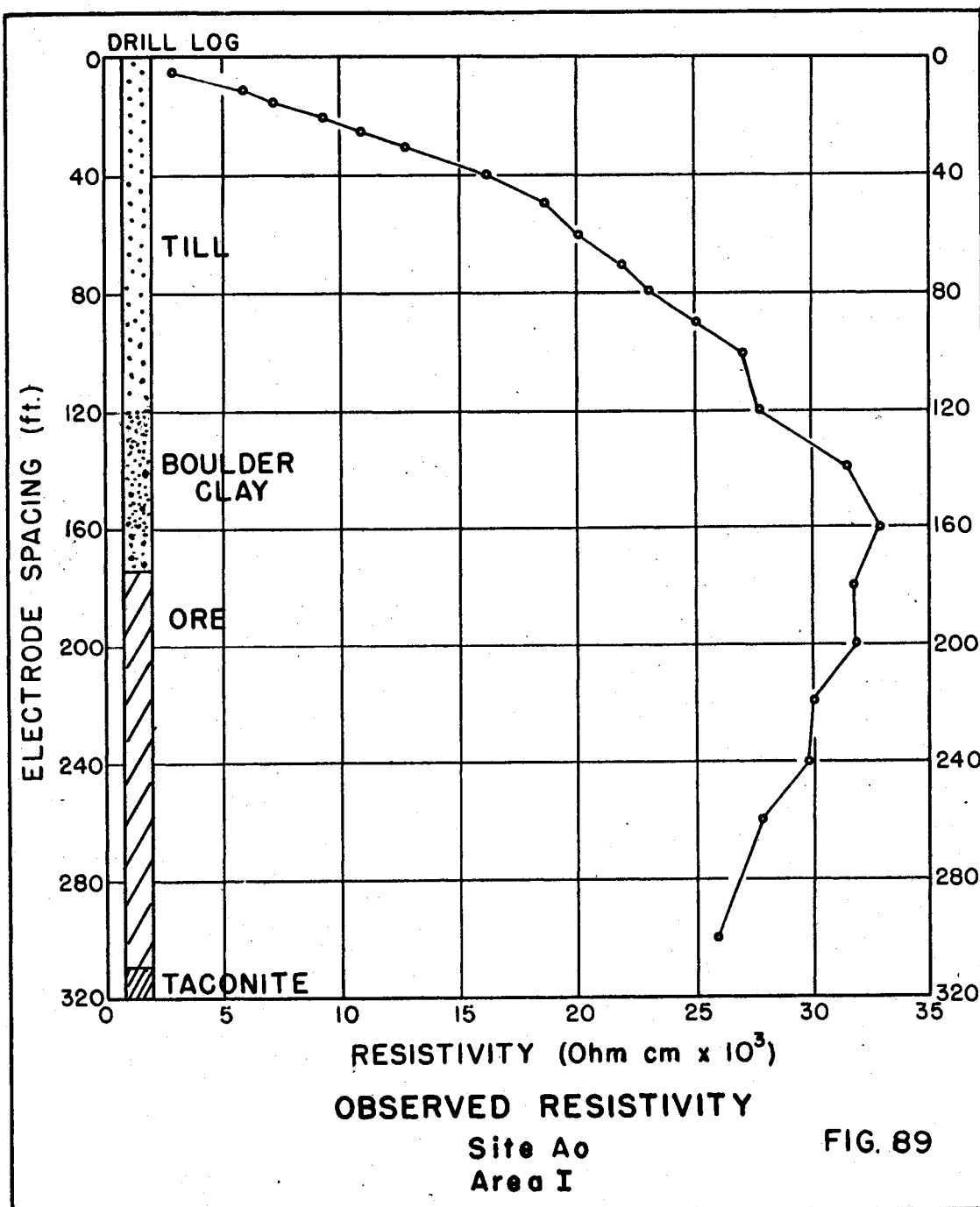
IV-6c Summary on Seismic Investigations

As indicated by the outcrop velocity studies, the seismic refraction method is not suitable for locating the soft oxidized ores of the Mesabi Range. The velocity of seismic propagation in the ore is no greater than that of the overlying glacial till and lower than that for water saturated sediments. As a result, the ore cannot be differentiated from till or detected below water table. However, it does appear possible to detect the underlying taconite by this method except where it underlies a perched water table. Where this occurs, the lower velocity of the unsaturated glacial drift and ore beneath the boulder clay layer causes downward refraction and erroneous depths are obtained for the deeper, high velocity, taconite layer. However, this situation was encountered on a wide spread basis in only one of the five areas investigated. In the other areas, the drill hole data indicated that the seismic results portrayed the taconite surface with sufficient fidelity to be used for mapping depressions where ore might occur.

IV-6d Electrical Resistivity Studies

In view of the failure of the seismic refraction measurements to detect ore, a series of test electrical resistivity depth measurements were carried out about site A₀ in Area 1. See Fig. 84. The Wenner configuration was used with DC current and porous pot potential electrodes. Fig. 89 shows the plot of the apparent resistivity values obtained for different electrode spacing intervals. The same data, plotted on a cumulative basis are shown in Fig. 90. Interpretation on this basis, as explained in the Antigo Survey, has been generally good. Breaks in slope are indicated for electrode spacings of 30, 62, 117, and 215 feet which are interpreted as representing those depths at which changes in resistivity occur. The adjacent seismic data indicated horizons at 45 and 120 feet and the drill log shows ore underlying till at 175 feet and taconite at 310 feet. As the depth of penetration in resistivity measurements is usually less than the electrode spacing by some proportional factor which varies with the local geology, it appeared these measurements might be useful. It was therefore decided to pursue the study further to find out if the break in slope of the resistivity curve at 220 feet could be correlated with the change from till to ore at 175 feet.

The areas chosen for study were the same as were used in making the seismic refraction studies. All of the areas were free of local subsurface conductors and regarded as good test areas for electrical measurement.



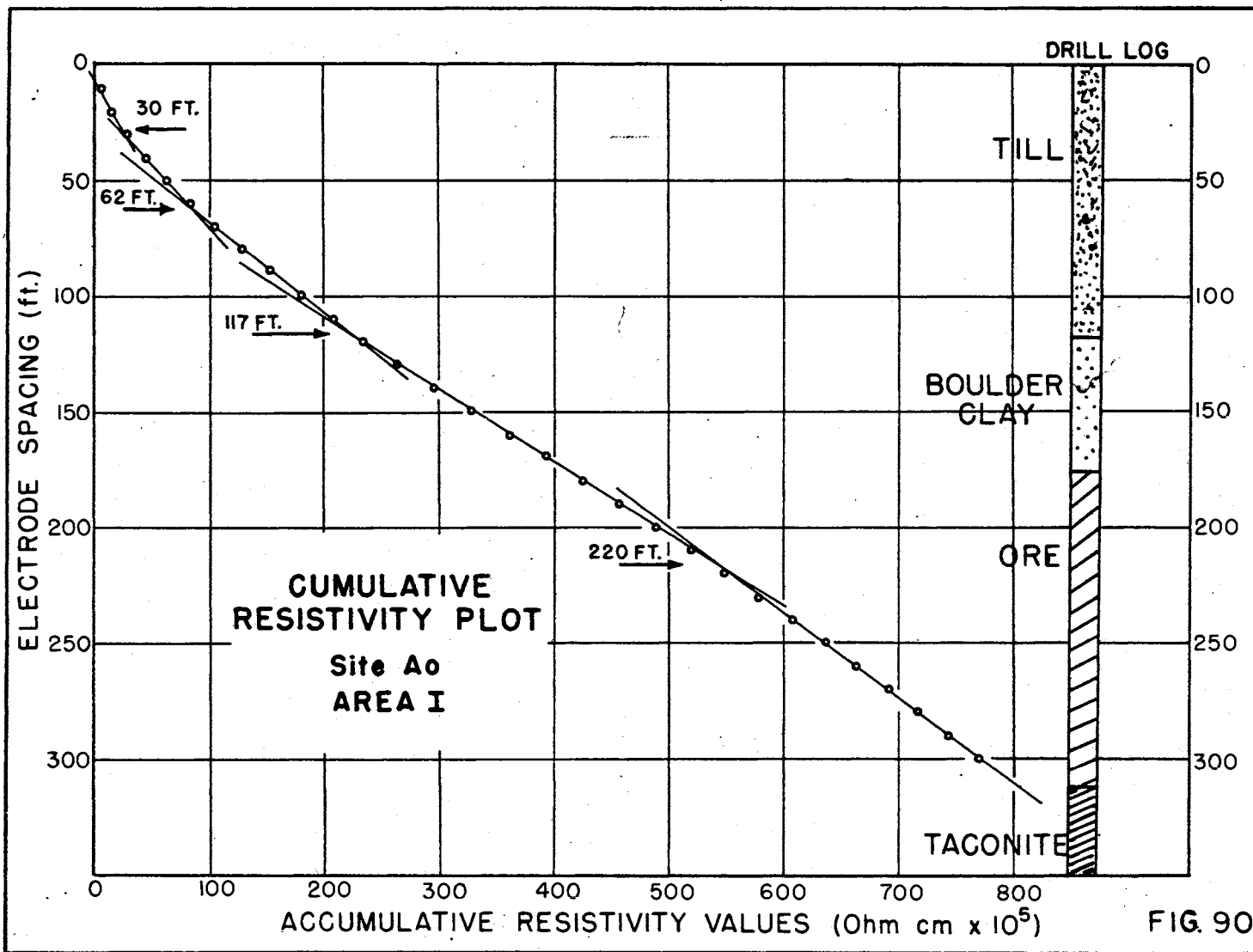


FIG. 90

IV-6d₁ Area 1

Four sets of electrical resistivity depth measurements were made in this area using the Wenner electrode configuration; also, two sets of measurements were made with unsymmetrical electrode configurations, and a test run made to compare the results obtained with metal potential stake electrodes with those using porous pot non-polarizing potential electrodes to see if there was any pronounced directional factor present. Two of the sets of measurements were made with the spreads oriented perpendicular to each other. The results of these special measurements showed that the Wenner electrode configuration gave the most easily interpreted results, and that non-polarizing potential electrodes should be used. On the test conducted with the electrode spreads oriented at right angles to each other, it was found that while the resistivity values obtained were numerically different for the same electrode spacing, the pattern of the resistivity graph obtained in each direction was essentially the same, and that comparable depths were indicated. See Fig. 91. However, it should be noted that whereas five horizons were indicated in one direction, only four were indicated in the other. In making the depth analyses, all of the resistivity values were plotted on a cumulative basis as a function of the electrode spacing, and these plots were compared with the projected log of the nearest diamond drill holes. Several "breaks" in slope on the graph were indicated at each location. As the drill hole data showed no changes in geology in the till, it was necessary to use the seismic data in order to establish complete correlations. All of the data are summarized in Table 44.

Table 44

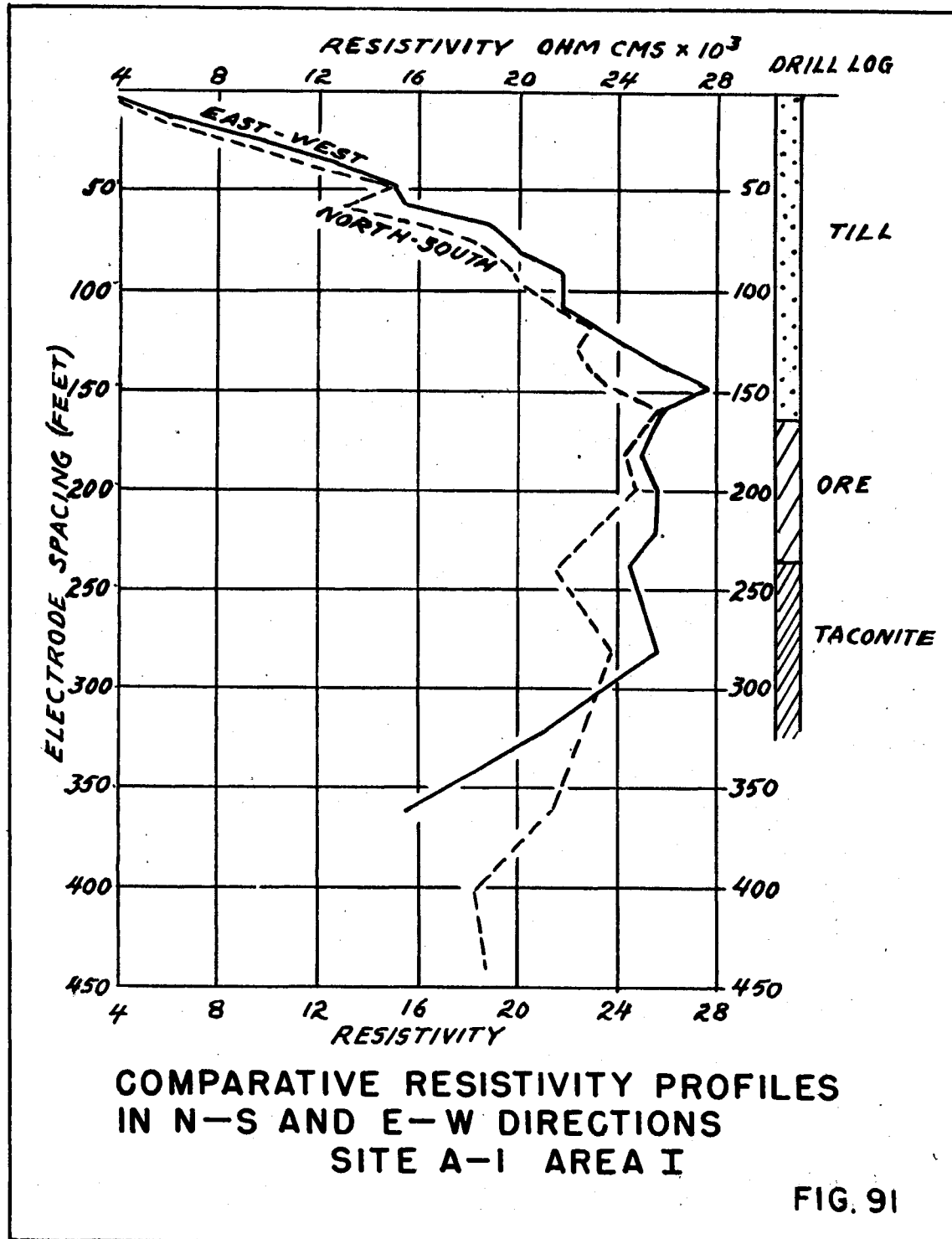
Electrical Resistivity Values, Area 1

Site	Electrode Spacing of Break in Slope						
	ρ_1	ρ_2	ρ_3	ρ_4	ρ_5	ρ_6	ρ_7
A ₀	30	62	117	---	215	---	---
A ₁ N-S	35	71	120	---	206	356	---
A ₁ E-W	42	83	120	---	---	316	---
A ₂	35	67	100	170	220	288	375
A ₃	25	57	100	159	210	308	413

Average Seismic Depths:

35(V₂) 122(V₃) 238(V₄)

A ₀	0 - till - 180 - ore - 298 - taconite
A ₁	0 - till - 165 - ore - 235 - taconite
A ₂	0 - till - 165 - ore and slate - 218 - taconite
A ₃	0 - till - 154 - ore and slate - 220 - taconite



On the basis of the seismic data for horizons above the boulder clay (V_3), it appears that ρ_1 can be correlated with material having velocity of about 4400 ft./sec. and tentatively identified as older till or the water table. ρ_2 has no known geologic or seismic counterpart but may represent sand or gravel within the till. ρ_3 appears to correlate with seismic horizon V_3 , the boulder clay. Although ρ_4 appears to correlate with the drill hole depth defining the till - ore boundary at sites A_2 and A_3 , this resistivity horizon is missing at the other sites, and the ρ_5 resistivity layer which does occur everywhere is correlated with the top of the ore. The ρ_6 layer is correlated with the lower cherty taconite, and ρ_7 is related to some such deeper geologic horizon as the underlying quartzite. The above correlations between the three sets of data are shown graphically in Fig. 92.

The data obtained in the other areas investigated were analyzed in a similar manner and correlations established from the drill hole and seismic data.

IV-6d₂ Area 3

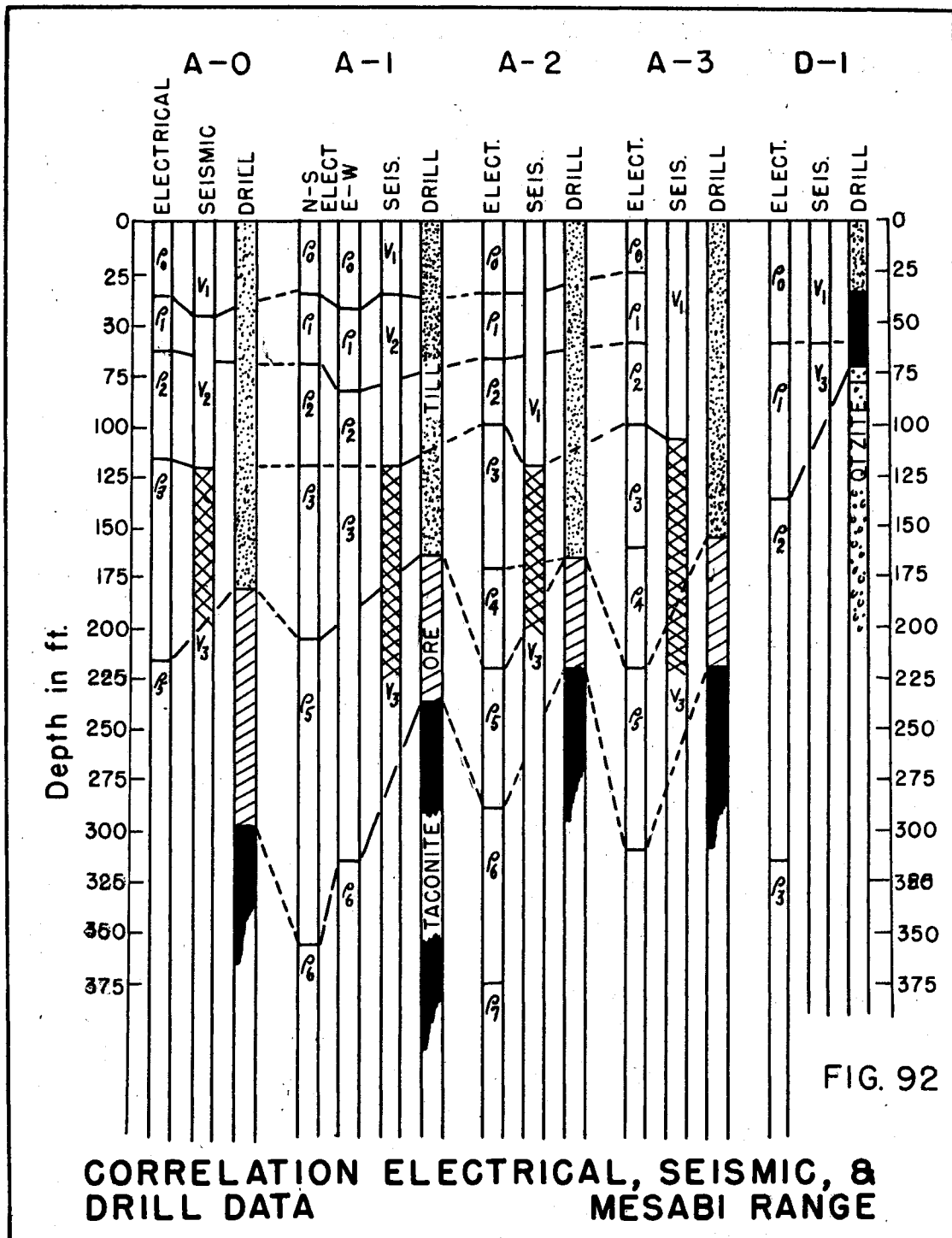
The location of the points of measurement in this area are shown in Fig. 86 and the results are summarized in Table 45.

Table 45

Electrical Resistivity Results, Area 3

Site	ρ_1	Electrode Spacing of Break in Slope			ρ_4
		ρ_2	ρ_3		
B-3	47	87	115		198
B-4	40	60	85		198
Average Seismic Depths:		85(V_2)			190(V_4)
B-3	0 - till - 48 - ore - 185 - taconite				
B-4	0 - till - 45 - ore - 180 - taconite				

In this area, only four resistivity layers are indicated below the surface layer. In correlating which of the "breaks" are related to the till - ore interface, that having the greatest change in slope was selected. This "break" occurs at too shallow a depth to be related to the taconite and as no pronounced discontinuity is indicated in the ore, this is the obvious break to select for defining the top of the ore. A graphical correlation of these resistivity, seismic and drill hole data is included in Fig. 92.



Two other sets of measurements with assymmetric electrode spreads were made in this area, but it was found that the results did not readily lend themselves to interpretation and for this reason have been omitted.

IV-6d₃ Area 4

The location of the single measurement made in this area is shown in Fig. 87 and the results obtained are given in Table 46.

Table 46

Electrical Resistivity Results, Area 4

Site	Electrode Spacing of Break in Slope		
	ρ_1	ρ_2	ρ_3
D-1	60	136	314
Seismic Depth: 22 to 62 feet (V_3) taconite			

D-1 0 - till - 34 - tachenite - 72 - conglomerate - 80 - quartzite

These measurements show only three resistivity layers beneath the surface layer. The upper break, ρ_1 , correlates with the depth of the taconite as indicated by both the seismic and drill hole data. ρ_2 appears to be related to the taconite - quartzite interface and the deeper horizon, ρ_3 , apparently is related to some rock member within the basement complex.

IV-6d₄ Area 5

The location of the measurements made in this area are shown in Fig. 88 and the results are summarized in Table 47.

Table 47

Electrical Resistivity Results, Area 5

Site	Electrode Spacing of Break in Slope						
	ρ_1	ρ_2	ρ_3	ρ_4	ρ_5	ρ_6	ρ_7
O-1	40	115	140	180	200	260	380
O-3	47	115	133	186	---	---	---
O-4	30	80	132	---	222	265	300
O-5	44	113	148	180	---	---	---
Seismic Depth:	110(V_2)			220(V_3)			

Table 47 (continued)

C-1	0 - till - 186 - slate and ore - 215 - taconite - 370 - quartzite
C-3	0 - till - 25 - taconite - 145 - slate - 192 - taconite
C-4	0 - till - 172 - ore - 240 - taconite
C-5	0 - till - 25 - taconite - 130 - slate - 180 - quartzite

The drill hole data and the geologic cross-section (Fig. 88) both indicate it would be misleading to assume horizontal layering of geologic lithologic units in correlating the resistivity horizons. The apparent horizontal layering indicated by the correlation chart of Fig. 93 and Table 47 down through the ρ_3 horizon, actually cuts across geologic lithologic units and therefore must be related to some factors other than rock type. Presumably, these would be changes in either the degree of water saturation or in the chemistry of the ground water.

IV-6d₅ Summary of Electrical Measurements

It appeared, with the exception of Area 5, that electrical resistivity values could be used to delineate one or more horizons in the glacial till, the top of the ore, the taconite surface and, in some cases, a formational break either within the taconite or below it. The electrode spacings delineating the different electrical resistivity layers, while appearing to give a direct correlation with depth for the near surface layering indicated by the seismic measurements, were apparently related to the deeper geologic horizons by some constant which differed with the different areas. These relationships and the constants derived for each layer are summarized in Table 48 and are shown graphically in Fig. 92 and Fig. 93.

That the constants, while appearing to be unique for each of the areas studied, are actually related to depth of the horizon as well as the lithology is shown in Fig. 94. It is seen that there is a very large change in value with depth for the near surface layer, defined seismically as having a velocity between 4000 and 5000 ft./sec., and probably representing an older till or water table. It will also be seen that when the taconite gets near to the surface, its depth value coincides with this horizon which elsewhere occurs in the till. This suggests that the horizon is actually the water table. The constant for the V_3 horizon, characterized by a velocity of 7000 ft./sec. and identified as boulder clay in the side of the open mine pit in Area 1, likewise shows a definite variation with depth. The same is true for the top of the ore. In the case of the taconite surface, the constant varies systematically for all depths greater than 180 feet. However, when the taconite is within 50 feet of the surface, the constant is comparable to that of the V_1 horizon, which, as has been pointed out, is believed to represent the water table. Presumably, this would also apply to the ore horizon where it approaches the surface.

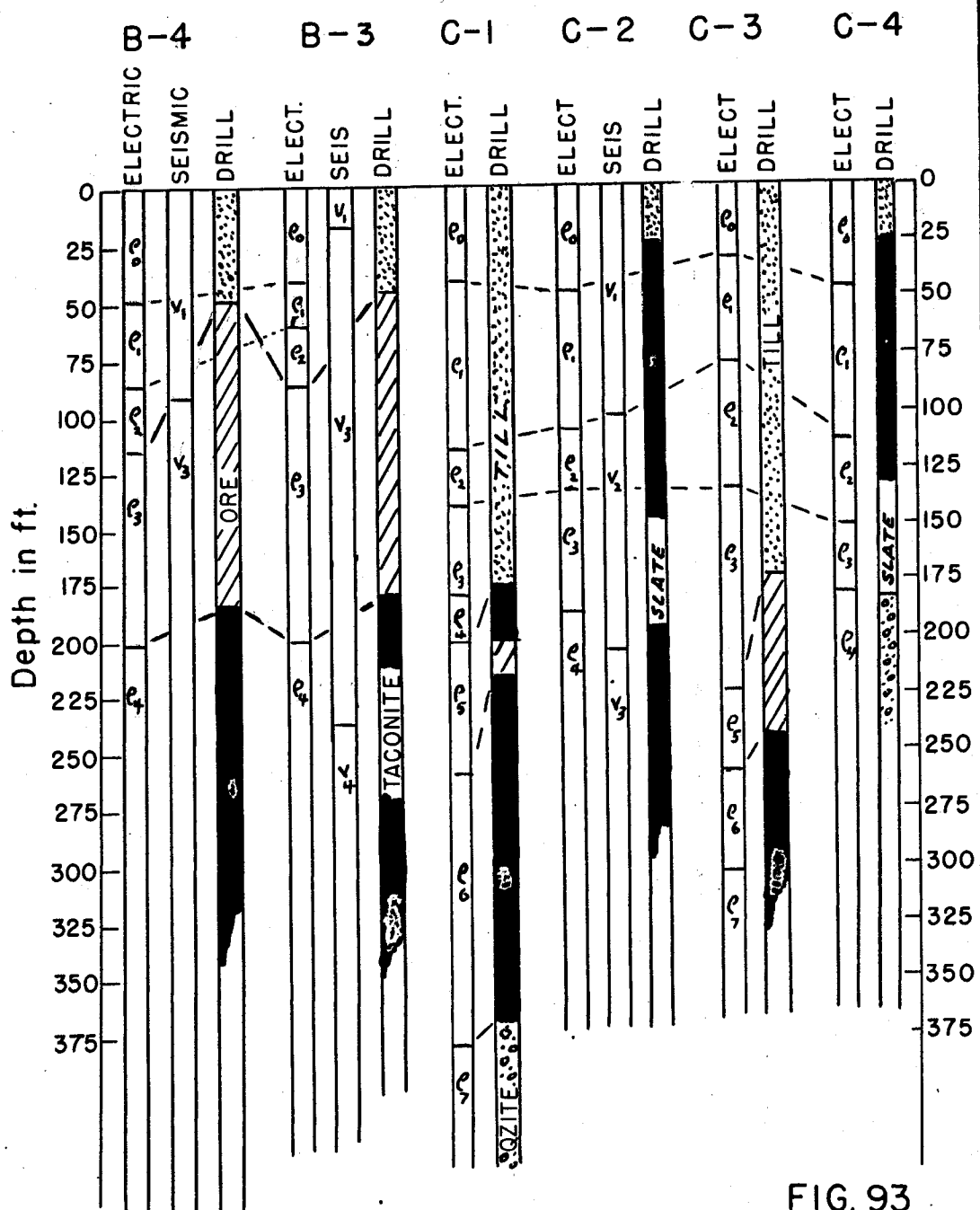


FIG. 93
CORRELATION ELECTRICAL, SEISMIC, &
DRILL AREA
MESABI RANGE

Table 48
Table of Electrical Resistivity Coefficients
Mesabi Range, Minnesota

Area 1

Site	Electrical Horizon	Seismic Horizon	Geologic Horizon	V ₂	Coefficient K*		
					V ₃	Ore	Taconite
A ₀	A ₁ 35 ft. ρ ₂ 115 ρ ₅ 225	V ₂ 45 ft. V ₃ 120	Ore 180	1.29	1.05	.80	
A _{1N}	ρ ₁ 35 ρ ₃ 120 ρ ₅ 205 ρ ₆ 355	V ₂ 35 V ₃ 117	Ore 164 Tac. 235	1.00	.97	.79	.66
A _{1E}	ρ ₁ 43 ρ ₃ 120 ρ ₆ 315	V ₂ 35 V ₃ 117	Tac. 235	.82	.97		.74
A ₂	ρ ₃ 100 ρ ₅ 220 ρ ₆ 290	V ₃ 118	Ore 165 Tac. 220		1.18	.75	.76
A ₃	ρ ₃ 100 ρ ₅ 220 ρ ₆ 310	V ₃ 110	Ore 155 Tac. 220		1.10	.71	.71
Average K				1.03	1.05	.76	.72

Area 3

B ₃	ρ ₃ 115 ρ ₄ 200		Ore 50 Tac. 185			.45	.93
B ₄	ρ ₃ 85 ρ ₄ 198	V ₄ 190	Ore 45 Tac. 180			.52	.91
Average K						.48	.92

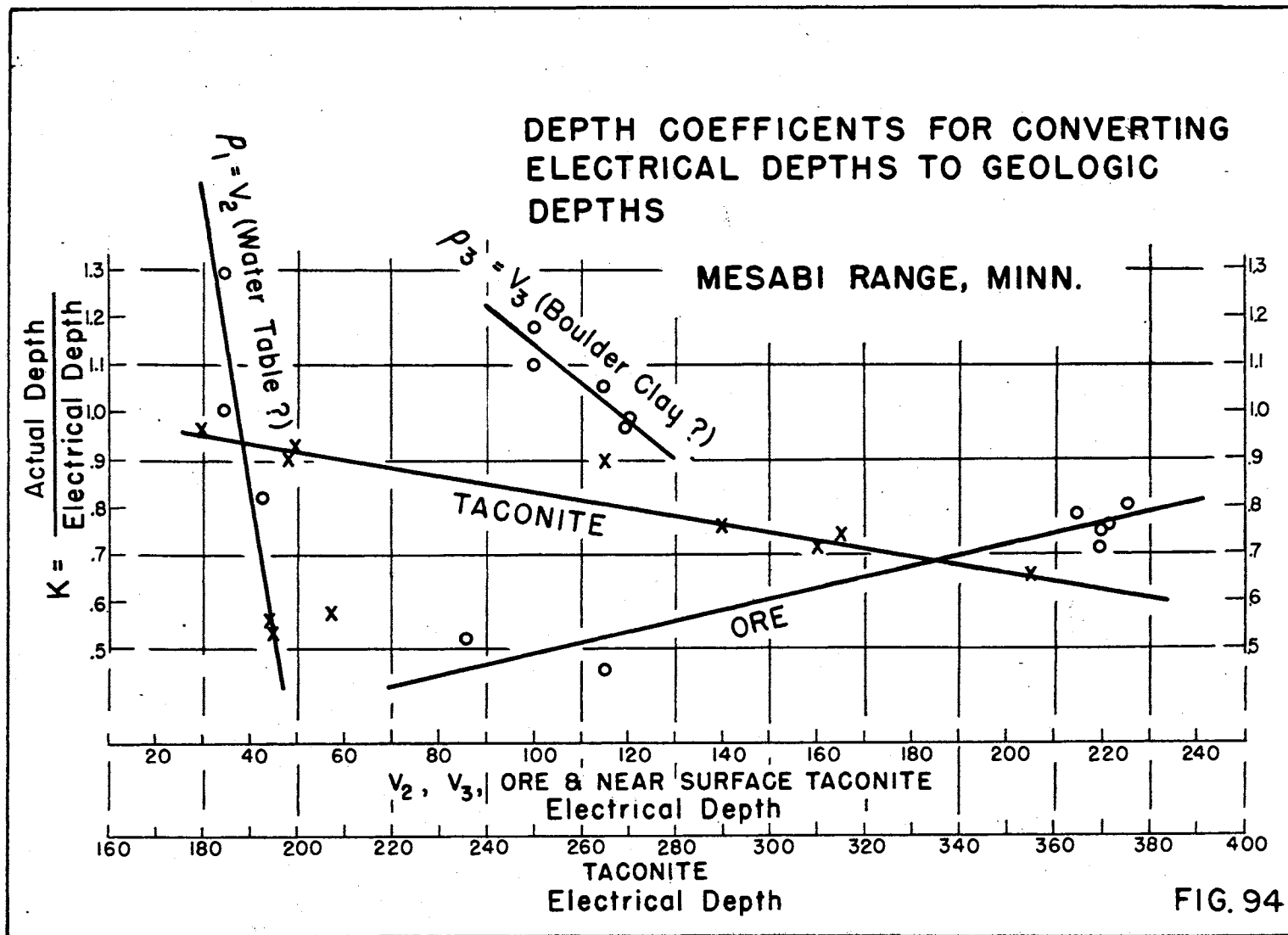
* Coefficient K = $\frac{\text{Seismic or Geological Horizon}}{\text{Electrical Horizon}}$

Table 48 (continued)

<u>Area 4</u>					
Site	Electrical Horizon	Geologic Horizon	Ore	Coefficient K*	
	ρ_1 58	Tac. 50		.59	
	ρ_2 137	Qtzite 80			.59
		Average K		<u>.59</u>	<u>.59</u>
<u>Area 5</u>					
C_1	ρ_3 180 ρ_7 380	Tac. 175 Qtzite 370		.97	.97
C_3	ρ_1 45	Tac. 25		.55	
C_4	ρ_5 222 ρ_6 265	Ore 170 Tac. 240	.76	.90	
C_5	ρ_1 45 ρ_4 180	Tac. 25 Qtzite 180		.55	1.00
		Average K	.76	.55(shallow) .93(deep)	.98

*Coefficient K = $\frac{\text{Geological Horizon}}{\text{Electrical Horizon}}$

Since there is nothing distinctive about the resistivity values for identifying a horizon as is the case with seismic values, a major problem in using resistivity is the correlation of breaks in the resistivity curve with the appropriate geologic horizon. It is therefore necessary to establish control from drill hole data. If used on this basis, the method would be useful for outlining reserves as well as prospecting. It has been demonstrated for many years by the work of the Ground Water Division of the Illinois Geological Survey that such measurements can be used successfully with this type of empirical interpretation. Much of the subsurface geology of that state has been worked out by the use of electrical resistivity measurements so interpreted, and drilling has proven the results to be correct approximately 90 % of the time.



IV-7 - Electro-magnetic Investigations
Along the Boundary of the Keweenaw Volcanic Flows
Northern Wisconsin

IV-7a General Statement

The Keweenaw basic lava flows of Upper Michigan, Wisconsin and Minnesota are known to be mineralized in several areas. The most spectacular occurrence being the native copper and copper-oxides found on the Keweenaw Peninsula in Michigan. In Wisconsin, the known mineralization is limited to minor amounts of metallic sulphides and copper along the southern boundaries of the flows. This investigation was undertaken to see if these occurrences could be located and extended using electro-magnetic methods.

IV-7b Electro-magnetic Study

The instruments used consisted of a 42 inch vertical primary coil energized with a 2000 cycle per second alternating current with a search (receiving) coil having a diameter of 12 inches which was mounted so that it could be rotated 360 degrees about both a horizontal and vertical axis. The field procedure followed is that described in the Appendix.

IV-7c Barabee Test, Ashland County

This area, located in SE $\frac{1}{4}$ SE $\frac{1}{4}$, Sec. 32, T 45N, R3-W, is one in which some sulphide mineralization had been found by surface prospecting. Five traverses were run in the vicinity of the old test pit and the dip results showed no pronounced near surface conductor. However, null widths (position of minimum signal) of 3° and 4° observed immediately adjacent to the pit did however indicate a conductor in the area.

Two additional traverses, each about a half mile long, were run about a half mile west of the area across Trout Brook, and although dips as large as 8° were obtained, they are of questionable validity since all were observed in areas adjacent to marked changes in topography. Phantom dips are apt to be obtained under such conditions due to misalignment of the coils, as it is not always possible to see the receiving coil so that the plane of the sending (energizing) coil can be oriented in the correct azimuth. To check on this at Trout Brook, two sets of measurements were made for each of the traverses; one with the energizing coil 300 feet north of the sending coil and one with the energizing coil 300 feet south of the search coil. All measurements were carried out "in line" with

observations at 50 foot intervals. As the marked dips which were observed on the first series of measurements were not obtained at the same locations when the energizing coil was moved to the other side of the receiving coil, it seems fairly certain that the observed dips here were related more to misalignment than the presence of any conductor. See Fig. 95.

IV-7d Davis Hill Area, Bayfield County

In this area, conglomerate and lava flows have been intruded by gabbro, and near the gabbro contact some traces of copper mineralization have been reported. A series of "in line" east-west traverses were established so as to cross this contact. No pronounced dip anomalies were observed except where power lines were crossed, and although null widths of 4° to 10° were found, they appeared to be associated with areas of swampy ground or else with areas of conglomerate in which there was probably as high water content. However, in one area having a local dip of 3° with a null width of 3° , some trace of iron and copper sulphide mineralization was noted.

The general conclusion reached from these investigations was that good conductors were absent in areas surveyed, although the presence of local weak conductors was indicated.

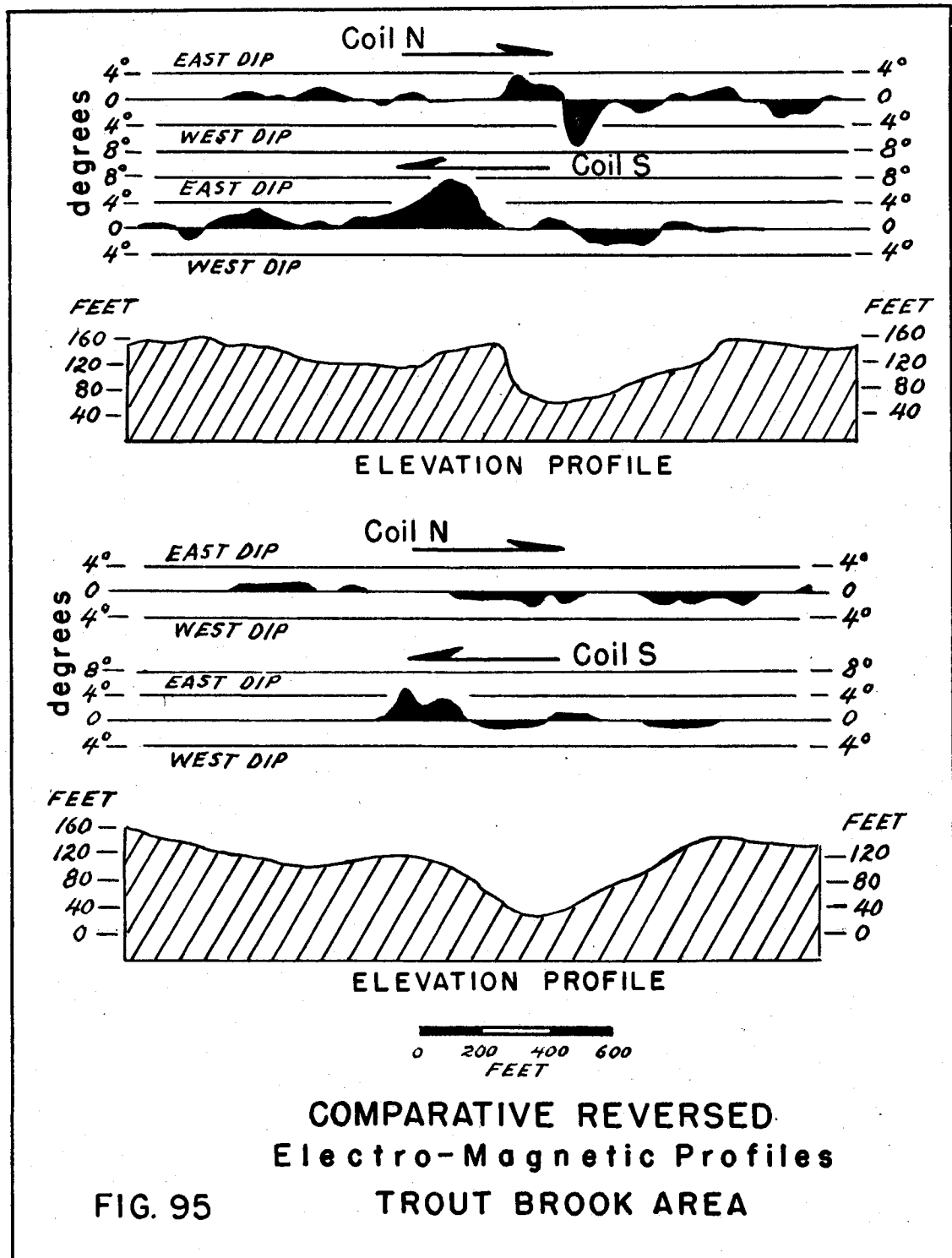
IV-8 - Magnetic Survey of Peridotite Body

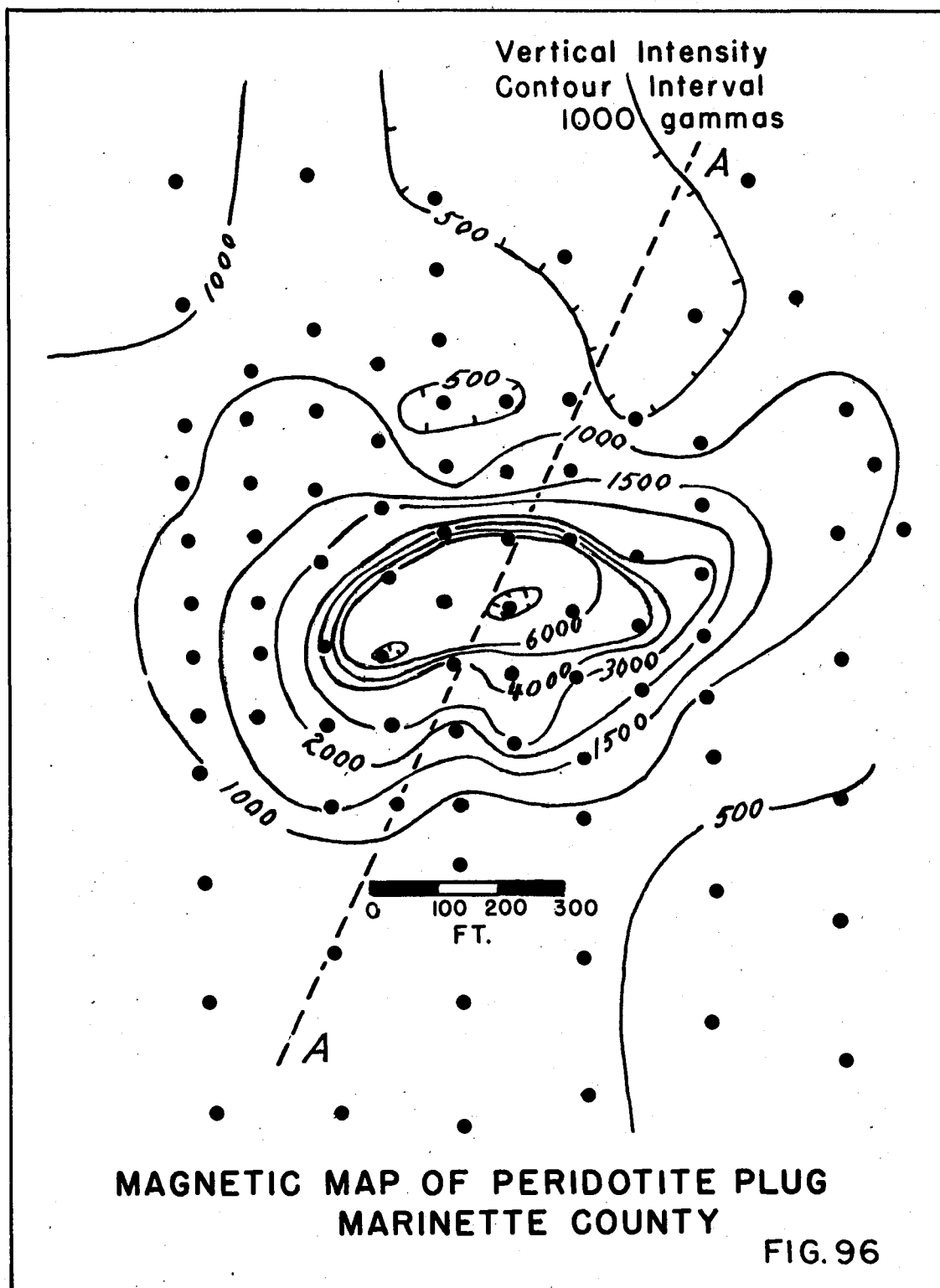
IV-8a General Statement

This investigation was made to outline the areal extent of a peridotite body which outcrops from beneath a surface cover of glacial drift in Sec. 24, T 36N, R 21E of Marinette County. The presence of asbestos in the outcrop indicated that it might be developed commercially if the body were extensive enough. As magnetite was found to be an abundant accessory mineral in the peridotite, magnetic measurements were chosen as the most suitable geophysical method to outline the horizontal extent of the body.

IV-8b Magnetic Survey

One hundred and sixty magnetic observations were made with an Askania vertical component variometer. Of these, approximately one half were on a reconnaissance basis with observations every 100 feet along traverses roughly 200 feet apart, and the balance located so as to form a 40 foot grid of stations over the peridotite outcrop and the area immediately adjacent. The data were corrected for diurnal field changes and latitude effects and the resulting anomalies plotted and contoured. See Fig. 96.





The variation observed in local anomaly values is over 6500 gammas, with a single magnetic "high" depicted whose dimensions are roughly 200 feet by 300 feet. This magnetic anomaly has a local relief of 5500 gammas, and is offset slightly to the south of the center of the outcrop area. A weak anomaly area of opposite sign is indicated to the north.

The above observations suggest that the peridotite body is a vertical elongate pipe-like body. The anomaly pattern is very similar to that which would be produced by a vertical bar magnet as the upper pole, near to the surface, would be dominant giving rise to a very sharp anomaly profile as is observed here. See Fig. 97.

As the magnetic anomaly conforms so closely to the outcrop area of the peridotite, it is obvious that the observable peridotite represents the entire areal extent of the body which is too small for commercial exploitation.

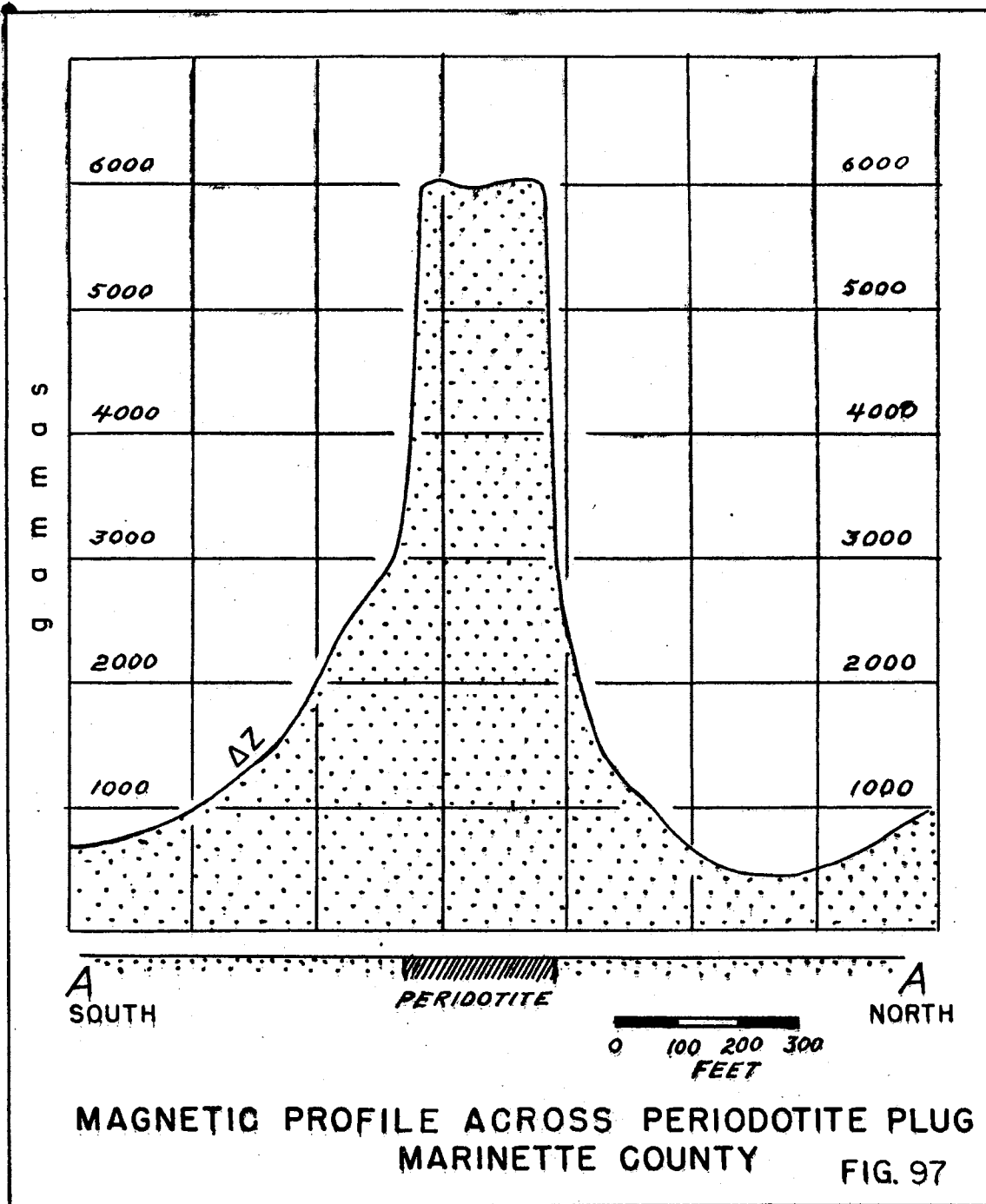
IV-9 - Lead - Zinc Deposit Gravity Study, Shullsburg, Wisconsin

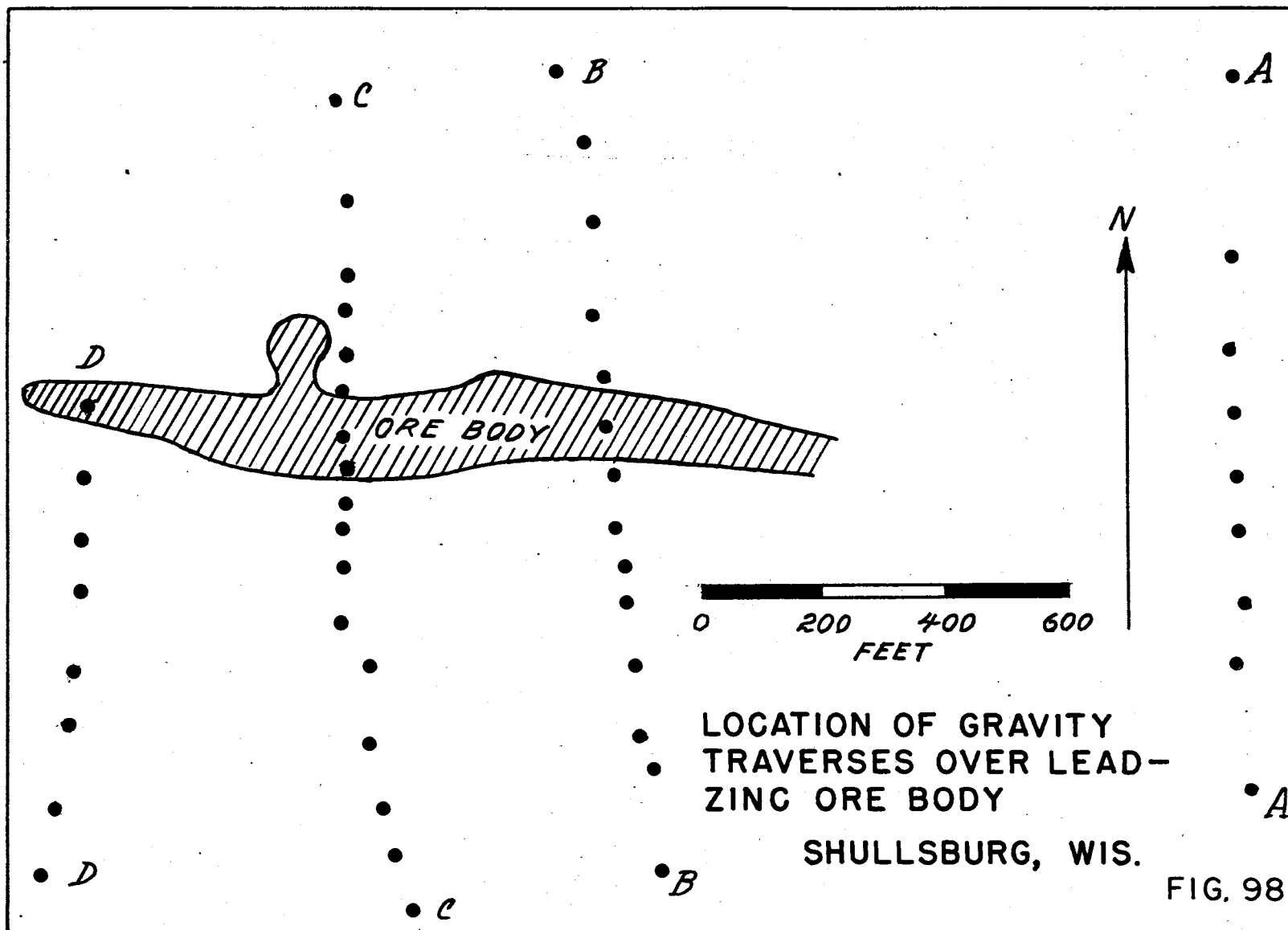
IV-9a General Statement

The lead-zinc deposits in Wisconsin occur in gently folded limestones and dolomites of Ordovician age with the ore occurring as fillings along joints, inclined fractures (pitches), and bedding planes (flats). Deposition appears to be predominantly galena in the upper levels, and sphalerite at depth; most of the ore bodies are within 250 feet of the present surface. As the deposits appear, for the most part, to be limited to the synclinal folds, it was felt that gravity observations might serve to depict favorable structure even if the mineralized areas themselves could not be directly located. The test area chosen was one in which there was a known ore body that as yet had not been mined.

IV-9b Gravity Survey

Two gravity traverses were established across the strike of the ore body having sufficient length to completely bracket both the mineralized area and any associated structure in the limestone. A third partial traverse was also run which started over the ore body. For comparative purposes, a fourth traverse was established parallel to the others that crossed an area that was believed to be mineralized. The average station spacing used was 100 feet along each traverse. The locations of the stations and their relation to the ore body are indicated in Fig. 98.



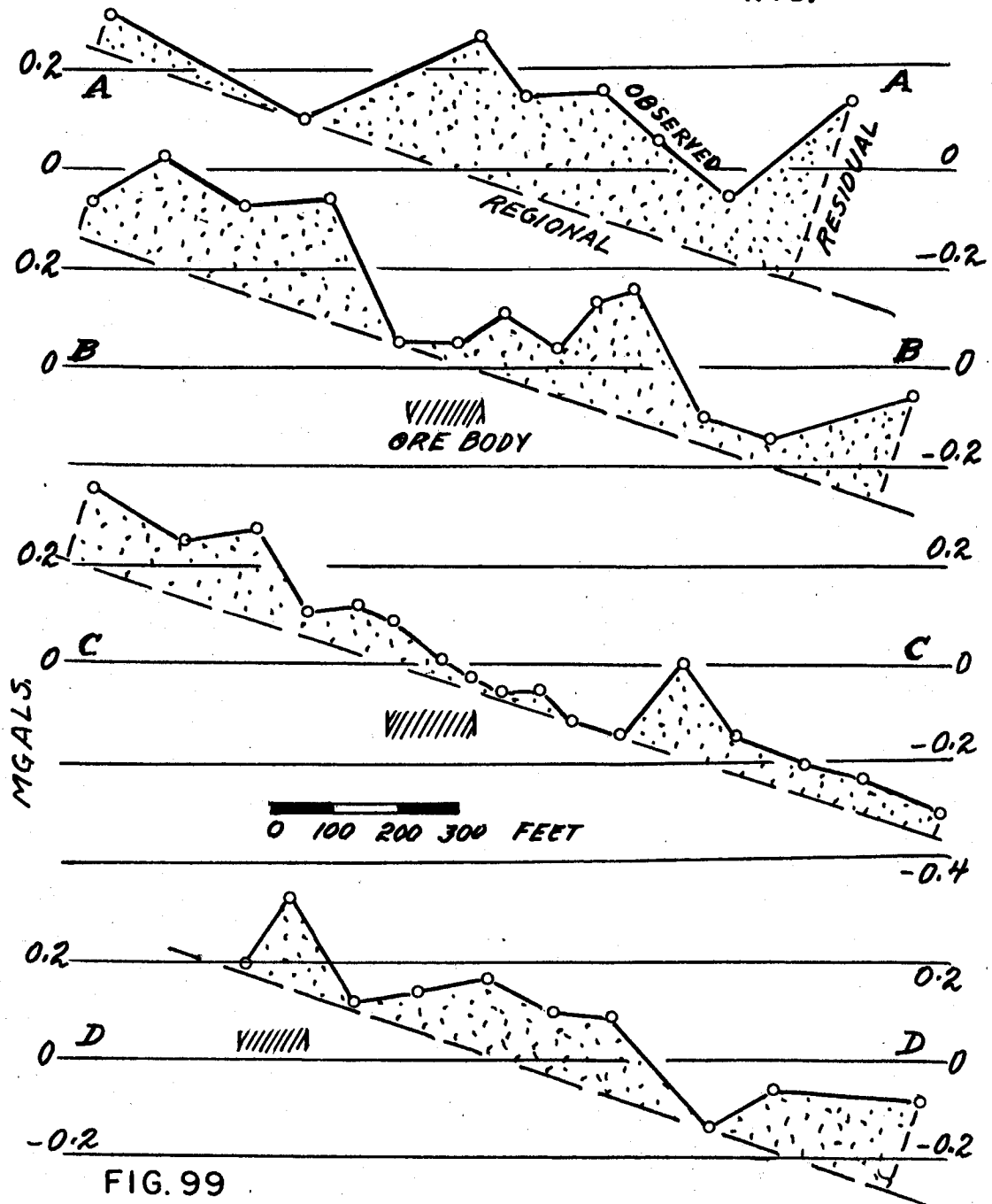


The observations were reduced to give Bouguer anomalies and the results along each traverse are shown in Fig. 99. The most striking feature on these profiles is the pronounced regional gradient; however, if this regional effect is removed, there appears to be a systematic series of residual "highs" and "lows" whose dimensions are about those of the known folding in the area. On the two complete traverses, B-B and C-C, it is seen that the ore in each case lies in an area having residual gravity minimum which was interpreted as being synclinal. It is also noted that a gravity "high" occurs either over or immediately adjacent to the reported position of the ore. This latter observation may be entirely fortuitous, but is suggestive enough to warrant more detailed work.

IV-9c Conclusion

On the basis of the limited amount of work done, it appears that the gravity method is applicable to mapping the subsurface geologic structure in the lead-zinc district of Wisconsin, and may also be used to locate areas of mineralization. The residual anomaly values, however, are less than one mgal, and careful detailed work with a high precision instrument is required.

GRAVITY ANOMALY TRAVERSES, SHULLSBURG, WIS.



Part V

General Geologic Studies

V-1 - General Statement

In the foregoing sections it has been shown how geophysical methods are being used to help solve problems in applied geology connected with water supply, engineering and mineral exploration. In addition to these investigations, several purely scientific geologic studies are being undertaken in various parts of the state. The nature of these studies is quite variable and as most of them will not be completed for some time to come, a few words will suffice at this time to describe their nature and the progress that has been made on each.

V-2 - Subsurface Topographic Studies

V-2a Lake Mills - Waterloo - Fond du Lac Areas

The water supply investigation at the Emmon Blaine Farm near Lake Mills indicated the presence of a buried ridge of basement rocks which was over a thousand feet high. It was shown that through the use of seismic, gravity and magnetic measurements, in connection with available well data, it was possible to follow this ridge for over 20 miles. The geophysical measurements are being extended to include what appears to be a parallel ridge to the east near Hartford, and to the Fond du Lac region in the north where similar subsurface ridges are indicated by well data. As these ridges are believed to be the remnants of old mountain ranges that at one time crossed Wisconsin, a more complete knowledge of their location and distribution pattern will be of considerable help in understanding the basic geologic framework within the state, as well as the movement of underground water.

V-2b Madison Area

It is known from well data that the pre-glacial Yahara River flowed in a valley over 500 feet deep through what is now the City of Madison. As was indicated by the seismic studies at the Willows Athletic Field, tributary valleys over 150 feet in depth also occur. Since it is not feasible to carry out seismic or magnetic measurements in the city proper, and as shooting of explosives in the lakes bounding the city is strongly discouraged by the State Conservation Department, a gravity study is being made of the area to see if the pre-glacial drainage pattern of the area can be mapped. Fig. 100 shows the gravity station network developed to date.

GRAVITY STATION
MAP

MADISON
&
VICINITY

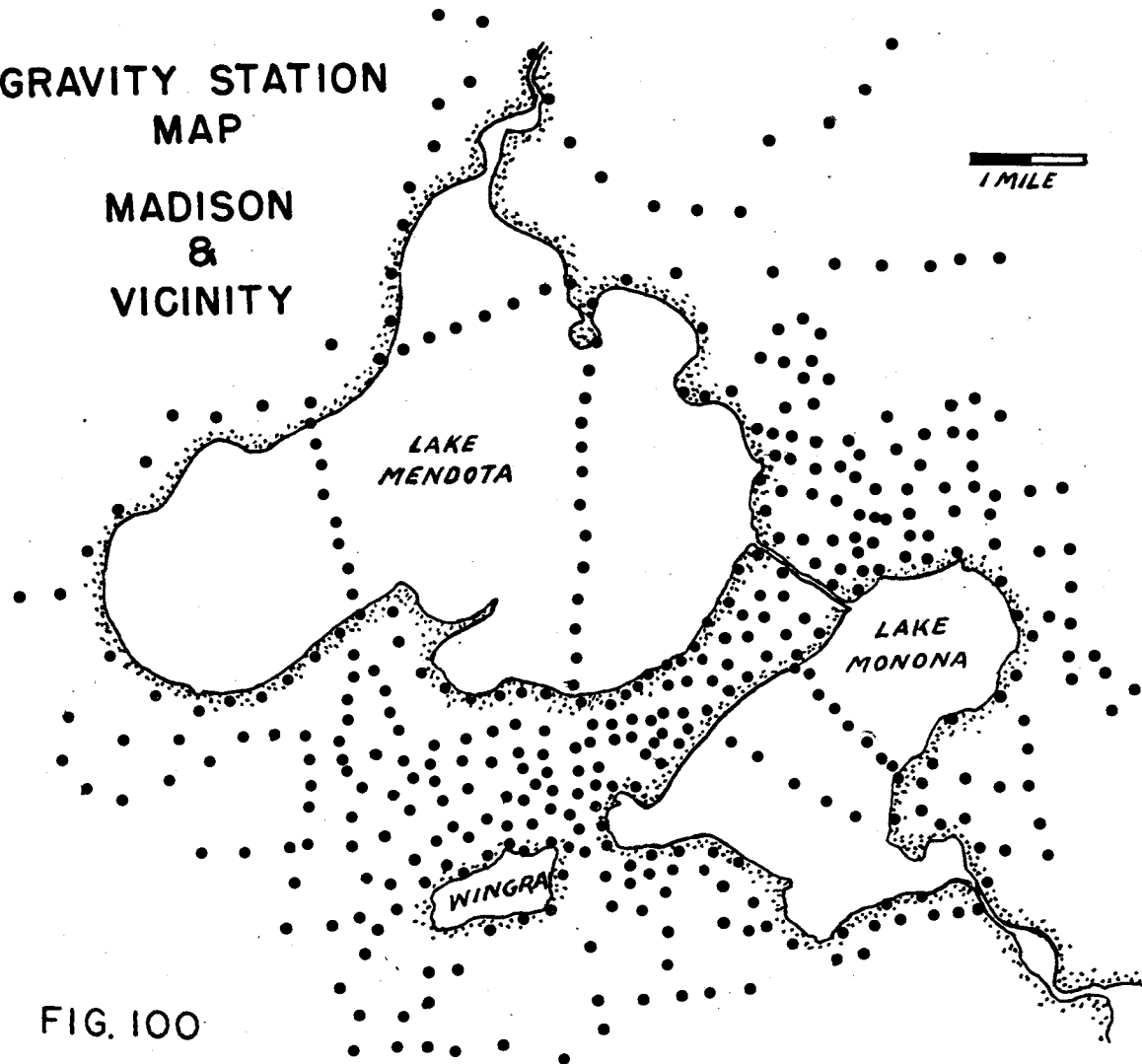
1 MILE

LAKE
MENDOTA

LAKE
MONONA

WINGRA

FIG. 100



V-3 - Crypto-Volcanic Structure Investigations

In several areas in Wisconsin, there are localities in which there is evidence of marked local structural disturbances involving both upward and downward movement. As this structural derangement suggests what might occur if an active volcanic pipe had been present in the area which never actually reached the surface, these are referred to as crypto (hidden) volcanic structures. One such structure that has been well mapped geologically occurs at Des Plaines, Illinois just south of the Wisconsin - Illinois state line. A gravity investigation is being made of this area to see if a local gravity anomaly is associated with the structurally deranged area. If a volcanic pipe is present at depth, a gravity maximum would be expected in the area. If a negative anomaly is associated with the area, the structure could result from a possible salt dome type of intrusion or the collapse of a cavernous area developed by solution. Enough work has been done on this study to indicate that a negative gravity anomaly is present. Since the gravity anomaly area is considerably larger than the known area of structural displacement as determined from well logs, it is planned to carry out supplementary seismic measurements to ascertain if the complex structure does extend as far as is indicated by the gravity measurements.

V-4 - Petrologic Investigations

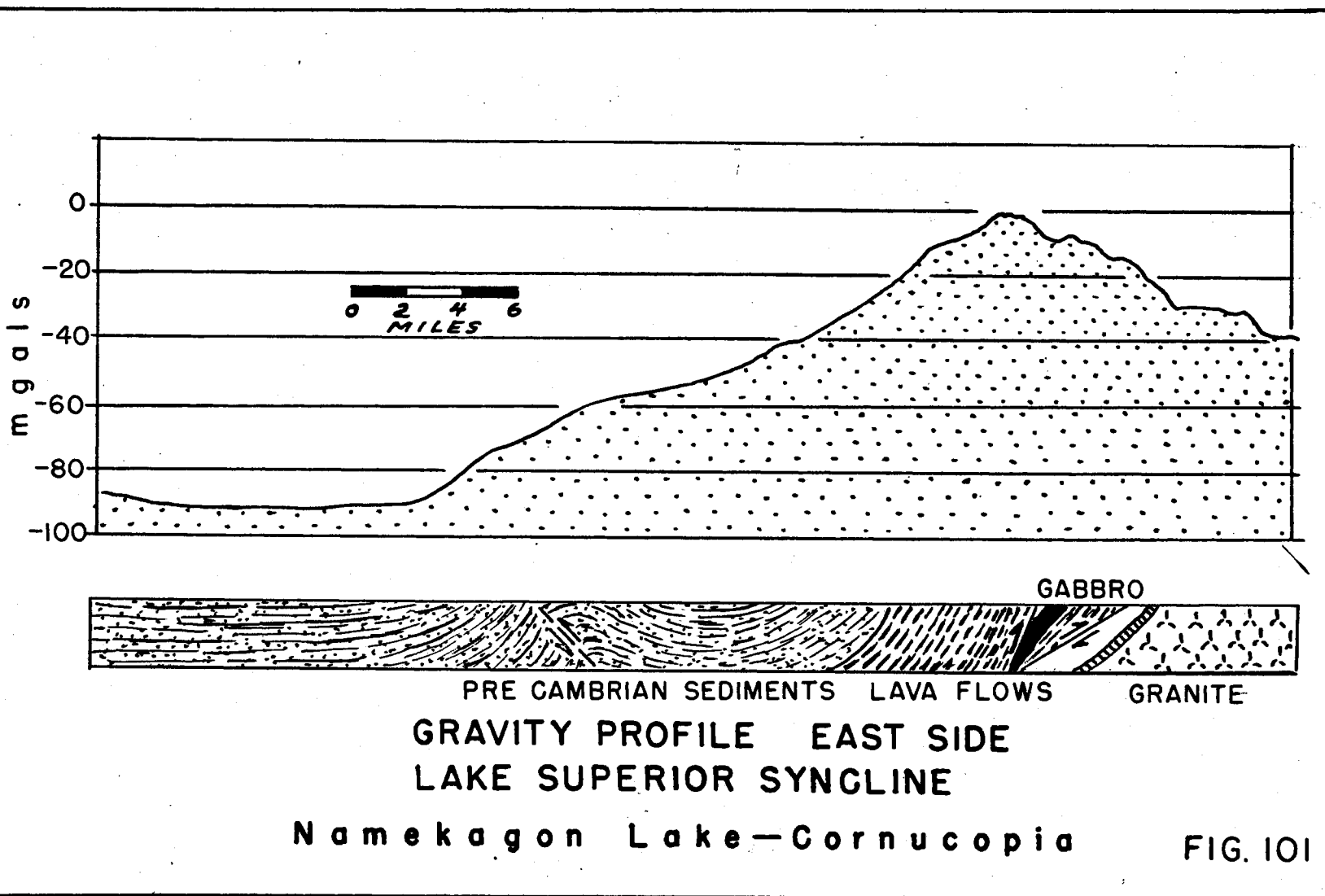
One of the major problems in geology is whether or not plutonic igneous rocks are derived by differentiation from a parent magma of basic composition. Granites, for example, may either be the result of such a process, or they may represent sediments that were granitized at depth.

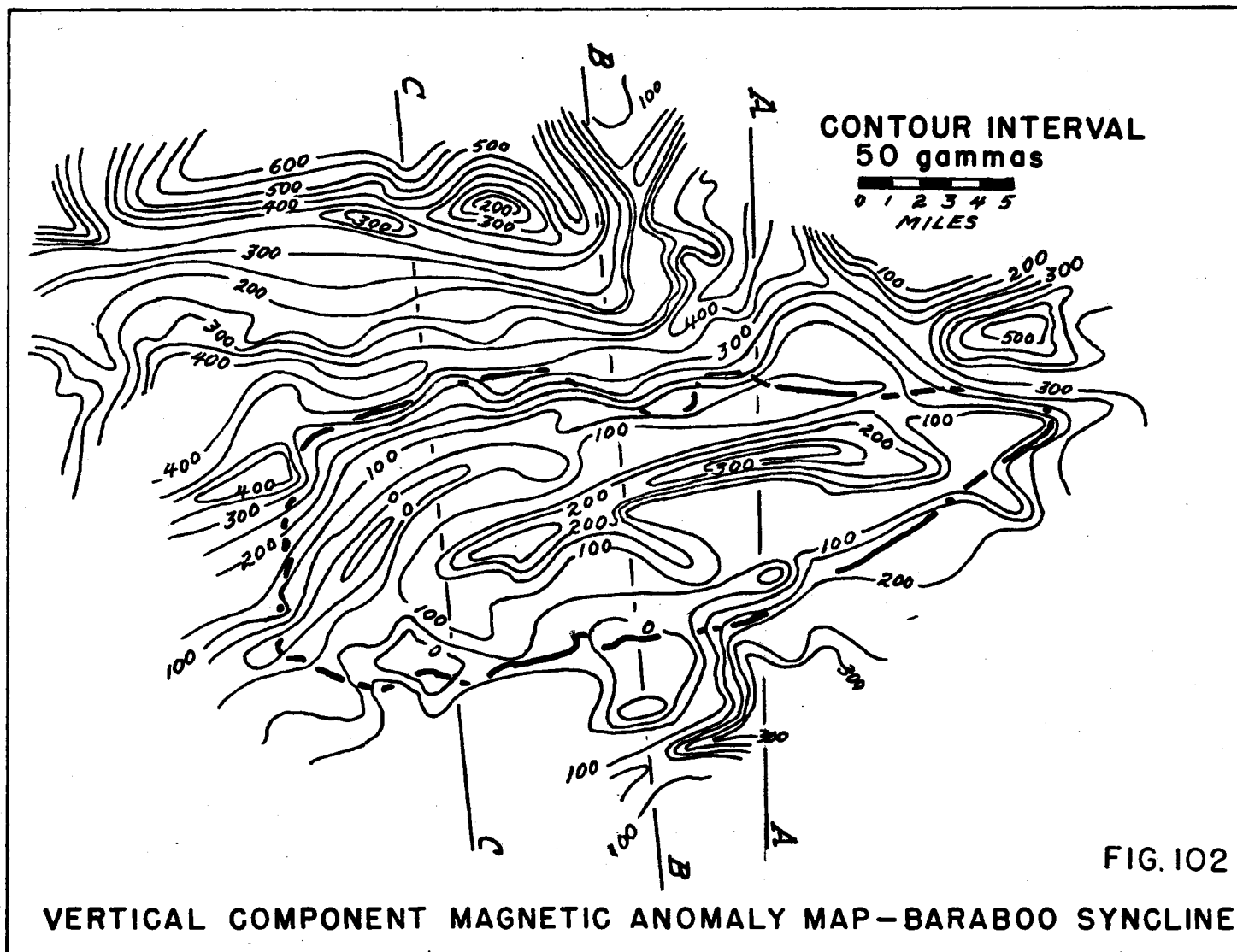
Similarly, there are different theories concerning the origin of basic rock occurrences. Under the granitization concept, these rocks constitute an expanding "front" from a granitic mass. Under the magmatic theory, such mineral assemblages would sink as early, high density differentiates. As the resulting mass distribution should be markedly different, a series of gravity studies are being made to see if these data can be used to ascertain which or where each process seems to apply in Wisconsin. Three areas are being studied: the Wausau area, where there is syenite and diorite; the Mellen area, where there is granite and gabbro; and the west shore of Lake Superior, where the thick basic rock sheet known as the Duluth lopolith appears to have differentiated in place giving rise to gabbro and granite.

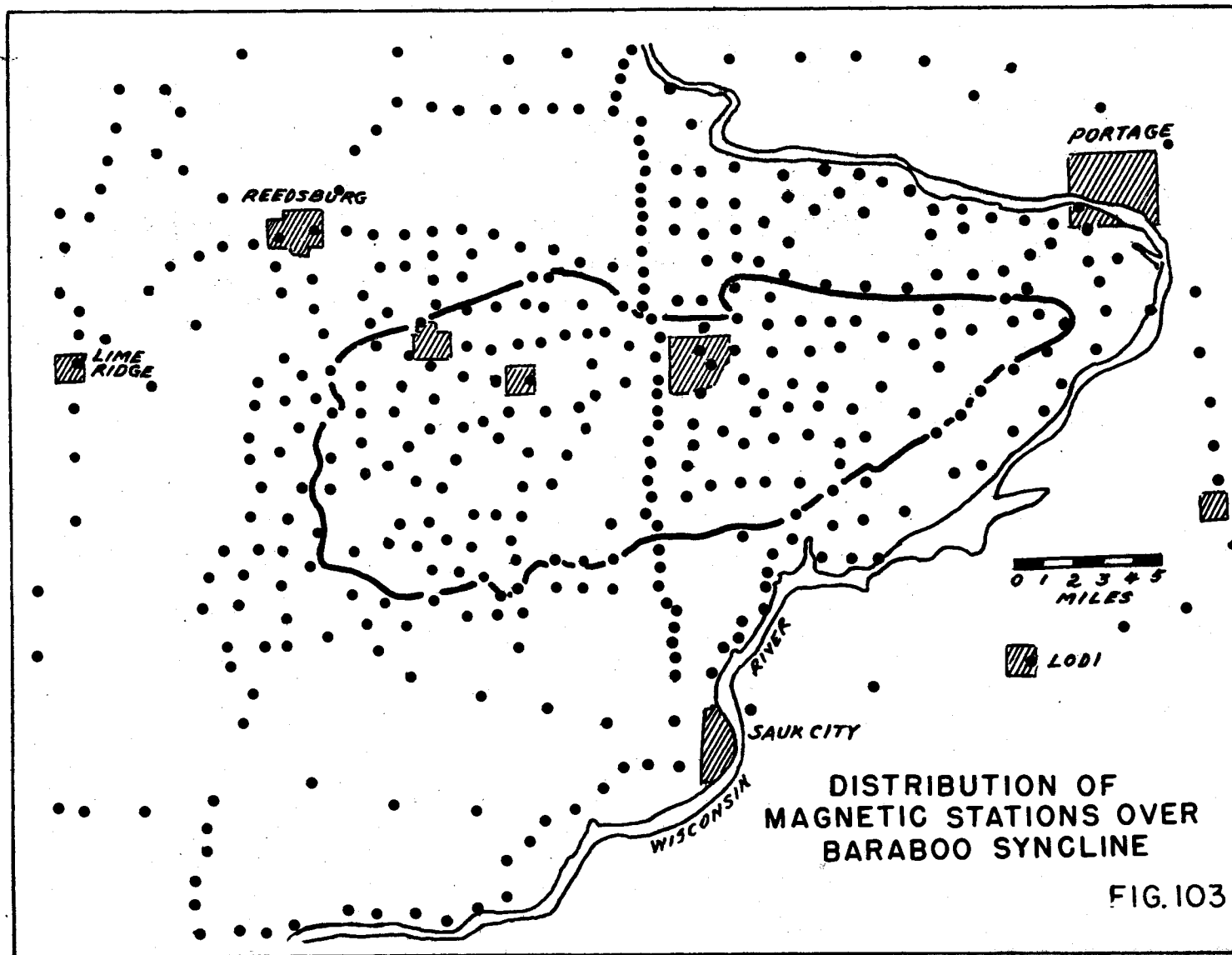
V-5 - Structural Studies

Two structural studies are being conducted. One involves the Lake Superior Syncline and the other, the Baraboo Syncline. Gravity, magnetic and seismic studies are being undertaken in connection with each area. An outstanding feature associated with the Lake Superior Syncline is the large gravity anomaly (90 mgals) observed in crossing it. This anomaly is related to Keweenaw basic volcanic flows which are enfolded in the sediments. See Fig. 101. On the basis of the large anomaly, it appears that this structure, with its associated lavas, extends southwest into central Kansas where it abruptly terminates.

Comment has already been made in connection with the study of the Baraboo Syncline on the magnetic anomalies associated with the iron bearing Freedom Formation, and the fact that a pronounced anomaly also occurs just off the north flank. Fig. 102 shows the anomaly pattern as developed from the station network of magnetic observations that has been established over the area. A similar network of gravity observations has been completed, and it is planned to supplement these measurements with seismic studies.







Part VI

Appendix

on

Geophysical Theory and Method of Reductions

VI-1 - Gravity Methods

VI-1a Gravity Theory

The fundamental expression for gravitational attraction is:

$$F = \frac{\gamma m_1 m_2}{r^2} . \quad \text{Eq. (1)}$$

in which F = force of attraction.

γ = the gravitational constant (6.67×10^{-8}).

m_1 and m_2 = two respective masses.

r = distance between mass m_1 and mass m_2 .

Newton's Second Law of Motion states:

$$F = ma , \quad \text{Eq. (2)}$$

in which m = mass.

a = acceleration.

If the two expressions are equated equal to each other and m_1 and m_2 are taken as unit masses, then:

$$a = \frac{\gamma m_2}{r^2} . \quad \text{Eq. (3)}$$

If m equals the mass of the earth, then the attractive force on a unit mass would equal the acceleration imparted to a falling body at the surface of the earth. If the earth is assumed to be approximated by a sphere,

$$\begin{aligned} a &= \gamma \frac{4/3 \pi R^3 \sigma}{R^2} . \\ &= \gamma 4/3 \pi R \sigma \end{aligned} \quad \text{Eq. (4)}$$

in which R - radius of the earth.

σ - the density of the earth.

However, as the earth is not a sphere but approaches an oblate ellipsoid of revolution, rotating about its minor axis, the value of gravitational acceleration increases from the equator towards the poles. This is due both to the decrease in radius in progressing toward the poles and to the decrease in the outward normal component of centrifugal acceleration due to rotation. The following expression evaluates both effects and gives the sea level value of gravity at any latitude.

$$G_0 = 978.049 (1 + 0.0052884 \sin^2 \phi - 0.0000059 \sin^2 2\phi) \quad \text{Eq. (5)}$$

in which G_0 = sea level gravity.

ϕ = latitude of point of observation.

This expression is based on a change in radius of the earth from 6,378,388 meters at the equator to 6,356,909 meters at the poles. The equatorial gravitational value (978.049) is an empirically determined value based on observed values of gravity at different places corrected to the equator on the basis of the above change in dimensions.

The actual value of gravitational acceleration at any place, however, will vary from that determined by Eq. 5 because of elevation, the density of the rocks present, and the thickness of the underlying crustal material. As the geologic factors can only be partially evaluated, the corrections that are applied to the sea level value of gravity, as determined by Eq. (5), usually allow for only the effects associated with a change in elevation; that is, the effect of the vertical gradient due to change in elevation and the effect of the included rock mass.

$$\begin{aligned} \text{Effect of change in elevation alone} &= -0.3086 \text{ mgals/meter} \\ &\quad \text{or} \\ &= -0.09406 \text{ mgals/foot,} \end{aligned} \quad \text{Eq. (6)}$$

where a mgal = 0.001 cm/sec².

$$\begin{aligned} \text{Effect of included rock mass} &= +0.04185 \sigma \text{ mgals/meter} \\ &\quad \text{or} \\ &= +0.01276 \sigma \text{ mgals/foot} \end{aligned} \quad \text{Eq. (7)}$$

where σ is the density of the rocks present.

If the area is hilly, an additional correction is required to allow for the effect of the mass of hills rising above the observation site, and the deficiency in mass associated with valleys below the site.

The method of determining the correction, while not difficult, is laborious as it requires that all of the surrounding terrain within a radius of about 15 miles be evaluated in terms of differences in elevation from that at the observation site for small areal compartments. The gravitational effect for each is computed and the sum of the effects in all compartments applied as a correction.

The sum of the above corrections applied to the sea level value of gravity constitutes the theoretical value of gravity. This usually differs from the observed value, and the difference between the two is the anomaly. It is the anomaly values which have to be interpreted as to their geological significance.

VI-1b Observed Gravity

Observed values of gravity are determined on the basis of the difference in instrumental readings between two points, one of which is used as a base. The instruments commonly used, gravimeters, are all subject to "drift"; that is, a change in reading with time due to non-elastic stretching of the spring system. As the rate of drift is not uniform and varies with temperature and pressure, it is necessary to make frequent repeat observations at a base station. By using such repeat observations for control, all the intervening readings can be corrected for this effect. These corrected readings are then made relative to some base station value. In order to get the relative difference between sites converted from gravimeter scale units to gravity units (mgals), these differences must be multiplied by the scale constant of the instrument.

If the absolute gravity value at the base station is known, then all the stations can be put on an absolute basis. In Wisconsin, the primary gravity base used for absolute values is in the basement of Science Hall on the campus of the University of Wisconsin in Madison, where the absolute gravity value, determined by 12 sets of observations between Madison and the national gravity base in Washington, is $980.3686 \text{ cm/sec}^2$.

VI-1c Example of Gravity Reductions

An example of a complete set of gravity reductions is as follows:

Observed Data and Drift Correction Sheet

Station	Time	Instrument Reading	Drift Correction	Corrected Reading
1	10:00	2416	—	2416
2	10:15	2118	-1	2117
3	10:30	2041	-2	2039
1	11:00	2420	-4	2416

Reduction Sheet

Station	Corrected Reading	Difference from Base 1	Difference x Scale Constant (K = 1 mgal)	Absolute Gravity (Observed) (cm/sec. ²)
1	2416	—	—	980.3688
2	2117	-299	-29.9	980.3389
3	2039	-377	-37.7	980.3311

Theoretical Gravity

Sta.	Latitude	Elevation	Sea Level Gravity	Elevation Correction	Mass Correction	Terrain Correction
2	42°10.0'	100 ft.	980.3741 ⁽¹⁾	9.4 mgal ⁽²⁾	3.4 mgal ⁽³⁾	0.2 mgal ⁽⁴⁾

1. Sea Level Gravity from tables based on Eq. (5).
2. Elevation correction = $.09406 \times 100 = 9.4$ mgals.
3. Mass Correction with (σ) = $2.67 = .01276 \times 2.67 \times 100 = 3.4$ mgals.
4. From tables and topographic map = 0.2 mgal.

Theoretical gravity = Sea Level Gravity	980.3741
- Elevation Correction	- .0094
+ Mass Correction	+ .0034
- Terrain Correction	- .0002
	<u>980.3679</u>

Gravity Anomaly = Observed Gravity - Theoretical Gravity	
For Station 2 = 980.3389 - 980.3679	
Anomaly = - 0.290 = - 29 mgals	

VI-1d Residual Anomaly Values

The bulk of most anomaly values is related to mass distributions lying several miles beneath the surface and only a small portion, which is related to near surface geologic features, is important from an exploration standpoint; it is therefore necessary to separate the two. Several methods are used in making the separation, and they all entail considerable labor. The simplest form of residual separation is that based on profiles as illustrated in Fig. 13. Other methods involve the use of a grid system for averaging the regional effect and subtracting it, or a map of the regional trends is drawn by inspection and subtracted from the observed anomaly map. There are also second derivative maps that can be prepared. The success of the method used in each case will depend mostly on how well the areal extent of the residual is gauged in subtracting the regional.

VI-1e Gravity Interpretation

The interpretation of the residual anomalies, once they have been separated, usually requires the computation of the gravitational effect of one or more geologic models that appear reasonable in the light of the known geology and the sign, magnitude and pattern of the contoured residual gravity anomaly. As there are always two unknowns, the depth and density contrast involved, it is not possible to get a completely unambiguous interpretation. Even if the calculated effect exactly matches that of the residual anomaly pattern, it is nearly always possible to find another set of equally probable conditions that would also match the anomaly; for this reason, gravity methods are not recommended for depth studies. Their principle and most successful application is in outlining the locations of buried mass abnormalities related either to geologic structure or to changes in petrology.

VI-2 - Magnetism

VI-2a General Statement

Magnetism is visualized as being caused by groups of elemental magnets distributed throughout a body and aligned in chains with their north and south poles alternating so as to attract each other. If similar poles were adjacent, there would be a repulsion rather than attraction. The fundamental expression for the force between magnetic poles is:

$$F = \pm \frac{1}{\mu} \cdot \frac{P_1 P_2}{r^2}, \quad \text{Eq. (8)}$$

in which P_1 and P_2 = the strength of the poles.
 r = to the distance between the poles.
 μ = permeability = 1 for air.
 \pm indicates the force may be an attraction or repulsion.

Permeability is a measure of the lines of magnetic force that can pass through a unit cross-sectional area. Materials are described as ferromagnetic when $\mu \gg 1$, paramagnetic when $\mu > 1$, and diamagnetic when $\mu < 1$. Examples of ferromagnetic materials are nickel, cobalt, and iron. Examples of diamagnetic materials are sulphur, bismuth, and quartz.

Other magnetic quantities that must be considered are as follows:

- (1) Magnetic field strength (H): the magnetic field is represented by "lines of force", and the field strength is the number of lines per square centimeter in a section perpendicular to the direction of flow. Lines of force are directed outward from one pole and inward to the other pole. These can best be seen by sprinkling iron filings on a piece of paper held over a magnet.
- (2) Susceptibility (K): a measure of the ease with which a body becomes magnetized by induction; that is, the ease with which the internal elemental magnets are oriented into chains.
- (3) Polarization (I): a measure of the number and the degree of orientation of the elementary dipole magnets in a body. Polarization is really a measure of the intensity of magnetization, and it plays the same role in magnetism as does density in gravitational studies.

$$I = KH, \quad \text{Eq. (9)}$$

where H is the field strength of the earth's magnetic field = 0.6 oersteds. K, the susceptibility, is usually governed by the percentage of the mineral magnetite present and can be expressed as:

$$K = K_m P, \quad \text{Eq. (10)}$$

Where K_m = the susceptibility of powdered magnetite
 = $300,000 \times 10^{-6}$ cgs. units.
 P = percentage by volume of magnetite in a rock.

The common magnetic unit used in exploration studies is the gamma.

$$1 \gamma = 10^{-5} \text{ oersted (gauss)}$$

1 oersted = field strength when a force of 1 dyne is exerted on a unit pole. A unit pole is defined as when two equal poles exert a force of 1 dyne when 1 centimeter apart.

VI-2b Magnetic Quantities Measured

The earth has a magnetic field similar to that which would be produced by a small dipole magnet at its center with the negative (S) magnetic pole oriented toward the North geographic pole. A compass aligns itself in the resultant magnetic field so that its positive (N) pole points toward the area where the lines of force converge over the negative (S) pole. A dip needle measures the inclination of the earth's field and its position will vary from horizontal at the equator to vertical over the pole area. Other instruments measure the change in total intensity or its vertical or horizontal components. Fundamental relations are as follows:

$$F = \frac{H}{\cos i} \quad , \quad \text{Eq. (11)}$$

in which F = total intensity.

H = horizontal component of total intensity.

i = angle of inclination (dip) from the horizontal.

$$F = H + V \quad \text{Eq. (12)}$$

in which V = vertical component of total intensity.

$$\frac{V}{H} = \tan i \quad \text{Eq. (13)}$$

In the United States, the range in the above values are approximately:

V = 0.4 to 0.6 oersted; 40,000 to 60,000 gammas.

H = 0.14 to 0.28 oersted; 14,000 to 28,000 gammas.

i = 55° to 75° .

The other magnetic quantity that can be used in exploration work is the declination (d), the departure of magnetic North from the true North. The variation in " d " within the United States is from 24° E in the northwest states to 20° W in the northeast states.

However, these quantities are not static. There is a long period secular (change) in magnetic field strength and direction, and superimposed upon this is a short period diurnal cyclic change and also occasional magnetic storms. The latter generally are associated with sun spot activity. There is no true theoretical magnetic intensity value at anyone place, only a constantly changing value that is determined empirically. Every ten years it is necessary to prepare new charts and tables to describe the earth's magnetic field. These charts evaluate the probable secular change to be expected, but not the diurnal changes; as a result, the theoretical intensity, as determined in common practice, does not include the diurnal change. The effect of the diurnal change is applied to the observed magnetic values in much the same way that the drift correction is applied in establishing observed gravity values. In contrast to drift readings which must be established for the particular instrument in use, the diurnal correction in magnetics can be taken with an auxiliary instrument maintained at any base station. The anomaly, as in gravity, is the difference between the corrected observed magnetic readings and theoretical values as determined from the charts referred to above.

VI-2c Example of Magnetic Reduction

An example of reductions for measurements made with a vertical component variometer is given below. This instrument, described in Part I, must be oriented so that the horizontal component of the earth's field does not influence the readings. This is done by aligning the instrument so that the axis of rotation of the magnetic element lies in the magnetic meridian. Two readings are taken; one with the north pole of the instrument pointing East and one with it pointing West. If the instrument is not compensated for changes in temperature, an additional correction has to be applied for the effect of such changes.

Observed Data						Diurnal	Corrected
Sta.	Time	N in W	N in E	Average	Temperature	Correction	Reading
1	10:00	52.4	52.6	52.5	20.1	---	52.5
2	10:15	48.7	48.5	48.6	20.2	-0.1	48.5
3	10:30	54.3	54.3	54.3	20.2	-0.2	54.1
1	11:00	52.9	52.7	52.8	20.3	-0.3	52.5

Anomaly Reduction

Sta.	Corrected Reading	Change from Base	Gammas Change		Theoretical Change from Base	Anomaly
			Cal. x	Scale K		
			(K = 108)			
1	52.5	---	---	---	---	---
2	48.5	-4.0	-40	8	+108	-308

VI-2d Analysis of Anomaly Values

As with gravity it is frequently necessary to separate the effects of deep seated geologic controls from those related to near surface geology. Analysis of the anomaly values is similar to that used in interpreting gravity anomalies, namely the magnetic effects of different geologic models are computed and compared with the observed anomaly pattern. However, in contrast to gravity studies, where there are only two principal unknown factors, there are five such unknown factors in magnetics. The polarization contrast and depth from which the anomaly originates are analogous to the density contrast and depth factor in gravity. In addition, the direction of the earth's field and the orientation and geometry of the disturbing element also have pronounced effects upon the anomaly. This is because most magnetic polarization is not an inherent feature of the body, but is induced by the earth's field. If the body is of a lath-like shape, with its long axis oriented parallel to the direction of the earth's field, two magnetic poles will be induced near the extreme ends. As one will exert an attraction and the other a repulsion on the magnetic element of the instrument, the measurement always represents the net effect of the two. The near pole will always exert the dominant effect and, in the above case, a narrow sharp magnetic "high" would be produced because the distance to the lower remote pole will be much greater than that to the upper pole. If the same body were oriented with its long axis perpendicular to the earth's field, the induced poles would lie along the two sides and be very close together. Here the effect of the lower pole would cancel most of that produced by the upper pole and a weak but broad magnetic high would result. An additional effect related to the inclination of the earth's field, where vertical component or horizontal component measurements are being used, is that of magnetic latitude. Near the equator, the inclination is slight, and as a result, the vertical component is very small. Poles will be induced on the north-south faces of bodies giving pairs of weak anomaly areas having opposite sign. At high latitudes where the inclination is great, the vertical component of the earth's field will be dominant, and poles will be induced on the upper and lower faces of bodies with single anomaly areas whose magnitude will be governed by the pole separation.

As all these factors must be evaluated in making an interpretation, it is seen that magnetic studies present a much more complex problem than is encountered in gravity. The principal use of magnetics, therefore, has been limited to outlining areas having rocks or minerals of high magnetic susceptibility.

VI-3 - Electrical Resistivity Measurements

VI-3a General Statement

Resistivity or specific resistance (ρ) is defined for a homogenous material by the expression:

$$R = \rho \frac{L}{A} \quad \text{Eq. (14)}$$

in which R = the observed resistance in ohms.
 L = the length of the sample tested.
 A = the cross-sectional area of the sample.

The resistivity unit is the ohm centimeter.

When an electric current enters the ground, which is assumed to be homogenous, the potential at any distance from the current source is:

$$V = \frac{\rho I}{2\pi r} \quad \text{Eq. (15)}$$

in which V = potential.
 ρ = resistivity of material.
 I = current.
 r = distance from current source.

Eq. 14 assumes that this potential occurs everywhere on the surface of a hemispherical bowl of radius " r ". That is, the potential at a depth equal to " r " is the same as that observed at " r " distance on the surface from the current source.

In carrying out electrical resistivity measurements, four electrodes are commonly placed in a line with an equal spacing (a) between them. This is called the Wenner electrode configuration. A measured current is applied between the two end electrodes and differences in potential are recorded between the two central electrodes, as was illustrated in Fig. 5.

With this arrangement, the potential at electrode (P_1) due to the current entering the ground at C_1 is $\rho I/2\pi a$. There is also a potential due to the current leaving the ground at C_2 , $-\rho I/2\pi 2a$. The net potential at P_1 is :

$$\begin{aligned} V_1 &= \frac{\rho I}{2\pi a} - \frac{\rho I}{2\pi 2a} \\ &= \frac{\rho I}{2\pi} \left[\frac{1}{a} - \frac{1}{2a} \right] \\ &= \frac{\rho I}{2\pi} \left[\frac{1}{2a} \right] \end{aligned} \quad \text{Eq. (16)}$$

In the same way it is found that the net potential (V_2) at the other potential electrode, P_2 , is :

$$\begin{aligned} V_2 &= \frac{\rho I}{2\pi} \left[-\frac{1}{a} + \frac{1}{2a} \right] \\ &= -\frac{\rho I}{2\pi} \left[\frac{1}{2a} \right] \end{aligned} \quad \text{Eq. (17)}$$

The difference in potential measured between P_1 and P_2 is:

$$\begin{aligned} V &= V_1 - V_2 \\ V &= \frac{\rho I}{2\pi a} \end{aligned} \quad \text{Eq. (18)}$$

The resistivity, as determined using the Wenner configuration, is therefore:

$$\rho = 2\pi a \frac{V}{I} \quad \text{Eq. (19)}$$

in which V = potential difference in volts.
 I = current applied in amperes.
 a = distance between electrodes.

As the distance between electrodes is increased, the effective depth of penetration of the current into the ground also increases. However, as the rock mantle is not homogenous but is stratified in layers with different specific resistances, there will be changes observed in the resistivity values with change in spacing. The value with each spacing represents a composite derived from several different rock layers. Because of this, only the relative change in values are diagnostic, and a plot of measured resistivity values as a function of electrode spacing is used to detect changes in geology with depth.

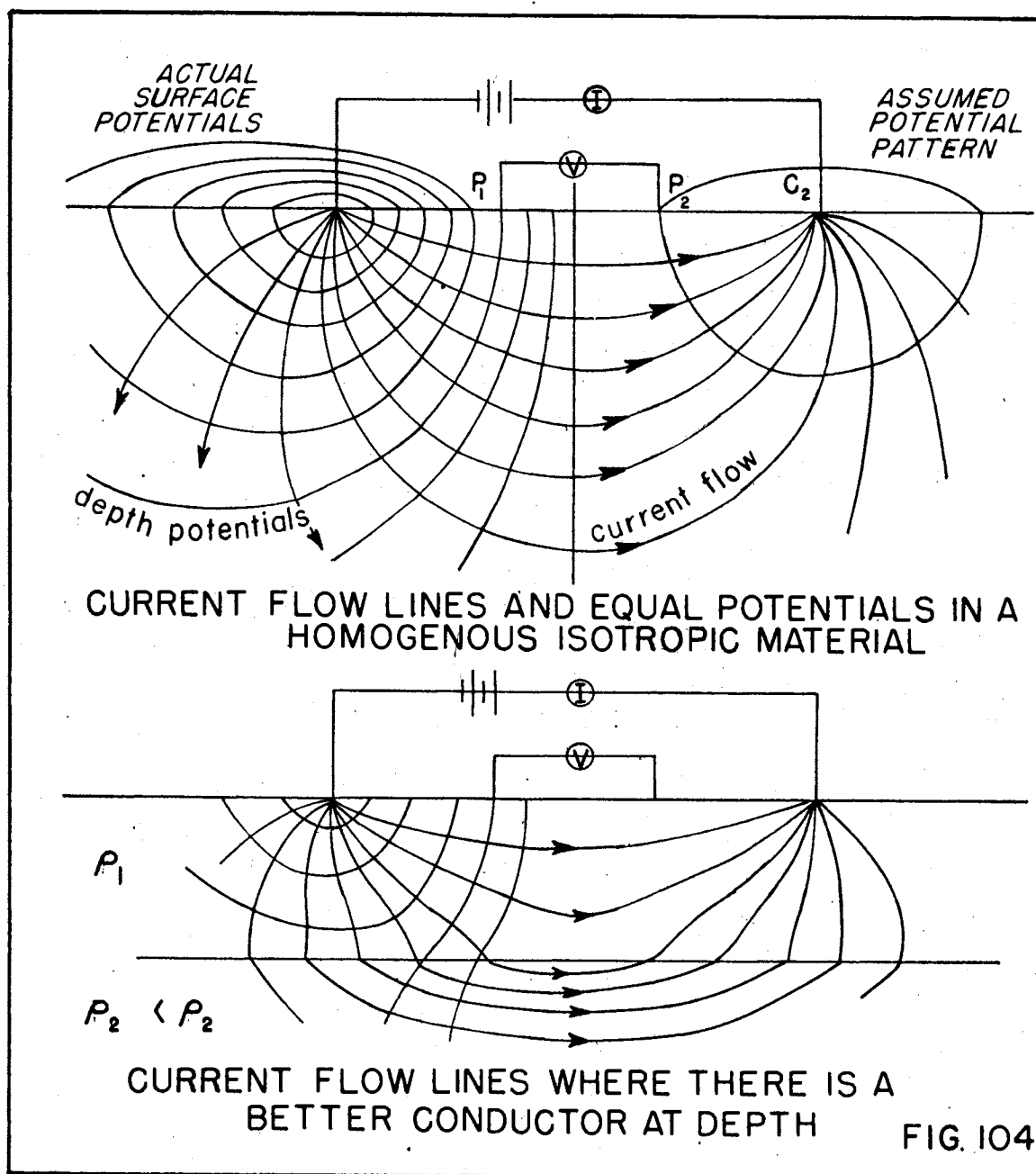
The interpretation of resistivity data in terms of actual depths at which changes in geology occur is a controversial subject, and without going into the arguments involved, it will suffice to say that no theoretical approach or empirical interpretation method has proved to be universally applicable. The rule of thumb assumption that the depth of penetration equals the electrode spacing is based on the idea that the equipotential lines describe a hemisphere around the current electrode. From Fig. 104, it is seen that this does not conform to the equipotential pattern actually obtained. The effective depth of penetration is always less than the electrode spacing, although how much less is a variable quantity depending upon many factors that cannot always be evaluated. The number of layers present, their thickness, and the relative change in resistivity of each combine to make the depth of penetration vary in different areas. Further, the observed changes can also be caused by horizontal changes in resistivity as the electrode spacing is increased. For these various reasons, it has been found that resistivity data, taken in connection with depth investigations, can frequently only be interpreted reliably where local well data can be used to establish an empirical calibration standard, but even this method cannot be used successfully where there are marked horizontal changes in the geologic column. Seismic data have shown this last factor to be a very real hazard in central and northern Wisconsin where the total section of sedimentary cover is no greater than the relief on the underlying crystalline complex; the same problem occurs in southern Wisconsin where the buried pre-glacial surface is composed of limestone which also has a high resistivity.

Other factors that influence the results, such as difference in moisture content of the soil, depth of penetration of the electrodes, and changes in chemistry, can be eliminated through the use of alternating current or non-polarizing electrodes. The effect of buried conductors, such as pipe lines, while not subject to correction, can usually be recognized as spurious.

VI-3b Reduction of Resistivity Data

An example illustrating the reduction of data taken for a resistivity determination is as follows:

Current (I)			Potential Difference (V)		
between C ₁ & C ₂			P ₁ and P ₂		
Forward	Reverse	Average	Forward	Reverse	Average
Current	Current		Current	Current	
27	27	27	16.6	29.9	23.3



Electrode
Spacing (a)
(feet)

Resistivity
 $V/1.2\pi(30.28a)$
(ohm cms.)

70

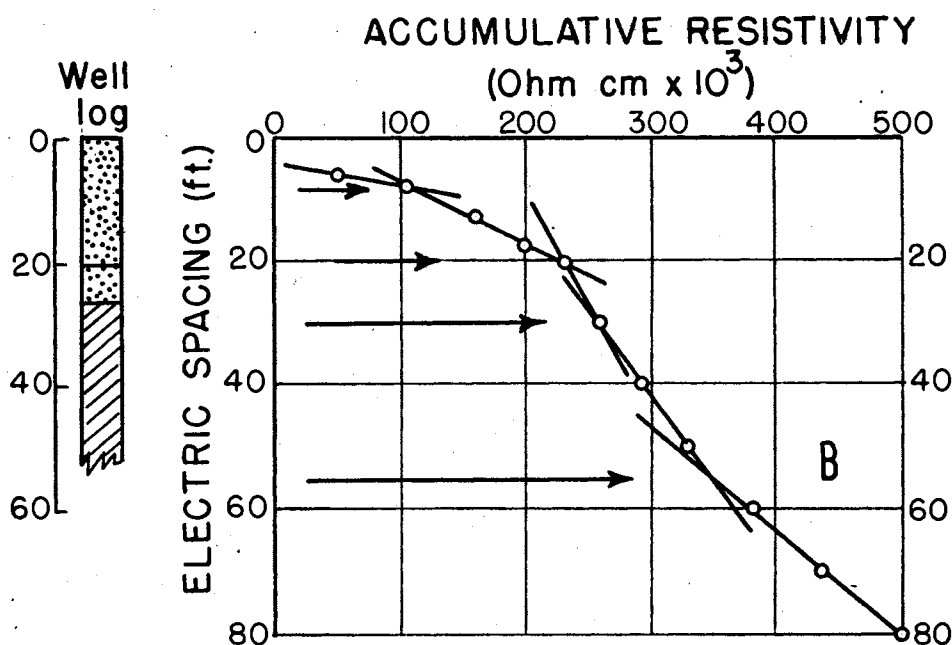
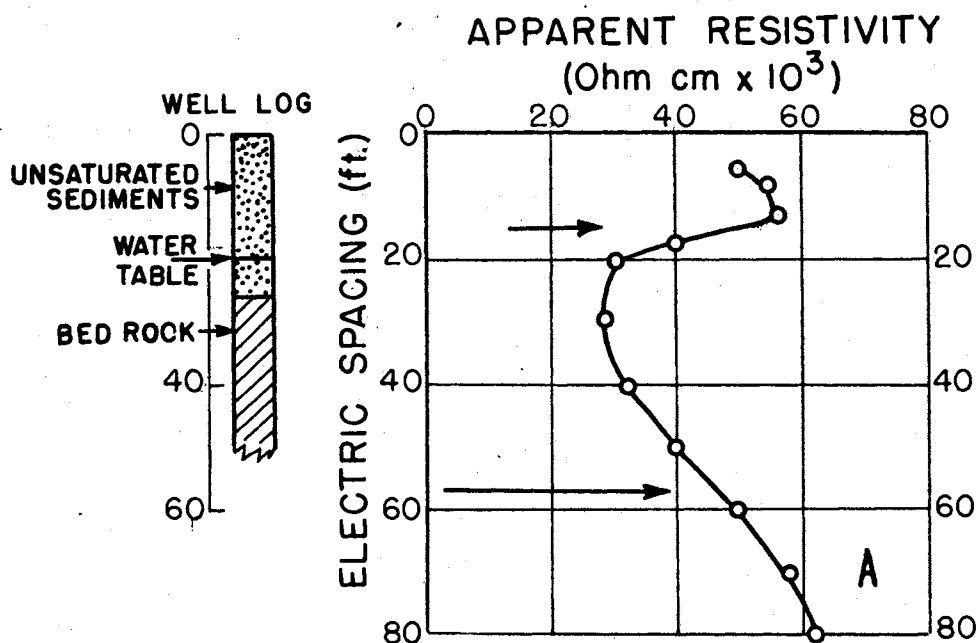
21450

Fig. 105 shows a typical graph of observed resistivity values plotted as a function of electrode spacing, and also an alternative method of plotting whereby the cumulative resistivity values are plotted as a function of the electrode spacing. The latter method, referred to as the Moore or cumulative method, is one largely used in making empirical interpretations. The electrode spacing at which there are changes in slope of the straight line segments drawn through the points are interpreted as being depths at which there are subsurface changes in geology. In interpreting the observed resistivity curve, inflection points and points of marked change in rate of line curvature are interpreted as being related to subsurface changes in geology.

Although several theoretical methods of interpreting electrical resistivity measurements have been devised that are applicable for simple geologic situations involving two to three layers, it is seldom that situations as simple as these are encountered, and as a result, the methods are not generally applicable. As was shown by the tests conducted at Antigo (Part II), the Moore (cumulative) empirical method of interpretation gave results that agreed on the whole better with the seismic results than those based on any other method of interpretation.

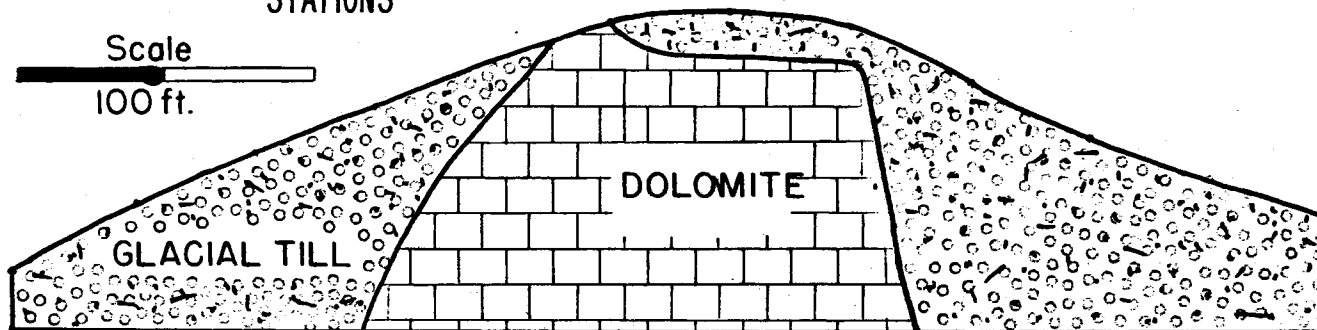
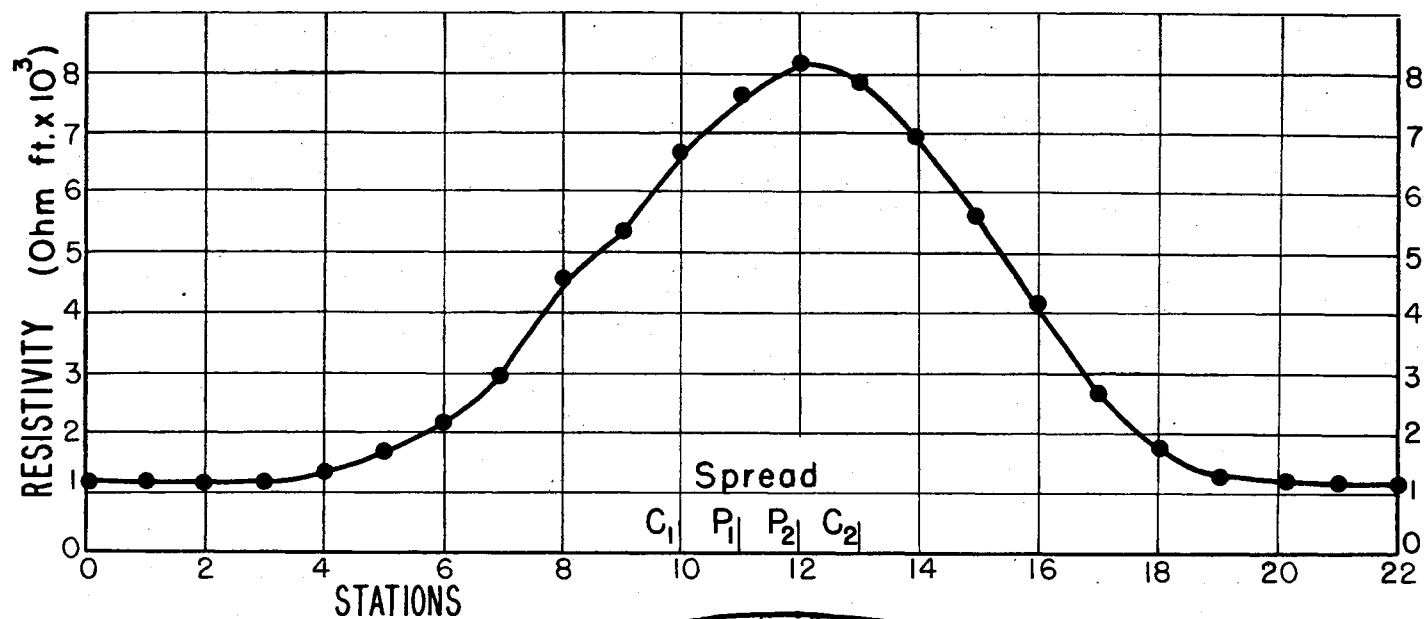
VI-3c Traverse (Constant Depth) Resistivity Measurements

In using electrical resistivity measurements to investigate horizontal variations in the subsurface geology, the Wenner configuration of electrodes can be employed so as to probe to a constant depth along a traverse; that is, the entire spread of electrodes is advanced along the traverse maintaining a constant electrode spacing. The interval of advance is usually that of the distance between a single pair of electrodes. Observations and reductions are carried out as in making resistivity studies of changes in geology with depth, but the results are plotted as a profile. Where changes in resistivity are encountered that are of wide extent as compared to the total length of the spread of electrodes, they can be regarded as valid. Fig. 106, for example, shows the change in resistivity observed in crossing a dolomite ridge buried beneath glacial till. However, where the changes in resistivity have a width less than, or approximately the same as, the distance between a pair of electrodes, the resistivity values cannot be regarded as showing directly the changes in subsurface resistivity. The reason for this is illustrated in Fig. 107.



**2 EMPIRICAL METHODS OF INTERPRETING
RESISTIVITY DATA AS COMPARED TO
WELL LOG AT SITE**

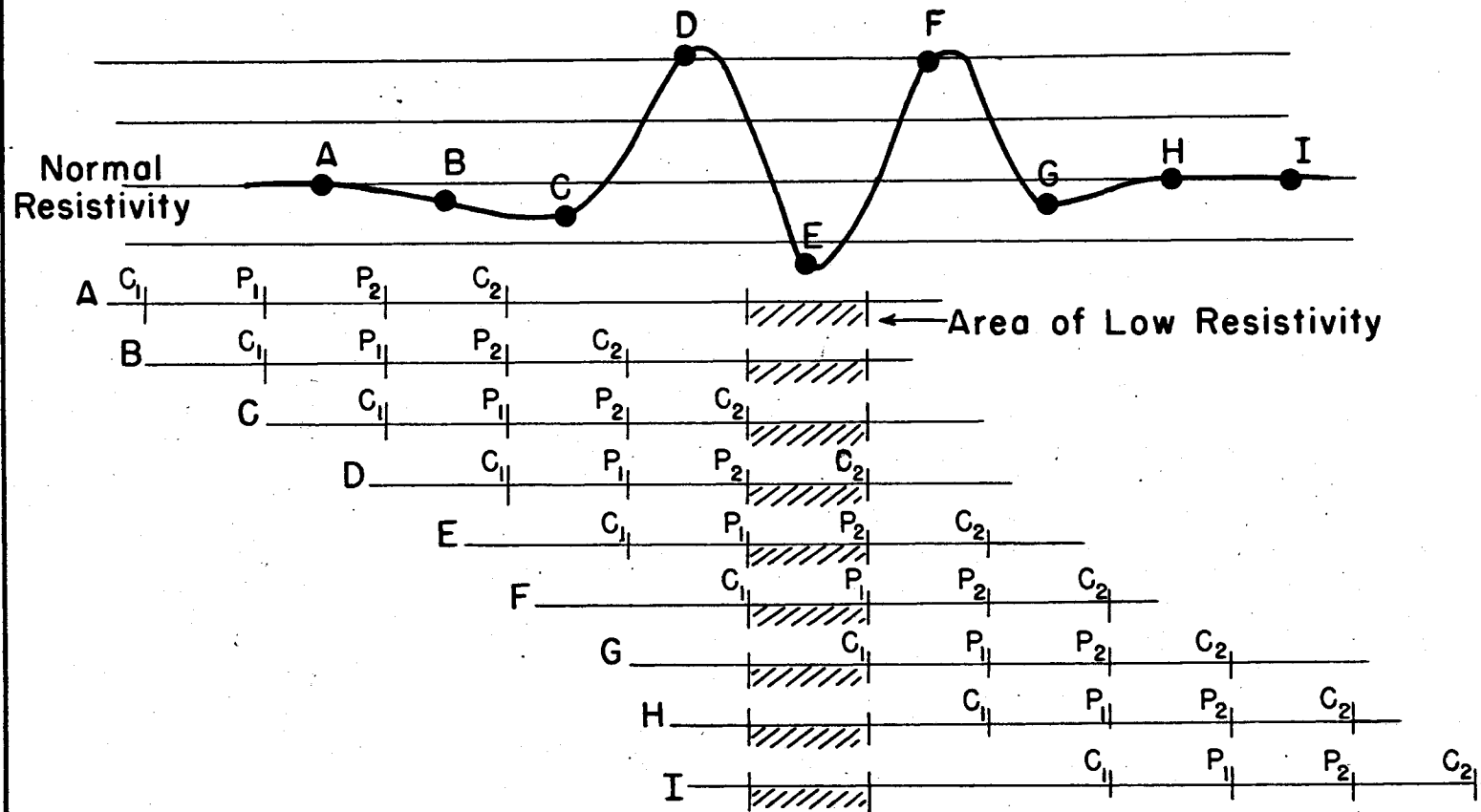
FIG. 105



CONSTANT DEPTH RESISTIVITY TRAVERSE ACROSS
DOLOMITE RIDGE COVERED BY GLACIAL TILL

FIG. 106

AFTER KURTENACKER WIS. HIGHWAY DEPT.



EFFECT OF LOCAL ANOMALOUS RESISTIVITY AREA
WHEN RUNNING CONSTANT DEPTH RESISTIVITY TRAVERSE

FIG. 107

As the local zone of lower resistivity (higher conductivity) is approached, the distortion of the equipotential lines away from the conductor, due to convergence of the current lines towards it, decreases the potential difference between P_1 and P_2 . Therefore, for positions B and C, there is a decrease in apparent resistivity. At position D there is a small potential drop between C_2 and P_2 because the conductor lies between these electrodes, but there is a large potential change between C_1 and P_1 . The resulting large potential difference between P_1 and P_2 gives an abnormally high resistivity value. At position E, the conductor lies between P_1 and P_2 , and there is, as a result, a low apparent resistivity value. For the other positions going away from the conductor, the situations are analogous to those observed in approaching the conductor. If the local anomalous area had involved a poorer conductor instead of a better conductor, the distortion pattern would have been reversed.

VI-3d Remarks on the Interpretation of Traverse Measurements

Sand and gravel layers in till generally are found to be characterized by high resistivity values. High values also are observed where till overlies a bedrock ridge of limestone or granite, but in the cases where shale is involved, the opposite relation may be observed.

To understand these relations, it must be remembered that, in addition to the electrical properties of the rocks themselves, the chemistry of the water filling the pore spaces plays an important and frequently dominant role in determining the resistivity value. Water derived by infiltration from the surface will have its chemistry determined by the mineral composition of the rocks which are leached as the water percolates downward through them. Clays, in addition to percolating water, also have chemically combined water, and the chemistry of the water present affects both their permeability and resistivity. A calcium base clay is flocculent and relatively pervious, whereas a sodium base clay is deflocculated and impervious. As glacial till usually contains a considerable amount of clay, a contrast in resistivity between such material and sand or gravel is to be expected. The clay material has a better electrical conductivity and a lower resistivity than the sand which is made up principally of quartz grains which have a high resistivity.

Water in sediments laid down under marine conditions may be saline or fresh depending upon the degree to which fresh water from surface sources has been able to flush out the original water of deposition. The reverse process may also take place due to contamination from nearby salt layers. Another factor influencing the resistivity of sediments is the degree that crystallization or cementation has taken place.

VI-4 - Seismic Methods

VI-4a General Statement

The seismic methods depend upon determining the velocity of propagation of sound waves generated by an explosion through earth materials and analyzing the refraction and reflection phenomena at the interfaces (boundaries) between rock layers which are characterized by different acoustic velocities.

The velocity of sound is dependent upon the type of impulse variously described as compressional waves, transverse waves, Rayleigh waves, and Love waves, as well as the physical characteristics of the material. These physical characteristics are described in terms of the following elastic constants:

- (1) Bulk Modulus (K): a measure of the ratio of stress (force per unit area) applied to the induced strain (volume of distortion produced).

$$\begin{aligned} \text{Stress} &= \frac{F}{A} \cdot & \text{Strain} &= \frac{\Delta V}{V} \cdot \\ K &= \frac{F/A}{\Delta V/V} = \frac{FV}{A \Delta V} \cdot \end{aligned} \quad \text{Eq. (20)}$$

- (2) Young's Modulus (E): is a measure of the ratio of the stress applied to the strain induced where simple compression or tension are involved. In tension, the strain is an elongation distortion, and in compression, it is a shortening distortion. For both situations, strain = $\frac{\Delta L}{L}$.

$$E = \frac{F/A}{\Delta L/L} = \frac{FL}{A \Delta L} \cdot \quad \text{Eq. (21)}$$

- (3) Rigidity or Shear Modulus (n): a measure of the ratio of stress to strain for simple shear. A shearing stress is exerted as an opposing couple and the displacement involves no change in volume. The displacement ΔL , therefore, is one involving only a change in shape such as the distortion of a rectangle into a rhombus.

$$n = \frac{F/A}{\Delta L/L} = \frac{FL}{A \Delta L} \cdot \quad \text{Eq. (22)}$$

- (4) Poisson's Ratio (σ): a measure of a geometric change in shape. For a body under compression, as a cylinder, there will be a shortening ΔL and an increase in diameter ΔD .

The ratio of the distortional change in diameter to that in length is Poisson's ratio.

$$\sigma = \frac{\Delta D/D}{\Delta L/L} . \quad \text{Eq. (23)}$$

- (5) Lamé constants (λ and μ): a pair of mathematical constants which relate the other elastic constants for a material to each other.

$$\lambda = \frac{6 E}{(1 + \sigma)(1 - 2\sigma)} . \quad \text{Eq. (24)}$$

$$\mu = \frac{E}{2(1 + \sigma)} \quad \text{Eq. (25)}$$

Of the sound waves transmitted through the ground, only the compressional waves need be considered for purposes of seismic investigations. These waves progress as an alternate compression and rarefaction, and are the first to be recorded, as they have the highest velocity of all the seismic waves. For this reason, there is little ambiguity in identifying their arrival. The expression for their velocity is:

$$v = \sqrt{\frac{K + 4/3 \mu}{\rho}} = \sqrt{\frac{\lambda + 2\mu}{\rho}} = \sqrt{\frac{E}{\rho} \left[1 + \frac{2\sigma^2}{1 - \sigma - 2\sigma^2} \right]} \quad \text{Eq. (26)}$$

where ρ is the density of the material.

When a velocity discontinuity is encountered at depth, the seismic waves have part of their energy reflected back towards the surface from the surface of discontinuity, and part refracted across the boundary into the underlying layer.

VI-4b Fundamentals of Refraction Method

It is found, as with light, that the degree of refraction (change in direction of propagation) of sound waves depends upon the difference in velocity of transmission on opposite sides of an acoustic boundary, and follows the relations set forth in Snell's Law. See Eq. (27).

$$\frac{\sin i}{\sin r} = \frac{V_1}{V_2} . \quad \text{Eq. (27)}$$

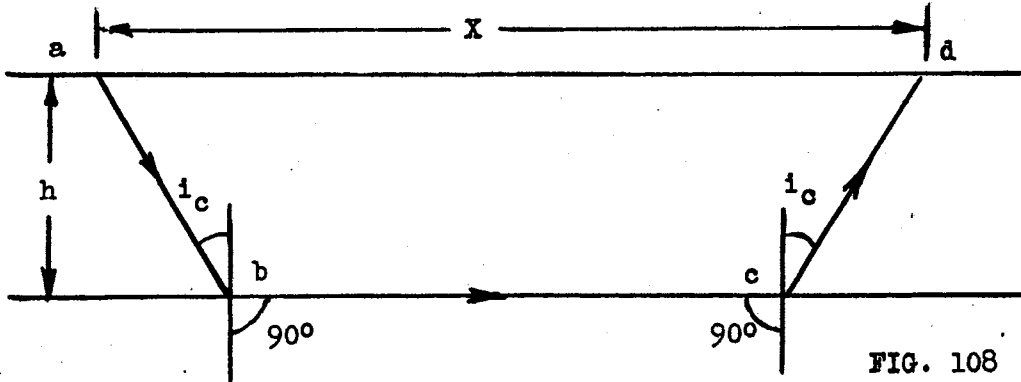
in which i = angle of incidence.
 r = angle of refraction.
 V_1 = velocity in incidence layer.
 V_2 = velocity in refracted layer.

When the angle of refraction is 90° and $\sin r = 1$, " i " is termed the critical angle of incidence.

$$\sin i = \frac{V_1}{V_2} .$$

At the critical angle, the refracted wave does not penetrate into the underlying layer but travels along the interface with the velocity in the underlying layer. As the wave advances along the boundary, energy will also be refracted back to the surface at the same angle as the critical incident angle. This phenomenon is the basis of the refraction method and its successful application depends upon there always being an increase in velocity with depth.

The refracted path for a sound wave generated at point "a" and received at point "d" is shown in Fig. 108.



From this figure, it is seen that the refracted travel path a,b,c,d, can be described as:

$$\text{Path abcd} = 2 \frac{h}{\cos i} + x - 2(h \tan i) , \quad \text{Eq. (28)}$$

in which i = critical angle.
 h = depth to the second layer.

The travel time along this path is:

$$T = \frac{2h}{\cos i V_1} + \frac{(x - 2h \tan i)}{V_2} , \quad \text{Eq. (29)}$$

which can also be expressed as follows:

$$T = \frac{2h}{\cos i V_1} + \frac{x}{V_2} - \frac{2h \sin i}{V_2 \cos i} .$$

From Snell's Law, $\sin i = \frac{V_1}{V_2}$.

$$T = \frac{x}{V_2} + \frac{2h}{\cos i V_1} - \frac{2h \sin i}{\frac{V_1}{\sin i} \cos i}$$

$$T = \frac{x}{V_2} + \frac{2h}{\cos i V_1} (1 - \sin^2 i)$$

$$T = \frac{x}{V_2} + \frac{2h}{\cos i V_1} \cos^2 i$$

$$T = \frac{x}{V_2} + \frac{2h \cos i}{V_1} \quad \text{Eq. (30)}$$

The travel time equation (Eq. 30) can be expressed entirely in terms of velocity values through the relation:

$$\sin i_c = \frac{V_1}{V_2} \quad .$$

then $\cos i_c = \sqrt{1 - \sin^2 i} = \sqrt{1 - \frac{V_1^2}{V_2^2}} = \frac{1}{V_2} \sqrt{V_2^2 - V_1^2}$

$$T = \frac{x}{V_2} + \frac{2h \sqrt{V_2^2 - V_1^2}}{V_1 V_2} \quad \text{Eq. (31)}$$

To determine the depth of the second layer, it is only necessary to know the velocity values V_1 and V_2 , and the travel time. These can be obtained from a graph of the observed travel time of the compressional waves in going from the point of origin to each of the detectors.

For a two layer situation such as outlined above, the graph would appear as shown in Fig. 109. The first line segment (A to B) represents travel via the direct path from the point of origin S to detectors 1, 2 and 3, and the slope of this line is $1/V_1$. The second line segment (B to C) represents travel via the deeper but quicker path. The slope of this line is $1/V_2$. The distance (X_c) from the shot point to which the break in the travel time plot occurs at B is known as the critical distance, the distance beyond which the quickest route from the shot point to the surface detectors is via the longer path.

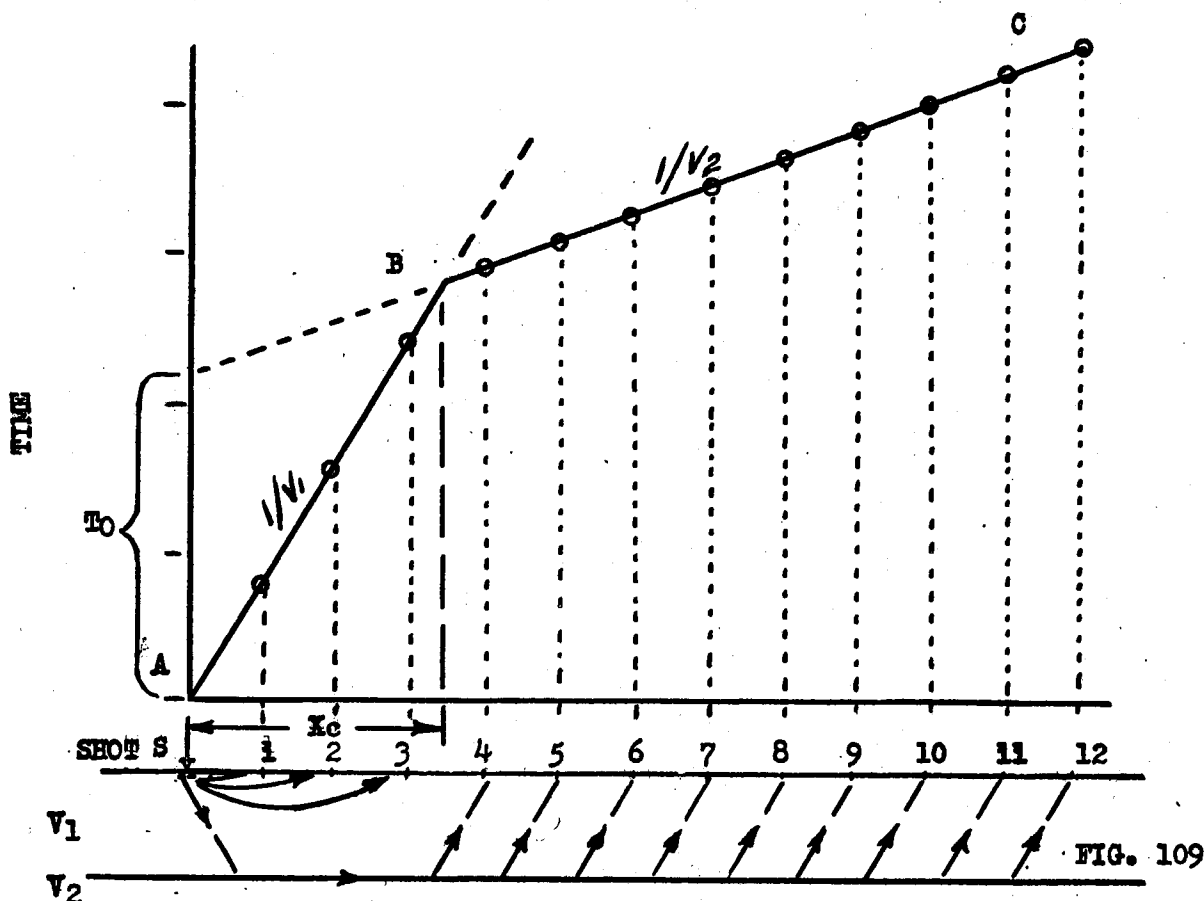


FIG. 109

At the critical distance, it is seen that the travel time via a direct path in the surface layer with velocity V_1 is the same as that where part of the travel path follows the refracted wave along the $V_1 - V_2$ interface. Therefore:

$$\frac{x_c}{V_1} = \frac{x_c}{V_2} + \frac{2h \sqrt{V_2^2 - V_1^2}}{V_1 V_2} \quad \text{Eq. (32)}$$

Solving for "h":

$$\begin{aligned} h &= \frac{x_c}{2} \left[\frac{1}{V_1} - \frac{1}{V_2} \right] \frac{V_1 V_2}{\sqrt{V_2^2 - V_1^2}} \\ h &= \frac{x_c}{2} \frac{V_2 - V_1}{\sqrt{V_2^2 - V_1^2}} \\ h &= \frac{x_c}{2} \sqrt{\frac{V_2 - V_1}{V_2 + V_1}} \quad \text{Eq. (33)} \end{aligned}$$

All of the quantities needed can be determined directly from the graph, and the depth "h" solved for directly.

The depth can also be computed from what is known as the "Intercept Time". The travel time, expressed in Eq. (30), is:

$$T = \frac{x}{V_2} + \frac{2h \cos i}{V_1}.$$

When "x" equals zero this expression is reduced to:

$$T_0 = \frac{2h \cos i}{V_1} \quad \text{Eq. (34)}$$

where T_0 is the intercept value on the travel time coordinate for the line segment defining the velocity in the second layer. See Fig. 109.

The following example demonstrates that both methods give identical results. In all cases a correction must be applied to the travel times for the difference in elevation of the detectors and that at which the sound source (shot) is located.

Seismic Example 1

Observed Data

Detector	Corrected Travel Time to Detector	Distance from Shot Point	Data from Travel Time Plot
1	0.05 sec.	250	$V_1 = 5000 \text{ ft./sec.}$
2	0.10	500	$V_2 = 14,000 \text{ ft./sec.}$
3	0.20	1000	$T_0 = 0.193 \text{ sec.}$
4	0.30	1500	$x_c = 150 \text{ ft.}$
5	0.34	2000	
6	0.37	2500	
7	0.41	3000	
8	0.45	3500	

Depth calculations on the basis of Time Intercept (Eq. 30):

$$T_0 = \frac{2h \cos i_c}{V}$$

$$h = \frac{T_2 V_1}{2 \cos i}$$

$$\sin i = \frac{V_1}{V_2}$$

$$\sin i = \frac{5000}{14000} = .3562$$

$$\cos i = .9344$$

$$h = \frac{.193 \times 5000}{2 \times .9344}$$

$$h = 518 \text{ feet}$$

Depth calculations on the basis of critical distance (Eq. 33):

$$h = \frac{x_c}{2} \sqrt{\frac{v_2 - v_1}{v_2 + v_1}}$$

$$h = \frac{1500}{2} \sqrt{\frac{14000 - 5000}{14000 + 5000}} = 750 \sqrt{\frac{9000}{19000}}$$

$$h = 750 \sqrt{.474} = 750 \times .69 = 518 \text{ feet.}$$

When more than two layers are involved, the particular ray that will be refracted at 90° at the lowest interface "n" is defined by the ratio:

$$\sin i_n = \frac{v_1}{v_n}.$$

This can best be seen from a specific example as the three layer situation shown in Fig. 110.

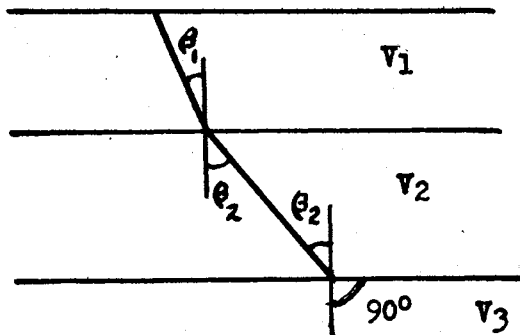


FIG. 110

In this case, θ_2 is the critical angle at the $v_2 - v_3$ interface. From plain geometry, it is seen that θ_2 is also the refracted angle at the $v_1 - v_2$ interface. Expressing the incident and refracted angles in terms of the velocity values according to Snell's Law:

$$\frac{\sin \theta_1}{\sin \theta_2} = \frac{v_1}{v_2}$$

$$\sin \theta_2 = \frac{\sin \theta_1 v_2}{v_1}$$

$$\frac{\sin \theta_2}{\sin 90^\circ} = \frac{v_2}{v_3}$$

$$\sin \theta_2 = \frac{v_2}{v_3}$$

therefore:

$$\frac{\sin \beta_1 V_2}{V_1} = \frac{V_2}{V_3} \quad \text{and} \quad \sin \beta_1 = \frac{V_1}{V_3} \quad \text{Eq. (35)}$$

The same relations could be developed for any number of layers.

For a three layer problem, the thickness of the first layer having velocity V_1 is obtained as in the previous example using the time intercept for the line segment defining the velocity V_2 . The thickness of the second layer in which the velocity is V_2 is determined from the expression:

$$T_{02} = \frac{2h_1 \cos \beta_1}{V_1} + \frac{2h_2 \cos \beta_2}{V_2} \quad \text{Eq. (36)}$$

where T_{02} is the time intercept for the line segment defining the velocity V_3 . h_1 is the thickness of the first layer determined independantly as a two layer problem, and $\sin \beta_1 = V_1/V_3$, $\sin \beta_2 = V_2/V_3$.

An example of a depth computation where three layers are involved is as follows:

Seismic Example 2

Data from Travel-Time Graph

$$\begin{array}{ll} V_1 = 5000 \text{ ft./sec.} & T_{01} = .193 \text{ sec.} \\ V_2 = 14000 \text{ ft./sec.} & T_{02} = .398 \text{ sec.} \\ V_3 = 20000 \text{ ft./sec.} & \end{array}$$

As previously calculated (see seismic example 1):

$$h_1 = \frac{T_{01} V_1}{2 \cos \alpha} \quad \alpha = \text{critical angle of incidence at } V_1 - V_2 \text{ interface.}$$

$$h_1 = 518 \text{ feet}$$

$$T_{02} = \frac{2h_1 \cos \beta_1}{V_1} + \frac{2h_2 \cos \beta_2}{V_2}$$

$$\sin \beta_1 = \frac{V_1}{V_3} = \frac{5000}{20000} = 0.25, \quad \cos \beta_1 = 0.967$$

$$\sin \beta_2 = \frac{V_2}{V_3} = \frac{14000}{20000} = 0.70, \quad \cos \beta_2 = 0.714$$

Substituting in Eq. (36):

$$.398 = \frac{2(518)(.967)}{5000} + \frac{2h_2 (.714)}{14000}$$

$$.0001023 h_2 = .398 - .200$$

$$h_2 = \frac{.198}{.0001023} = 1938 \text{ feet}$$

$$\text{Total Depth} = h_1 + h_2$$

$$= 518 + 1938 = 2456 \text{ feet.}$$

For a four layer situation:

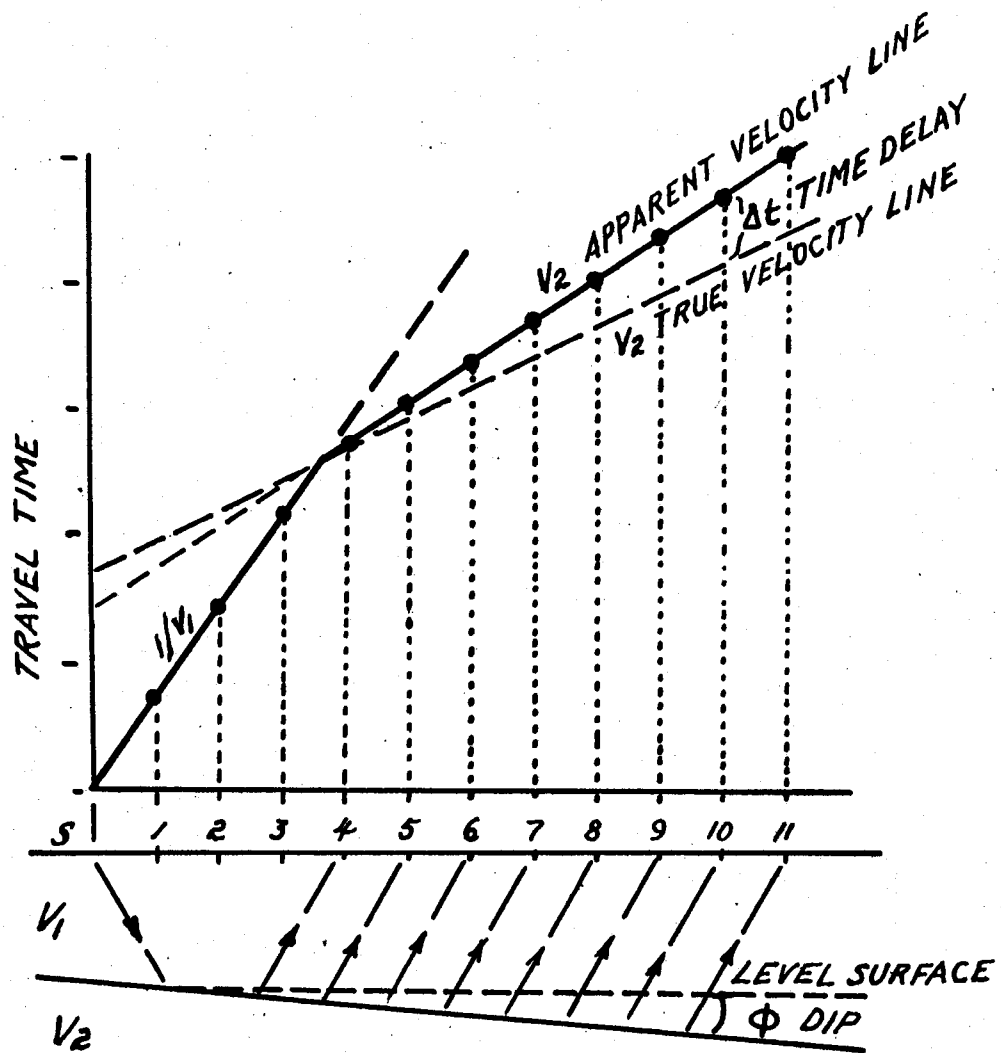
$$T_{03} = \frac{2h_1 \cos \delta_1}{V_1} + \frac{2h_2 \cos \delta_2}{V_2} + \frac{2h_3 \cos \delta_3}{V_3} \quad \text{Eq. (37)}$$

$$\sin \delta_1 = \frac{V_1}{V_4}, \quad \sin \delta_2 = \frac{V_2}{V_4}, \quad \sin \delta_3 = \frac{V_3}{V_4}$$

$$\delta_3 = \text{incident angle refracted } 90^\circ \text{ at the } V_3 - V_4 \text{ interface.}$$

In all cases it is assumed that the velocity increases with depth. If the velocity decreases with depth, the incident ray would be refracted downward into the underlying layer, and no record of the low velocity horizon would be obtained. This happens, however, only where limestones overlie other sediments, or where igneous rocks are interbedded in sediments. For all other geologic situations, the effects of compaction and cementation with depth (usually also a measure of geologic age) results in an increase in velocity with depth.

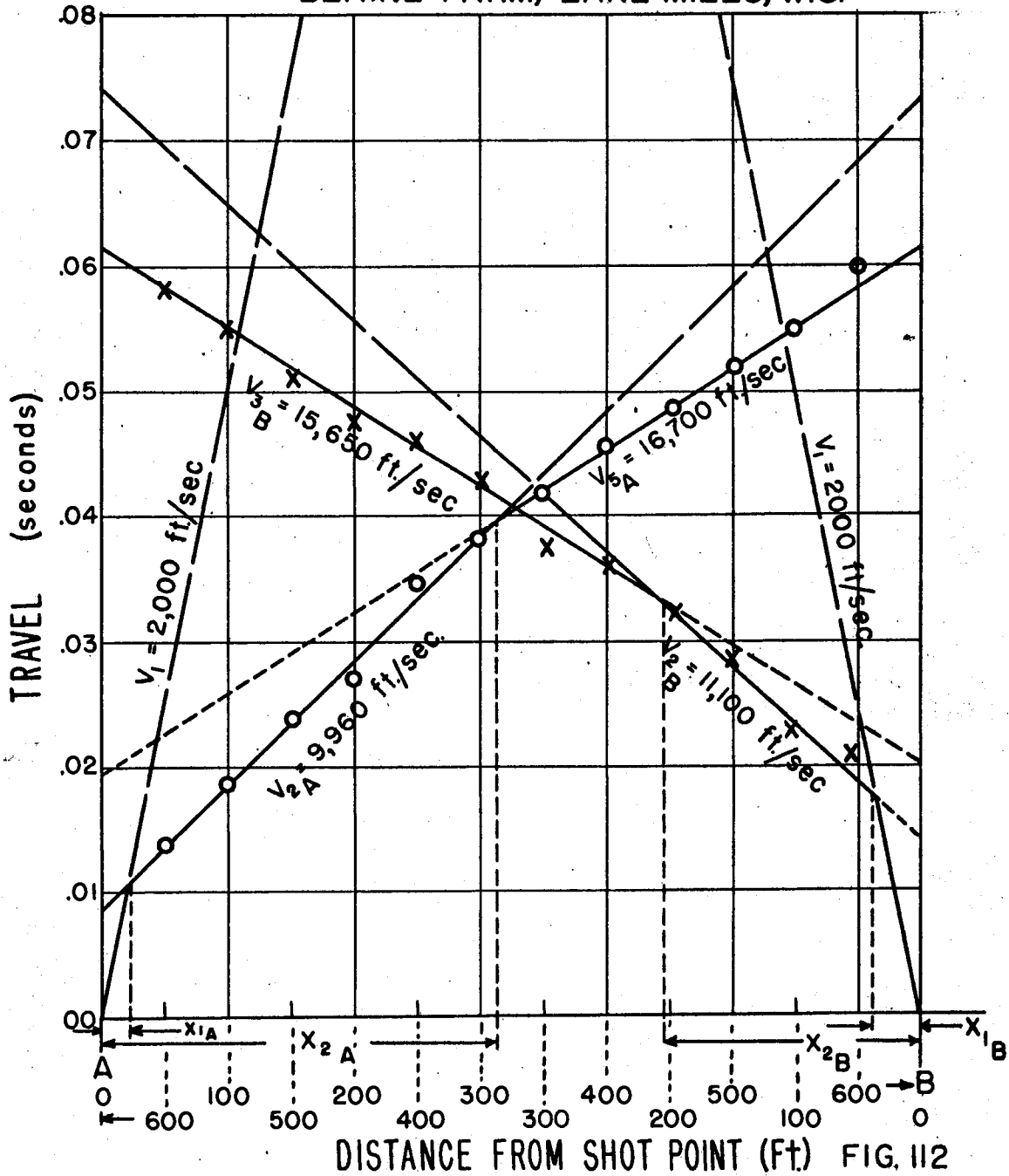
When the strata at depth are not flat-lying, but are dipping, it is necessary to modify both the field procedure and mode of analysis. If a horizon is dipping away from the shot point, the thickness of the overlying layer gets progressively greater with a consequent lag in the time of arrival over that which would have been obtained if there had been no dip. As a result, the velocity value derived from the slope of the travel time graph segment defining V_2 gives an apparent velocity that is less than the true value. This can be seen by reference to Fig. 111. Similarly, the apparent velocity for the dipping layer will be higher than the true value when shooting up dip.



EFFECT OF DIP ON V_2 VELOCITY LINE OF TRAVEL-TIME GRAPH

FIG. III

REVERSE TRAVEL TIME GRAPH
LOCATION 3
BLAINE FARM, LAKE MILLS, WIS.



As it may not be known whether subsurface layers are dipping or not, the only safe procedure is to make two series of measurements in opposite directions and compare the travel time graphs. This technique is called reverse shooting. If the underlying beds are horizontal, the intercept times for each layer will be the same in either direction. With dipping layers, the intercept times will always be greater in the down dip direction. The total travel time, however, in either direction will be the same. See Fig. 112.

If shooting were carried out in one direction only, the assumption of horizontal layering in such an area would obviously lead to erroneous conclusions concerning the rock types present.

The equation for the travel path and travel time in either direction can be developed along the same lines as was shown in determining the equations for horizontal layering. For a multilayer situation, as shown in Fig. 113, the expressions for depth are given below.

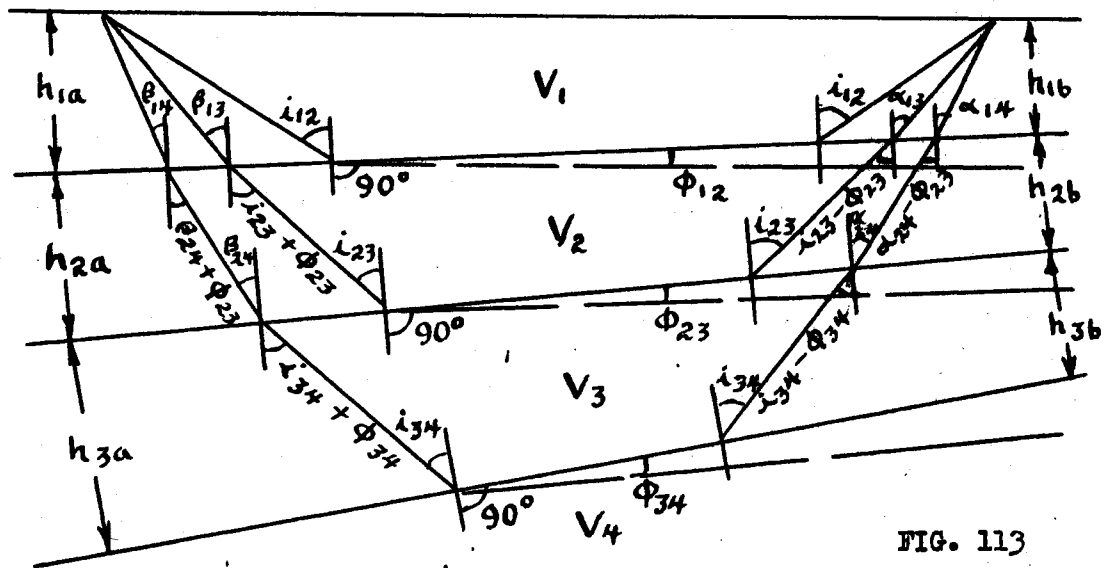


FIG. 113

- (1) For a two layer situation with a single dipping interface: On the basis of the critical distance (X_c) when shooting down dip,

$$\frac{X_{cb}}{V_1} = \frac{2h \cos i}{V_1} + \frac{X_{cb}}{V_1} \sin (i + \phi)$$

$$\text{or } 2h = \frac{X_{cb}}{\cos i} [1 - \sin (i + \phi)]$$

Eq. (38)

Since "h" here is measured perpendicular to the dipping horizon, the vertical depth $h_z = h / \cos \phi$. Therefore:

$$h_z = \frac{X_{cb} [1 - \sin(i + \phi)]}{2 \cos \phi \cos i} \quad \text{where} \quad \frac{V_1}{V_{2b}} = \sin(i + \phi) \quad \text{Eq. (39)}$$

For shooting up dip:

$$h_z = \frac{X_{ca} [1 - \sin(i - \phi)]}{2 \cos \phi \cos i} \quad \text{where} \quad \frac{V_1}{V_{2b}} = \sin(i - \phi) \quad \text{Eq. (40)}$$

Using the time intercept method, the expression is the same as for horizontal layering, but it is necessary to determine the true velocity value.

$$T_{0a} = \frac{2h \cos i}{V_1} \quad \frac{V_1}{V_{2a}} = \sin(i - \phi)$$

$$\text{or} \quad \frac{V_1}{V_{2b}} = \sin(i + \phi)$$

$$h_z = \frac{T_{0a} V_1}{2 \cos i \cos \phi} \quad \frac{V_1}{V_2} = \sin i$$

Knowing the depth at one of the shooting points, that at any distance "x" along the line of measurement can be determined as: $h_2 + \tan \phi x$ down dip, or $h_2 - \tan \phi x$ up dip.

(2) For a three layer problem with two dipping layers:

$$T_{02a} = \frac{2h_2 \cos i_{23}}{V_2} + h_1 \frac{\cos \alpha_{13} + \cos \theta_{13}}{V_1} \quad \text{Eq. (41)}$$

and

$$\frac{V_1}{V_{3a}} = \sin(\alpha_{13} - \phi_{12}) \quad \frac{V_1}{V_{3b}} = \sin(\theta_{13} + \phi_{12})$$

$$\frac{V_1}{V_2} = \frac{\sin \alpha_{13}}{\sin(i_{23} - \phi_{23})} = \frac{\sin \theta_{13}}{\sin(i_{23} + \phi_{23})}$$

$$\frac{V_2}{V_3} = \sin i_{23}$$

- (3) For four layer problem with three dipping layers:

$$T_{03a} = \frac{2h_3 \cos i_{34}}{V_3} + \frac{h_2(\cos \alpha_{24} + \cos \theta_{24})}{V_2} + \frac{h_1(\cos \alpha_{14} + \cos \theta_{14})}{V_1} \quad \text{Eq. (42)}$$

$$\frac{V_1}{V_{4a}} = \sin(\alpha_{14} - \phi_{12})$$

$$\frac{V_1}{V_{4b}} = \sin(\theta_{14} + \phi_{12})$$

$$\frac{V_1}{V_2} = \frac{\sin \alpha_{14}}{\sin(\alpha_{24} - \phi_{23})} = \frac{\sin \theta_{14}}{\sin(\theta_{24} + \phi_{23})}$$

$$\frac{V_2}{V_3} = \frac{\sin \alpha_{24}}{\sin(i_{34} - \phi_{34})} = \frac{\sin \theta_{24}}{\sin(i_{34} + \phi_{34})}$$

$$\frac{V_3}{V_4} = \sin i_{34}$$

In all cases "h" is measured perpendicular to the dipping surface, and the vertical depth involved will be $h_z = h/\cos \phi$.

The general procedure followed in working up reverse profile data are as follows:

- (1) From the travel time graph the values for V_1 , V_{2a} , V_{2b} , V_{3a} and V_{3b} are determined and the intercepts T_{01a} , T_{01b} , T_{02a} , T_{02b} , etc., read or the critical distances X_{ca} and X_{cb} determined.
- (2) On the basis of the velocity ratios the angle of incidence and inclination are solved for:

Example:

$$\frac{V_1}{V_{2a}} = \sin(i_{12} - \phi_{12})$$

$$\frac{V_1}{V_{2b}} = \sin(i_{12} + \phi_{12})$$

$$\text{adding, } \frac{V_1}{V_{2a}} + \frac{V_1}{V_{2b}} = 2 \sin i_{12}$$

subtracting,

$$\frac{V_1}{V_{2a}} - \frac{V_1}{V_{2b}} = 2 \sin \phi_{12}$$

- (3) With the above values the depth can be solved by substitution in the basic equation for determining the depth.

When the subsurface geology involves irregular surfaces rather than plane surfaces, as discussed up to now, the travel time plots will show abnormalities which can be used as a means of determining the nature of the irregularity and also estimating their magnitude.

In Fig. 114, the effect of a limited vertical offset is indicated when shooting across it in opposite directions. The change in thickness of the upper layer (V_1) with velocity results in the time offset (Δt) indicated in the V_2 line segment of the travel time graph. The displacement (Z) can be computed as :

$$Z = \frac{\Delta t V_1}{\cos i} = \frac{\Delta t V_1 V_2}{\sqrt{V_2^2 - V_1^2}} \quad \text{Eq. (43)}$$

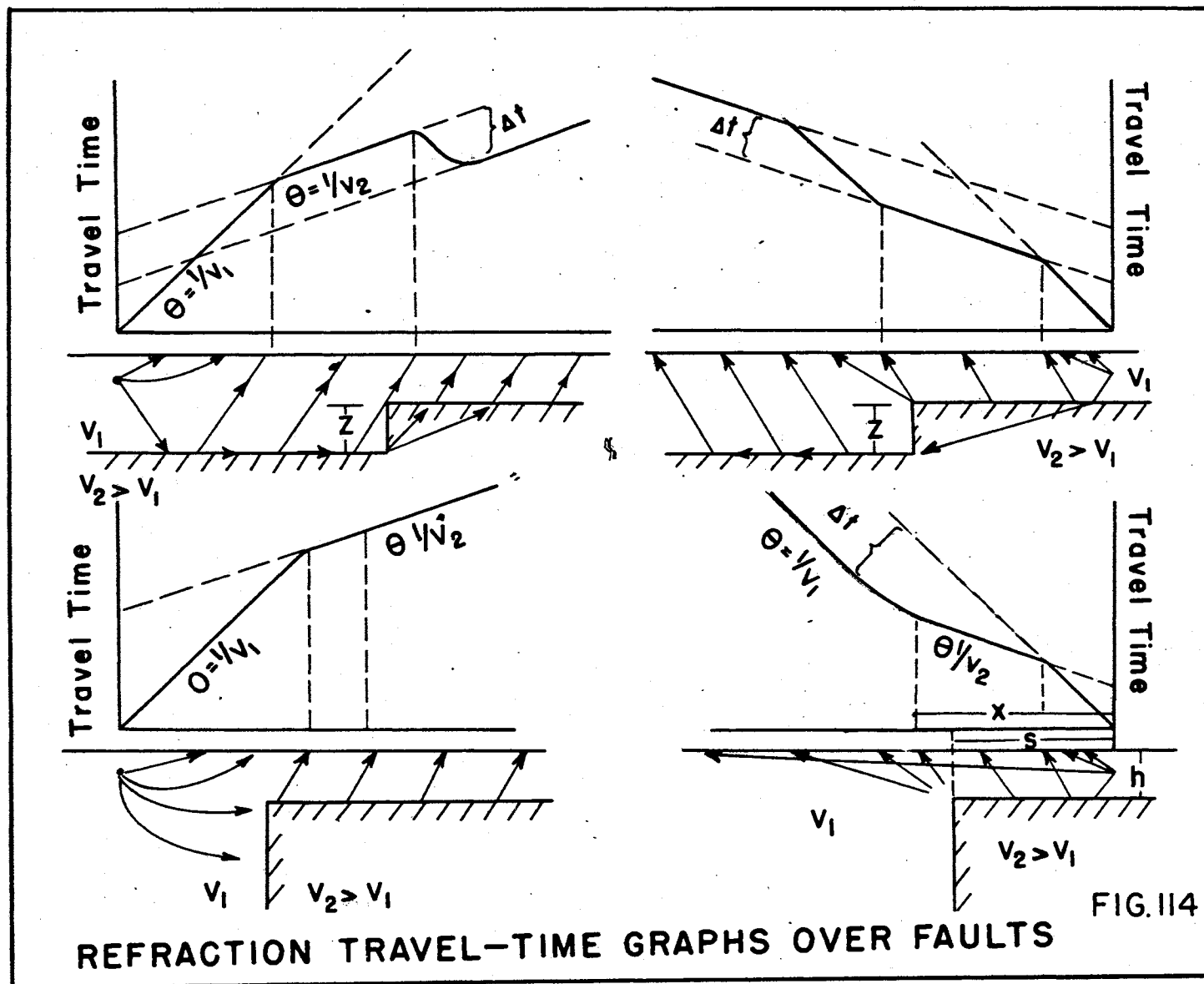
The effect of a large vertical displacement is also shown in Fig. 114, when shooting across it in opposite directions. Although the amount of the displacement cannot be computed in this case, the location of the displacement at "S" distance can be determined.

$$S = X - h \tan i \quad \text{Eq. (44)}$$

where X = distance where the break in the V_2 line segment of the travel time graph occurs. " h " is the computed thickness of the surface layer at the shot end of the line. Angle " i " is defined from the relationship $\sin i = V_1/V_2$.

Although the above discussions consider the simpler types of subsurface geologic structure, in practice more complex ones are encountered such as ridges or valleys between the two ends of a reverse shooting profile. It frequently happens that when such features are near to one shot point, they will show up in shooting in one direction but not in the other. For this situation to occur with a valley, for example, it must lie inside the critical distance from the shot point.

In rough terrain, relative changes in the elevation of the various detectors to each other and the shot point will require an auxiliary set of calculations to correct all observed travel times to a fixed datum plane before the travel time graph can be constructed.



VI-5 - Electro-Magnetic Method

VI-5a General Statement

When an electric current is passed through a coil of wire, a magnetic field will be created around the conductor. By using numerous insulated turns on a circular frame and an alternating current, a strong electro-magnetic field can be created. Such a magnetic field will cut into the earth and induce voltage variations which in turn will set up electrical currents in the earth, and these currents will have a secondary magnetic field associated with them which will distort the primary field set up by the energizing coil at the surface. The better the subsurface conductor, the greater will be the distortion of the primary field.

The above describes the basis of the electro-magnetic method, and the only measurements required are those for the distortion of the primary field.

Quantities that can be measured are magnetic flux, magnitude of the vertical or horizontal component of the magnetic field, magnitude and direction of the resultant magnetic field and phase of the electric or magnetic field. As a rule, the magnitude and direction of the resultant field are the quantities measured. This is done with a secondary search coil whose operation is described in the next section.

VI-5b General Theory

The results obtained are influenced by the relative electrical conductivity of the subsurface conductor to the surrounding rock, the length of the conductor, the mutual inductance between the coil and conductor, the frequency of the energizing current, the current in the energizing coil, and the electrical resistivity of the overburden.

In view of the complex nature of the theory, it will only be considered in general terms. The electromotive force (e.m.f.), E_0 , created by the energizing coil produces an alternating current, I_0 , in the subsurface conductor which in turn induces an electromotive force, E_s . The search coil is acted upon by both the primary e.m.f. (E_0) and the secondary e.m.f. (E_s). The overburden acts as a shield whose effect varies approximately as the square of the frequency of the current in the primary energizing coil.

The search coil is gimbal mounted on a tripod so as to have both a vertical and horizontal axes of rotation, and a minimum signal (null) will be obtained when the search coil is tangent to the field of the energizing coil (vertical and perpendicular to the plane of the

energizing coil). A minimum signal also will be obtained with the search coil horizontal and perpendicular to the plane of the energizing coil. A maximum signal will be obtained when the search coil is vertical in the plane of the energizing coil. In all cases it is assumed that the elevation of both coils is the same; i.e., the axis of rotation of the search coil is at the same elevation as the center of the energizing coil. The orientation of the search coil relative to the secondary field produced by a subsurface conductor, is such that a minimum signal (null) will be obtained when the plane of the search coil is tangent to the circular magnetic field surrounding the conductor created by the induced current.

The actual orientation for a minimum signal, therefore, will depend upon whether there is a buried conductor present or not, although the minimum signal position will always be obtained when the search coil is tangent to the resultant field of both the primary and secondary sources.

With the energizing coil vertical and its plane pointed toward the search coil, if any angle from the vertical (dip) of the search coil, or direction of the search coil (strike) is obtained other than that pointing toward the energizing coil, there is evidence of the presence of a buried conductor.

VI-5c Field Procedure

General procedure and data recorded are as follows:

- (1) Point the energizing coil in a vertical position toward the search coil.
- (2) Level the search coil tripod.
- (3) Set the vertical arc at 90° so that the plane of the search coil is vertical in gimbal.
- (4) Rotate the coil about the vertical axis of the tripod until a minimum signal is obtained.
- (5) Clamp the coil ring and turn the coil still in the vertical position through 90° , the position for maximum signal. (gimbal axis will be pointed at the energizing coil.)
- (6) Rotate the coil about the horizontal gimbal axis until a minimum signal is obtained. This will define the dip.
- (7) Record the magnitude and direction of dip and sharpness of the null (minimum signal) in degrees.

The method employed in traversing an area involves setting up both coils along a line parallel to the suspected strike of the buried conductor and then advancing this line sideways so as to always maintain the same azimuthal orientation. The amount of advance is governed by the estimated depth to the conductor. In general, about one half of the estimated depth is used. Similarly, the distance between the energizing and search coil is determined as equal to about three times the estimated depth.

Since the energizing coil must be "sighted" at the search coil, this requires either cutting lines of sight in wooded country or else using magnetic orientation. In areas of marked magnetic anomalies, the latter procedure may induce considerable errors in the results, as was demonstrated at Trout Brook. See Fig. 95.

Where the country rock has disseminated conductors either as mineral material or water, the null positions found will be very broad. The presence of a more homogenous material, even if a poor conductor, will be indicated in such areas by obtaining sharper nulls.

In Fig. 115, strike and dip curves obtained over a buried sheet conductor are shown for vertical orientation and for a dip of about 45° . In each case the dip curve is at about zero value where the strike value is a maximum, and this position in general coincides with the axis of the conductor, and hence permits its position to be mapped. The direction of dip of a conductor is determined on the basis that the smallest angle of dip occurs on the hanging wall side.

VI-6 - Conclusion

For those desiring a more complete exposition on the methods of reduction and interpretation of data and the theory underlying them, the following texts are recommended.

General technical discussion suitable for reader without an advanced mathematical background.

Geophysical Prospecting for Oil by L.L. Nettleton
McGraw Hill Co. New York, 1940 .

An Introduction to Geophysical Prospecting by Milton Dobrin
McGraw Hill Co., New York, 1953.

Complete technical discussion requiring an advanced knowledge of mathematics.

Geophysical Exploration by Carl Heiland
Prentice Hall Co., New York, 1940.

Exploration Geophysics by J.J. Jakosky
Trija Publishing Co., Los Angeles, Calif. 1950.

